Autoantibodies that drive extraintestinal manifestations of gluten-related disorders are developed in the gut

Thesis submitted in fulfillment of the requirements of the degree of Doctor of Philosophy

2017

Ana Mafalda Reis

School of Dentistry,

Cardiff University

Acknowledgments

First, I would like to thank Professor Daniel Aeschlimann for the patience and time he spent with me that allow me to submit this thesis. I would also like to thank Dr. Xiaoqing Wei for the support and expertise in immunology. A thank you to Dr. Vera Knauper and Dr. Sharon Dewitt for their words of encouragement during the course of this PhD. A special thank you (and 'Sorry!') to my 'lab partner' Rhiannon Griffiths for her friendship and for putting up with my frustrations.

I would like to acknowledge Coeliac UK and Cardiff University, School of Dentistry for funding this research.

To my family back in Portugal, thank you for all your love! To my dad and my sister, thank you for all your great advice and for always believing in me (even at times when I didn't). To my good friends Bruno, Andreia and Leila: thank you for your loyalty (Even though I've neglected you in the last few years. I will make it up to you!). To the Cardiff gang: this journey wouldn't have been the same without your craziness and I will be forever grateful for your friendship!

I would like to thank The Gambles: Charlotte, George and Gil for making me feel like I was part of the family, and for the endless support and encouragement.

To Mike: thank you for your love, patience, strength and for making me laugh! You make me a better person and always support me in pursuing my dreams. I wouldn't have been able to endure this PhD without you.

Summary

Coeliac disease is reported to affect around 1% of the western population, with ingestion of gluten typically initiating inflammation of the bowel. Current diagnostic assays based on biomarkers of gluten sensitivity are only specific for patients with classical gastrointestinal symptoms, such as those displayed in coeliac disease. However, studies have shown that gluten sensitivity can manifest with symptoms other than those related to inflammation of the bowel, notably neurological symptoms including ataxia and neuropathy. Identification of gluten sensitive patients, with a predisposition to develop neurological deficits, is crucial to prevent irreversible damage to neural tissue, as this tissue has a poor intrinsic repair capacity.

A novel transglutaminase, TG6, has been discovered and shown to be predominantly expressed by a subset of neurons in the central nervous system. Furthermore, anti-TG6 IgG and IgA autoantibodies have been shown to be prevalent in gluten ataxia, independent of intestinal involvement. Therefore, TG6 antibodies have been identified as possible biomarkers to diagnose those patients that may be at risk of developing neurological disease in association with gluten sensitivity.

The aim of this project was to develop a mechanistic understanding of autoantibody development and extraintestinal disease-manifestations. Specifically, the research aimed to determine whether autoantibody development to TG6 occurs in conjunction with that of TG2, i.e. in the gut, or if it has its origin in independent events.

By immunofluorescent analysis of intestinal biopsies, this research was able to detect, for the first time, the presence of TG6-reactive B-cells and plasma cells in the intestinal mucosa of patients presenting with gluten-related disorders. Additionally the research was able to identify macrophages as possible sources of TG6 at the intestinal level.

These findings have led to the proposition that autoantibodies that drive the extraintestinal manifestiations of gluten related disorders are developed in the gut.

Table of Contents

List of abbreviations

AA – amino acid
AGA - anti-gliadin antibodies
AM – acetomethylester
ATP – adenosine-5'-triphosphate
BCR - B-cell receptor
BSA - bovine serum albumin
CEB – cell extraction buffer
CD – coeliac disease or cluster of differentiation
CMV – cytomegalovirus
CNS - central nervous system
COP – coat protein complex
CPPD – calcium pyrophosphate dihydrate
C (Cys) - cysteine
D (Asp) – aspartic acid
D2 – second part of the duodenum
Da - Dalton
DGP - deaminated gliadin peptides
DH - dermatitis herpetiformis
DMEM – Dulbecco's Modified Eagle Medium
DMSO – dimethyl sulfoxide
DTT – dithiothreitol
E.coli - Escherichia coli
ECM – extracellular matrix
EDTA – ethylenediaminetetraacetic acid
EGTA - ethylene glycol-bis(β-aminoethyl ether)-N,N,N',N'-tetraacetic acid
EGF – epidermal growth factor
ELISA – enzyme-linked immunosorbent assay
EMA – endomysium antibodies
FXIIIa – factor XIIIa
FBS – fetal bovine serum
FFPE - formaldehyde fixed and paraffin embedded

FITC - fluorescein isothiocyanate

GA - gluten ataxia

GAD - glutamic acid decarboxylase

GALT – gut-associated lymphoid tissue

GDP – guanosine-5’-diphosphate

GFD – gluten-free diet

G proteins – guanine nucleotide-binding proteins

GRD - gluten related disorders

GTP – guanosine-5’-triphosphate

H (His) – histidine

HEPES – 4-(2-hydroxyethyl)-1-piperazineethanesulfonic acid

HLA-DQ – human leukocyte antigen, DQ subregion

HRP – horseradish peroxidase

HSP - heat shock protein

ISA - idiopathic sporadic ataxia

IL – interleukin

INF-γ – interferon γ

LB medium – Luria-Bertani medium

LPS – lipopolysaccharide

MALT - mucosa-associated lymphoid tissue

MHC – major histocompatibility complex

MSA-C - multiple system atrophy -cerebellar variant

MW – molecular weight

NK cells – natural killer cells

NHS - N-hydroxysuccinimide

OD - optical density

PAGE - polyacrylamide gel electrophoresis

P2X7 - ligand gated ion channel 7

PBS – phosphate buffered saline

PCR – polymerase chain reaction

PEN - penicillin

PMSF – phenylmethanesulfonyl fluoride

Q (Gln) - glutamine

RCD - refractory coeliac disease

SCA - spinocerebellar ataxia

scFv – single-chain variable fragment

SDS – sodium dodecyl sulfate

SF - Spodoptera frugiperda

STREP – streptomycin

TAE – Tris-Acetate EDTA buffer

TBS – Tris-buffered saline

TGF-β – transforming growth factor β

TNF-α – tumour necrosis factor α

TPA – 12-O-tetradecanoylphorbol-13-acetate

UV - ultraviolet

W (Trp) - Tryptophan

WA - wheat allergy

WMA - white matter abnormalities

wt - wild type

Chapter 1 Introduction

1.1 The transglutaminase family

The transglutaminase (TG) family consists of a group of enzymes related in function and structure, which mediate post-translation modification of proteins. In the human genome, 9 TG genes have been identified, of which 8 are encoding catalytic active enzymes: TG1, TG2, TG3, TG4, TG5, TG6, TG7 and Factor XIIIa (FXIIIa). The remaining gene codes for a catalytically inactive protein, erythrocyte membrane protein band 4.2, found as a structural protein in erythrocytes (Iismaa et al. 2009).

TGs evolved from the papain family of proteases and are products of different genes arising from duplication and rearrangement of an ancestral proto-gene (Grenard et al., 2001; Lorand & Graham, 2003; Thomas et al., 2013). Therefore, is not surprising that there's a high degree of structural conservation between the TG family members. They share a similar protein structure that consists of 4 structurally distinct domains: 1 N-terminal β-sandwich, 1 catalytic core and 2 C-terminal β-barrel domains (Yee et al., 1994; Pinkas et al., 2007). Additionally, TG1 and FXIIIa contain a pro-peptide before the N-terminal β-sandwich that is cleaved for enzyme activation (Iismaa et al. 2009). Fig. 1.1 demonstrates the relationship between TGs gene organization and protein structure.

Apart from protein band 4.2, all transglutaminases share the same amino acid sequence at the active site (the equivalent of Cys277, His335 and Asp358 in human TG2) and conserved Trp241 and Trp332 residues that stabilize the transition state during catalysis (Liu et al. 2002).

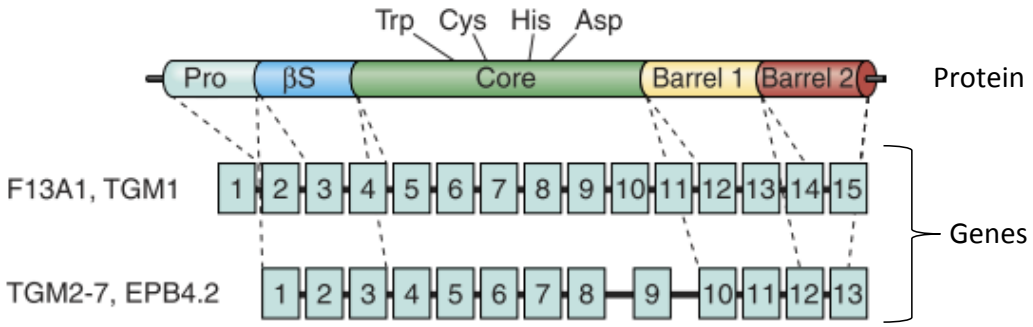

Fig. 1.1 Genomic organization of transglutaminases (adapted from Iismaa et al. 2009)

1.2 Enzymatic reactions mediated by transglutaminases

TGs are able to catalyse at least 5 types of post-translational protein modifications. These enzymes preferably target the γ-carboxamide group of the side chain of glutamine residues, located within unstructured flexible regions of protein substrates (Hohenadl et al., 1995). The desired glutamine seems to depend more on its accessibility than on the primary sequence surrounding it, although there seems to be sequence specificity (Stamnaes et al., 2010). Also, TGs do not react with the free amino-acid glutamine (Folk & Finlayson, 1977; Mehta & Eckert, 2005).

Modification of the γ-carboxamide group of the glutamine residue depends on the nature of the substrates available and catalyzed reactions can be grouped into transamidation, hydrolysis or esterification (Fig. 1.2) (Aeschlimann & Thomazy 2000).

The reaction starts when a glutamine-containing protein or peptide (acceptor substrate) reacts with the active site cysteine, transiently acylating its thiol group to form a covalently linked γ-glutamyl-thioester (acyl-enzyme intermediate). This step is rate-limiting and results in the release of ammonia (Lorand & Graham 2003). This initial acylation step can be followed either by reaction with water or by binding of a second substrate, such as an amine or an alcohol, to cleave the thioester bond (the deacylation step) with generation of the hydrolysed, transamidated or esterified product and enzyme regeneration (Folk, 1980; Beninati & Piacentini, 2004; Mehta & Eckert, 2005; Iismaa et al., 2009).

Transamidation reactions can result in crosslinking of proteins by formation of a N^{ε}(γ-glutamyl)lysine isopeptide bond between the glutamine residue of one protein and the ε-amino group of a deprotonated lysine residue present in another protein. Other transamidation reactions can result in the amine or polyamine incorporation into the acceptor glutamine residue or acylation of a lysine residue on the donor protein (Lorand & Graham 2003). Hydrolysis will occur in the absence of a second donor substrate, when a water molecule will drive the reaction. This leads to deamidation of the glutamine residue on the acceptor substrate. Given the aqueous environment, it remains to be structurally explained why reaction with water occurs in some instances but not others. Hydrolysis can also occur in the presence of an already crosslinked polypeptide, by cleavage of the isopeptide bond, demonstrating reversibility of the second step of the reaction.

The reactions of transamidation compete between each other and with esterification, and are reversible. However, both reactions leading to hydrolysis proceed only in one direction (Lorand & Graham 2003).

The reactions catalysed by TGs are essential for biological processes such as blood coagulation, skin barrier formation, and extracellular matrix (ECM) assembly (Iismaa et al. 2009).

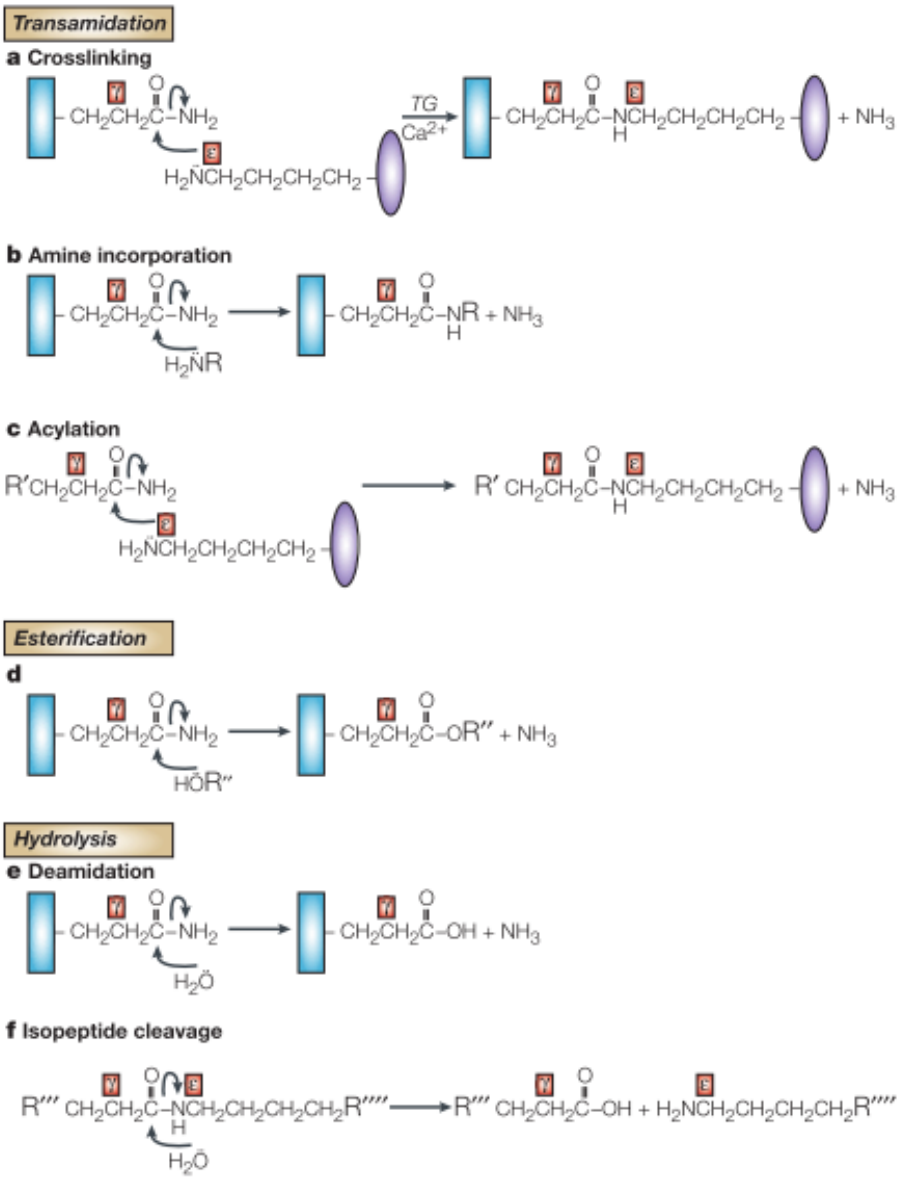

Fig. 1.2 Post-translational reactions catalysed by transglutaminases. TGs mediate Ca^{2+}-dependent acyl-transfer reactions that can be grouped into transamidation (a, b, c), esterification (d) or hydrolysis (e, f). Type of reaction is dependent on the second nucleophile donor. Gln acceptor residue (blue rectangle); Lys donor residue (purple ellipse); R (side chain of primary amine); R' (Gln containing peptide); R'' (a ceramide); R''' and R'''' (the side chains in branched isopeptides). Retrieved from Lorand & Graham 2003.

1.3 Biological function of transglutaminases

Different members of the TG family have different distribution patterns and different biological functions (Table 1.1). For example, the presence of TGs is important in the differentiation of keratinocytes, with TG1 and TG5 being involved in the crosslinking of epidermal proteins and formation of cornified envelopes in the epidermal cells (Mehta & Eckert 2005). FXIII takes part in the coagulation cascade and catalyzes the formation of γ-glutamyl-ε-lysine cross-links between fibrin chains, thus stabilizing the fibrin clot during blood coagulation (Bagoly et al., 2012). TG2 is ubiquity expressed and is involved in the stabilization of the extracellular matrix by selectively crosslinking proteins (Aeschlimann & Thomazy, 2000). Also, deamidation of peptides by TG2 is critically related to the pathogenesis of coeliac disease (Sollid, 2002).

For the purpose of this project, I will introduce TG members TG2, TG3 and TG6, as they are closely related (H. Thomas et al., 2013) and implicated in gluten-sensitivity disorders, which is the context of this project (Hadjivassiliou et al. 2010).

1.4 Transglutaminase 2

1.4.1 Protein expression and function

Transglutaminase 2 (TG2), also known as tissue transglutaminase, was first discovered by the Waelsch group in 1957 (Sarkar, Clarke, & Waelsch, 1957). It is encoded by *TGM2* on human chromosome 20q11-12 and has a molecular weight of ≈77kDa. TG2 is the only member of the transglutaminase family that is ubiquitously expressed at substantial levels and hence makes up above 90% of transglutaminase activity in many tissues in mammals (Lorand & Graham, 2003). Because of its wide distribution, TG2 is the most studied enzyme of the TG family and consequently, several of its intra and extracellular functions have been delineated. The protein is found in epithelium, myeloid cells and many mesenchymal-derived tissues including

smooth muscle cells, chondrocytes, osteoblasts and fibroblasts (Aeschlimann & Thomazy, 2000). On a cellular level, it is predominantly a cytosolic protein (80%), but it can also be found associated with the cell membrane (10-15%) and nuclear membrane (Lorand & Graham, 2003).

Table 1.1 The transglutaminase family – expression, function and links with disease

Protein	Synonyms	Tissue expression	Function	Disease
TG1	TG_k, keratinocyte TG	Keratinocytes, Brain	Cornified-envelope formation	Lamellar ichthyosis
TG2	tissue TG, TG_c, Ghα	Ubiquitous	Cell adhesion and motility, matrix assembly, signal transduction, cell survival, apoptosis, cell differentiation and many others	Coeliac disease
TG3	TG_e, epidermal TG	Epidermis, hair follicle, brain	Cell-envelope formation	Dermatitis herpetiformis
TG4	TG_p, prostate TG	Prostate	Semen coagulation	Unknown
TG5	TG_x	Ubiquitous except for CNS and lymphatic system	Cornified cell envelope formation	Peeling skin syndrome
TG6	TG_y	Testis, lung, CNS	Unknown	Gluten ataxia Spinocerebellar ataxia
TG7	TG_z	Ubiquitous	Unknown	Unknown
FXIIIa	Fibrin-stabilizing factor, fibrinoligase, plasma TG	Platelets, placenta, synovial fluid, astrocytes, macrophages, dendritic cells	Blood clot formation, wound healing, embryo implantation during pregnancy	Bleeding disorders Spontaneous abortion
Band 4.2	B4.2	Erythrocytes, bone marrow, spleen	Scaffolding protein in membrane of erythrocytes	Hereditary spherocytosis

Although investigated extensively, TG2 function in the body is still unclear, as many roles have been proposed, some of which are contradictory. In part this relates to the complexity added by its many proposed activities: transamidase, GTPase, disulphide isomerase, receptor ligand or structural protein, and the possible overlap in functions between members of the TG family. TG2 has been associated with stabilisation of the extracellular matrix and mineralization of skeletal tissues (Aeschlimann et al. 1995), cell survival (Boehm et al. 2002), neuronal differentiation (Tucholski et al. 2001), injury repair and inflammatory responses and programmed cell death (Aeschlimann & Thomazy 2000) among many others functions. Surprisingly, studies on TG2 knock-out mice revealed no overt developmental abnormalities, no obvious defects in organ function and normal reproduction (Laurenzi & Melino, 2001). The lack of obvious abnormalities in TG2 deficient mice may be explained by the activity of other TGs (FXIIIa in particular) that partially compensate for TG2 deficiency (Mehta & Eckert 2005). However, deficiencies are clearly evident when these mice are analysed in injury or disease models (Aeschlimann & Knauper, 2016), supporting a key role for the enzyme in tissue repair processes.

1.4.2 Protein structure and regulation of enzymatic activity

Similar to other members of the TG family, TG2 is composed of four domains: 1 N-terminal β-sandwich, 1 catalytic core and 2 C-terminal β-barrel domains. The catalytic triad is formed by the residues cysteine (C277), histidine (H335) and aspartate (D358). The active site C277 is situated in the catalytic core, in a pocket formed by three α-helices and stabilized by two tryptophan residues (W241 and W332). The core domain is connected to N-terminus of β-barrel 1 by a flexible loop (S. Liu et al., 2002; Pinkas et al., 2007).

Catalytic activity of TG2 is allosterically regulated by binding of calcium ions (Ca^{2+}) or guanine nucleotides (GTP/GDP) (Achyuthan & Greenberg, 1987; Begg et al., 2006). Nucleotide binding lowers the affinity for Ca^{2+} and decreases the accessibility of glutaminase donor substrate to

the TG2 substrate-binding pocket by inciting TG2 to adopt a “closed” conformation (compact form), masking the active site and therefore inhibiting its transamidation activity (Fig. 1.3A) (Casadio et al., 1999; S. Liu et al., 2002; Pinkas et al., 2007). The GTP-bound compact conformation of TG2 can be changed by calcium concentrations of >0.2mM. Enzyme activation requires binding of at least three Ca^{2+} ions. Activated TG2 adopts an expanded ellipsoid structure, whereby the two C-terminal β-barrels rotate almost 180˚ into the plane of the core/β-sandwich domain of the enzyme, revealing its active site and allowing substrate access (Fig. 1.3B) (Pinkas et al. 2007). This unusual large conformational change could potentially expose self-epitopes normally not present within the tissue and drive immunological responses (Pinkas et al., 2007). In fact, the production of autoantibodies against TG2 has been detected in the context of coeliac disease (Dieterich et al., 1997).

Binding of nucleotide or Ca^{2+} is mutually exclusive and hence guided by the respective affinity constants and local Ca^{2+}/nucleotide concentrations. Since calcium concentration is normally lower inside the cell (<10μM) compared to the extracellular environment (1.5-2mM), cytosolic TG2 remains in a GTP-bound inactive conformation.

Once secreted, TG2 binds Ca^{2+} and assembles immediately in the ECM or binds tightly to the cell surface (Lorand & Graham, 2003). However, the secretion mechanism of TG2 still needs to be fully elucidated. A recent study from our group shows that the externalization process is controlled by purinergic signalling, and more specifically P2X7 receptor (Adamczyk et al., 2015). Some reports suggest that extracellular TG2 activity is short-lived as the enzyme undergoes oxidative inactivation (Stamnaes et al. 2010).

TG2 is the only member of the transglutaminase family for which clear evidence exists that it also functions as a signal transducing G protein, i.e. in hormone receptor signalling (Lesort et al. 2000). Its GTPase activity is linked to regulation of transmembrane signalling through cell surface receptors such as α1-adrenergic receptor or oxytocin receptor (Fesus & Piacentini, 2002).

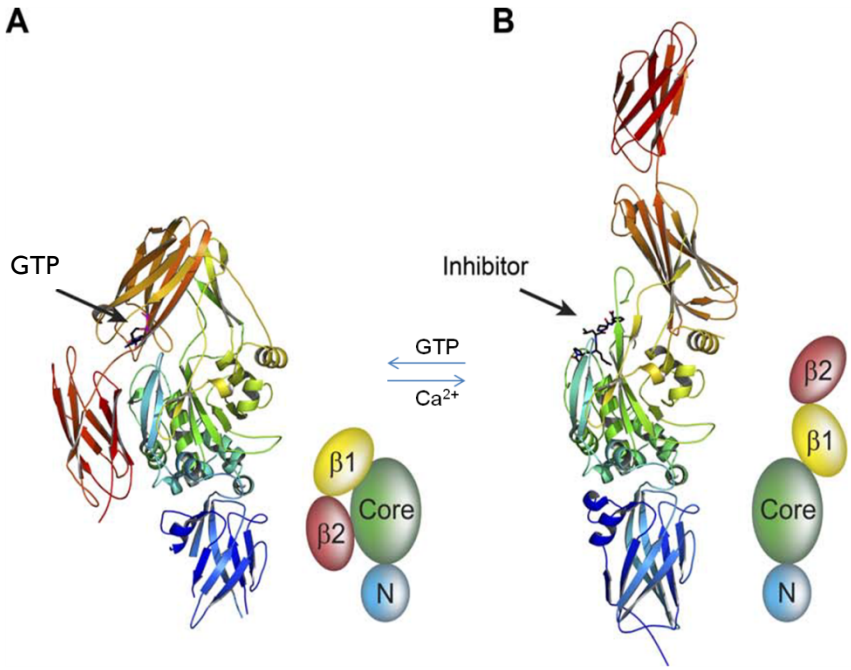

Fig. 1.3 Crystal structures of GDP-bound and inhibitor-bound TG2. The N-terminal β-sandwich is shown in blue (N), the catalytic domain (core) in green, and the C-terminal β-barrels (β1 and β2) in yellow and red, respectively. (A) GDP-bound TG2. (B) TG2 inhibited with the active-site inhibitor Ac-P(DON)LPF-NH_2 (adapted from Pinkas et al. 2007).

The transamidating and GTPase activities of this protein are mutually exclusive: Ca^{2+} bound TG2 has no GTPase activity, whereas GTP-bound TG2 does not exhibit transamidase activity (Feng et al. 1999).

As a transamidase, in addition to crosslinking proteins in a Ca^{2+} dependent manner, TG2 can modify proteins by amine incorporation and site-specific deamidation. In addition, when externalized from cells, it can non-covalently bind to integrins, fibronectin and other proteins of the extracellular matrix to modulate cell-matrix interactions (Fesus & Piacentini, 2002; Stephens et al., 2004).

A large number of substrates have been identified in intracellular compartments, including the cytosol, nucleus and mitochondria, as well as on the cell surface and in the extracellular matrix (Csosz et al., 2008). Hence, the enzyme can have a variety of functions dependent on the local context.

1.4.3 TG2 in pathological processes

The importance of studying the pleiotropic functions of transglutaminases emerged from the understanding that deficiency or aberrant activity of these enzymes has a major contribution to the pathophysiology of blood and skin disorders and in various inflammatory, autoimmune and degenerative diseases (Iismaa et al., 2009).

Upregulation or aberrant activity of TG2 has been linked with a number of different diseases. The enzyme has been implicated in various pathological states including cancer, atherosclerosis, fibrosis, neurodegenerative disorders as Alzheimer's, Parkinson's and Huntington's disease and various autoimmune conditions including diabetes (Lesort et al., 2000; Porzio et al., 2007). The common factor being a role of TG2 in the altered inflammatory responses associated with these conditions. The most convincing evidence has been accumulated to suggest a major role of TG2 in coeliac disease (Dieterich et al., 1997). This will be discussed in detail in section 1.8.2.

1.5 Transglutaminase 3

Transglutaminase 3 (TG3), also known as epidermal transglutaminase, is an enzyme encoded by TGM3 on human chromosome 20q11-12. TG3 is an unusual member of the TG family in that this protein is synthesized as an inactive ≈77kDa zymogen that is proteolytically activated by cathepsin-L to become an active 50/27kDa complex (Iismaa et al., 2009). The zymogen consists of four folded domains that share a common structure with other TGs. Activation of the zymogen requires cleavage at Ser469, located in a hinge region that separates the catalytic core and β-barrel 1 domains. The resulting 50/27kDa fragments remain associated together in the active enzyme (Ahvazi et al. 2002).

The crystal structure of TG3 has been solved in the presence of Ca^{2+} (Ahvazi et al., 2002). The acquired data revealed that the presence of 3 Ca^{2+}ions is required for enzyme activity (Fig. 1.4). The first Ca^{2+}-binding site

seems to be constantly occupied and this Ca^{2+} ion cannot be removed without protein denaturation. Although this binding site is crucial for TG3 activity it is not sufficient. The remaining two Ca^{2+}-binding sites are unsealed by cleavage of the zymogen. Occupation of the second Ca^{2+} binding site prompts a small structural change, however, it is the binding of the third Ca^{2+} ion that mediates the crucial conformational change and full enzyme activation. This allows for exposure of residues Trp236 and Trp327, involved in stabilization of TGs active site.

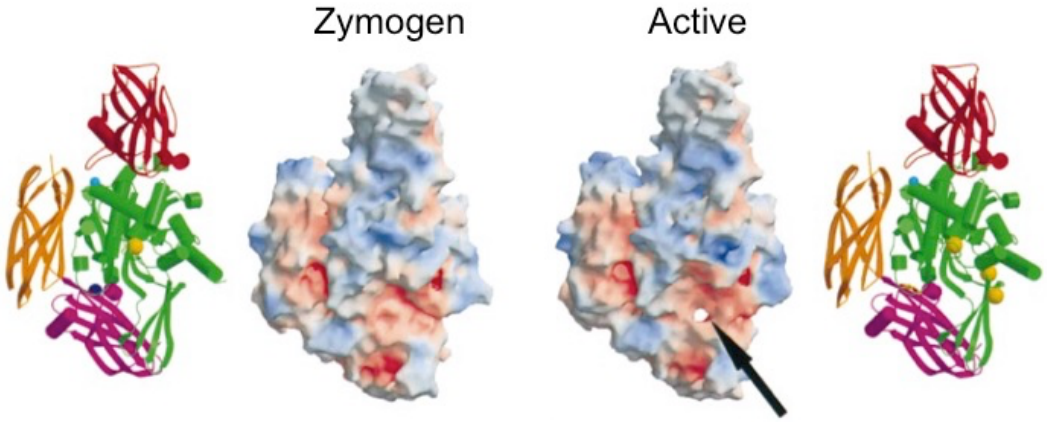

Fig. 1.4 Structural comparison of TG3 zymogen and active form. The electrostatic surface potential maps are shown in the centre. The acidic regions are coloured red and the basic regions in blue. Calcium ions are shown as yellow spheres. The arrow indicates a channel that opens after binding of a Ca^{2+} in site 3. On the left and right are secondary structure images of the zymogen and activated TG3 in the same orientations (retrieved from Ahvazi et al. 2003).

Similarly to TG2, TG3 has been reported to interact with guanine nucleotides (Ahvazi et al., 2004). TG3-GTP binding is associated with substitution of Ca^{2+} with Mg^{2+} at the third calcium-binding site. This binding causes a conformation change that culminates in enzyme inactivation through closing of the active site channel. Subsequent hydrolysis of the bound GTP and nucleotide dissociation results in a reversion of the enzyme to the active state. Calcium-activated TG3 is inhibited by GTP at low μM concentrations.

TG3 functions involve the cross-linking of trichohyalin and keratin intermediate filaments to harden the inner root sheath, which is critical for

hair fibre morphogenesis and the assembly of the cornified envelope of the stratum corneum in terminally differentiated keratinocytes (Beninati & Piacentini, 2004). It is also known that TG3 knockout mice display no obvious defect in skin development, and no evident changes in barrier function or ability to heal wounds, as TG3 is compensated-for by other TG family members. On the other hand $TG3^{-/-}$ mice present thinner hair with major alterations in the cuticle cells and hair protein cross-linking markedly decreased, suggesting that without TG3 expression, the hair cuticular cells are directly compromised (John et al., 2012).

TG3 has been implicated in the gluten-sensitivity related disorder Dermatitis Herpetiformis (Sárdy et al., 2002; Stamnaes et al., 2010) and this will be covered in section 1.8.3.

1.6 Transglutaminase 6

Transglutaminase 6 (TG6) is an enzyme encoded by the TGM6 gene on human chromosome 20q11, located in the same gene cluster with TGM3 and in close proximity to TGM2 (Grenard et al. 2001). TG6 has a molecular mass of ≈79kDa. Not much is yet known about this protein. Its close relationship with TG2 led to speculation that they could have comparable properties, in terms of activities and regulation by Ca^{2+} ions and nucleotides Fig. 1.5 (H. Thomas et al., 2013).

TG6 is widely expressed in murine brain tissue such as cerebral cortex, olfactory lobe, cerebellum and also the spinal cord (H. Thomas et al., 2013). The expression pattern during central nervous system (CNS) development in the cortical plate suggests its involvement in neuronal differentiation (H. Thomas et al., 2013). A comprehensive study of TG6 in the central nervous system of adult mice showed robust expression of this enzyme in brain regions involved in locomotive control. In the cerebellum, neurons expressing TG6 were present in both the cerebellar cortex and nuclei. TG6 is also expressed in Purkinje cells, which are the only neurons responsible for sending output from the cortex (Liu et al., 2013).

The physiological role of TG6 at the molecular level in the CNS remains to be elucidated. However, TGM6 has been reported to be the causative gene for a form of spinocerebellar ataxia (SCA 35) (Wang et al., 2010), and TG6 importance has been highlighted by the original identification of its involvement in autoimmune ataxia (Hadjivassiliou et al., 2008).

Fig. 1.5 Model of the structure of full-length human TG6. The overall structure modelled based on the calcium activated TG3 structure. Cylinders and arrows denote α-helical and β-strand conformations, respectively. The four domains (β sandwich, catalytic core, β-barrel 1, β-barrel 2) are depicted in different colours. The position of three bound calcium ions is shown by yellow spheres (retrieved from Thomas et al. 2013).

TG6 has specifically been implicated in gluten ataxia pathophysiology (Hadjivassiliou et al. 2008). This topic is going to be discussed in detail below.

1.7 Gluten

The development of agriculture about 10,000 years ago led to major changes in the composition of human diet. One of those changes was the

introduction of gluten-containing cereal such as wheat, barley and rye, as a major component of daily food intake. These form the basis of a variety of flour and other cereal-based food products consumed throughout the world (Anna Sapone et al., 2011). The introduction of these cereals in human diet created the conditions for the advent of human diseases related to gluten exposure.

Gluten was one of the initial protein fractions described by chemists, being described for the first time by Beccari in 1728 (see translation by Bailey 1941).

Gluten is the main structural protein complex formed by the prolamins gliadin and glutenin and is present in the starchy endosperm cells of wheat grain (Shewry et al. 2002). Gliadin is an alcohol-soluble monomeric component with a molecular weight between 30 and 60kDa. Glutenin is a large alcohol-insoluble complex stabilized by disulphide and noncovalent bonds (Rubin et al. 1992).

These proteins are rich in the amino acids proline (~15%) and glutamine (~35%), which give them distinctive features that contribute to their immunogenic properties. The high proline content makes gluten resistant to proteolytic degradation within the gastrointestinal tract, as the human body lacks gastric and pancreatic enzymes with post-proline cleaving activity. The high glutamine content makes gluten a good substrate for TG2 (Stepniak & Koning, 2006). As a result, immunogenic/immunotoxic peptides accumulate and are transported by retrotranscytosis across the intestinal epithelium where they initiate a detrimental adaptive and innate immune response in genetically susceptible individuals (Iismaa et al., 2009).

1.8 Gluten-related disorders

Gluten-related disorders (GRD), which affect 1-2% of the general population, are a group of immune-mediated diseases with diverse manifestations, caused by dietary exposure to wheat gluten, or related protein from barley and rye. As wheat is an ingredient used in many food products, exposure to relatively large amounts of gluten starts very early in

life. Gluten is introduced into the diet as early as 6 months of age, with a child of 12 months typically eating between 6 and 9 g of gluten daily (Koning et al. 2005).

Symptoms of gluten-related disorders usually disappear with a gluten-free diet (GFD) and reoccur with gluten ingestion. The best known GRD is coeliac disease (CD), however there are others that may not involve gastrointestinal manifestations, such as gluten ataxia and dermatitis herpetiformis (Iismaa et al., 2009)

1.8.1 Wheat allergy

Wheat allergy (WA) is a type I hypersensitivity immunologic reaction to wheat proteins. It occurs in individuals previously sensitized to the allergen gluten (A. Sapone et al., 2012).

IgE antibodies have a strong predisposition to bind to mast cells and basophils, which possess high-affinity receptors for the Fc-portion of IgE. When a mast cell or a basophile containing cytophilic IgE antibodies is re-exposed to gluten, a multivalent binding of the antigen to more than one IgE molecule causes the cross-linkage of adjacent IgE antibodies. This leads to the aggregation of the cytoplasmic portion of the IgE Fc-receptor complexes and consequently, activation of signal transduction pathways (Cotran et al. 1999). This triggers a release of primary and secondary mediators, such as histamine or pro-inflammatory cytokines and will lead to the typical symptoms of an acute allergic reaction. IgE mediated allergy to wheat may be presented with various severity from simple urticaria to anaphylaxis (Lee et al., 2013)

Wheat allergy is common among bakers and is commonly known as Baker's Asthma. It affects 4% to 10% of bakery workers in European countries as they are constantly exposed to this allergen, present in wheat, rye and soybean flour. Symptoms among this group are usually asthma and allergic rhinitis (Sander et al., 2011).

1.8.2 Coeliac disease

Coeliac disease (CD), also known as gluten sensitive enteropathy, is one of the most common gluten-related disorders, and affects approximately 1% of the general population. CD is a type IV hypersensitivity, initiated by the ingestion of gluten and related proteins, and is characterized by an increased permeability in the small intestine, allowing for enhanced passage of antigens and the activation of an innate and adaptive immune responses, in susceptible individuals (Koning et al., 2005). Typical symptoms include chronic diarrhoea, fatigue and weight loss, associated with a lesion in the upper small intestine, characterized by villous atrophy, crypt hyperplasia, increased number of intraepithelial lymphocytes and a chronic inflammatory response driven by the lamina propria lymphocytes. These symptoms usually disappear when the patient starts a gluten-free diet (GFD), as the $CD4^+$ T cell response driving the disease process is gluten-dependent. When there is no response to a GFD, a condition called refractory coeliac disease (RCD) may have been developed (Hadjivassiliou et al., 2010).

RCD should be considered when all other causes for failure to improve on a gluten-free diet have been excluded. It is defined as having the classical symptoms and small intestinal inflammation that persist after one year on a strict GFD. Histological findings consist of raised intraepithelial lymphocytes and crypt hyperplasia, with progression of the inflammation to villous atrophy. Symptoms of RCD are similar to the ones observed in CD: diarrhoea, malabsorption and weight loss as well as vitamin and mineral deficiencies (Ludvigsson et al., 2012). RCD is divided into two types, based on special studies of flow cytometric analysis of lymphocytes performed on small intestinal biopsies (Semrad, 2008). Type I is characterized by a normal T-cell population spread along the intestinal lining, usually with good response to treatment with steroids or azathioprine and a good prognosis. Type II presents with abnormal T-cell population spread along the intestinal lining. It has a poor response to steroid treatment, often requiring intravenous nutrition. Individuals with Type II RCD have a high risk of developing T-cell lymphoma.

1.8.2.1 The genetics of coeliac disease

CD is an autoimmune disease that has genetic, environmental and immunological components (Vader et al., 2002). A high prevalence among first-degree relatives of CD patients indicates that the susceptibility to develop CD is strongly influenced by inherited factors. The genetic influence in CD is also supported by a high concordance rate (75%) in monozygotic twins (Koning et al., 2005).

It is known that CD, as well as other GRD, is strongly associated with specific human leukocyte antigen (HLA) genes. About 95% of CD patients are positive for HLA-DQ2.5 (DQA1*05,DQB1*02) encoded in *cis* or *trans* with the remaining 5% carrying HLA-DQ8 (DQA1*03,DQB1*0302) (Fig. 1.6) (Sapone et al., 2012; Sollid & Jabri, 2011). Individuals that carry these genes have a relative risk of disease development increased by 30-fold when compared to HLA-association seen in many other auto-immune diseases such as type I diabetes or rheumatoid arthritis (Koning et al., 2005).

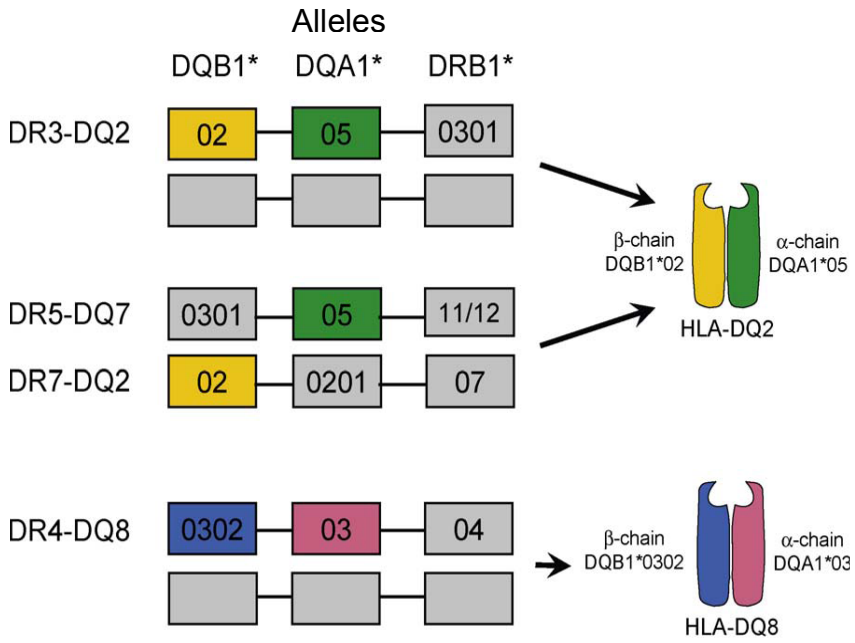

Fig. 1.6 HLA gene association in coeliac disease. The majority of CD patients express the HLA-DQ2 heterodimer encoded by DQA1*05 and DQB1*02 genes, either in cis (top row) or trans (bottom row). The remaining patients that are DQ2-negative express DQ8 encoded on the DR4-DQ8 haplotype (retrieved from Qiao et al. 2009).

In CD, HLA of a specific type is an indispensable, but not sufficient factor for disease development, and most individuals who express these genes will never develop CD (Sollid & Jabri, 2011). HLA-genes contribute about 40% of genetic load but other genes are involved in the pathology of the disease. The involvement of non-HLA genes in CD is yet to be understood. About 40 other genes have been shown to confer a small amount of risk each, but these are not shown among CD patients and therefore this does not explain disease heritability (Mistry et al., 2015).

Although HLA genes are specific for CD, non-HLA genes contribute more to the genetic background of CD than HLA genes. Each non-HLA gene adds only a modest contribution to disease development (Sollid, 2002). Risk variants for CD have been found in the 4q27 region harbouring IL2 and IL21 genes (van Heel et al., 2007). IL-2 is a cytokine secreted by antigen-stimulated T-cells and is involved in T-cell activation and proliferation. IL-21, another T-cell derived cytokine, enhances B-cell, T-cell, and natural killer cell proliferation and IFN-γ production. They are both implicated in the mechanism of other autoimmune diseases, such as type 1 diabetes and rheumatoid arthritis, suggesting that this region can represent a general autoimmune disease risk locus (Catassi & Fasano, 2008).

The region that has been linked most consistently to CD is on the long arm of chromosome 5 (5q31–33) (Greco et al., 2001). This region is rich in possible candidates for susceptibility genes, including the Th2 cytokine cluster, which is related to Crohn's disease, the lipopolysaccharide receptor gene CD14; Tmp1, which controls interleukin-12 (IL-12) responsiveness, IL12B, which is implicated in type-1 diabetes and *Tim*, which is implicated in asthma (Sollid, 2002). In fact, most of the genes now implicated in CD identified by the Genome Wide Association Studies have a role in modulating the immune response (Mistry et al., 2015).

1.8.2.2 Pathomechanisms of coeliac disease

For most dietary proteins, it is true that they are broken down into small, non-immunogenic fragments by proteases in the intestinal lumen.

However, the gluten protein gliadin is highly resistant to luminal and brush-border proteolysis, and large fragments remain intact after digestion, such as the 33mer peptide derived from α-gliadin that is the major T-cell epitope in CD (Stamnaes et al., 2010). This is due to its high content of proline residues.

The physiological role of the HLA-system is to present peptide fragments of antigens to T-cells. HLA-DQ2 and HLA-DQ8 molecules could confer susceptibility to CD by presenting gluten peptides to specific $CD4^+$ T cells in the intestinal mucosa. In fact, Halstensen and colleagues reported that *in vitro* stimulation of small-intestine biopsies with gluten results in the activation of $CD4^+$ lamina-propria T cells in biopsies of treated individuals who have coeliac disease, but not in controls (Halstensen et al. 1993).

Both HLA molecules have a preference for peptides with negatively charged amino acids at multiple anchor positions. However, the negatively charged anchor residues are differentially located along the binding grooves of the two MHC molecules (Fig. 1.7). HLA-DQ2.5 favours negatively charged residues at positions P4, P6 and P7 (Johansen et al. 1996) whereas DQ8 prefers negatively charged residues at positions P1 and P9 (Godkin et al., 1997). Hence, different peptides are immunodominant epitopes in individuals carrying the respective HLA's.

This binding is highly specific and it is the ability to form stable peptide-MHC complexes that appears to be a key factor for the *in vivo* generation of T-cell responses and development of coeliac disease (Sollid & Jabri, 2011).

Interestingly, gluten proteins normally contain few negatively charged residues. Reports that coeliac derived T-cells primarily recognize deamidated gluten peptides, brought TG2 into the context of the disease (Sjöström et al., 1998). TG2 is known to catalyse a deamidation reaction in the absence of a second donor substrate. It has also been reported that the ratio of deamidation to transamidation, in the presence of primary amines, is markedly increased at a pH below 7.3 (Fleckenstein et al., 2002). With duodenum pH being ≈6 (Fallingborg, 1999) it is possible that deamidation of gluten peptides in the gut is mediated by TG2. Furthermore, TG2 expression

was also shown to be increased in active coeliac disease, which may lead to enhanced deamidation of gluten peptides (Molberg et al., 1998).

As mentioned, gluten peptides are ingested as part of a normal diet and survive small bowel digestion because of their high content of proline and glutamine residues. This also makes gluten peptides preferable targets for TG2.

Gluten peptide deamidation by TG2 is highly sequence context specific. The glutamine residue (Q) is not a target of the enzyme in the sequences QP and QXXP but can be modified in the sequence QXP (Vader et al., 2002). Selective modification of glutamine by TG2 can result in the generation of a large repertoire of gluten peptides that can bind to HLA-DQ2 or HLA-DQ8 and stimulate T cells in the intestine of CD patients. In fact, the sequence specificity of TG2 is reflected in the bias of T-cell epitopes that have been linked to coeliac disease (Stamnaes et al., 2010).

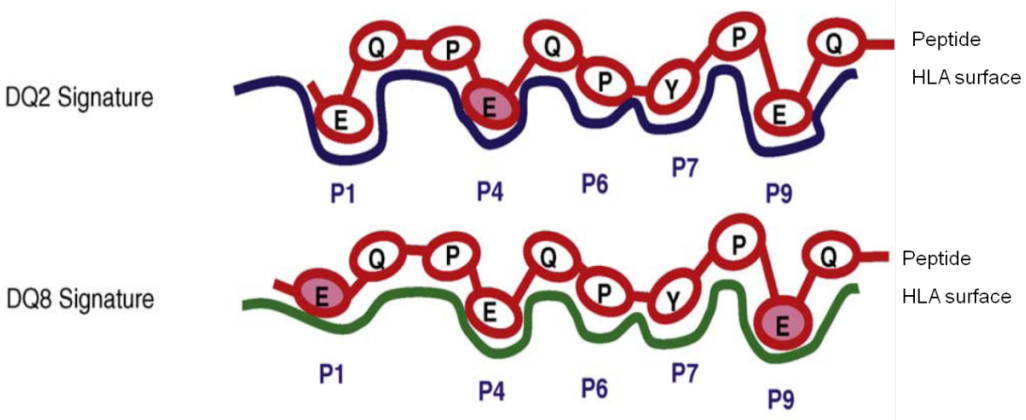

Fig. 1.7 Peptide binding signatures of DQ2 and DQ8 molecules. The DQ2 and DQ8 epitopes recognized by lesion derived T cells of CD patients share the same 9 amino acid core sequence. This sequence contains three glutamate residues formed by TG2-mediated deamidation in positions P1, P4 and P9. DQ2 prefers negatively charged glutamate residue in P4 whereas DQ8 prefers glutamate in P1 and P9 (adapted from Qiao et al. 2009).

The hallmark of coeliac disease is the presence of antibodies reactive to TG2 (autoantigen) in addition to antibodies reactive to gluten (Dieterich et al., 1997). Both anti-TG2 and anti-gluten antibodies disappear once coeliac patients commence a strict gluten-free diet and reappear upon gluten challenge. Hence, production of autoantibodies is gluten driven.

Antibodies are produced by plasma cells, which differentiate from B cells after recognition of antigen by the B-cell receptor (BCR). On average, 10% of plasma cells in the coeliac lesion are specific for TG2 (Roberto Di Niro et al., 2012). Such a response to a single target is highly unusual. However, the mechanism by which production of antibodies against the self-protein TG2, in response to exposure to a foreign antigen still remains to be elucidated. It has been proposed that production of TG2 reactive antibodies is related to T-cell help to TG2-specific B cells by gluten-specific T cells (Fig. 1.8) (Sollid et al. 1997).

It is possible that TG2 forms stable complexes with gluten peptides, either through crosslinking or as a reaction intermediate (Stamnaes et al., 2010). These complexes could be bound by surface immunoglobulins on TG2-specific B cells and subsequently internalized. Deamidated gluten peptides could then be presented in the context of HLA-DQ2 or HLA-DQ8 to gluten-reactive T-cells. T-cells would then become activated, and TG2-specific B-cells could receive cognate help from gluten-specific T cells, leading to production of anti-TG2 antibodies. The interaction between T cells and B cells not only gives rise to antibodies, but also amplifies the anti-gluten T-cell response. It has been shown that monoclonal anti-TG2 antibodies recognize the N-terminal part of the enzyme. (Stamnaes et al. 2015). As lysine residues of TG2 involved in isopeptide bonds are mainly present in the C-terminal part of TG2, the N-terminal part of the enzyme is free to bind to TG2-reactive antibodies. Furthermore, there is evidence that complexes of gluten-TG2 can be bound by TG2-specific BCRs, internalized and processed, thereby releasing the covalently linked gluten T- cell epitopes for MHC class II presentation to T cells (Roberto Di Niro et al., 2012; Jorunn Stamnaes et al., 2015). However, evidence that these events take place *in vivo* is still lacking.

TG2-gluten peptide complexes may also activate DQ2 or DQ8 restricted T-helper cells that proliferate and produce mainly Th1-type cytokines, such as interferon-gamma (IFN-γ). The secretion of IFN-γ activates the release of enzymes that can damage the intestinal mucosa, with a loss of villous structure. Th1 cytokines will in turn lead to higher

expression of the HLA-DQ molecules and also TG2 and thereby, an increase in gluten peptide presentation, creating a chronic feedback loop driving the inflammatory process as long as gluten is introduced in the diet (Tjon et al. 2010).

When interacting with epithelial cells, macrophages and dendritic cells in the lamina propria, toxic gluten peptides provoke an innate immune response, up-regulating the expression of different mediators such as interleukin 15 (IL-15). This leads to a massive increase of intraepithelial lymphocytes and is ultimately responsible for the damage of the mucosal matrix (Ferretti et al. 2012; Shewry 2009). This later response is primarily responsible for villous destruction and hence generation of the flat mucosa, the hallmark of CD.

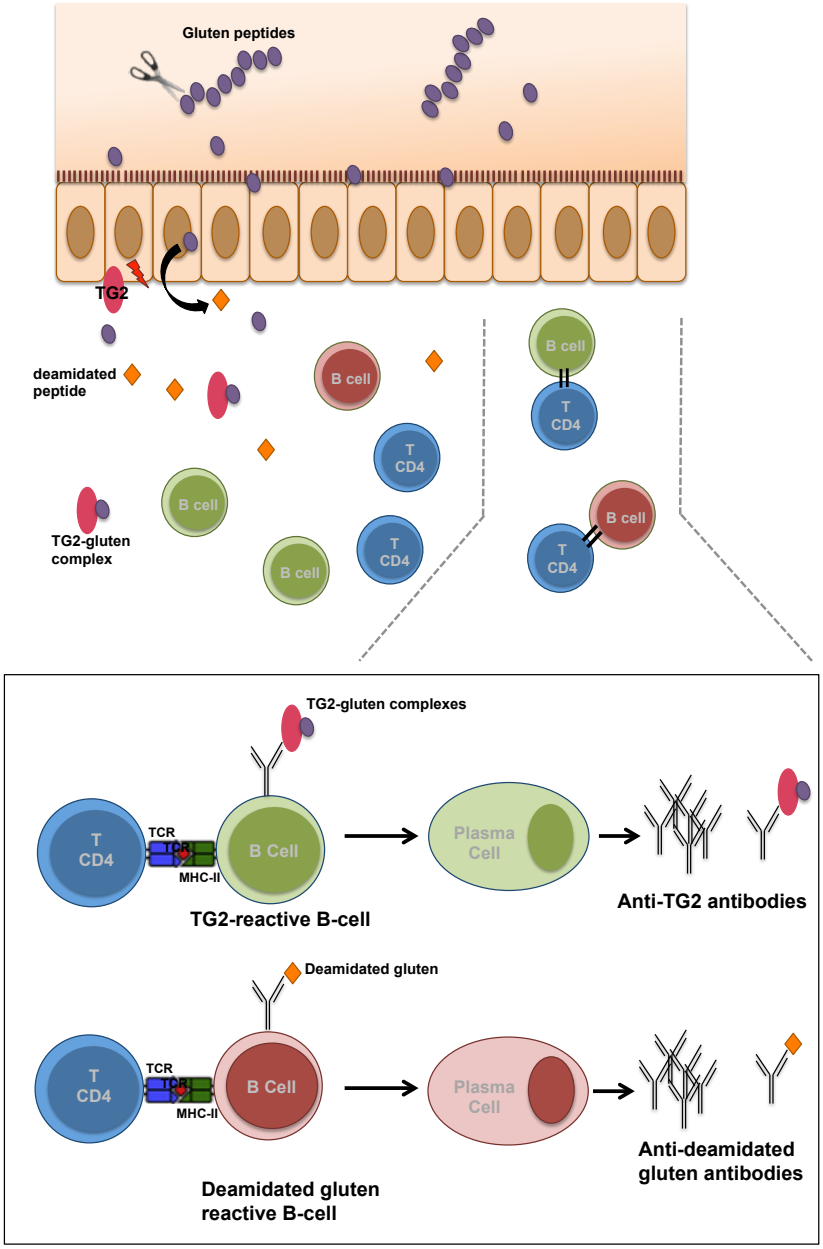

Fig. 1.8 Antibody production in the context of coeliac disease. Gluten-reactive $CD4^+$ T cells provide help to both TG2-reactive B-cells and (deamidated) gluten-reactive B-cells. TG2 forms stable complexes with gluten peptides. TG2-gluten complexes are internalized by TG2-reactive B-cells through BCR-mediated endocytosis. After internalization, (deamidated) gluten peptides in addition to TG2 derived peptides can be presented following breakdown of the complexes. Deamidated peptides can bind to MHC-II (HLA-DQ2 or HLA-DQ8) and be presented to T cells. Thereby, gluten-reactive T-cells provide help to TG2-reactive B-cells for subsequent production of antibodies against the self-protein. Interaction of gluten-reactive T-cells with gluten-reactive B-cell leads to production of antibodies against (deamidated) gluten peptides. (Adapted from Du Pre 2015)

1.8.2.3 Diagnosis and treatment

Diagnosis of CD cases by screening of the population is an important objective, since early institution of a GFD may prevent long-term sequels, such as osteoporosis, CNS disease, secondary autoimmunity, or even malignancy. A firm diagnosis of CD can only be established after a representative small intestinal biopsy, revealing a flat jejunal mucosa with absence of normal intestinal villi (Fig. 1.9).

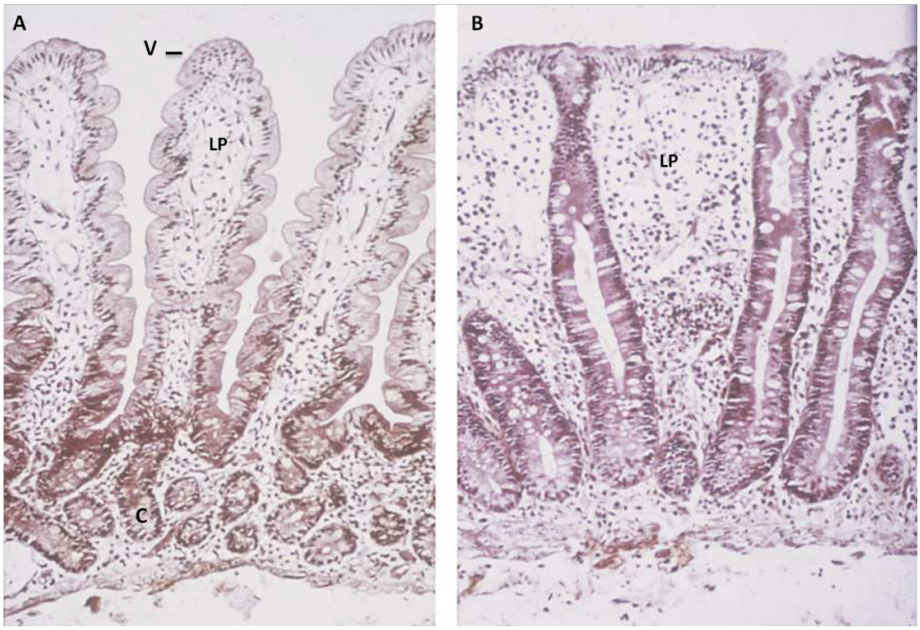

Fig. 1.9 Normal and coeliac-disease small-intestine mucosa. A - Histology of a normal small intestine showing villi (V) and crypts (C). B - The coeliac mucosa is characterized by villous atrophy, enlarged hyperplastic crypts and increased infiltration of lymphoid cells in the lamina propria (LP) and epithelium (adapted from Sollid 2002).

Histological examination further demonstrates a cellular infiltration of the lamina propria by plasma cells and lymphocytes. Small intestinal changes can vary from a nearly normal mucosa with increased intra-epithelial lymphocytes to a completely flat mucosa, depending on the stage of disease and amount of gluten consumption (Catassi & Fasano, 2008).

The diagnosis of CD should not depend only on intestinal biopsy, but also on the clinical features, genetic profile and serology of the patient. The availability of highly accurate serologic tests, developed after identification of

TG2 as the autoantigen in CD, greatly facilitates the diagnosis of this disease. Most patients were initially tested for conventional IgA and IgG anti-gliadin (AGA) antibodies and IgA anti-endomysium antibodies (EMA). Anti-gliadin antibodies are not disease-specific and are frequently found in the normal population. With the identification of TG2 as the target CD autoantigen recognised by EMA, the development of easy to perform and observer-independent ELISA tests has also become possible (Koning et al., 2005).

CD-specific antibodies comprise auto-antibodies against TG2, including endomysial antibodies (EMA), and antibodies against deamidated forms of gliadin peptides (DGP). A test for CD-specific antibodies is the first tool that is used to identify individuals for further investigation to diagnose or to rule out CD.

It is now recommended that the initial test be IgA class anti-TG2 from a blood sample. If total serum IgA is not known, then this also should be measured. In subjects with either primary or secondary humoral IgA deficiency, at least 1 additional test measuring IgG class CD-specific antibodies should be done (IgG anti-TG2, IgG anti-DGP or IgG EMA, or blended kits for both IgA and IgG antibodies) (Husby et al., 2012).

Tests measuring antibodies against DGP may be used as additional tests in patients who are negative for other CD-specific antibodies but in whom clinical symptoms raise a strong suspicion of CD. Tests for the detection of IgG or IgA antibodies against native gliadin peptides (conventional gliadin antibody test) should not be used for CD, as they lack specificity (Husby et al., 2012).

Currently there is no known cure for CD. However, most of the patients show substantial improvement when subjected to a GFD, and can live a relatively normal, symptom-free life.

1.8.3 Dermatitis herpetiformis

Dermatitis herpetiformis (DH) is an autoimmune disease that was first described by Louis Duhring in 1884 (Duhring, 1884). It may be present at any

age but generally begins between the ages of 15-40. Its prevalence is thought to be about 1/10,000 in the UK (Fry, 1995).

DH presents with skin pruritic polymorphic lesions mainly distributed in typical areas such elbows, forearms, buttocks, knees and scalp (Bolotin & Petronic-Rosic, 2011a). Histologically, the disease is characterized by subepidermal blistering and accumulation of neutrophils at the dermal papillae, while the most common immunological finding consists of granular IgA deposits along the basement membrane, mainly localized in the dermal papillae (Bolotin & Petronic-Rosic, 2011b).

Patients with DH produce two IgA antibody populations against TG3. The first binds TG3 exclusively, whereas the second cross-reacts between TG3 and TG2. However, only TG3 seems to colocalize with skin IgA deposits found in DH patients, suggesting that TG3 rather than TG2 is the primary autoantigen in this disease (Sárdy et al. 2002). A more recent study, further demonstrates that detection of IgA antibodies against TG3 is a highly sensitive test for the primary diagnosis of DH (Rose et al., 2009).

DH is a multifactorial disease and its pathogenesis involves environmental, genetic and autoimmune factors. Genetically, patients presenting with DH show the same high prevalence of HLA-DQ2 and DQ8 haplotypes as CD (Spurkland et al., 1997).

A potential explanation for the pathological mechanism of DH is that in susceptible individuals the development of skin lesions is related to an active chronic bowel inflammation as a result of persistent gluten consumption (Bonciani et al., 2012). This initially leads to a local immune response and the production of mucosal IgA in the bowel. Circulating IgA (anti-TG3) binds to the skin. The immune response in the small intestine results in increased levels of circulating cytokines, which may partially activate neutrophils as well as T-cells and endothelial cells. Exposure to UVB light and microtrauma to the skin increase local cytokines production, leading to the release of neutrophils, deposition of IgA at the dermo-epidermal junction, and thus to the development of DH skin lesions (Bonciani et al., 2012). A mouse model has indeed shown that circulation derived antibodies can recapitulate the blistering condition in transplanted skin (Zone et al., 2011).

Similar to CD, DH symptoms usually disappear once the patient starts a gluten-free diet.

1.8.4 Gluten Ataxia

Neurological disorders have only recently been recognised as potential presenting manifestations of coeliac disease. They have been reported to occur with a frequency of up to 10% in coeliac disease patients (Lagerqvist et al. 2001). Gluten ataxia (GA) is one of the most common neurological manifestations in the context of gluten-sensitivity, with a prevalence of about 35% (Hadjivassiliou et al., 1998)

The presence of an enteropathy in gluten-related neurological disorders is not a requirement. In fact, the majority of patients with GA do not have overt gastrointestinal symptoms and only a third of patients with GA will have evidence of enteropathy on biopsy. (Hadjivassiliou, 2003)

GA is the most common and potentially treatable type of cerebellar ataxia. It usually presents as pure cerebellar ataxia, with gaze-evoked nystagmus and other ocular signs of cerebellar dysfunction also commonly observed (Hadjivassiliou et al., 2010). The majority of GA patients express the HLA-DQ2 or DQ8 genes (Hadjivassiliou, 2003)

Just like TG2 in a CD intestine and TG3 in a DH skin, TG6 was discovered to be the primary autoantigen in the CNS in GA (Hadjivassiliou et al., 2008, 2013). TG6 shares genetic, structural and enzymatic properties with TG2 and TG3. In fact, it has been shown that TG6 can catalyse the reactions that drive T and B cells responses (Stamnaes et al., 2010).

TG6 is a transglutaminase primarily expressed in neural tissue (H. Thomas et al., 2013). Furthermore, extensive deposition of TG6 has been found to colocalize with perivascular IgA deposits around brain vessels in post-mortem examination of a GA patient, suggesting that deposition of characteristic antibody complexes could involve targeting of TG6 (Hadjivassiliou et al., 2008). It is also known that patients with GA have an immunological response (autoantibodies) primarily directed against TG6 even in the absence of enteropathy (Hadjivassiliou et al., 2008).

Furthermore, this disease may also be associated with antibody cross-reactivity between antigenic epitopes on Purkinje cells and gluten proteins (Hadjivassiliou et al., 2010).

The observed IgA deposits indicate that vasculature-centred inflammation may compromise the blood-brain barrier, allowing persistent exposure of the CNS to the gluten-related pathogenic antibodies, and therefore, may be the trigger of nervous system involvement (Hadjivassiliou et al. 2008). Evidence supporting that such antibodies may potentially be pathogenic comes from experiments in mice. Boscolo and colleagues demonstrated that sera from a patient suffering from a gluten-related disorder, contain antibodies capable of causing ataxia when transferred into the central nervous system of mice (Boscolo et al., 2007, 2010). As recombinant TG-specific scFv 'antibodies' that lack the Fc region lead to a loss of motor function, this implicated an scFv-antigen interaction rather than Fc receptor-triggered immune response in the disease process. The risk of developing neuronal damage could also be related, at least in part, to the presence of anti-TG2 antibodies in the cerebrospinal fluid. Indeed, in some GA patients, intrathecal anti-TG2 antibody production has been detected (Boscolo et al., 2007). Even though anti-TG2 antibodies are able to cause dramatic effects in mice, they are not sufficient to explain the diverse neurological conditions associated with gluten sensitivity, and why only a fraction of CD patients are affected. In line with this, results obtained using serum from a GA patient suggest the presence of additional anti-neural antibodies that may be involved in ataxia, as this patient had no circulating anti-TG2 antibodies (Boscolo et al., 2007). This neural reactivity has been linked to the presence of antibodies reacting with TG6 (Boscolo et al., 2010).

One of the critical differences between GA and CD/DH is that, even though GA patients also seem to respond to a GFD (Hadjivassiliou et al. 2003), the brain has a limited potential to regenerate, unlike the skin and the gastrointestinal epithelium. Thus, the degree of permanent functional deficit will depend on the amount of Purkinje cell loss sustained by the cerebellum by the time gluten is eliminated form the diet (Hadjivassiliou et al. 2003). An

early identification of these patients is therefore essential, as they will suffer from irreversible damage to the neural tissue.

1.9 The aims of the project

The variation in manifestation of gluten-related disorders indicates that the immune system reacts to gliadin in different ways. This could be due to the genetic background in the individuals affected. Of all the GRD, CD is the only one with a clear understanding of the pathological mechanism. However, it is also crucial to improve the understanding of the pathophysiology of extraintestinal disease including DH and GA in order to develop appropriate diagnostic protocols and potential strategies for therapy beyond GFD.

In this project, I aim to develop a mechanistic understanding of autoantibody development and extraintestinal disease manifestations.

Within this context, I intend to answer the following main question: Does autoantibody development to TG6 occur in conjunction with that to TG2, i.e. in the gut, or does it have its origin in independent events?

Answering this question would widen our understanding of the pathomechanisms involved in gluten ataxia and could later be used in the development of novel therapies in the disease context.

Therefore, the following topics formed the basis for the research I have undertaken:

1. Are TG6-specific plasma cells developed at the level of the gut in GRD patients?
2. Investigate whether B-cells specific for TG6 and TG2 are present in the gut of all patients with GRD or restricted to patients with distinct manifestations, such as GA.
3. Identify what cells in the gut express TG6, i.e. is a specific subset of macrophages the source of TG6.

Chapter 2 Materials and Methods

2.1 Protein concentration determination

Protein concentration was derived from the absorbance reading at 280nm through spectrophotometric analysis (Beckman Coulter, DU 800), using the Beer-Lambert Law c=absorbance/(ε·d), where ε is the theoretical extinction coefficient of a specific protein (calculated using ProtParam software from ExPASy Bioinformatics Resource Portal) (Table 2.1) and d=cuvette diameter (d=1cm).

Table 2.1 Theoretical extinction coefficient used for calculation of protein concentration.

Protein	Theoretical extinction coefficient (ε) at Abs 0.1%
rhTG2	1.35cm^2/g
rhTG6	1.45 cm^2/g
Hemocyanin	1.39 cm^2/g

2.2 SDS polyacrylamide gel electrophoresis (SDS-PAGE)

Denaturing SDS-PAGE was performed using Novex 4-20% Tris-glycine polyacrylamide gels supplied by Invitrogen. Protein samples were mixed with an equal volume of 2x sample loading buffer comprised of 25mM Tris/HCl, pH 6.8, 39mM EDTA, 4% (w/v) SDS, 30% (v/v) glycerol, 0.3% (w/v) bromophenol blue and 2% (v/v) β-mercaptoethanol. Samples were boiled for 2min at 98°C and a specific amount of protein was loaded per lane along side a molecular weight standard - 30μg of Amersham Low Molecular Weight Marker (GE Healthcare). Electrophoresis was performed at a constant voltage of 125V/cm^2 and ~35mA for 2h. Running buffer was composed of 25mM Tris/HCl, pH 8.8, 192mM glycine and 0.1% w/v SDS.

2.3 Coomassie blue staining

Coomassie blue staining solution was prepared by adding 3g/L of Coomassie blue R-250 powder to a solution containing 10% v/v glacial acetic acid, 40% dH_2O and 50% (v/v) methanol. When described, SDS and Native gels were stained overnight with gentle agitation. Excess staining was removed by serial washes with a solution of 25% isopropanol and 10% acetic acid in dH_2O followed by serial washes with a solution of 10% isopropanol and 10% acetic acid in dH_2O.

2.4 Real-time fluorescence assay for determining transglutaminase isopeptidase activity

Transglutaminase enzymatic activity was determined by a real-time fluorescent assay previously developed by our group and described by Adamczyk et al., 2013. TG isopeptidase activity was quantified by measuring changes in fluorescent levels over time, resulting from the hydrolysis of an isopeptide bond of a quenched fluorescent probe, Abz-APE(γ-cad-Dnp)QEA λ max=418nm (A102; Zedira, Darmstadt, Germany). Reaction kinetics were captured at 37°C in black optical bottom 96-well plates (165305, Nunc) using a FLUOstar Optima or OMEGA plate reader (BMG LABTECH). The reaction was carried out in 100µl of assay buffer containing 50mM Tris/HCl, pH 7.5, 10mM glycine methylester, 100mM NaCl, 50µM Abz-APE(γ-cad-Dnp)QEA, 5mM DTT, and indicated concentration of TG2. For determining TG6 isopeptidase activity, glycine methylester and NaCl concentrations were raised to 50mM and 300mM, respectively. The pH adjustment to 7.5 was carried at 37°C.

Well-specific fluorescence was measured during 400s (10x 40s) and cleavage of the quenched substrate was triggered by automated injection of Ca^{2+} (2 or 10mM) at cycle 10. For control samples, 10µl of H_2O were injected instead of Ca^{2+}. Using a plate-mode protocol, fluorescence was measured using the 320ex nm excitation filter and the 440nm emission filter (top optics, gain set to 2450). Substrate conversion was measured for a 1h period and

fluorescent acquired every 40s (a total of 90 cycles). Well-specific fluorescence of the first 8 cycles was averaged and subtracted from the curves obtained after Ca^{2+}-injection. Control curves (no Ca^{2+} injection) were subtracted from the data to account for fluorescence bleaching and the final data was fitted using linear regression.

2.5 Statistical analysis

Data were analyzed using the GraphPad Prism® software version 7.0b or the IBM SPSS statistical software. The data presented corresponds to the mean ± standard deviation (SD). For contingency tables the χ^2 test was conducted. A p value of ≤0.05 was considered as significant.

2.6 Expression and purification of rhTG2

Recombinant human TG2 (rhTG2) was successfully expressed and purified using a modified protocol based on the methodology described by Hadjivassiliou et al, 2008. *Escherichia coli* BL21 was transformed with constructs containing native TG2 sequence with an added His_6-tag to the N-terminus that were already available within the group. *E.coli* transformed with the expression constructs was streaked onto Luria–Bertani-Agar (LB-Agar) plates containing 50μg/ml of ampicillin and grown overnight at 37°C. A single colony was selected and grown in baffled Erlenmeyer flasks, with LB broth containing 50μg/ml of ampicillin and incubated at 200rpm, 37°C to an optical density of 0.6 at 600nm. When the required optical density was reached, TG2 expression was induced by adding L-Rhamnose to a final concentration of 0.5% w/v. The suspension was incubated for 24h at 150rpm at 20°C. Bacteria were collected by centrifugation at 12128x g for 30min, at 4°C in a Sorvall centrifuge. Bacterial pellets were used or otherwise frozen at -20°C.

Bacterial pellet was resuspended in buffer A1 (50mM Na_2HPO_4, pH 8.0, 300mM NaCl) and cell lysis performed using three passages through a Stansted pressure cell homogenizer (Harlow, Essex, UK) at 1.2bar. The bacterial lysate was then diluted with A1 buffer to a final volume of 100ml and

cleared from insoluble material by ultracentrifugation at 47808x g for 30min, at 4°C using a Sorvall centrifuge. Protein was applied to a 5ml His-Trap HP column (GE healthcare) pre-equilibrated in buffer A1 at 4°C using a flow rate of 2ml/min. The resin was initially washed with buffer A1 until an A280 of 0.02, and then with 10% buffer B1 (50mM Na_2HPO_4, pH 8.0, 300mM NaCl, 300mM imidazole) before eluting TG2 with 50% buffer B1. Eluted material was diluted 3-fold with 20mM Tris/HCl, pH 7.2, 1mM EDTA and further purified by ion exchange chromatography using a HR10/10 column packed with Resource Q15 resin (GE healthcare) equilibrated in buffer A2 (20mM Tris/HCl, pH 7.2, 1mM EDTA, 100mM NaCl). TG2 was eluted as a single peak within a 20-column volume gradient of 0 to 60% buffer B2 (20mM Tris/HCl, pH 7.2, 1mM EDTA, 1M NaCl). Purified rhTG2 was stored at -20°C.

RhTG2 purity was analysed by SDS-PAGE followed by staining with Coomassie brilliant blue R.

2.7 Expression and purification of rhTG6

RhTG6 was expressed in *Spodoptera frugiperda*, SF9 insect cell line using a baculovirus expression system containing the human TG6 sequence with an added His_6-tag to the C-terminus.

Cells were expanded in Erlenmeyer flasks to a desired volume and cell density, infected with the virus and cultured for 96h. Cells were harvested using centrifugation at 190x g for 15min at 4°C. The supernatant was discarded and the cell pellet resuspended with lysis buffer and kept on ice. Cell lysis was performed using three passages through a Stansted pressure cell homogenizer (Harlow, Essex, UK) at 1bar, followed by ultracentrifugation at 47808x g for 30min at 4°C. Protein was incubated with 1ml of Ni^{2+}-Sepharose 6 Fast Flow resin (GE Healthcare) for 45min at 4°C on an orbital shaker. The suspension was centrifuged at 180x g for 7 minutes and supernatant removed. The resin was resuspended and washed in a series of specific buffers before being eluted in a buffer containing imidazole. Purified TG6 was buffer exchanged to 10mM Tris/HCl pH 7.8, 500mM NaCl, 10mg/ml sucrose using a pre-equilibrated PD10 desalting column containing 8.3mL of

Sephadex™ G-25 resin (GE Healthcare). Purified rhTG6 was lyophilized and stored at -20°C. Upon use, samples were reconstituted to the same original volume.

2.8 Chemical labeling of rhTG2, rhTG6 and hemocyanin (in solution)

TG2 was chemically labeled with commercially available fluorescent dye Atto-565 NHS ester or Atto-647N NHS ester (Cat. No: 72464 and 18373, Sigma Aldrich). Protein was buffer exchanged to 50mM Borate/NaOH, pH 8.5, 150mM NaCl or 0.1M Na_2HPO_4/NAH_2PO_4, pH 7.6 using a pre-equilibrated PD10 desalting column containing 8.3mL of Sephadex™ G-25 resin (GE Healthcare). Buffer exchanged TG2 (≈1mg) was added to the column and eluted by adding 1.5 column volumes of borate or sodium buffer while collecting 0.5ml fractions. Absorbance at 280nm for the different fractions was measured through spectrophotometry using a Beckman Coulter DU800 spectrophotometer. Fractions containing the highest concentration of protein were pooled and used for labeling process. The pooled protein working solution was ≈1mg/ml. Protein was incubated with or without 1mM GTP for 1min. Subsequently, a 3-fold or 10-fold molar excess of Atto-dye over protein was added and incubated for 2h at room temperature in the dark and with gentle agitation. Excess free dye was blocked by incubation with 1M ethanolamine for 15min. Labelled protein was separated from free label using the same desalting column, re-equilibrated in 10mM Tris/HCl, pH 7.4, 150mM NaCl. Labelled TG2 was eluted from the column by adding 1.5 column volumes of Tris-buffer while collecting 0.5ml fractions. Spectroscopic analysis of collected fractions was performed and fractions containing eluted labelled TG2 were pooled. The same labelling process was performed at 4°C with an increased incubation time to 4h, and blocking time to 1h.

Labelling of TG6 was initially carried out in solution as per TG2, however some adjustments had to be made to buffer conditions to keep TG6 in solution. Labelling buffer was composed of 0.1M Na_2HPO_4/NaH_2PO, pH 7.8, 500mM NaCl, and 10mg/ml sucrose. Protein was then buffer exchanged

as before to yield a protein solution for labelling of about 1mg/ml. Labelling was performed with a 3-fold molar excess of Atto-565 NHS ester over protein and in the presence of 5mM GTP. Labelled TG6 was eluted while returned to 10mM Tris/HCl, pH 7.8, 500mM NaCl and 20% glycerol.

Hemocyanin from *Limulus polyphemus* hemolymph was purchased from Sigma. Labelling of hemocyanin was performed, as per TG2, using the following modifications: hemocyanin (≈1mg) was labelled with Atto-565 NHS ester in 0.1M Na_2HPO_4/NAH_2PO_4, pH 7.6, in the presence of a 140-fold molar excess of dye over protein and no added GTP. The remaining steps of the labeling process were kept the same as for TG2. Use of labeled Hemocyanin is described in chapter 5. Labelled proteins were stored at -20°C until further use.

2.9 Chemical labelling of rhTG6 (in column)

RhTG6 was also labelled during purification. This was performed before the elution step of the Ni^{2+}-chelating column. TG6/sepharose slurry (≈1ml) was washed twice with a buffer containing 0.1M sodium phosphate, pH 7.8 and 300mM NaCl before being collected by centrifugation for 1min at 180x g. Total amount of TG6 present in the Ni^{2+}-slurry mixture was extrapolated from previous purification experiments and determined to be ≈500μg at ≈6.3μM. A 3 or 10-fold molar excess of Atto-565 dye over protein was used for labelling, which was added to the 1 or 2ml volume of slurry, respectively. Labelling was performed for 1h at room temperature, in the dark, with constant shaking. Purification of labelled TG6 was performed as per non-labelled TG6. Purified labelled TG6 was buffer exchanged to 10mM Tris pH 7.8 500mM NaCl, 10mg/ml sucrose using a PD10 column.

2.10 Labeled protein concentration determination

Final concentration of labeled proteins was estimated from standard curves generated from serial dilutions of Atto-565 or Atto-647N dyes. Both labelled proteins and a series of 2-fold dilutions of the relevant dye (Neat to

1:128) were subjected to spectrophotometric analysis. Atto-dye concentration in original solution was the same as that used for the correspondent labeling process. Absorbance at 280nm and 565nm or 647nm was measured, and respective standard curves created. The corrected absorbance value at 280nm of the labelled protein was estimated by calculating label molar concentration in the protein solution and subtracting the correspondent 280nm absorbance contribution. Final protein concentration was then calculated using the Beer-Lambert Law.

2.11 Protein concentration as determined by Bradford assay

Labeled protein concentration was also assessed by Bradford assay. Bradford protein assay was performed according to the protocol provided by the manufacturer (Bio-Rad, USA). In order to calculate protein concentrations, bovine serum albumin (BSA) was used as a standard (20 – 2000 μg/ml). 10μl of each standard and sample, as well as appropriate blanks, were placed into wells of a 96-well plate, to which 200μl of dye reagent solution/well was added. Dye reagent was obtained by diluting 1 part Dye Reagent Concentrate with 4 parts double distilled H_2O water before filtering through a Whatman grade 1 filter to remove particulates. The plate was sealed and agitated thoroughly for 30s, and incubated for 5min at room temperature. Absorbance was read at 590 nm using a plate reader. The standard curve for BSA was derived by linear regression and protein concentrations calculated from the standard curve.

2.12 Native polyacrylamide gel electrophoresis (Native-PAGE)

A native polyacrylamide gel electrophoreses was performed to analyse conformational changes in TG2 upon co-factor binding. Native-PAGE was undertaken using Novex 10% Tris-Glycine polyacrylamide gels supplied by Invitrogen (EC6078BOX). Where indicated, protein samples were incubated with 600μm of GTP for 1min prior to electrophoresis. Protein samples were mixed with an equal volume of 2x sample loading buffer

containing 200mM Tris/HCl pH 6.8, 30% glycerol, 0.2% w/v bromophenol blue and 20mM DTT to prevent sample oxidation. The gel running buffer comprised of 25mM Tris/HCl pH 7.8 and 192mM glycine. Where indicated, an additional 25μM GTP was added to the running buffer. The gel/chamber was placed in an ice-water bath and electrophoresis was carried out for 3 h at 100V/cm^2, 35 mA. The pH adjustment for all solutions was carried out at 4°C.

2.13 'In gel' incorporation of FITC-cadaverine by TG2

Native gels, pre-loaded with specified TG2 samples, were washed 3x 5min in TBS (20mM Tris/HCl, pH7.4 150mM NaCl), before overnight incubation at 37°C, with a solution containing 50mM MOPS/NaOH, pH6.5, 10mM $CaCl_2$, 1mM DTT and 100μM FITC-cadaverine (81504, ANASPEC). The following day, gels were extensively washed (≈10 changes of buffer) in TBS for 24h. FITC-cadaverine incorporation and other described fluorophores were visualized by scanning the gels with the Typhoon 9400 variable mode imager (GE Healthcare) using the following settings: for visualization of FITC, the 488nm blue laser line was used for excitation in combination with a 520nm band pass filter; for visualization of Atto-565 NHS ester the 532nm laser line was used together with a 560nm long pass filter; and for visualization of Atto-647N, the 633nm laser line was used together with a 670nm band pass filter. Photomultiplier tube voltage was set to obtain the best possible image without affecting the legitimacy of the results.

2.14 TG2 inhibition with active site-directed inhibitors

Two different TG2 site-directed irreversible inhibitors were purchased from Zedira, Germany: B003 (tert-Butyloxycarbonyl-(6-Diazo-5-oxonorleucinyl)-LGlutaminyl-L-Isoleucinyl-L-Valinmethylester) and Z006 (Benzyloxycarbonyl-(6-Diazo-5-oxonorleucinyl)-L-Valinyl-L-Prolinyl-L-Leucinmethylester).

TG2 (10μg) was mixed with a core solution containing 5mM $MgCl_2$ and 5mM Tris/HCl, pH 8.3, +/- 50μg N-Voy (supplied by Expedeon). Protein was incubated on ice until needed or incubated at 37°C for 30min. Additional TG2 samples were inhibited by incubating the protein at 37°C supplemented with 50μM B003 in 2 sequential steps of 30min. In the second step, 10mM $CaCl_2$ +/- 1mM putrescine were added. Samples were used as described. In a similar experiment, inhibition of TG2 was carried out as described, but this time no N-Voy was added and incubation of B003 was carried at 4°C.

In experiments using Z006, TG2 (10μg) was mixed with the same core solution as described above. Inhibition of the enzyme was achieved by incubating the protein at 4°C, supplemented with 50μM Z006 in 2 or 7 sequential steps of 30min. In the second step, 10mM $CaCl_2$ was added.

2.15 *In vitro* incorporation of FITC-cadaverine by TG2

Different forms of TG2 (B003 inhibited, wt, open, E329) were mixed in a solution containing 50mM Tris/HCL pH8.3, 5mM $MgCl_2$, 5mM DTT, 100μM FITC-cadaverine and either 1mM EGTA or 10mM $CaCl_2$. Samples were then incubated at 37°C for 20min in a warm-bath or on ice as specified. Samples were run on a SDS-PAGE, and gels scanned using the Typhoon 9400 variable mode imager as described in 2.13.

2.16 Inhibition of TG2 with Z006 for protein crystallization

TG2 ($8.3x10^{-8}$mol) was incubated with a 10-fold molar excess of Z006 inhibitor. Total volume of the reaction was calculated to keep DMSO concentration at 1% (the inhibitor is stored in DMSO). TG2 was initially diluted to 1mg/ml with 20mM Tris/HCl pH7.5. The inhibition took place in two different steps. Firstly, 40% of the total volume of Z006 was diluted to 1ml and added to the protein solution over a 30min period at 4°C, by dripping the inhibitor with a syringe while stirring. In the second step, the remaining 60% of inhibitor were diluted to 1.5ml and added to the protein simultaneously with

1ml of $CaCl_2$ (10mM final concentration) solution over a 60min period at 4°C while stirring. The calcium solution will drive the remaining non-inhibited TG2 to its open conformation, allowing irreversible binding of Z006. Note that, before the second step, TG2 was further diluted to reach the total volume of reaction, while accounting for added volume of inhibitor and $CaCl_2$. Inhibited protein was concentrated using a Centiprep Ultracel YM-10 concentrator (Millipore), according to manufacturer specifications, to a volume of ≈2-3ml. Inhibited TG2 was buffer exchanged to the more appropriate storage buffer of 10mM Tris/HCl pH 7.5, 100mM NaCl, by using a pre-equilibrated PD10 column. Protein was centrifuged for 10min at 16000x g, at 4°C to remove any aggregates and analysed by spectrophotometry. Final protein concentration was calculated using Beer-Lambert Law.

2.17 Crystallisation of Z006-inhibited TG2

Crystallisation of inhibited TG2 was attempted using methodology based on the previously published crystallization experiments by Pinkas et al., 2007.

Inhibited TG2 (6.8mg/ml; 87,7μM) was plated for crystallisation in the presence of either no ligand (Apo) or one of two different amines (ligand A or B). Ligands were used at 10-fold molar excess over protein. Three different precipitant buffers were used. The base of all buffers was a 100mM HEPES, pH7.2, solution, to which ammonium sulphate was added to three different concentrations: 1M, 2M and 3M. These buffers were also used +/- 15% glycerol, and +/- N-Voy (20-fold molar excess over protein). Different ratios of protein-precipitant were seeded: 2:1; 3:2; 1:1 and 1.3:2 to obtain protein concentrations of approximately 13.5mg/ml, 10mg/ml, 6.7mg/ml and 4.4mg/ml respectively.

Crystallisation was performed using vapour diffusion, sitting drop methodology. Protein, ligands and precipitants were loaded into 96-well plates using a Phoenix Liquid Handling System robot. Plates were scanned at day 0, 1, 5, 7, 15 and after 1 month.

In a second crystallisation experiment, inhibited TG2 (6.1mg/ml) and ligands were loaded as before, but using different precipitant buffers. The precipitant buffer used was 100mM HEPES, 2M ammonium sulphate at pH 6.8, 7.2, 7.4, 7.5, 7.7 and 8.0. Crystallisation was carried out with and without 15% glycerol and no N-Voy. Plates were scanned at day 0 and 1, 5, 7, 13 days and also after 1 month.

2.18 Tissue processing and sectioning of D2 intestinal biopsies

Intestinal biopsies from the second part of the duodenum (D2) were obtained from the Gastroenterology Service of the Royal Hallamshire Hospital in Sheffield, with the approval of the Yorkshire Research Ethics Committee and after consent forms were signed by the patients. Biopsies were collected by a specialist gastroenterologist, through endoscopy and processed on the site by the author of this study.

All biopsies were rinsed in sterile PBS (137mM NaCl pH7.3, 0.3mM KCl, 0.8mM Na_2HPO_4, 1.5mM KH_2PO_4) and immediately processed after collection according to 3 different protocols: rapid freezing without fixation, cryopreservation after fixation, and paraformaldehyde fixation and paraffin embedding.

For rapid freezing without fixation, biopsies were snap-frozen in liquid nitrogen and transferred into a container pre-equilibrated at -80℃.

For cryopreservation after fixation, samples were first fixed in 0.5% paraformaldehyde/PBS for 2h at RT, and then in 4% paraformaldehyde/PBS overnight with gentle agitation. The tissue was washed extensively in PBS over 12-24h with several changes, transferred into small containers, soaked overnight in a 1M sucrose/PBS solution and subsequently in 2.3M sucrose/PBS solution for 5-6h or until equilibrated. Samples were then frozen on a block of dry ice and afterwards overlaid/embedded in tissue freezing medium (OCT) for sectioning.

Samples processed according to both of these protocols were stored at -80°C.

For paraffin embedding, D2 biopsies were initially fixed in 4% paraformaldehyde/PBS twice for 24h with gentle agitation and washed extensively in PBS over 48h with several changes. Tissue processing then followed the routine paraffin embedding protocol in the histopathology laboratories at the School of Dentistry, Cardiff University.

Orientation of biopsies was performed so a transversal section of intestinal crypts and villi were observed. D2 biopsies were cut at -27°C in a cryostat or at RT on a general microtome. Sections were cut to a thickness of 3μm and tissue was collected onto gelatin-coated glass slides. Slides were stored at -80°C or RT, according to type of tissue processing used.

2.19 Immunofluorescence staining

Cryosections were air-dried overnight prior to immunostaining. Paraffin sections were deparaffinised for 10min in xylene before rehydration by dipping slides 3-5x in decreasing concentrations of 100%, 90% and 70% ethanol and distilled water.

Sections were washed twice in TBS for 5min. To prevent non-specific binding, tissue was blocked in 1% BSA/TBS for 30min at RT. Sections were incubated, in the dark, for 10min with labeled TG2 or 1h at RT with labeled TG6 or labeling reagents as detailed in Table 2.2. As a control, Hemocyanin was incubated at the same concentration and for the same time as corresponding labeled TG. Sections were then washed 3 times for 5min in TBS. When specified, secondary antibody was incubated for 1h at RT in the dark. All labeling reagents were diluted in 1%BSA/TBS, as specified, before centrifugation for 5min at 10000x g. Sections were finally washed 3 times for 5min in TBS and mounted in Vectashield® mounting medium containing DAPI supplied by Vector labs.

2.20 Cell counting

Adherent cells were detached from the growing surface with 1ml trypsin/EDTA solution (0.05%) (Invitrogen) and left for 2-5 min at 37°C.

Trypsin was 'inactivated' by addition of 5ml of medium containing 10% fetal bovine serum (FBS) and cells were collected by centrifugation for 5 min at 400x g. The non-adherent cells were collected by centrifugation at 400x g for 5 min.

Cells were suspended in appropriate medium. Desired volume of cell suspension was mixed with Trypan Blue solution (0.4%) (Sigma) in 1:1 ratio. A total of 10µl of cell suspension was loaded into a Neubauer counting chamber and unstained cells counted according to the manufacturer's protocol.

Table 2.2 List of labelling reagents used in immunofluorescent staining of D2 intestinal biopsies

Name	Species	Final concentration	Catalog number and manufacturer
Atto-565 TG2	Human	10µg/ml	in house labeling
Atto-565 TG6	Human	20µg/ml	in house labeling
Atto-565 hemocyanin	*Limulus polyphemus*	10µg/ml or 20µg/ml	in house labeling
FITC-conjugated anti-human IgA α-chain	Goat	1.5µg/ml (1:1000)	109-095-011, Jackson Immuno Research
Anti-human CD138	Mouse	4µg/ml (1:25)	MCA2459GA, AbDSerotec
Anti-human CD20cy	Mouse	1:100	M0755, Dako
Anti-mouse IgG (H+L) secondary antibody Alexa Fluor 488	Donkey	4µg/ml (1:500)	A21202, Invitrogen
VECTASHIELD® Mounting Medium with DAPI	NA	1.5µg/ml	H-1200, Vector Labs

2.21 THP-1 cell culture. differentiation and activation

Human monocytic leukemia cells (THP-1) were kindly gifted by Dr. Xiaoqing Wei. THP-1 cells were grown in RPMI 1640 medium (Sigma) supplemented with 10% FBS (Gibco), 2mM L-glutamine (Gibco) and antibiotics (100 µg/ml streptomycin, 100 U/ml penicillin) (Gibco). Cells were maintained at 37 °C in a humidified incubator with 5% CO_2.

Cells were seeded in complete RPMI medium at $0.5x10^5$ cells/cm^2. Differentiation into a resting macrophage stage was achieved by supplementing the medium with 12-O-Tetradecanoyl-phorbol-13-acetate (TPA) (50ng/ml in dimethyl sulfoxide (DMSO)) (Merck Millipore, 524400) for 48h. When specified, cells were further polarized into pro-inflammatory M1 or anti-inflammatory M2-type macrophages by adding to the medium granulocyte-macrophage colony-stimulating factor (rhGM-CSF) (20ng/ml in dH_20) (ImmunoTools, 11343113) or macrophage colony stimulating factor (rhM-CSF) (20ng/ml in dH_2O) (ImmunoTools, 11343123) for 3 days. After 3 days, activation of macrophages was promoted by stimulation for 4h or 24h with 100ng/ml bacterial lipopolysaccharide (LPS) from *Salmonella sp.* or $1x10^5$ heat killed candida (HKC) (both kindly donated by Dr Xiaoqing Wei). Total RNA was extracted from the cells at the described time points according to methodology described in section 2.24.

2.22 Mouse bone marrow derived macrophages: isolation, culture and differentiation

Culture and differentiation of mouse bone marrow-derived macrophages was performed based on methodology used within our department and provided by Dr. Xiaoqing Wei and Dr. Niels Hans.

An appropriate number of adult mice were sacrificed by CO_2 exposure or cervical dislocation. The femurs were removed aseptically, with care to retain the intact bone, and not to expose the bone marrow. Muscle tissue was removed from the bone and femurs were stored on ice, in 1640 RPMI medium supplemented with L-glutamine, 10% FBS, 100u/ml penicillin and

100µg/ml streptomycin. Bone marrow was harvested from femurs by flushing with complete RPMI medium. The hip and knee joints were removed using a scalpel and 0.5-1 ml of RPMI was flushed through the femur, via a cut in one end, using a syringe and needle. The recovered cells were pooled in a centrifuge tube and spun at 400x g for 5min. The cell pellet was resuspended in 1ml of red blood cell lysis buffer, containing ammonium chloride, and incubated for 90s. A large excess of fresh RMPI was added and centrifuged at 400x g for 5min. The pellet was resuspended in appropriate volume of RPMI and cells were counted. Cells were seeded at a density of $0.6x10^5$cells/cm^2 and cultures for 7 days in complete RPMI medium supplemented with 20ng/ml mGM-CSF or 20ng/ml of both mM-CSF and mIL-4 (cytokines were kindly donated by Dr Xiaoqing Wei). Medium was changed every 3 days. After day 7 cells were trypsinised as describe in section 2.20 and re-seeded on a 24-well plate at a density of $1.25x10^5$cells/cm^2. Cells were allowed to adhere overnight. On the following day, macrophage activation was promoted by stimulation with 100ng/LPS for 2, 6 or 24h. Total RNA was extracted at these time points and processed as described in section 2.24.

2.23 Human PBMC derived macrophages: isolation, culture and differentiation

Peripheral blood samples were obtained from Cardiff University, School of Dentistry, with the approval of the Research Ethics Committee: REC10/MRE09/28 and after consent forms were signed by the volunteers. Peripheral blood monocyte cells (PBMC) were purified from total blood solution as described below.

Approximately 15ml of peripheral blood was collected into a syringe containing 10U/ml of heparin and diluted 1:1 with cold RPMI1640 serum free medium. The diluted blood was divided into 8 ml fractions and carefully laid over 5ml of Ficoll-Paque Premium (GE, 17-5442-02), in Falcon tubes. Tubes were centrifuged at 510x g for 25 min at 4°C, with lowest settings for brake and acceleration. After centrifugation, the upper layer was aspirated with a

Pasteur pipette to within 0.5cm of the opaque interface containing mononuclear cells. The opaque interface was carefully transferred into a clean Falcon tube and washed by adding 10ml of serum-free medium followed by centrifugation at 400x g for 10min, 4°C (brake 0, acceleration 0). Cells were resuspended in 5 ml of serum-free medium and a second wash was performed in the same way. The pellets from all tubes (from the same patient) were combined and resuspended in 1-2ml of serum-free medium, depending on size of the pellet. Cells were counted with a haemocytometer after lysis of remaining erythrocytes through addition of 2% acetic acid. They were then seeded at a density of $1x10^6$cells/ml and cultured for 7 days, at 5% CO_2 and 37°C with 1640 RPMI medium supplemented with 10% FBS, L-glutamine, 100u/ml penicillin and 100µg/ml streptomycin and either 20ng/ml rhGM-CSF or 20ng/ml rhM-CSF (ImmunoTools) for M1 and M2 differentiation, respectively. Medium was exchange every 3 days. On day 7, cells were washed, trypsinised and counted as described in section 2.20.

Cells were re-seeded at a density of $0.5x10^5$cells/cm^2 and allowed to adhere overnight. The following day, cells were stimulated with either complete medium only, 100ng/ml LPS or $1x10^5$cells HKC for 4h. Cells were prepared and total RNA extracted as described in section 2.24.

2.24 Isolation of total RNA and reverse transcription

Cells were washed 3 times with pre-warmed (37°C) PBS. Isolation of purified total RNA was achieved by using RNeasy mini kit (Qiagen), according to manufacturer specifications. The concentration of total RNA was estimated from the OD260/280 ratio, determined using a Nanovue (GE Healthcare). Total RNA was stored at -80°C as an ethanol precipitate: 1µl of glycogen (5mg/ml), 1/10 of the total volume of 3M sodium acetate, pH5.2, and 2.5x volume of 100% ethanol. For recovery, the precipitated RNA was collected by centrifugation at 12,000 x g for 20min at 4°C. The pellet was washed with 80% ethanol and collected again by centrifugation in the same conditions for 10min. Pellet was briefly air-dried and reconstituted in nuclease free H_2O.

Reverse transcription was carried using SuperScript^{TM}II Reverse Transcriptase enzyme (Invitrogen). For a 20µl reaction volume, 500ng of total RNA were used. The following components were added into a nuclease-free microcentrifuge tube: 1µl of 0.5µg/µl Oligo$(dT)_{15}$ (Promega), 1µl dNTP Mix (10mM each), specified RNA and nuclease free H_2O to bring the volume up to 13µl. Mixture was heated to 65°C for 5min and quick chilled in ice The following reagents were then added: 4µl of 5x First-Strand Buffer and 2µl of 0,1M DTT (Invitrogen). Samples were incubated for 2min at 42°C and 0.5µl of enzyme was added. Samples were incubated at 42°C for 52min and then at 95°C for 2min, followed by quick chill on ice and a further addition of 0.5µl of enzyme. The incubation at 42°C was repeated. The reaction was finally stopped by incubation at 70°C for 15min. Samples were stored at -20°C until further use.

2.25 Analysis of M1 and M2 cell markers by qPCR

Samples were tested for gene expression of different M1 and M2 markers, as specified, by real-time quantitative polymerase chain reaction (qPCR) using the forward (f) and reverse (rev) primers described in Table 2.3. Where described, hGAPDH or mβ-Actin were used as internal control genes.

The different fragments were amplified using 40 cycles in a total reaction volume of 20µl. The amplification of 5µl cDNA (1µl diluted 5-fold) was performed using 10µl of Mesa Green 2x PCR master mix (Eurogentec), 0.2µl of SYBR green reference dye (Sigma, R4526) and 0.5µM of each primer. Data was acquired using the QuantStudio™ 6 Flex Real-Time PCR System and the parameters described in Table 2.4.

All samples were run in triplicate. The relative expression of each sample was acquired using the $2^{-\Delta\Delta}$Ct method, after normalizing for internal control gene. Results are shown in comparison to a control sample.

Table 2.3 Primers used for analysis of M1 and M2 markers by qPCR.

Name	Sequence
miNOS f P1	5’ - TGGCTCGCTTTGCCACGGACGAGACGGA - 3’
miNOS rev P2	5’ – GGAGCTGCGACAGCAGGAAGGCAGCGGG - 3’
mArg1 f P1	5’ - AGCTGGCTGGTGTGGTGGCAGAGGTCCA - 3’
mArg1 rev P2	5’ - GGGTGGACCCTGGCGTGGCCAGAGATGCT - 3’
mβ-Actin f P3	5’ - TCTTTGCAGCTCCTTCGTTGCCGGTCC - 3’
mβ-Actin rev P4	5’ - GTCCTTCTGACCCATTCCCACCATCACAC - 3’
hIL-12p40 f	5’ - CCCTGGTTTTTCTGGCATCTCCCCTCGT - 3’
hIL-12p40 rev	5’ - GAGGACCACCATTTCTCCAGGGGCATCC - 3’
hEBI3 f P1	5’ - AAACTCCACCAGCCCCGTGTCCTTCATT - 3’
hEBI3 rev P2	5’ - CGGTGACATTGAGCACGTAGGGAGCCAT - 3’
hGAPDH f	5’ - TCCTCCTGTTCGACAGTCAGCCGCATC - 3’
hGAPDH rev	5’ - GGTGACCAGGCGCCCAATACGACCAAAT - 3’

Table 2.4 Parameters used for amplification by real-time quantitative PCR

Stage	Temperature	Duration	N. of cycles
Activation of polymerase	95°C	2min	1
Denaturation	95°C	15s	40
Annealing	60°C	30s	
Elongation	72°C	30s	
Melt Curve	95°C	15s	1
	60°C	1min	1
	95°C	15s	1
Completion	4°C	∞	1

2.26 Screening of transglutaminase expression by PCR

cDNA was amplified using polymerase chain reaction (PCR) and the forward (f) and reverse (rev) primers as described in Table 2.5.

Table 2.5 Primers used for transglutaminase amplification in THP-1 samples.

Name	Sequence
hTG1 f	5' - ACCCTGTGACCATGCCAGTG - 3'
hTG1 rev	5' - GCTGCTCCCAGTAACGTGAGG - 3'
hTG2 f	5' - ATGAGAAATACCGTGACTGCCTTAC - 3'
hTG2 rev	5' - CAGCTTGCGTTTCTGCTTGG - 3'
hTG3 f	5' - GCTGTTGGGTAACCTGAAGATCG - 3'
hTG3 rev	5' - GCTACGTCGATGGACAACATGG - 3'
hTG4 f	5' - TCACGTCTTTCCAGTACCCTGAGT - 3'
hTG4 rev	5' - CAGGCTTTCCAAAGAGAACTTGAC - 3'
hTG5 f	5' - CAAAGAGCATCCAGAGTGACGAGCGGG - 3'
hTG5 rev	5' - GGGCTGTCCTGGCTCAGTGATGTGGGC - 3'
hTG6 f	5' - GTGAAGGACTGTGCGCTGATG - 3'
hTG6 rev	5' - CGGGAAGTGAGGGCTTACAAG - 3'
hTG7 f	5' - CCTCATCAATGGGCAGATAGC - 3'
hTG7 rev	5' - CTTGACCTCGTTGCTGCTGA - 3'
hFXIII f	5' - GACCAATGAAGAAGATGTTCCGT - 3'
hFXIII rev	5' - GAAGGTCGTCTTTGAATCTGCAC - 3'
h36B4 f	5' - AGATGCAGCAGATCCGCAT - 3'
h36B4 rev	5' - ATATGAGGCAGCAGTTTCTCCAG - 3'

The different TG fragments were amplified using 40 cycles in a total reaction volume of 25μl. The amplification of 1μl cDNA was performed using 1.25U of GoTaq G2 hot start DNA Polimerase (Promega, 5U/μl) and 0.25μM of each primer in the presence of 5μl Flexi buffer (Promega), 2mM $MgCl_2$ (Promega) and 10mM dNTPs (New England Labs) and parameters as specified in Table 2.6.

Table 2.6 Parameters used for transglutaminase amplification by PCR

Stage	Temperature	Time	N. of cycles
Activation of polymerase	94°C	2min	1
Denaturation	94°C	30s	40
Annealing	60°C	45s	
Elongation	72°C	45s	
Completion	72°C	7min	1
	4°C	∞	1

For analysis, the amplified PCR products were separated on a 1% agarose gel containing 1.25mM ethidium bromide in TAE running buffer (40mM Tris/acetate, pH 8.5, 2mM Na_2EDTA). Electrophoresis was performed under constant voltage (100V/cm^2) and bands were visualized by UV exposure using a gel-doc system (BioRad). Bands were quantified based on subjective observation of two independent subjects.

2.27 Analysis of TG2 and TG6 expression by qPCR

Analysis of TG2 and TG6 expression was performed by qPCR, using the forward (f) and reverse (rev) primers and probes described in Table 2.7. h36B4 was used as the internal control gene. Human primer and probe sequences were able to amplify mouse cDNA due to the high degree of homology between sequences in the two species.

The different TG fragments were amplified using 50 cycles in a total reaction volume of 25μl. The amplification of 1μl cDNA was performed using 12.5μl of 2x TaqMan Fast Advanced Master mix (Applied Biosystems) and primers at the described concentration (Table 2.7). Data was acquired using the QuantStudio™ 6 Flex Real-Time PCR System and the parameters described in Table 2.8.

All samples were run in triplicate. The relative expression of each sample was acquired using the $2^{-\Delta\Delta}$Ct method, after normalizing for internal control gene, h36B4. Results are shown in comparison to a control sample.

Table 2.7 Primers and probes used for qPCR analysis of TG2 and TG6 expression and respective final concentrations used

Name	Sequence	Final Concentration
mTG2 f	5' - CGAATCCTCTACGAGAAGTACAGC - 3'	150nM
mTG2 rev	5' - GTCAAACGCCAAAACGAACC - 3'	150nM
hTG2 probe	5' - AGCTACCTGCTGGCTGAGAGAGATCTC - 3'	175nM
mTG6 f3	5' - CAGCAGTGGTAGGAGTGACAG - 3'	300nM
mTG6 rev 7	5' - CTCTTGGAAGGGGTTATGTTG - 3'	600nM
mTGy probe	5' - CAAGGACAGCTAAGTATTGAGGTGCCCAG - 3'	200nM
h36B4 f	5' - AGATGCAGCAGATCCGCAT - 3'	300nM
h36B4 rev	5' - ATATGAGGCAGCAGTTTCTCCAG - 3'	300nM
h36B4 probe	5' - AGGCTGTGGTGCTGATGGGCAAGAAC - 3'	100nM
hTG3 f	5' - GCTGTTGGGTAACCTGAAGATCG - 3'	300nM
hTG3 rev	5' - GCTACGTCGATGGACAACATGG - 3'	300nM
hTG3 probe	5' - CGGAGTGGCACCAAGCAACTGCTCGC - 3'	100nM
hTG6 f	5' - GTAAAGGACTGTGTGCTGATG - 3'	300nM
hTG6 rev	5' - TGGGAACTGTGAGCTGACAAG - 3'	300nM
hTG6 probe	5' - CTTCTCCAAGGACAGCTAAGTATTGAG - 3'	100nM

Table 2.8 Parameters used for amplification of TGs in mouse macrophages by qPCR

Stage	Temperature	Duration	N. of cycles
Activation of polymerase	95°C	20s	1
Denaturation	95°C	15s	50
Annealing/Elongation	60°C	30s	
Completion	4°C	∞	1

Chapter 3 Protein purification and chemical labelling

3.1 Introduction

Gluten containing diets have been a part of the Western world lifestyle for centuries or even millennia. On average, the consumption of gluten is approximately 10g to 20g per day in most European countries, and it is also rapidly increasing in Eastern countries. With gluten disorders affecting most of the Western world, and coeliac disease being estimated to affect 1% of the population in these countries, it is natural that gluten related disorders are a research focus of the scientific community. Importantly, TG2 has been recognised as the predominant auto-antigen in coeliac disease for almost 20 years (Dieterich et al. 1997). More recently, a novel transglutaminase, TG6, has been identified and linked to the autoantibody response specifically in the gluten associated neurological manifestations of the autoimmune disease, and gluten ataxia in particular (Hadjivassiliou et al. 2008). Even though both gluten ataxia and more often coeliac disease have been studied across the world by many groups, the mechanism for the development of these antibodies against transglutaminase enzymes is still not fully understood. It is known that TG2 catalyses highly specific deamidation of gluten peptides and most gluten peptides identified as TG2 substrates also serve as T-cell epitopes (Arentz-Hansen et al. 2000), and hence drive the immune response.

It has been suggested that production of antibodies against TG2 is a T-cell driven event and relates to the uptake of TG2-gluten peptide complexes by pre-existent TG2-specific B cells (Sollid et al. 1997). In fact, it has recently been shown that B-cells expressing TG2-specific B-cell receptors (BCRs) are able to take up and present TG2-gliadin complexes in an antigen presenting cell manner leading to the activation of gluten-specific T-cells (Du Pre & Sollid 2015; Di Niro et al. 2012).

The understanding of the mechanistic role of TG6 in gluten ataxia is still quite limited. Stamnaes et al (2010) have shown that, in a similar way to TG2, TG6 is able to deamidate gluten peptides containing the most common

CD gluten T-cell epitopes. The enzyme has also been shown to form TG6-gluten peptide complexes that could act in a hapten-carrier fashion and lead to presentation of gluten by auto-reactive B-cells to elicit T cell help. Although it has been suggested that TG6 antibody populations could originate from epitope spreading as a consequence of considerable homology between human transglutaminases (Grenard et al 2001; Stamnaes et al 2010), recent data by Hadjivassiliou suggests the independent involvement of TG6 in the pathogenesis of gluten ataxia, as antibodies in most patients do not cross-react between different transglutaminase isoforms (Hadjivassiliou et al. 2008). However, as TG6 is primarily expressed in the central nervous system, it is unclear whether these immune events occur at the level of the gut or the brain.

Demonstration of TG6-specific B-cells or TG6 expression in the human small intestine would substantiate that production of autoantibodies in GA could originate in the small intestine even though the symptoms and predominant disease manifestation are extraintestinal.

To address this, human TG2 and TG6 were expressed, purified and fluorescently labelled for use in immunohistochemical assays. Labelled protein will allow us to assess the presence of TG2 and TG6-specific B cells in small intestine biopsies of patient with gluten-related conditions. In this project, TG2 is being used as a proof of principle/reference point as it has been more extensively studied in the gluten disorders context and relevant TG2-specific B-cells are evidently present in the small intestine (Di Niro et al. 2012). It is also a protein that is comparatively easier to work with than TG6, which is difficult to produce recombinantly in active form. Furthermore, enzymatic activity of labelled proteins will be assessed, to ensure that enzymatically functional TG2 and TG6 are obtained, as autoantibodies against TG2 have been shown to be conformation dependent (Seissler et al. 2001; Iversen et al. 2013).

The aims of the chapter:

1. To express and purify TG2 and TG6 enzymes.
2. To establishment a protocol for chemical labelling of TG2 and TG6 with a fluorescent dye.
3. To assess labelled enzymes enzymatic activity using a fluorogenic activity assay.

3.2 Results

3.2.1 Expression and purification of coeliac disease autoantigen TG2

Detailed methodology can be found in section 2.6 of chapter 2. Briefly, RhTG2 was successfully expressed and purified using a modified protocol based on the methodology described by Hadjivassiliou et al, 2008. *Escherichia coli* BL21 transformed with constructs containing native TG2 sequence with an added His_6-tag to the N-terminus were already available within the group. *E. coli* was grown in LB medium and expression of TG2 was induced by addition of rhamnose. Bacteria were collected by centrifugation and resuspended in purification buffer. Harvesting of expressed protein was achieved by lysis of bacterial cells using a Stansted pressure cell homogenizer. RhTG2 was purified from the lysate using Ni^{2+}-chelating affinity chromatography followed by further purification through anion exchange chromatography (Fig. 3.1A). RhTG2 purity was analysed by sodium dodecyl sulfate polyacrylamide gel electrophoresis (SDS-PAGE) under reducing conditions, followed by staining with Coomassie brilliant blue R (Fig. 3.1B).

SDS electrophoresis showed the successful purification rhTG2 from the starting material (S). A lot of the proteins in the lysate mixture did not bind to the nickel affinity column (F) and from the proteins that bound unspecifically or weakly, the majority could be flushed out with 30mM imidazole. RhTG2 was eluted effectively from the column with 150mM imidazole.

During anion exchange chromatography, rhTG2 eluted as a second peak (P2) with 210-280mM NaCl. Two other peaks were observed: peak 1 (P1) was detected using 150mM NaCl and corresponds to non-specifically bound protein. P3 (P3), detected at 1M NaCl, could possibly correspond to DNA.

Although rhTG2 was successfully purified to a high degree, it was still possible to observe some additional bands at ≈45kDa, 30kDa and 25kDa in the denaturing electrophoresis. Previous studies within the group using mass

spectrometry, have shown that the bands were TG2 degradation products (personal communication, Prof D. Aeschlimann).

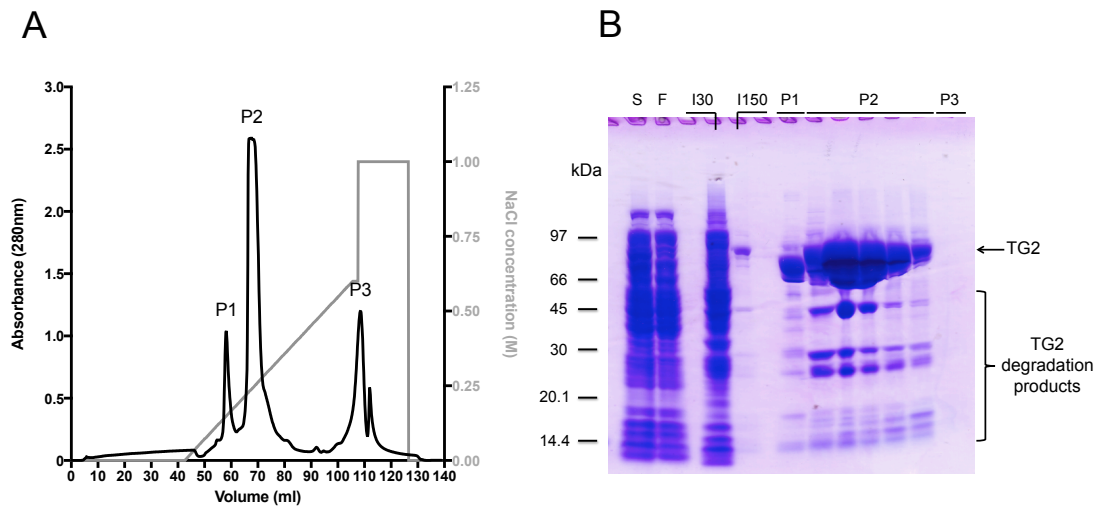

Fig. 3.1 Purification of rhTG2 A: Absorbance spectrum of anion exchange chromatography on Source Q15 column. P1 corresponds to unspecific bound protein, P2 corresponds to TG2 and P3 possibly corresponds to DNA. **B:** SDS-PAGE (4-20% PA gel, reducing conditions) analysis of different fractions of TG2 purification. S corresponds to starting material; F corresponds to Ni^{2+}-chelating affinity chromatography flow through; I30 and I150 correspond to proteins eluted with 30mM and 150mM imidazole. P1, P2 and P3 correspond to fractions of the peaks observed during anion exchange chromatography with P2 corresponding to eluted TG2.

Fractions (Fig. 3.2A) containing purified TG2 were pooled and spectroscopic analysis for absorbance was performed (Fig. 3.2B). Final concentration of the protein was calculated using the Beer-Lambert Law c=absorbance/(ε·d), where ε is the theoretical extinction coefficient of the protein (ε(TG2)=1.35cm^2/g – calculated using ProtParam software from ExPASy Bioinformatics Resource Portal) and d=cuvette diameter (d=1cm). Concentration of TG2 was calculated to be approximately 2.30mg/ml for the preparation shown in Fig. 3.2 and total yield of protein was ≈15mg.

To assure protein enzymatic activity, a real-time fluorescent assay was carried out. This assay monitors transglutaminase activity by determining its isopeptidase activity. It was previously developed by researchers within our group and is based on the hydrolysis of an isopeptide bond of a quenched fluorescent probe, Abz-APE(γ-cad-Dnp)QEA (Abz=2-

aminobenzoyl; cad-Dnp=2,4-dinitrophenyl-cadaverine). The probe is derived from the substrate sequence APQQEAL in osteonectin, and mimics a cross-linked TG reaction product. Hydrolysis of the isopeptide bond by TG2 releases the quencher (Dnp) and therefore generates an increase in light emission from the fluorophore (Abz) at λ max=418nm (Adamczyk, Heil, & Aeschlimann, 2013a). For the reaction to occur, TG2 needs to be activated by adding calcium.

Protein was prepared according to the protocol described by Adamczyk et al. 2013, and analysis was carried out using the FLUOstar OMEGA multidetection microplate reader. Substrate conversion was measured for 90 cycles. Calcium was injected in cycle 10 (400s), to activate the enzyme (Fig. 3.2C). Fluorescence was acquired every 40s and average fluorescence from the first 8 cycles was subtracted to normalize for well-specific fluorescence (Fig. 3.2D). The control (without enzyme activation) was subtracted from the data to account for fluorescence bleaching and the final data fitted using linear regression (Fig. 3.2E)

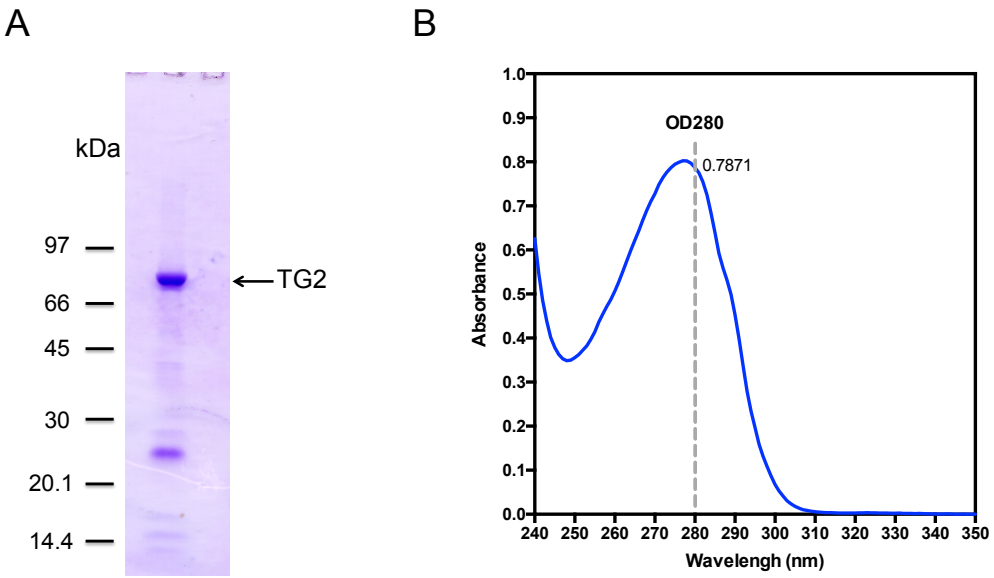

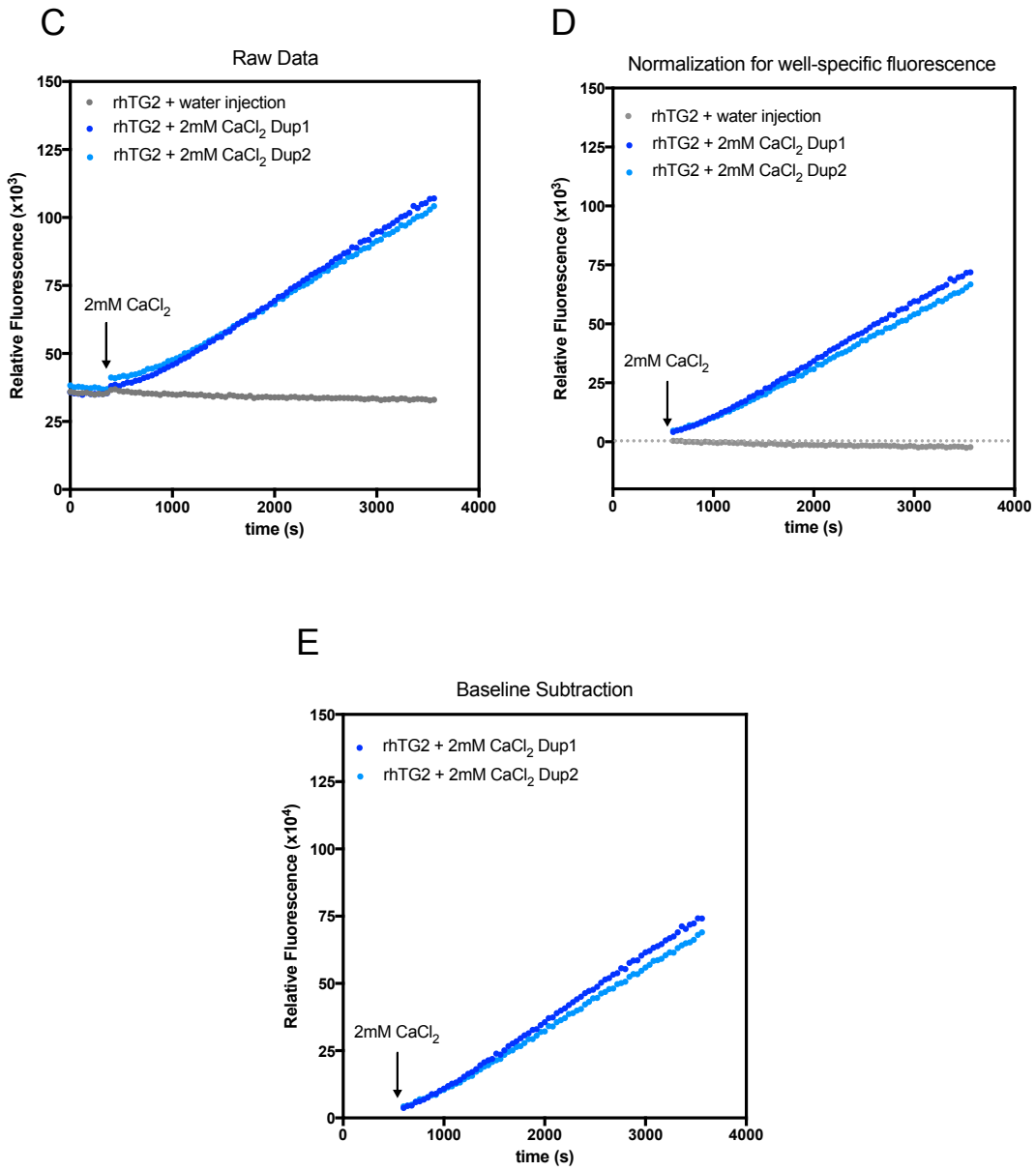

Fig. 3.2 Characterisation of purified rhTG2. A: SDS-PAGE (4-20% PA gel, reducing conditions) analysis of purified rhTG2 (pooled fractions). A band observed around the 80kDa mark was consistent with TG2 molecular weight of 77325g/mol. **B:** Absorbance spectrum for purified rhTG2. rhTG2 was diluted 1/4 to allow spectroscopic analysis and normalized for buffer. **C:** Raw data for TG2 isopeptidase real-time fluorescent assay. Reaction mixture containing ≈20μg/ml TG2 was injected at cycle 10 (400s) with either water (control) or 2mM $CaCl_2$. **D:** Data from TG2 isopeptidase assay after normalization for well-specific fluorescence (subtraction of the average of first 320s). **E:** Data from TG2 isopeptidase assay after subtraction of baseline fluorescence to account for fluorescence bleaching. As expected, rhTG2 is highly active after calcium injection and reaction rates can be determined from linear regression of data.

Absorbance spectrum and isopeptidase assay of purified rhTG2 showed the successful purification of an active form of the enzyme, which could subsequently be used for labelling.

3.2.2 Labelling of TG2 with NHS ester dye results in an enzymatically inactive enzyme.

Commercially available Atto-NHS ester dyes were purchased as the fluorescent labels of choice. In these well-established dyes, the activated *N*-hydroxysuccinimide (NHS) ester group readily reacts with primary amines, forming a chemically stable amide bond between the dye and the protein. Primary amines exist at the N-terminus of each polypeptide chain and in the side-chain of lysine (Lys, K) amino acid residues. The optimum pH range for NHS-ester coupling is physiologic to slightly alkaline conditions (pH 7.2 to 9.0) and hence ideal for protein labelling. At this pH, amino groups of proteins are unprotonated to a high degree and highly reactive towards the dye-NHS-ester. The reaction releases NHS (Fig. 3.3).

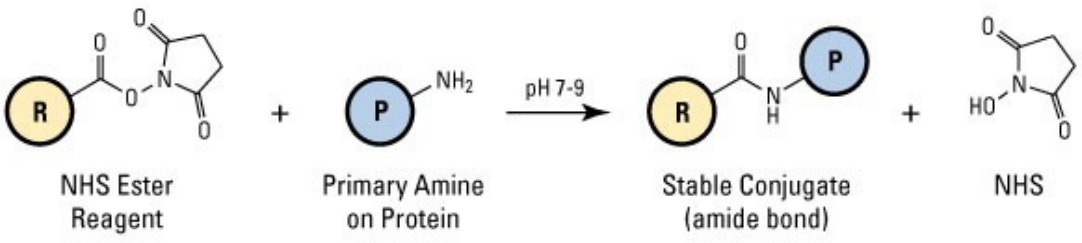

Fig. 3.3 NHS ester reaction with primary amine. R represents a labelling reagent; P represents a protein. NHS ester-activated labelling compound reacts with a primary amine optimally in pH 7 to 9, generating a stable amide bond. The reaction releases NHS (retrieved from ThermoFisher).

Atto-565 NHS ester was purchased and this dye is a red fluorophore belonging to the class of rhodamine dyes. It has a maximum excitation of 563nm and a maximum emission of 592nm, which will allows its use in double immunohistochemistry along side additional green labels already in stock in the laboratory.

Purified rhTG2 was fluorescently labelled by reaction with Atto-565 NHS ester dye, with the final aim to use the labelled enzyme in immunofluorescence assays on patient's gut biopsies. Since TG2 was stored in Tris-buffer, which contains amino groups and is therefore incompatible with the labelling reaction, a buffer exchange was performed. A borate buffer was chosen and pH was set to 8.5. This pH would lead to deprotonation of protein amino-groups (lysine residues) and allow for efficient reaction of the NHS dye with the protein. This pH will also be high enough to prevent rapid dye hydrolysis, this way making the labelling reaction highly efficient.

A PD10 desalting column was used for the buffer exchange process. This type of gel filtration chromatography (Sephadex^{TM} G-25) allows rapid separation of high molecular weight substances from low molecular weight substances. Molecules larger than the matrix pores would be excluded from the system and elute first, in the void volume of the column. Molecules smaller than the pores infiltrate them and, therefore, would elute later. It was therefore anticipated to observe an initial peak in the void volume corresponding to the protein and a second peak corresponding to the buffer salts.

The desalting column was equilibrated with borate buffer and TG2 was applied to the system. Fractions corresponding to 0.5ml were collected while adding additional buffer to the column. Fractions were then analysed using a UV/VIS spectrophotometer, measuring absorbance at 280nm.

The absorbance analysis showed that the protein eluted first, between fractions 7 and 9 with highest absorbance at fraction 8 (V_0≈4ml; OD280=0.27). As expected a salt peak (V_T≈12ml) was observed at fraction 24 (Fig. 3.4A).

Fraction 8 (Fig. 3.4B) was calculated to have a protein concentration of ≈0.8mg/ml. This fraction was used for the labelling reaction.

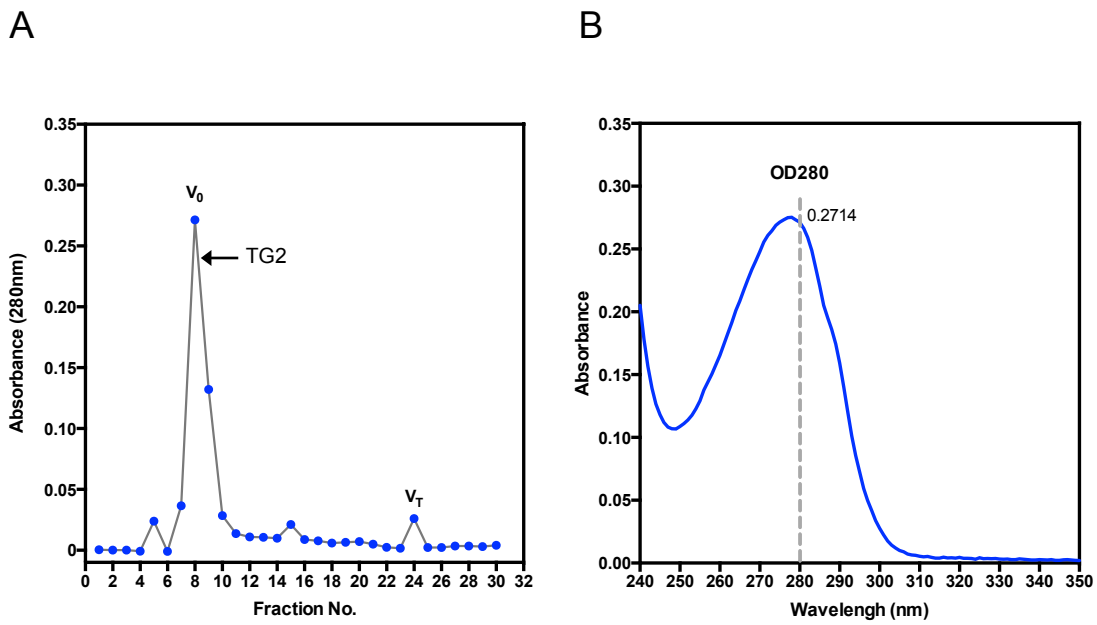

Fig. 3.4 Absorbance spectrum for buffer exchanged rhTG2. TG2 (0.5ml, 2mg/ml) was applied to PD10 column for buffer exchange. Fractions (0.5ml) were collected and diluted 1:4 for spectroscopic analysis. Data shown was corrected for buffer absorbance. **A:** Absorbance measured at 280nm for each fraction collected. Protein eluted between fractions 7 and 9 (V_0= void volume; V_T=total volume). **B:** Absorbance spectrum giving typical spectrum for protein with maximum absorbance near 280nm and no evidence of aggregation.

Fluorescent labelling of TG2 was performed in solution, initially using a 10-fold molar excess of Atto-565 NHS ester over protein. Labelled protein was separated from free label using the PD10 desalting column, while returning the protein to its initial, more adequate Tris-buffer. Fractions containing eluted labelled TG2 were pooled. Spectroscopic analysis confirmed the success of the labelling process, as a 280nm protein peak was observed along side the expected 565nm absorbance peak for the fluorophore (Fig. 3.5).

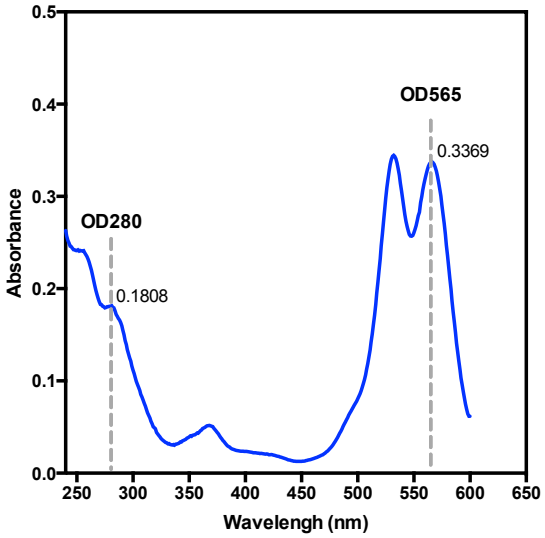

Fig. 3.5 Absorbance spectrum for Atto-565 labelled rhTG2. Data corrected for buffer absorbance. Sample was diluted 1:4 to allow spectroscopic analysis. Labelled protein was purified using a PD10 column. It was evident that labelling was successful based on the peak observed at 565nm corresponding to Atto-565 dye attached to rhTG2.

Final protein concentration and label density were estimated from a standard curve generated from serial dilutions of Atto-565 dye (Fig. 3.6). Since the fluorescent label contributes in part to the value obtained for OD280 of the sample (Fig. 3.6A), this had to be subtracted to obtain the real concentration of TG2. Labelled TG2 was calculated at a final concentration of ≈318μg/ml and a label density of approximately 2,7 label/TG2.

Protein concentration was also assessed independently by protein assay. Typical BCA assay could not be used as BCA-copper complex has a strong absorbance (562nm) that overlaps with the NHS-ester dye absorbance peak (565nm). Although a Bradford assay was performed, results obtained seemed to be unreasonable. As absorbance for this assay is measured at 595nm (Bradford, 1976), there could still be a juxtaposition of wavelengths between the assay substrate and the NHS dye that interfere with an accurate measurement.

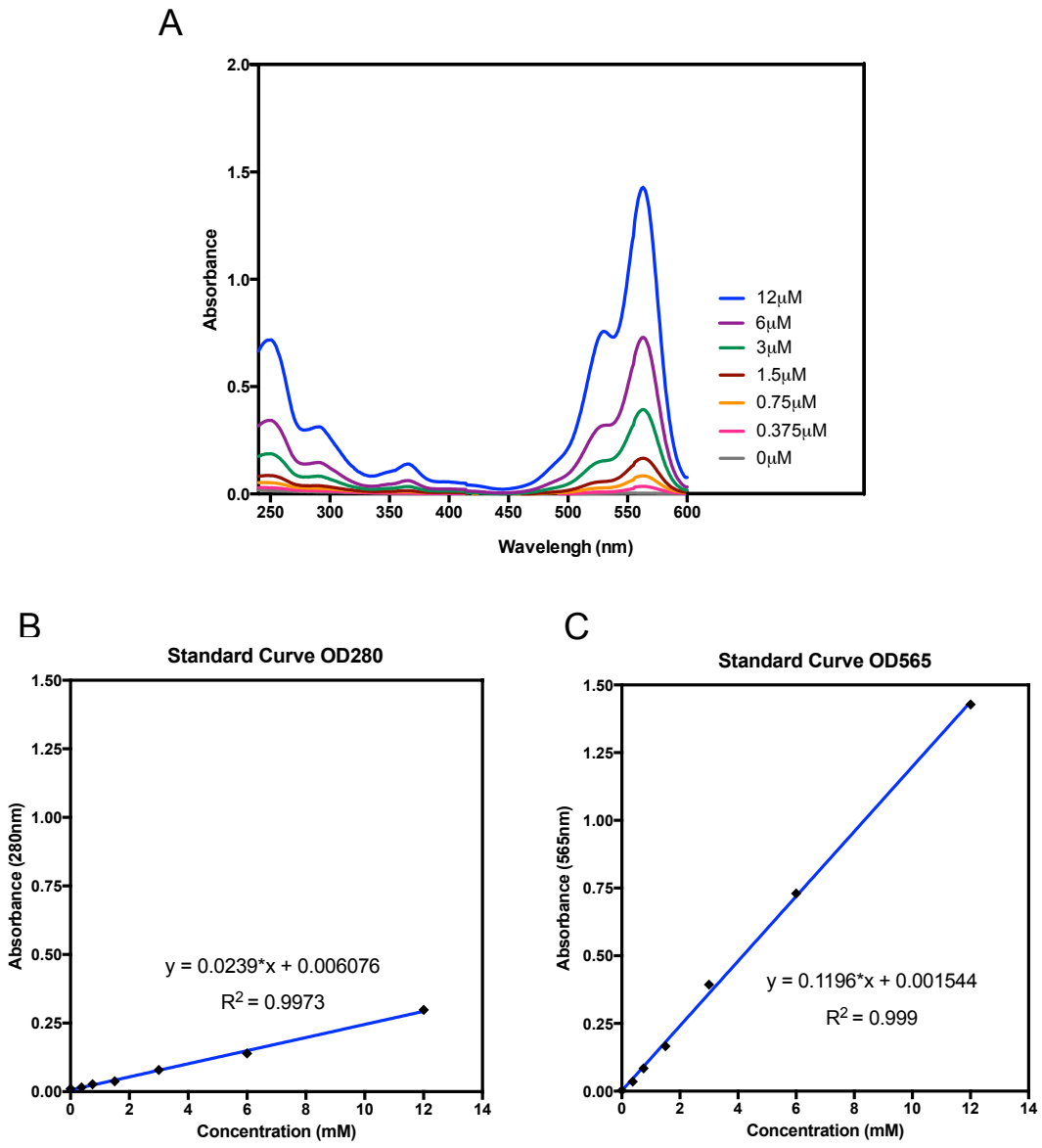

Fig. 3.6 Absorbance spectrum of fluorescent dye Atto-565 dilution series and standard curves. A: Serial dilution of Atto-565 NHS ester. Molar concentration varies from 0 to 12μM as indicated. Active ester component of dye was blocked by reaction with excess of ethanolamine prior to analysis. **B:** Linear regression analysis obtained from absorbance values at OD280 for different dye concentrations. **C:** Linear regression analysis obtained from absorbance values at OD565 for different dye concentrations. Standard curves were used to estimate the contribution to sample absorbance at 280nm and therefore to derive the protein-related absorbance at 280nm.

As labelled TG2 was going to be used to detect B-cell associated IgA in immunofluorescence on patient biopsies staining, functionality is likely to be of critical importance to the final results. Patient antibodies have been

shown to be conformation-dependent and folding of the enzyme may be critical for antibody recognition (Iversen et al., 2013; Seissler et al., 2001). To assure that the enzyme could adopt conformations associated with catalysis following labelling, isopeptidase activity was measured as before. Surprisingly, the transglutaminase activity assay showed that labelled TG2 retained little or no enzymatic activity when compared to the unlabelled control (Fig. 3.7). This suggested that modification with Atto-label was somehow interfering with the catalytic site or a conformational transition of the enzyme, leading to TG2 being inactive.

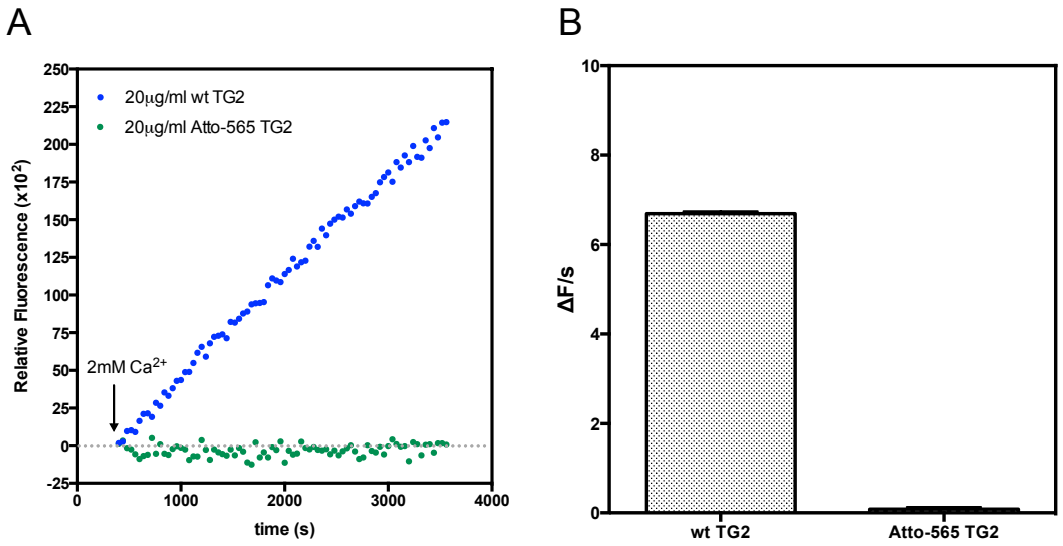

Fig. 3.7 Atto-565 labelled TG2 isopeptidase activity. A: Enzyme isopeptidase activity for 20μg/ml TG2 following injection of 2mM Ca^{2+}. Data was normalized for well-specific fluorescence and control curve (no Ca^{2+}) subtracted to account for fluorescence bleaching. Compared to unlabelled TG2 (blue), Atto-565 labelled TG2 (green) retained little or no enzymatic activity. **B:** Analysis of difference in change in fluorescence over time calculated from linear regression (±SD) analysis of the data for the period between 1500s and 2500s of a single experiment.

3.2.3 Fluorescent labelling of rhTG2 with NHS ester dye: influence of conformation

To overcome the fact that the labelling protocol yielded an inactive enzyme, a second labelling experiment was performed using a different approach. As mentioned in section 1.4.2, TG2 enzymatic activity is allosterically regulated by Ca^{2+} ions and the nucleotides GTP/GDP (Achyuthan & Greenberg, 1987; Begg et al., 2006). As a strong allosteric inhibitor, GTP supresses Ca^{2+} activated crosslinking activity. Also, GTP-binding leads to a structural change in TG2, which acquires a more compact "closed" conformation, decreasing the accessibility of the TG2 substrate binding-pocket and burying the enzyme active site within the protein (Venere et al., 2000). By adding GTP to the labelling reaction, it is expected that the consequential conformational change of TG2 to a closed form would prevent access of Atto-565 to primary amines located near to the catalytic site or substrate-binding pocket of the enzyme, and thereby prevent enzyme inactivation. Also, to reduce the extent of labelling in the reaction, the previously used borate buffer was changed to a sodium phosphate buffer with a lower pH of 7.6. Since the amount of label added to the reaction could have a negative impact on the enzyme activity, this was decreased to a 3-fold molar excess over protein.

The labelling process was performed as before with the exception of addition of 1mM of GTP to the labelling reaction (Fig. 3.8). Spectroscopic results obtained using the new methodology were similar to those previously obtained, with protein not showing signs of aggregation or precipitation. Final concentration of the eluted labelled protein was calculated as being ≈310μg/ml with a label density of 2,7 label/TG2.

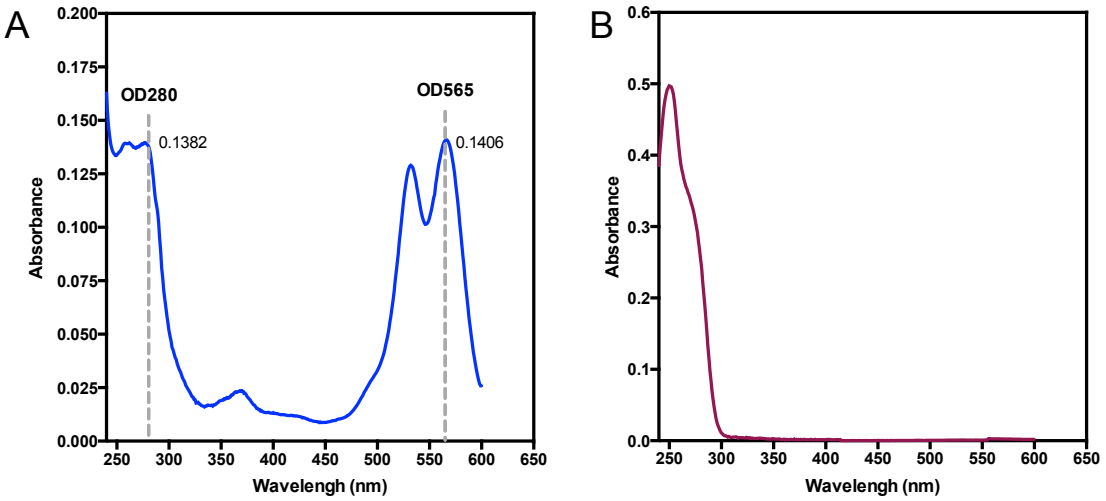

Fig. 3.8 Absorbance spectrum for Atto-565 labelled rhTG2. A: TG2 Labelling was performed in the presence of 1mM GTP. Labelled protein was purified using a PD10 column. Data was normalized for buffer. Sample was diluted 1:4 for spectroscopic analysis. The peak observed at 565nm corresponds to Atto-565 dye attached to the protein. **B:** Absorbance spectrum for GTP. Hence, absorbance at 280nm of GTP-bound TG2 is partially due to GTP, which has its maximum absorbance at 260nm.

Enzyme activity assay was repeated for the TG2 labelled in the presence of GTP, to find out if with the new labelling method could generate an active labelled enzyme. For this experiment, the concentration of calcium injected was increased to 10mM, to overcome the inhibitory effects of GTP and push the equilibrium for binding of allosteric co-factors towards GDP release and Ca^{2+} binding (Fig. 3.9). The isopeptidase assay showed that when labelling TG2 in the presence of GTP, the enzyme retained about 50-56% of its activity when compared to unlabelled control, even though the label density was comparable to that observed for the protein labelled in the absence of GTP (≈2.7 label/TG2 molecule).

A further experiment was conducted on a larger scale and similar results were observed (Fig. 3.9B). An enzymatically active labelled TG2 (≈1.22mg/ml) was obtained, which retained about 80% of its activity when compared to the wild type control. This percentage was higher than the one obtained in the previous experiment and might be related to the lower ratio of label to TG2 (0.78 label/protein).

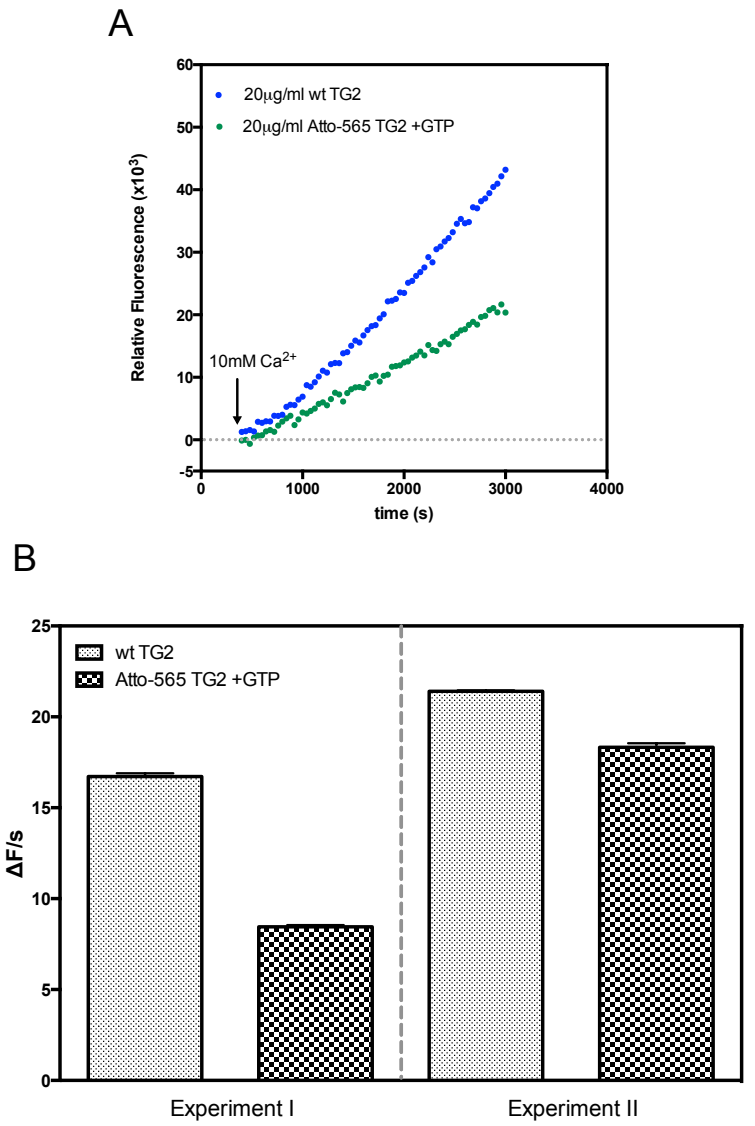

Fig. 3.9 Isopeptidase activity of TG2 labelled with Atto-565 in the presence of 1mM GTP. A: Enzyme isopeptidase activity of 20µg/ml TG2 following injection of 10mM Ca^{2+}. Data was normalized for well-specific fluorescence and control curve (no Ca^{2+}) subtracted to account for fluorescence bleaching: FLUOstar OPTIMA (gain 3000). Concentration of calcium injected was increased from 2mM to 10mM to compete for the inhibitory effect of GTP. Compared to unlabelled TG2 (blue), Atto-565 labelled TG2 (green) retained approximately 50% of its enzymatic activity. **B:** Comparison of fluorescence change for non-labelled and labelled TG2 calculated from linear regression (±SD) analysis of the data for the period between 1500s and 2500s in 2 independent experiments.

3.2.4 TG2 labelling: is influence of conformation label specific?

Being aware that label itself could also play a part in TG2 final conformation and enzyme activity I decided to repeat the labelling experiment using a chemically different Atto-NHS ester dye. Atto-647N also emits light in the red spectral region and has a maximum excitation of 644nm and a maximum emission of 669nm.

Even though Atto-565 and Atto-647N NHS-ester compounds react with proteins in the same way, they are chemically different (Fig. 3.10). Therefore, even though likely attached at the same or overlapping side chain permutations, the adjacent protein interactions may be very different, and hence, effect on overall protein structure be very different. Different structures could have an impact on enzyme activity. This experiment enabled the determination as to whether the lack of enzyme activity after labelling without GTP was label-dependent or not.

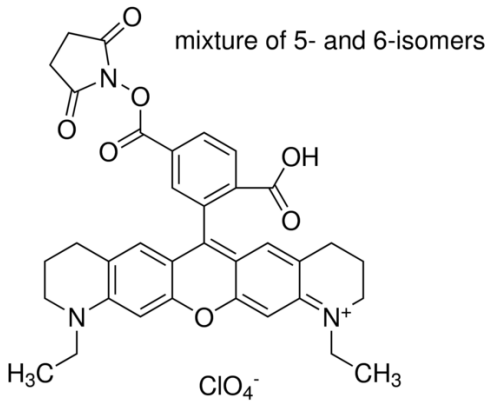

Atto-565 NHS ester

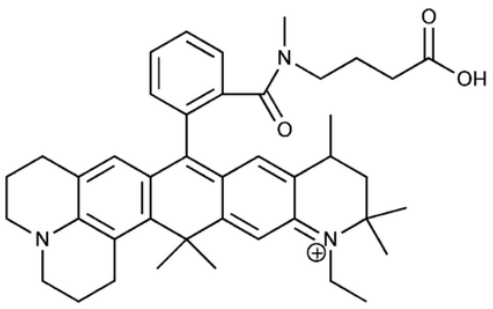

Atto-647N fluorophore

Fig. 3.10 Chemical structures of Atto-565 and Atto-647N dyes. Note details on Atto 647N NHS-ester compound were not publically available and therefore the unmodified dye is shown.

The labelling process was repeated in the same way as with Atto-565 NHS-ester dye, using 0.1M sodium phosphate as labelling buffer. Experiments were again performed in the absence/ presence of 1mM GTP.

Results obtained when labelling TG2 with Atto-647N were overall similar to the ones observed for the Atto-565 dye (Fig. 3.11). TG2 labelled in the absence of GTP was calculated to have a final concentration of ≈217μg/ml with a label density of 2.6 label/TG2. TG2 labelled in the presence of GTP was calculated to have a final concentration of ≈96μg/ml with a label density of 6.5 label/TG2 (higher than the one obtained in the previous experiment). As observed before, when labelling was performed in the absence of GTP, labelled protein seemed to lose its catalysis capacity, which was maintained if the nucleotide was present during labelling. When comparing the isopeptidase activity of the two Atto-647N-labelled proteins with its correspondent unlabelled control it was evident that labelled TG2+GTP had a relative activity 5x higher than its -GTP pair, despite its apparent higher label density (Fig. 3.11E).

A

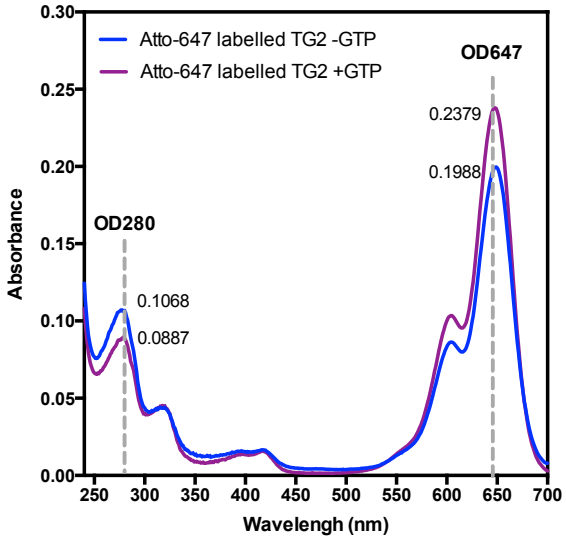
Atto-647 labelled TG2 -GTP
Atto-647 labelled TG2 +GTP
OD647
0.2379
0.1988
OD280
0.1068
0.0887
Absorbance
Wavelengh (nm)

B

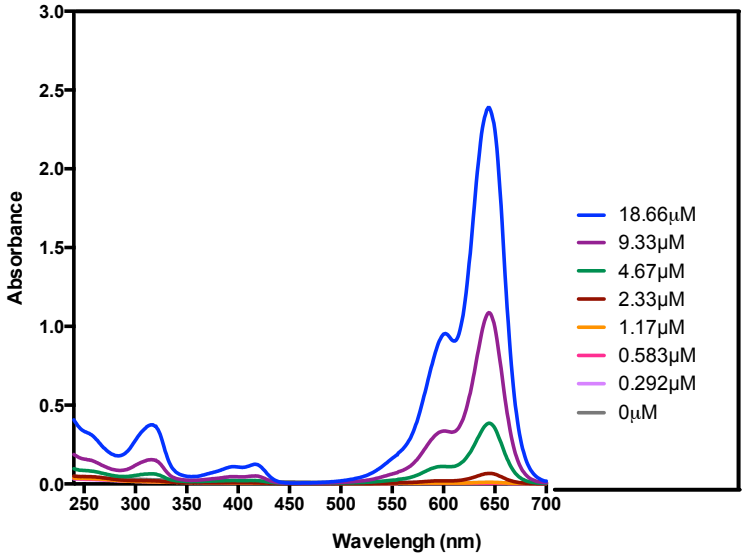
18.66µM
9.33µM
4.67µM
2.33µM
1.17µM
0.583µM
0.292µM
0µM
Absorbance
Wavelengh (nm)

C

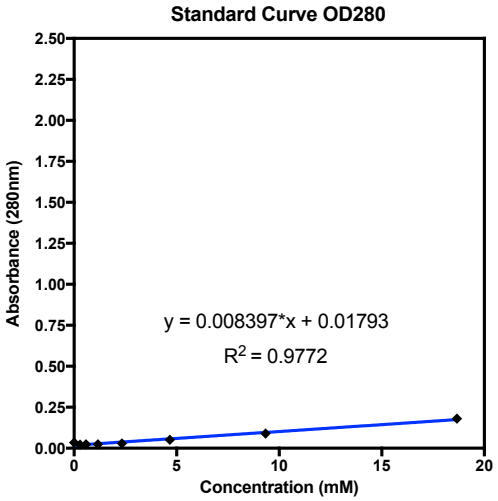
Standard Curve OD280
y = 0.008397*x + 0.01793
R2 = 0.9772
Absorbance (280nm)
Concentration (mM)

D

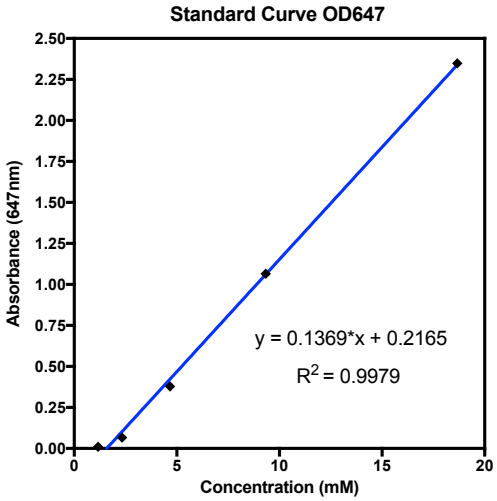
Standard Curve OD647
y = 0.1369*x + 0.2165
R2 = 0.9979
Absorbance (647nm)
Concentration (mM)

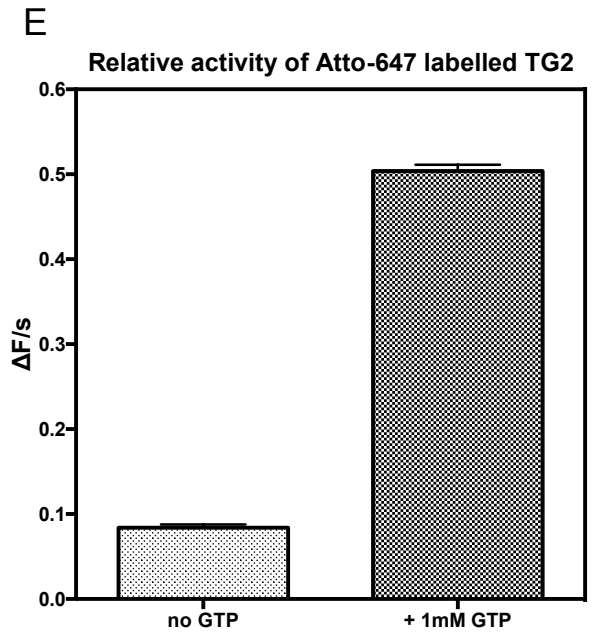

Fig. 3.11 TG2 labelling with Atto-647 N NHS ester. A: Absorbance spectrum for Atto-647 labelled rhTG2, labelled in the presence or absence f 1mM GTP. Data is normalized for buffer. Sample was diluted 1:4 for spectroscopic analysis. Labelled protein was purified using a PD10 Column. Successful labelling is indicated by the presence of a peak at 647nm corresponding to Atto-647 dye attached to the protein. **B:** Serial dilution of Atto-647N NHS ester. Molar concentration varies from 0 to 18.66μM. Dye was blocked by reaction with ethanolamine prior to analysis. **C:** Linear regression analysis of absorbance at 280nm for different dye concentrations. **D:** Linear regression analysis of absorbance at 647nm for different dye concentrations. Standard curves were used to calculate the label contribution to the protein absorbance at 280nm of a protein sample. **E:** Isopeptidase activity assay was carried out as in **Fig. 3.9**A. Comparison of relative fluorescence change for unlabelled TG2/ labelled TG2 calculated by linear regression (±SD) for the period between 1500s and 2500s. Atto-647 labelled TG2 retained little enzymatic activity (≈8%) when labelled in the absence of GTP.

3.2.5 Influence of temperature on conformation–specific labelling

Unfortunately, upon labelling it was evident that TG2 was aggregating at a higher rate than unlabelled protein with prolonged storage without freezing. TG2 aggregates were clearly observed as a pink deposit after centrifugation of labelled protein. As protein aggregation may be a significant factor contributing to loss of activity, it was decided to repeat the labelling process with Atto-565 dye but this time at a temperature of 4°C to prevent

protein aggregation. It is known that TG2 interaction with substrate at RT but not at 4°C render the protein prone to aggregation (presumably due to TG2 adopting the “open” conformation) (personal conversation with Professor Daniel Aeschlimann).

Buffer exchange of TG2 was performed using a PD10 column and 0.1M sodium phosphate buffer with pH adjusted to 7.6 at 4°C. The expected spectrum with maximum absorbance at 280nm was obtained (Fig. 3.12A). Since lowering the temperature was most likely going to slow the labelling reaction, the reaction time with NHS-ester was increased to 4h. Also, blocking time with 1M ethanolamine was increased to 1h. From the spectrophotometry wavelength scan (Fig. 3.12B) it was evident that both TG2 labelled in the presence and absence of GTP incorporated the Atto-565 label. Labelled TG2 -GTP was estimated to have a concentration of ≈780μg/ml and a label density of ≈4.4 label/protein. Labelled TG2 +GTP had a final estimated concentration of 930μg/ml and a label density of ≈6.4 label/protein, the highest label density obtained so far.

However, when performing the isopeptidase assay to assess protein enzymatic activity the results were not what was anticipated. Contrary to what was observed previously, TG2 labelled in the absence of GTP had some enzymatic activity (Fig. 3.12C). Although labelled TG2 -GTP was comparatively less active than labelled TG2 +GTP, the former retained ≈11% of its activity when compared to the unlabelled control. With labelling at RT, this value was close to 0. This suggests that the protein can be effectively labelled at 4°C while at the same time protecting protein functionality at least partially.

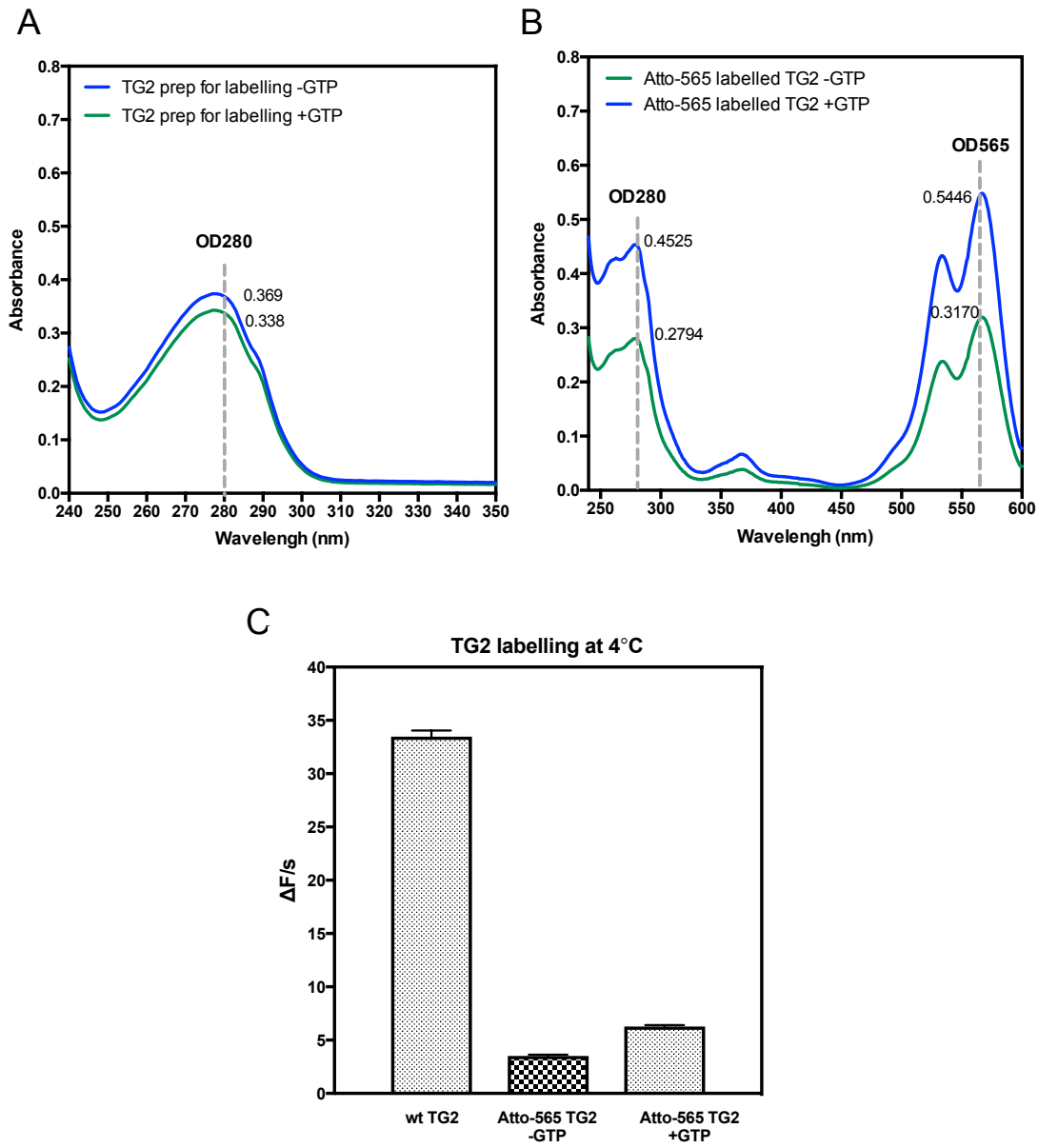

Fig. 3.12 Absorbance spectrum of TG2 labelled with Atto-565 at 4°C. A: ≈1mg of TG2 was applied to two PD10 columns each to enable protein buffer exchange. Fractions containing TG2 were pooled and samples were diluted 1:4 for spectroscopic analysis. **B:** Spectroscopic analysis of TG2 labelled +/- GTP at 4°C (data was normalized for buffer in graphs A and B). **C:** Isopeptidase assay was performed with generated labelled TG2 protein preparation as in **Fig. 3.9**A. Relative fluorescence change for unlabelled TG2 and TG2 labelled in the absence/presence of GTP was calculated by linear regression (±SD) for the period between 1500s and 2500s.

3.2.6 rhTG6 – protein purification

RhTG6 was expressed in *Spodoptera frugiperda*, SF9 insect cell line using a baculovirus expression system containing the human TG6 sequence with an added His_6-tag to the C-terminus. Insect cells were collected by centrifugation and resuspended in purification buffer. Expressed protein was harvested by lysis of insect cells using the Stansted pressure cell homogenizer. RhTG6 was purified from the lysate using Ni^{2+}-chelating affinity chromatography. Purified protein was analysed by SDS-PAGE under reducing conditions, followed by staining with Coomassie brilliant blue R (Fig. 3.13A). SDS-PAGE shows that the approach was successful in obtaining a single protein from the starting material with a molecular weight of ≈80kDa. Since it is known that TG6 has a calculated molecular weight of approximately 79kDa based on its sequence, this likely affirms that the band of purified protein corresponds to the protein of interest. The result is further confirmed by co-migration of this band in the gel with a TG6 standard. Purified TG6 was subjected to spectroscopic analysis, which showed a single peak with a maximum absorbance of around 270nm (Fig. 3.13B). The reason for the shift to lower wavelength of the absorbance maximum is unclear, but could be related to a nucleotide contamination, either specifically associated with the protein or in the form of DNA. Protein concentration was calculated to be 405μg/ml using absorbance at 280nm and Beer-Lambert law.

To ascertain that rhTG6 was enzymatically active, an isopeptidase activity assay was performed in a similar way as previously described with TG2. It has previously been shown that the quenched substrate is recognized by TG6 (Thomas et al. 2013). The assay showed a large increase in fluorescence over time after 2mM $CaCl_2$ injection, demonstrating enzyme activity (Fig. 3.13C). Water injection, as a negative control, showed the Ca2+-dependence of the reaction and thereby the assay specificity.

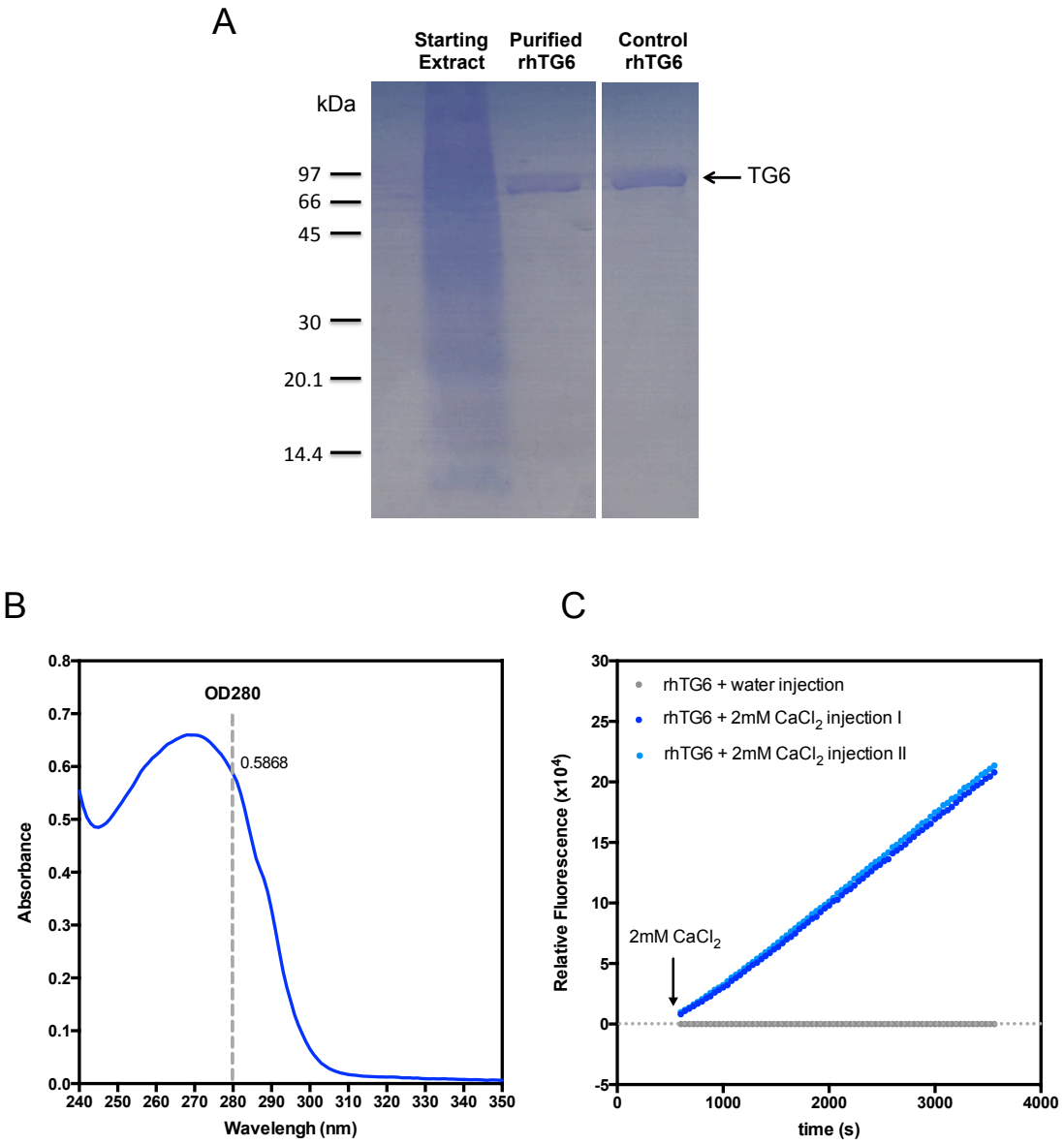

Fig. 3.13 Purification of rhTG6. A: SDS-PAGE (4-20% polyacrylamide gel) under reducing conditions showing starting material and final purified rhTG6 after staining with Coomassie blue R. When compared to the known TG6 standard it was evident that a purified band presented at the same molecular weight. Note. Samples were run on the same gel and cropping of the picture has not altered relative positions of bands. **B:** Absorbance spectrum of rhTG6 pool of purified protein corrected for associated buffer absorbance. Spectroscopic analysis of purified protein shows a single peak with maximum absorbance at ≈270nm. **C:** Enzyme isopeptidase activity of 20µg/ml TG6 following injection of 2mM Ca^{2+}. Data was normalized for well-specific fluorescence FLUOstar OPTIMA (gain 3000).

3.2.7 TG6 labelling with Atto-565 NHS ester (in solution)

Since the focus of the project was the role of TG6 in gluten related disorders, purified rhTG6 was labelled using the same principle as the approach described for rhTG2. As with labelled TG2, TG6 was labelled for future use in immunofluorescence assays.

The same 0.1M sodium phosphate buffer was used for the labelling process, but with the addition of 500mM NaCl, 10mg/ml sucrose and with the pH increased to 7.8. These conditions were previously found to preserve TG6 activity by researchers in our group. TG6 was buffer exchanged into sodium phosphate buffer using a PD10 column. Protein solution was cleared from any aggregates by centrifugation and spectroscopic analysis showed a non-aggregated protein, with maximum absorbance around 275-280nm, which was expected for highly pure protein (Fig. 3.14A). Labelling of TG6 was performed in solution with a 3-fold molar excess of Atto-565 NHS ester over protein and in the presence of 5mM GTP. A higher GTP concentration was employed due to the lower affinity of TG6 for GTP compared to TG2 (Thomas et al. 2013). Spectroscopic analysis of labelled TG6 showed that labelling of the protein was successful, as indicated by the presence of an absorbance peak at 565nm corresponding to the Atto dye (Fig. 3.14B). However, even though in principle successful labelling TG6 occurred, the modified protein appeared to aggregate at a high rate, showing a high degree of aggregation in the spectroscopic analysis immediately after completion of labelling reaction. Nevertheless, an isopeptidase assay was performed to assess labelled TG6 enzymatic activity. For this assay, the NaCl concentration of the reaction mixture was raised from to 125mM to 375mM, as a higher salt concentration is required for stability of TG6 (personal communication, Professor Aeschlimann). The activity assay showed a loss of activity of labelled TG6 when compared to its unlabelled control after 10mM $CaCl_2$ injection, with labelled TG6 retaining only ≈6% of its activity (Fig. 3.14C). There was also a loss of activity after buffer exchange of TG6, which highlights the sensitivity of TG6 to different chemical environments.

Labelled protein continued to rapidly aggregate over time and freezing of the samples lead to protein precipitation, making it impossible to use this material in our immunofluorescence assay.

3.2.8 TG6 labelling with Atto-565 NHS ester (on column)

To prevent loss of protein during buffer exchange step, it was decided to label TG6 while purifying it. It could be that, while attached to the nickel column TG6 has less flexibility to undergo conformational changes and therefore is less likely to aggregate.

RhTG6 was purified as described before, but this time, labelling of the protein was performed before the elution step from the Ni^{2+}-chelating column. TG6/sepharose slurry was washed twice with a buffer composed of 0.1M sodium phosphate, pH7.8 and 300mM NaCl to allow for labelling with Atto-565 dye. Total amount of TG6 present was extrapolated from previous purification experiments to be ≈500μg at ≈6.3μM. Based on this, a 3-fold molar excess of labelling reagent over protein was used, which was added to the 1ml volume of slurry. Labelling was performed for 1h at room temperature and protein purification continued as normal. Purified labelled TG6 was buffer exchanged to 10mM Tris pH 7.8 500mM NaCl, 10mg/ml sucrose using a PD10 column, for further analysis and storage. Spectroscopic analysis revealed a better quality protein (no aggregation) but also that labelling was not as efficient as expected (0.6 label/TG6).

Therefore, it was decided to increase the amount of label added from 3- to 10-fold molar excess, and to double the volume of the reaction mixture to achieve better mixing of the solid phase during the reaction. This change seemed to improve the labelling process. The results of three independent preparations of TG6 labelling are shown in Fig. 3.15A. Preparation I was calculated to have a final concentration of ≈160μg/ml and a ratio of ≈1.5 label/TG6. Preparation II was ≈290μg/ml and ≈1.2 label/TG6 and preparation III was ≈340μg/ml and ≈1 label/TG6. Overall the labelling of TG6 appeared to be quite reproducible. Although some aggregation was still evident from the spectra, this appeared to be minimal.

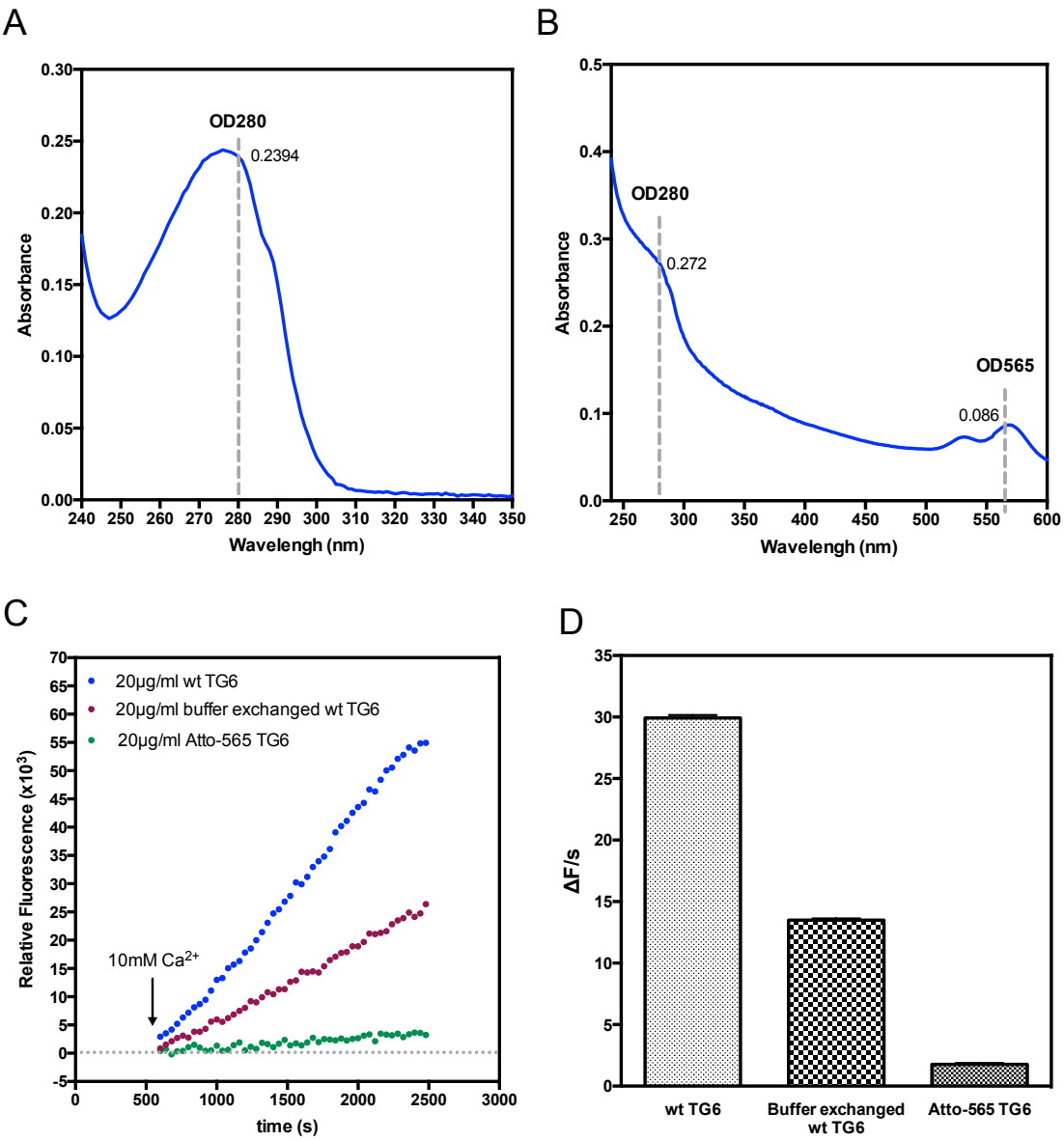

Fig. 3.14 Labelling of TG6 with Atto-565 NHS ester dye in solution. A: Absorbance spectrum of buffer exchanged TG6. Data normalized for buffer. **B:** Absorbance spectrum of Atto-565 labelled TG6. TG6 was labelled in the presence of 5mM GTP. Data normalized for buffer. Absorbance between 320nm and 450nm is indicative of protein aggregation (light scattering). **C:** Isopeptidase activity of unlabelled and Atto-565 labelled TG6. Data was obtained with ≈20µg/ml TG6, normalized for well-specific fluorescence and control curve without Ca2+-activation was subtracted to account for fluorescence bleaching: FLUOstar OPTIMA (gain 3000). Unlabelled buffer exchanged TG6 displays enzymatic activity but most of it is subsequently lost during labelling. Labelled TG6 retained only 6% of its activity when compared to the starting material control. **D:** Comparison of relative rate of fluorescence change for TG6, buffer exchanged TG6 and Atto-565 TG6 after 10mM $CaCl_2$ injection, obtained from linear regression (±SD) of the data for the period between 1250s and 2250s.

The labelled TG6 was subjected to the isopeptidase assay to evaluate enzyme activity. The three independent preparations of labelled TG6 displayed enzymatic activity, with relative activity varying from 16% to 43%, depending on preparation, when compared to its unlabelled control. Unlabelled TG6 was derived from the same TG6 preparation purified in parallel but omitting the labelling step.

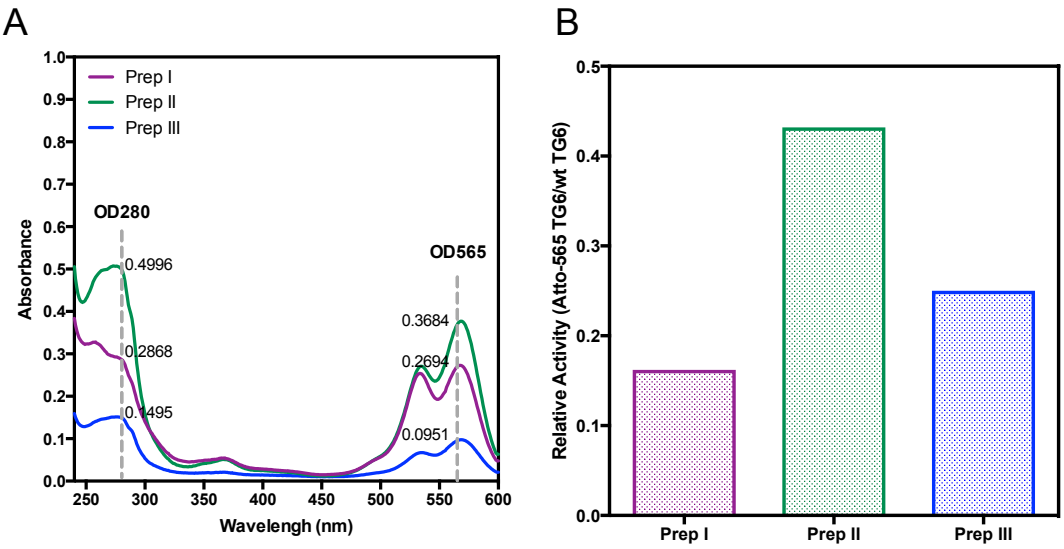

Fig. 3.15 On column Atto-565 labelling of TG6. A: Absorbance spectrum of Atto-565 labelled TG6 for 3 different preparations. Data normalized for buffer. The peak observed at 565nm corresponds to Atto-565 dye attached to the protein. **B:** Isopeptidase activity of ≈20μg/ml enzyme. Specific activity was derived as in **Fig. 3.14** and is expressed as relative activity compared to matched unlabelled protein.

Taken together, these data show that TG6 had been successfully labelled and purified for use in downstream assays.

3.2.9 TG6 labelling with Atto-565 – effects of labelling process on the protein

Although expression, purification and labelling of TG6 were quite successful, a rapid increase in aggregation over time was evident if the protein was stored at 4°C. Therefore, a batch of TG6 was monitored after labelling and purification process over a 3-day period (Fig. 3.16A). The initial

material was calculated to have a concentration of ≈94μg/ml. After 24h at 4°C an aliquot was taken and centrifuged for 10min at 16000x g to remove any aggregates. A pink pellet was detected in the tube after centrifugation. Spectroscopic analysis of the labelled TG6 showed a decrease in concentration of ≈18%. After 72h at 4°C, another aliquot was treated and analysed as before. At this time, although a pellet was not visible, the absorbance spectrum indicated high levels of aggregation of the protein, to an extent where further analysis was of no purpose and the experiment was therefore terminated. This showed that the labelled TG6 could not be stored at 4°C before use in downstream experiments.

In order to prevent loss of protein over time, another approach was attempted, and this involved TG6 lyophilisation. Unfortunately, loss of protein was still observed when reconstituting the protein into the original volume from the lyophilised form (Fig. 3.16B). As no suitable conditions for storage could be identified, the protein had to be prepared fresh for the planned immunofluorescence experiments.

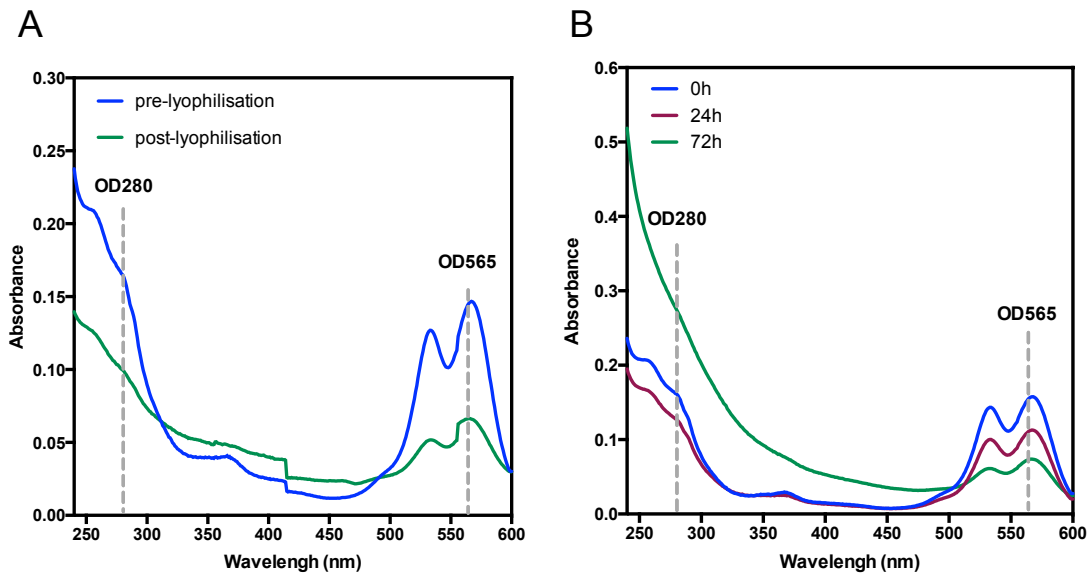

Fig. 3.16 Absorbance spectrum of Atto-565 labelled TG6. Data normalized for buffer. **A:** Spectroscopic analysis of labelled TG6 stored at 4°C over a 3-day period. A decrease in concentration was observed after 24h and high levels of protein aggregation were visible after 72h. **B:** Spectroscopic analysis of labelled TG6 before and after lyophilisation. Aggregation/loss of protein is visible after lyophilizing process.

3.3 Discussion

In this chapter, it was shown that successful labelling of the proteins involved in the autoimmune response in coeliac disease and gluten ataxia, i.e. TG2 and TG6 respectively, was achieved. The effects of fluorescent amine-labelling on TG2 functionality was analysed, with one of the most important findings being the positive effect that addition of the nucleotide GTP had on generating a labelled enzyme that was functional. This was important as autoantibodies have been shown to recognise antigen in a conformation-sensitive manner (Iversen et al. 2013; Seissler et al. 2001).

GTP is known to be an allosteric regulator of TG2, with the nucleotide having a negative regulatory effect that can be overcome by high concentrations of calcium (Venere et al., 2000). The TG2-GTP binding site has been shown to be located in a pocket between the first β-barrel and the catalytic core (Jang et al. 2014). The majority of the residues involved in GTP-binding come from the end of the first β-strand of the first β-barrel domain and the loop that connects it to the next β-strand (Arg476, Arg478, Val479, Ser482, Met483, Arg580, and Tyr583). Also, two residues from the catalytic core, Lys173 and Phe174, have been shown to contribute to the GTP interaction (Begg et al., 2006; Jang et al., 2014; S. Liu et al., 2002). In these experiments it was observed that reaction of TG2 with Atto-565 NHS ester led to absence of isopeptidase activity while the presence of GTP during labeling generated an enzymatically active protein.

More generally, NHS ester acts by reacting with primary amines, at the N-terminus or side chains of proteins. With 13 lysine residues present within the TG2 catalytic core alone it was possible that attachment of fluorescent label would result in structural changes that interfere with enzyme activation or catalysis. It could also mean that label-attachment blocks substrate access to the TG2 active site. That a more “open” conformation was linked to enzyme inactivation was supported by the fact that some isopeptidase activity was retained when labelling was performed at 4°C even in the absence of GTP. Lower temperatures reduce conformational transitions and hence reactions with residues available in the extended

conformation were substantially less likely. This interpretation is also consistent with the observation that the label density per protein molecule was not reduced under these labelling conditions. Hence, the availability of structurally/functionally critical residues must be the distinguishing factor.

GTP binding has been reported to cause a conformational change to TG2, shifting the protein to a closed conformation and burying the active site (Pinkas et al. 2007). With TG2 in a closed conformation and no access to the active site, labelling can only occur by reaction with lysines available on the surface of the protein. Such surface modification is apparently tolerated and an increase in substrate cleavage and release of quenched fluorophore is observed upon the conformational change induced by high concentrations of calcium. Jeon et al. have suggested that conformational changes caused by GTP binding may help maintaining enzyme stability physiologically, to display transamidation activity at high calcium concentration(Jeon et al. 2002).

Similar results were obtained when labeling TG2 using the same protocol but a chemically different fluorophore, Atto-647N NHS ester. As expected, when labeling was performed without incubation of the protein with GTP an enzymatically inactive TG2 was obtained, while pre-incubation of the protein with GTP led to an enzyme with isopeptidase activity. This result led to the conclusion that the lack of isopeptidase activity after labeling in the absence of GTP was not dependent on the nature of the fluorophore *per se* but the site at which the modification occurred, although both fluorophores used had relatively hydrophobic structures.

The same labeling principle was subsequently applied to the recognized gluten ataxia antigen, TG6. Initially, the same procedural approach was used as for TG2, i.e. attempted labelling of TG6 in solution. Even though buffer modifications were put in place and sucrose was added to stabilize TG6, this approach proved unsuccessful. Spectroscopic analysis of labelled TG6 showed high absorbance levels between 320nm and 450nm indicating substantial protein aggregation.

As the major problem appeared to be related with stability of TG6 in buffer conditions suitable for labelling, it was decided to label TG6 during its purification, when bound to a solid support. This approach prevents protein

aggregation during labelling and enables re-equilibration (refolding) of protein in appropriate buffer solution prior to elution from solid support. By this approach and a 10-fold molar excess of label over protein, a sufficiently high label density on TG6 (1-2 fluorophores per protein molecule) was obtained. Labelled TG6 showed isopeptidase activity using the in-house activity assay. Even though active, the specific activity of different preparation varied substantially, likely due to the propensity of the labelled protein to aggregate. It is unlikely that this result was related to excessive modification of protein with label as different preparations that had similar label/TG ratios had quite different enzymatic activity levels, and estimated label density was typically low (≈1-2 fluorophores per protein molecule). Instead, lower levels of activity were likely linked to protein aggregation.

TG6 seemed to be less stable after labelling with Atto dye as evident from the relatively rapid decrease in concentration of soluble protein and increase of aggregation over time. As no GTP was used during the solid-phase labelling process of TG6, Atto-565 could have modified the protein in critical positions that lead to protein insolubility. As these experiments were costly and of large experimental effort, no further optimization was undertaken, but a workable compromise adopted. Labelled TG6 was kept in the fridge and used for immunohistochemistry as soon as possible (within 24h) or frozen at -20°C. Although the freezing process led to loss of protein, such aggregates could be removed by centrifugation prior to the experiment and the concentration of the remaining soluble protein estimated from absorbance measurements. This proved to be a successful strategy, with results from downstream experiments being presented in chapter 5.

In conclusion a successful expression and purification of TG2 and TG6 was achieved. Furthermore, Atto-565 labelled TG2 and TG6 were produced, and they were shown to be enzymatically active.

Chapter 4 Transglutaminase: amine donor substrate binding and implications for deamidation reaction

4.1 Introduction

TG2 is the most widely expressed enzyme from the transglutaminase family in mammalian tissues. TG2's expression has been demonstrated at both intra and extracellular levels, with endothelial cells, smooth muscle cells and fibroblasts showing constitutive expression. In the context of autoimmune diseases TG2 has been recognized as the autoantigen in coeliac disease (Dieterich et al. 1997) as well as suspected to be involved in the pathogenesis of Alzheimer's, Parkinson's, Huntington's, osteoarthritis and breast and ovarian cancer (Iismaa et al., 2009).

Although there are numerous non-catalytic actions driven by TG2, the ability to introduce novel post-translational protein modifications in a calcium dependent way is what seems to relate this enzyme to so many autoimmune responses. In fact, the involvement of TG2 in the pathological process of coeliac disease is related to deamidation of gluten peptides (Arentz-Hansen et al. 2000) and formation of TG2-gluten complexes that culminates in the activation of gluten-specific T cells. These can then provide help to TG2-specific B cells and lead to production of antibodies against the self protein (Sollid 1997).

Amongst the types of post-translational protein modifications, TG2 is able to catalyse transamidation and hydrolysis of proteins and peptides. The enzyme active site, Cys277, initially targets a glutamine-containing protein or peptide resulting in a thiol-ester bound acyl-enzyme intermediate and release of ammonia (Folk, 1983). In a second step the intermediate complex can be attacked by an amine donor substrate (primary amines) resulting in a transamidated product. In some instances, water can replace the amine donor substrates driving the reaction towards hydrolysis. This leads to deamidation of the uncharged substrate glutamine and its conversion into the charged residue glutamate. Deamidation can also be a by-product of isopeptidase of an already cross-linked polypeptide.

Although it is known that deamidation of proteins by TG2 occurs, it still remains to be clarified why the protein has preference for this reaction, as the rich presence of primary amines would favour transamidation.

Boros et al. reported the TG2 selective deamidation of a glutamine residue in the small heat shock protein 20 (Hsp20) under conditions where other glutamine residues were transamidated (Boros et al. 2006). These results suggest that transamidation and also deamidation could be influenced by both substrate and reaction conditions. Stamnaes et al. also demonstrated that direct deamidation reactions in the presence of an acyl-acceptor were conditioned by peptide sequences as well as enzyme concentration. Good TG2 substrates were more prone to transamidation, and poorer substrates had a higher ratio of deamidation to transamidation (Stamnaes et al. 2008). Furthermore, these researchers also reported that TG2 could hydrolyse isopeptide bonds where both the acyl-donor and acyl-acceptor were peptides.

Previous work performed within our group (by Adamczyk) showed that a large difference in the concentration of two different amines (glycine methylester and Nα-acetyllysine methylester) was necessary to produce a transamidated product in TG2-mediated conversion of an already cross-linked substrate (Adamczyk, 2013). This suggests that the nature of the amine has an impact in the preference for transamidation or deamidation reactions by TG2.

Although a structure of TG2 in complex with an inhibitor that mimics a gluten-peptide has been solved (Pinkas et al. 2007), information on how amine-donor substrates interact with the enzyme is still lacking.

In this chapter, a series of experiments was undertaken leading to the suggestion that inhibited TG2 specifically interacts with an amine donor substrate. This culminated in an attempt to crystalize the enzyme complex. By solving this crystal structure, elucidation of how the nature of an amine donor substrate could lead to a transamidation or deamidation reaction could be forthcoming. Therefore, a report on TG2 interaction with different amine donor substrates could be beneficial for novel therapeutic targets in the context of gluten-related disorders.

The aims of the chapter:

1. To characterize inhibited rhTG2 by assessing its catalytic activity using a fluorogenic activity assay and an in gel enzyme assay and to compare it against wild-type and mutant forms.
2. To report on TG2 interaction with different amine donor substrates by crystallizing inhibited TG2 in the presence of two different amines.

4.2 Results

As shown in the previous chapter, TG2, when labelled in the absence of GTP, had no enzymatic activity in an isopeptidase assay. In contrast, TG2 labelled in the presence of GTP was enzymatically active. The fact that these results were observed for chemically different Atto-565 and Atto-647N labels (Fig. 4.1) suggests that this was not due to the presence of a particular fluorophore and that labelling was not a random event.

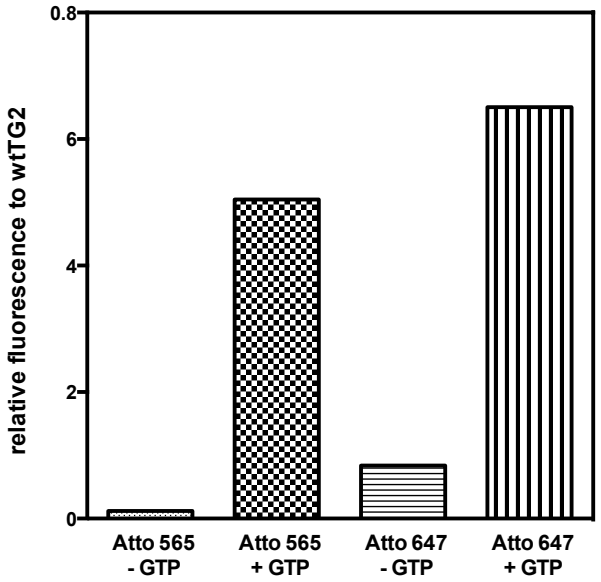

Fig. 4.1 Isopeptidase activity for TG2 labelled in the presence/absence of GTP. Each column represents relative fluorescence between labelled TG2 and wt TG2 after 2mM calcium injection. Linear regression slopes were used for calculations. Relative fluorescence demonstrates higher levels of enzymatic activity for the protein labelled in the presence of GTP when comparing to the one labelled in the absence of the nucleotide.

The above finding raised the question as to why GTP-bound TG2 was resistant to inactivation during protein labelling and as an extension to this, could there be a conformational difference between the active and inactive labelled TG2.

4.2.1 Structural differences of labelled TG2

It was suspected that the absence of GTP led to labelling at specific sites that could influence the conformation of the enzyme and hence prevent the catalytic cycle. It was therefore decided to run TG2 preparations, labelled in the presence and absence of GTP, on a native polyacrylamide gel electrophoresis (PAGE). A native PAGE is a non-denaturing type of electrophoresis. Here, molecules are separated based on both their charge-to-mass ratio and also their overall structure. This allows the analysis of proteins in their native conformation, as both the conformation and biological activity of proteins remain intact. One disadvantage of this method is that proteins may not separate in a predictable way, perhaps even remain as protein complexes (they cannot move through the polyacrylamide gel as quickly as SDS-bound, denatured proteins). Furthermore, it is important to keep the equipment cool to minimize the effects of heat denaturation and proteolysis in order to maintain the integrity of proteins during electrophoresis. The main advantage of this technique is that, because proteins remain in the native state, they may be visualised not only by general protein staining reagents but also by specific enzyme-linked staining.

To confirm that adding GTP prior to labelling had an effect on the overall structure of the protein and therefore its enzymatic activity, preparations of TG2 labelled in the presence or absence of GTP were run along side unmodified wild type control TG2 and a commercially purchased TG2 (T051 Zedira, Germany), conjugated with an inhibitor at the active site Cys residue in order to stabilize the open conformation. To determine whether the enzyme bound GTP and subsequently adopted the closed conformation, labelled TG2 preparations were incubated with an additional 600μM of GTP for 1min and, where indicated, 25μM of GTP was added to the running buffer to maintain GTP saturation during electrophoresis. The gel was analysed using the appropriate filters for the fluorophores using a phosphorimager to visualise labelled TG2. Gels were subsequently stained for total protein with Coomassie Blue R.

When comparing wt TG2 to open TG2 it was observed that they ran in similar positions in the absence of GTP (Fig.4.2). However, when GTP was added, a shift in the position of wt TG2 was observed, which was not true for the other form of the enzyme, as being covalently bound to the inhibitor, it cannot bind GTP.

Analysis of labelled TG2 showed a shift in the protein position when samples were pre-incubated with GTP. Additionally, there seemed to be a difference in the proportion of the protein able to bind GTP when comparing TG2 labelled in the presence as opposed to the absence of the nucleotide (Fig 4.2). The fraction of labelled TG2 capable of binding GTP was identified by the condition-dependent switch in migrating position, i.e. it ran at the same level as the wt control. Such results led us to the view that it is the enzyme able to bind GTP that constitutes the active fraction in the preparation.

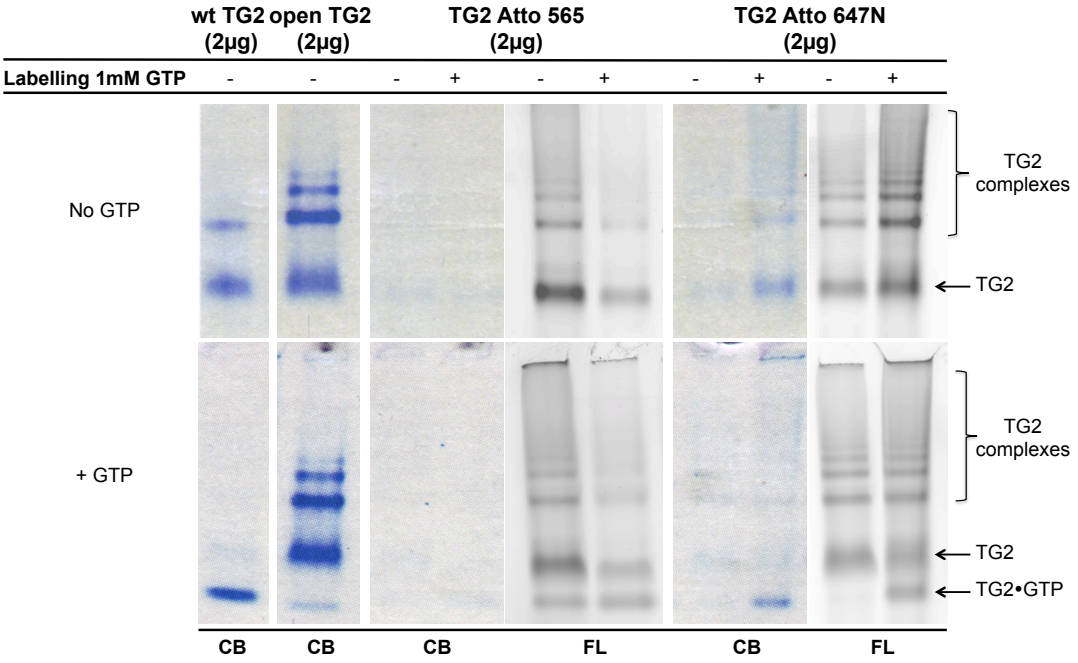

Fig. 4.2 Native PAGE for different variants of TG2. Atto-565 and Atto-647N labelled TG2 were run alongside wt and open TG2. The top panel correspond to the samples where no GTP was added prior to or during electrophoresis. The bottom panel corresponds to samples where 600µM GTP was added prior to electrophoresis. To maintain GTP saturation, 25µM GTP (final concentration) was added to the running buffer on the bottom panel. Coomassie blue R staining is shown as a blue colour. Fluorescence (grey colour) of Atto-565 labelled TG2 was visualized using a combination between the 532nm laser line excitation and a 560nm long pass filter for emission (PMT=470V). For Atto-647N labelled TG2 a 633nm laser line excitation and the 670BP30 filter for emission (PMT=430V) were used. The native electrophoresis showed that labelling in the absence of GTP resulted in enhanced loss of GTP-binding capacity. BP= band pass; PMT = photomultiplier tubes

4.2.2 Analysis of FITC-cadaverine incorporation of TG2

It was suspected that the band observed at a lower position in the gel when adding GTP was the active fraction of the labelled TG2. To understand if this hypothesis was correct, an 'in gel' enzyme activity assay was performed using the FITC-conjugated substrate, cadaverine. Cadaverine is a diamine compound that will act as an amine donor substrate for TG2 by mimicking a lysine side chain. Incubation of the gel with FITC-cadaverine, under appropriate conditions, enables the analysis of activity of different fractions of the enzyme within the gel. This is possible because TG2 has the ability to cross-link with the substrate and itself. That way, enzymatically active TG2, will be covalently modified with the fluorescent substrate.

The different variants of TG2 were run on a native PAGE in the presence of GTP, as previously shown. The gel was then incubated with a buffer solution containing calcium to activate the enzyme and allow substrate binding. After extensive washing over a 24h period, the gel was analysed for FITC fluorescence using a variable mode imager.

As previously observed, there appeared to be a shift in the migration position of the protein when labelling was performed in presence of GTP that does not appear in TG2 labelled in absence of the nucleotide. This was true for both Atto-565 and Atto-647N fluorophores (Fig. 4.3A), whereby the faster migrating bands correspond to the GTP-bound form of TG2. The retarded bands (higher position in the gel relative to TG2) correspond to TG2 complexes. When comparing Atto-565 or Atto-647N with the correspondent FITC-cadaverine labelling, it was evident that the faster migrating bands mentioned (TG2•GTP) actually corresponded to the active TG2, as they were the only bands where the enzyme interacted with the FITC-conjugated amine donor substrate.

FITC-cadaverine is expected to be covalently cross-linked to TG2 through the autocatalytic action of the enzyme. This result is confirmed by wild type TG2, which shows a strong band in the same position for FITC labelling (Fig. 4.3A). To further confirm this result, a second experiment was performed with an independently labelled batch of enzyme. This time, two

separate native PAGE gels were run, with and without the presence of 25μM in the running buffer (Fig. 4.3B). Results showed that a shift of the protein was only visible when the saturation of GTP in the gel was maintained (Fig. 4.3B right panel). This was true for wt TG2 and all variants of labelled TG2, even when pre-incubated with GTP. However, enzyme activity was demonstrated for the proteins labelled in the presence of GTP independent of whether GTP was present during electrophoresis. The difference in band intensity appears to be due to the 'sharpness' of the bands (compared to Coomassie blue) consistent with GTP promoting adoption of a defined, compact conformation. An interesting result was that a band shift was still observed for Atto-565 TG2 even though the protein was not previously incubated with GTP. Also, for Atto-565 labelled TG2 in the absence of GTP, a proportion remained GTP-sensitive (Fig. 4.3B right panel). This was an unexpected result, as the protein should not have the capacity to bind GTP. This might be related to residual non-labelled TG2 that was not affected by the labelling process and therefore subsequently behaved as wt TG2.

Another surprising result was that the irreversibly inhibited open TG2 also 'reacted' with the amine substrate (Fig. 4.3A right panel). It was speculated that either inhibitor conjugation was incomplete or the enzyme conformation represented by this "open form" had a high-affinity binding site for the amine donor substrate and therefore bound FITC-cadaverine non-covalently. To test if the FITC-cadaverine was non-covalently bound to the open TG2, different variants of TG2 were incubated *in vitro* with FITC-cadaverine in the presence of Ca^{2+}. The samples were analysed by SDS-PAGE (Fig. 4.3C). As this is a type of denaturing electrophoresis, if the cadaverine was not covalently bound to TG2, it should run in the gel front due to its low molecular mass. Along with open TG2 and wt TG2, two TG2 mutants were analysed. The TG2 C277S has a modified active site and therefore is enzymatically inactive. However, it should be able to bind glutamine donor substrate. The TG2 E329G is a Ca^{2+}-binding site mutation. Since calcium is required to bring about a conformation that harbours enzymatic activity, this variant was not expected to bind either the glutamine donor or the amine-donor substrate. The SDS gel showed that only the open

and wt TG2 were able to bind the substrate, presumably in a covalent way, as the FITC label was only detected in bands corresponding to these variants (Fig. 4.3C). Furthermore, the assay was specific, as Ca^{2+}-binding and active site mutant TG2 displayed no cadaverine incorporation. These results suggested that open TG2 had considerable residual activity, and that this contributed to the unexpected labelling in the ‘in gel’ assay (Fig. 4.3A).

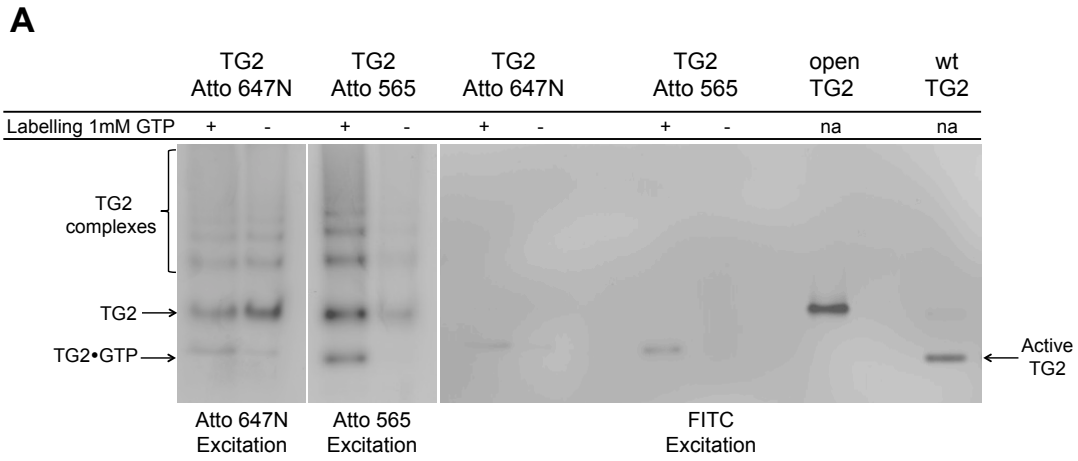
A
TG2 Atto 647N
TG2 Atto 565
TG2 Atto 647N
TG2 Atto 565
open TG2
wt TG2
Labelling 1mM GTP
+ - + - + - + - na na
TG2 complexes
TG2
TG2•GTP
Active TG2
Atto 647N Excitation
Atto 565 Excitation
FITC Excitation

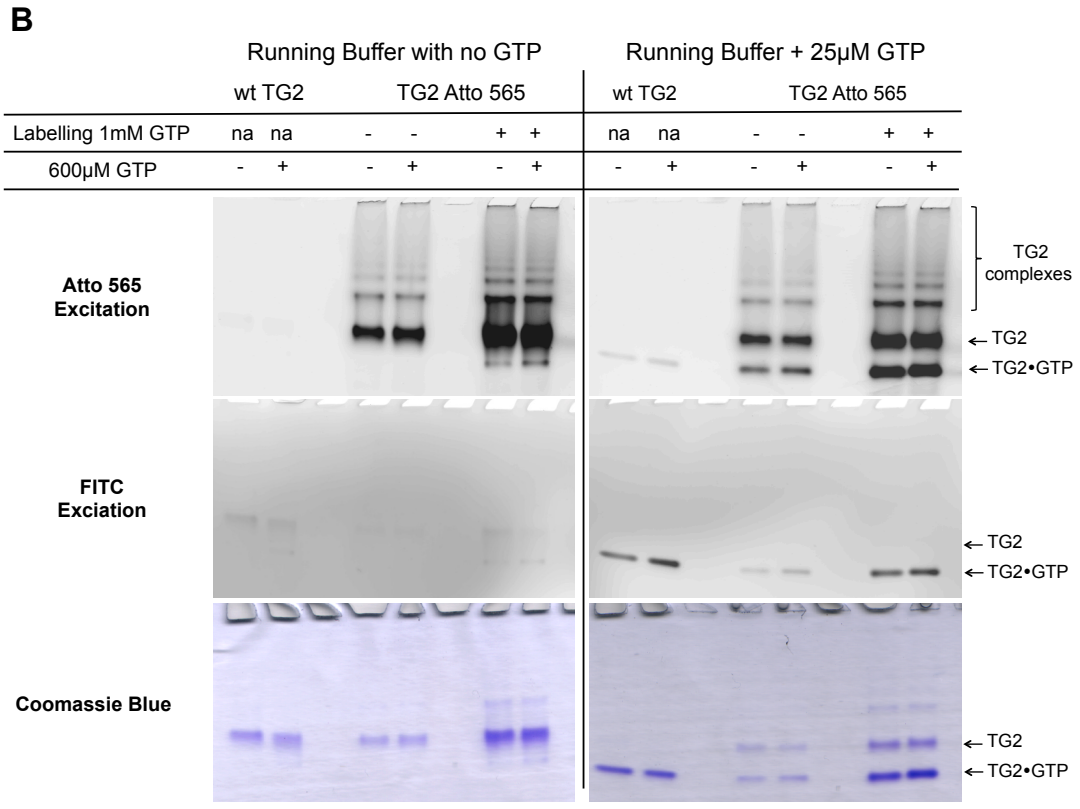
B
Running Buffer with no GTP
Running Buffer + 25μM GTP
wt TG2
TG2 Atto 565
wt TG2
TG2 Atto 565
Labelling 1mM GTP
na na - - + + na na - - + +
600μM GTP
- + - + - + - + - + - +
Atto 565 Excitation
FITC Exciation
Coomassie Blue
TG2 complexes
TG2
TG2•GTP
TG2
TG2•GTP
TG2
TG2•GTP

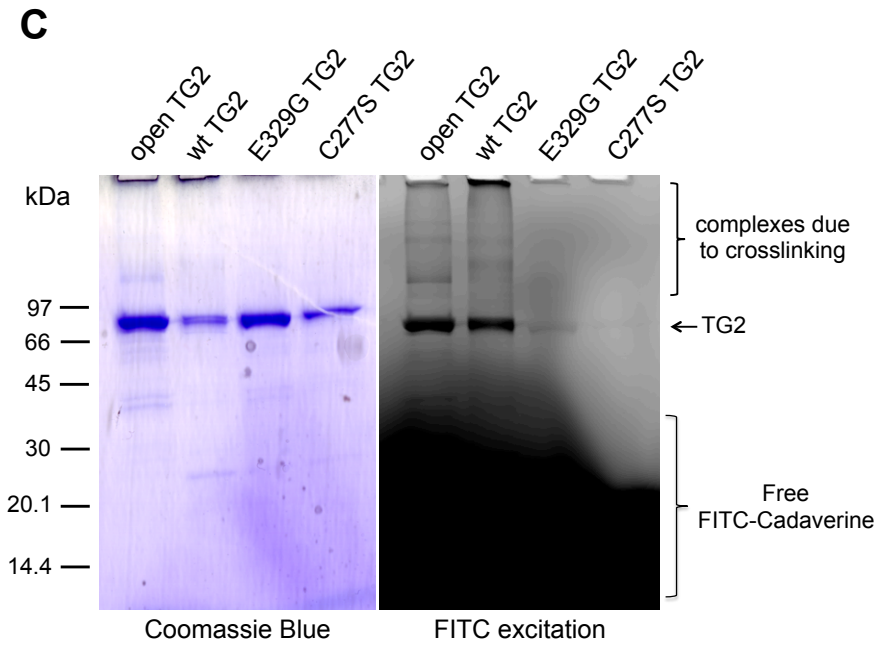

Fig. 4.3 'In gel' TG2 enzymatic activity as determined with FITC-cadaverine. A: 2μg of labelled TG2 were separated on a native PAGE, wt and open TG2 were used as controls. Samples were pre-incubated with 600μM GTP and electrophoresis was carried out in the presence of 25μM GTP. Gel was incubated with FITC-cadaverine solution in the presence of 10mM Ca^{2+}. The first panel corresponds to Atto-647N labelled TG2 visualized using a 633nm laser line for excitation together with a 670nm band pass filter for emission (PMT=450V). The second panel corresponds to Atto-565 labelled TG2 visualized using a 532nm laser line for excitation and a 560nm long pass filter for emission (PMT=500V). These images were captures prior to labelling with FITC-cadaverine. For visualization of FITC (third panel) a 488nm laser line was used for excitation and a 520nm band pass filter for emission (PMT=500V) Results show that the shifted band observed for both Atto-647N and Atto-565 labelled TG2 +GTP is the active fraction of the protein, as it incorporated the FITC-cadaverine. **B:** To prove that results were not influenced by addition of GTP, a second experiment was conducted where samples were pre-incubated +/-600μM GTP and electrophoresis was performed +/- 25μM GTP. A shift of the band was only observed in samples were GTP saturation was maintained during electrophoresis (right panel). These bands were also the ones able to react with the fluorescent amine substrate. **C:** SDS-PAGE of TG2 variants incubated *in vitro* with FITC-cadaverine substrate in the presence of 10mM Ca^{2+}at 37°C for 30min. Coomassie blue R staining is shown on the left, FITC-fluorescence on the right (for details see A). Enzymatically inactive TG2 mutants were not able to bind FITC-cadaverine covalently. Reaction of the fluorophore with open TG2 suggests this protein to have a considerable amount of residual activity.

4.2.3 Inhibition of TG2 with B003

To overcome the problem of residual activity of commercially purchased inhibited-TG2 and thereby verify whether interaction of FITC-cadaverine with the open TG2 relates to this residual activity or non-covalent binding, it was decided to generate our own rhTG2 in the open conformation. The compound tert-Butyloxycarbonyl-(6-Diazo-5- oxonorleucinyl)-LGlutaminyl-L-Isoleucinyl-L-Valinmethylester, a site specific irreversible inhibitor of TG2 known as B003 (Zedira, Germany) was purchased.

The TG2 protein was inhibited in two steps with a buffer containing 50µM B003, a 10-fold molar excess over protein. A solution containing 10mM $CaCl_2$ +/- 1mM putrescine was added in the second step. Ca^{2+} activation was employed to allow substrate access to the active site. Putrescine, like cadaverine, is a high affinity TG2 amide donor substrate (Folk & Finlayson, 1977). It was added to the reaction as a substrate 'competitor', to investigate if after adding this amide donor substrate the inhibited protein was still able to bind FITC-cadaverine. If the inhibited transamidation intermediate of the enzyme bound amide donor substrate strongly and the off-rate was very slow as suspected from previous experiments, then competition should be highly effective. Thereafter, inhibited TG2 as well as wt TG2, as a control, was rebuffered to remove free inhibitor and kept on ice until needed. An isopeptidase assay was performed to compare levels of enzymatic activity between wtTG2 and inhibited variants. Inhibited TG2, +/- putrescine, both showed little or no activity when compared to the wt control (Fig. 4.4A), leading to the belief that inhibition was successful. The inhibited proteins were also subjected to native PAGE analysis along side wt TG2 as a control. After electrophoresis, the gel was incubated with FITC-cadaverine as before (Fig. 4.4B) to assess transamidation activity/amine donor substrate interaction. As expected our control wt TG2 was able to bind and crosslink to the cadaverine. Although both variants of inhibited TG2 were shown to be inactive in the isopeptidase assay, some level of fluorescence in the 'in gel' assay was still detectable. Coomassie blue staining revealed that the inhibited TG2 preparations contained significant levels of protein complexes.

Given that the reaction was carried out at room temperature it was likely that autocatalytic crosslinking readily occurring in the presence of high Ca^{2+} concentrations was responsible for TG2 complex formation. However, it was also possible that the transamidation intermediate, open conformation TG2, was less stable and therefore formed non-covalent aggregates. These results were found to be inconclusive, as both the low levels of fluorescence in the gel assay and low enzymatic activity in the isopeptidase assay for inhibited protein could be related to TG2 complex formation and not the inability of the monomeric protein to bind or react with cadaverine.

A second experiment was carried out, this time with the addition of N-Voy to prevent protein aggregation. N-Voy are commercially available linear, uncharged, carbohydrate polymers with highly amphipathic properties. They are around 5kDa and designed to increase protein solubility whilst preventing aggregation. Their working mechanism is by association at multiple points with surface exposed hydrophobic patches of proteins to form multipoint reversible complexes (Expedeon, n.d.).

To assess the ability of N-Voy to prevent protein aggregation, 10µg of wtTG2 were incubated in the presence and absence of 50µg of N-Voy. As temperature is a critical factor in protein aggregation, incubation was carried out at either 4°C or 37°C. B003-inhibited protein was also incubated with N-Voy to test whether these carbohydrate molecules could prevent protein aggregation. The samples were analysed through native PAGE followed by incubation with FITC-cadaverine in the presence of Ca^{2+} (Fig. 4.4C).

When analysing wtTG2 incubated without N-Voy it was evident that temperature had a dramatic effect on protein aggregation. At 37°C, there was a high degree of protein aggregation, and this was not observed if the experiment is carried out at 4°C. Unfortunately, protein incubated in the presence of N-Voy showed up as a smear in the native gel, which indicated that, although the polymer bound to TG2 and stabilised it, it interfered with the electrophoretic separation of the protein into a distinct species and therefore was not suitable for our assay.

Since high temperatures seemed to have a negative effect on TG2 integrity, it was decided to perform the inhibition process at 4°C. TG2 (5µM in

25μl reaction volume) was inhibited by 50μM B003 at 4°C, followed by further inhibition in the presence of calcium in a second step. The inhibited protein was subsequently subjected to the isopeptidase assay as before (Fig. 4.4D). Results showed that inhibition of TG2 was successful, as inhibited protein showed no measurable activity.

To further confirm successful inhibition of TG2, inhibited TG2 (incubated at 4°C), wtTG2, open TG2 (commercial) and mutant E329G were incubated, *in vitro*, with FITC-cadaverine in the presence of 10mM $CaCl_2$ or 1mM EGTA and then separated on a SDS-PAGE to assess if FITC-cadaverine was covalently bound (Fig. 4.4E). TG2 E329 has a mutation in a glutamic acid residue that is essential for calcium binding to convert the enzyme into its active form. As expected, FITC-cadaverine binding was observed for wt TG2 incubated in the presence of calcium at both temperatures. Evidently reaction rates differed at these two temperatures, which can be clearly appreciated by the size and level of complex formation as well as loss of TG2 monomers. As expected, E239G mutant didn't show any incorporation of the substrate. Both commercially available and in house generated 'open' TG2 appeared to readily react with FITC-cadaverine but only when incubated in the presence of calcium at 37°C and this coincided with formation of covalently cross-linked complexes. Since inhibited TG2 incubated at 4°C did not show any measurable enzymatic activity, it was thought that the apparent association with cadaverine at 37°C might be related to residual activity. Although effective, conversion of TG2 into the inhibited 'open' conformation was clearly incomplete.

A

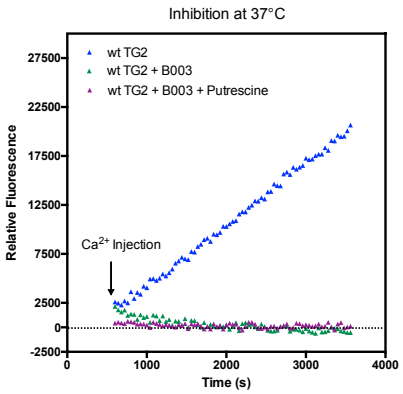
Inhibition at 37°C
wt TG2
wt TG2 + B003
wt TG2 + B003 + Putrescine
Relative Fluorescence
Ca2+ Injection
Time (s)

B

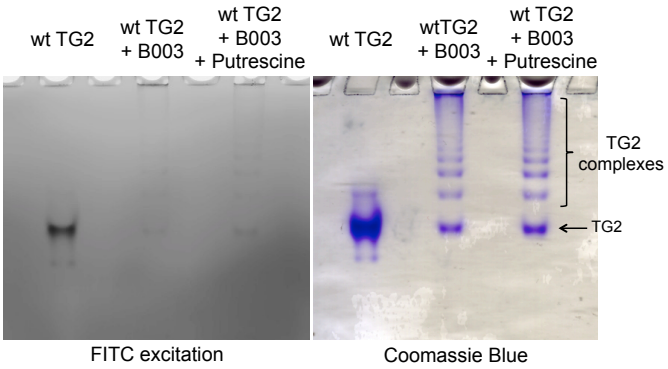
wt TG2
wt TG2 + B003 + Putrescine
wt TG2
wtTG2 + B003
wt TG2 + B003 + Putrescine
TG2 complexes
TG2
FITC excitation
Coomassie Blue

C

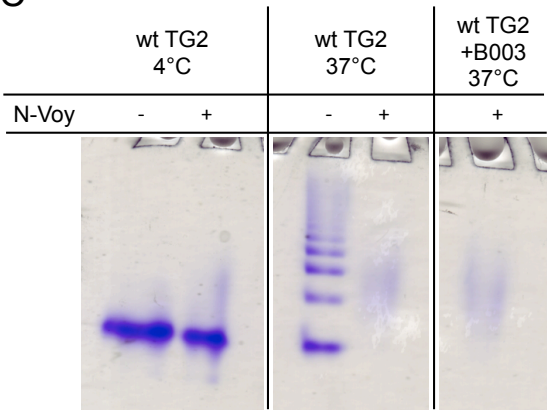
wt TG2 4°C
wt TG2 37°C
wt TG2 +B003 37°C
N-Voy
-
+
-
+
+

D

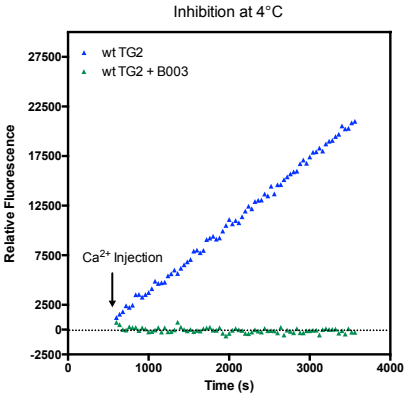
Inhibition at 4°C
wt TG2
wt TG2 + B003
Relative Fluorescence
Ca2+ Injection
Time (s)

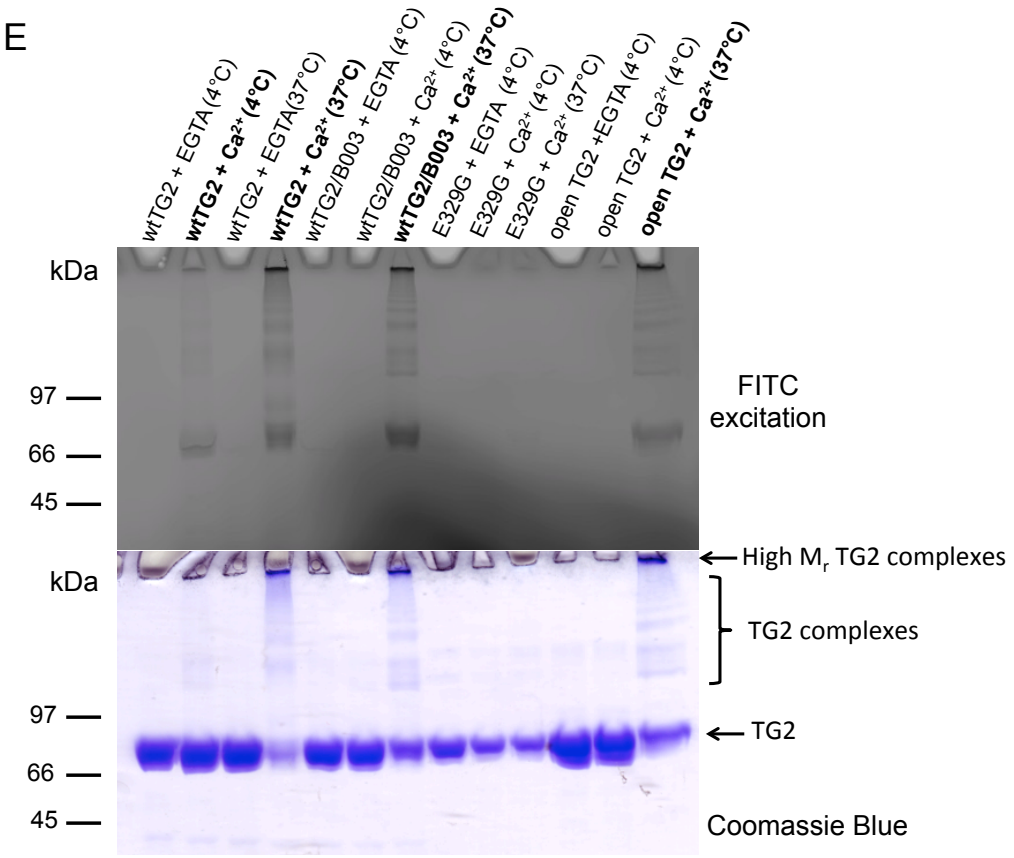

Fig. 4.4 Inhibition of TG2 with B003 compound. A: Isopeptidase activity of wtTG2 compared to B003 inhibited TG2 preparations +/- putrescine. Data for enzyme activity of 20µg/ml TG2, normalized for well-specific fluorescence and following subtraction of control curve to account for fluorescence bleaching: FLUOstar OPTIMA (gain 3000). Increasing of fluorescence over time following Ca^{2+} activation indicates that only wtTG2 is enzymatically active. **B:** Native PAGE of wt and B003 inhibited TG2 followed by 'in gel' activity assay with FITC-cadaverine. In both B and E, FITC-staining was visualized using a combination of the 488nm laser line for excitation and a 520nm filter for emission (PMT=500V). After visualising fluorescence, gel was stained with Coomassie Brilliant Blue R to visualise proteins **C:** Native PAGE of wt and B003 inhibited TG2 in the presence/absence of polymer N-Voy at 4°C and 37°C. N-voy seems to vastly alter electrophoretic mobility of TG2. **D:** Isopeptidase activity of wtTG2 against 4°C B003 inhibited TG2. Data for enzyme activity of 20µg/ml TG2, normalized for well-specific fluorescence and following subtraction of control curve to account for fluorescence bleaching: FLUOstar OPTIMA (gain 3000). Inhibition of TG2 was successful as there is no apparent activity. **E:** Different TG2 preparations were incubated with FITC-cadaverine in the presence of 10mM $CaCl_2$ or 1mM EGTA at either 4°C or 37°C for 20min. Thereafter proteins were separated on a 4-20% SDS-PAGE gel under reducing conditions and detected by visualising FITC-fluorescence followed by Coomassie blue R staining. Lanes in bold show FITC-bound protein.

4.2.4 Multiple step inhibition of TG2 with B003

To tackle the fact that binding of FITC-cadaverine by 'open' TG2 could be due to residual activity it was decided to drive inhibition of TG2 with B003 to completion using a multiple step approach. Ten different steps of inhibitor treatment were undertaken (Table 4.1) and remaining activity was assessed by *in vitro* incubation with FITC-cadaverine in the presence of calcium. Protein was incubated for 15min periods with B003 and temperature was increased according to the steps detailed in Table 4.1. A separate inhibition of TG2 with 250μM B003 was also performed in two steps. Firstly TG2 was incubated with 250μM B003 for 30min at 4°C and then incubated with another 250μM B003 in the presence of 10mM $CaCl_2$ for 30min at 37°C. All inhibited samples and control wt TG2 were incubated with FITC-cadaverine *in vitro*, and then separated on a SDS-PAGE.

Table 4.1 Steps employed for successive inhibition of TG2.

Step	Temperature	Reagents added
1	4°C	+ 50μM B003
2	4°C	+ 50μM B003 + 10mM $CaCl_2$
3	4°C	+50μM B003
4	10°C	+50μM B003
5	10°C	+50μM B003
6	20°C	+50μM B003
7	20°C	+50μM B003
8	37°C	+50μM B003
9	37°C	+50μM B003
10	37°C	+50μM B003

Results showed a decrease in residual activity with increasing B003 inhibitor over the first 7 steps of inhibition (Fig. 4.5). However, a single inhibition with 250μM of B003 seems to be as effective as 7 consecutive steps of inhibition with 50μM B003.

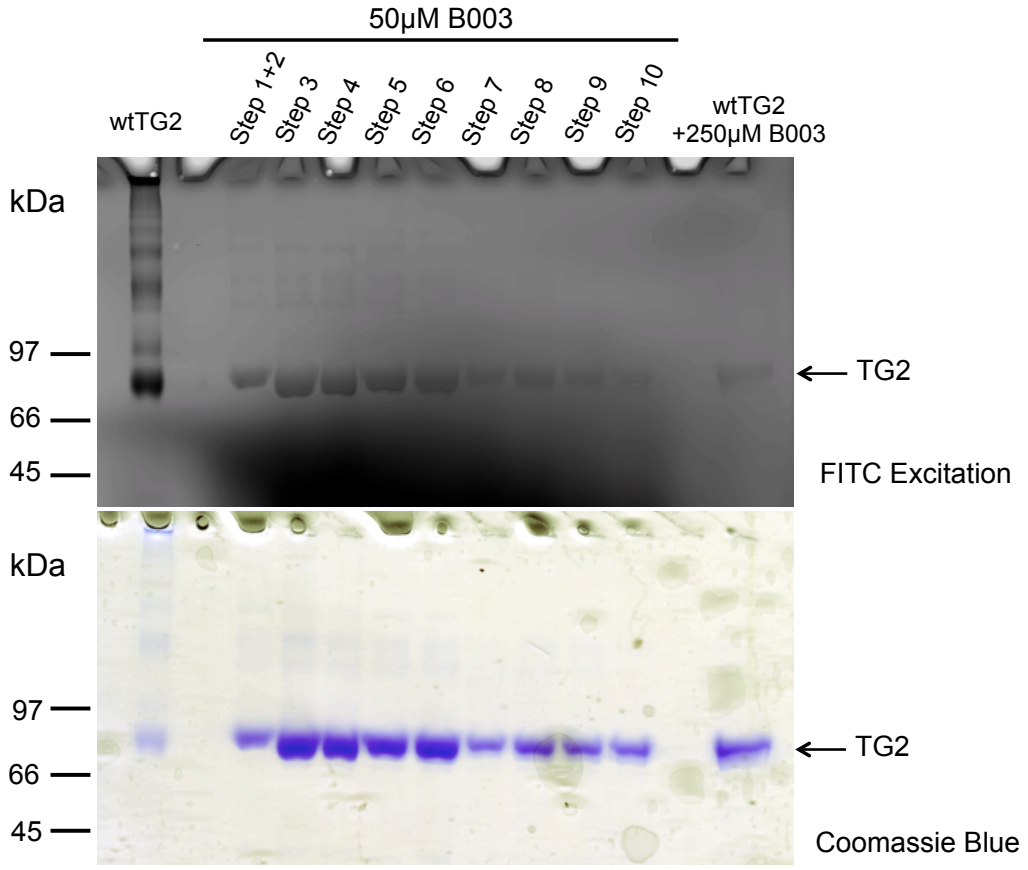

Fig. 4.5 Stepwise inhibition of TG2 with B003. Following inhibitor treatment, samples were pre-incubated *in vitro* with FITC-cadaverine and Ca^{2+}. Samples were separated on a 4-20% SDS-PAGE gel under reducing conditions. FITC incorporation into TG2 (top row) was visualized using a combination of the 488nm laser line excitation and a 520nm filter (PMT=500V). Gel was subsequently stained with Coomassie Brilliant Blue to reveal proteins.

4.2.5 Inhibition of TG2 with different active site-directed inhibitor

It was decided to inhibit rhTG2 using a different active site-directed inhibitor. Benzyloxycarbonyl-(6-Diazo-5-oxonorleucinyl)-L-Valinyl-L-Prolinyl-L-Leucinmethylester, also known as Z006, was purchased from Zedira. This inhibitor was selected as it is the same one used by the company to generate the previously used commercial 'open' TG2 and because a crystal structure for this variant was available. Although it is likely that B003 modified TG2 is in the 'open' conformation, for Z006 there was direct evidence to substantiate this (Pinkas et al., 2007). Using this inhibitor would allow study to assess if the abundant binding of FITC-cadaverine previously observed for purchased 'open' TG2 was due to residual transamidation activity or a high affinity interaction.

As before, TG2 was inhibited in 2 steps or 7 steps at 4°C with B003 or in 2 steps with Z006. Z006 was employed at the same concentration as B003. Half of the volume of the samples was separated by native gel electrophoresis. The gel was then incubated overnight with FITC-cadaverine in the presence of calcium at 37°C. The second half of the volume of the samples was incubated, *in vitro*, with FITC-cadaverine, and calcium at 37°C for 20 minutes and then subjected to SDS-PAGE. Running the two different types of electrophoresis for the same samples would allow the elucidation of whether interaction of TG2 with the fluorescent substrate was due to transamidation or binding, and if it was indeed covalently bound. If a covalent bond was not present it would not be possible to observe any fluorescence after denaturing electrophoresis.

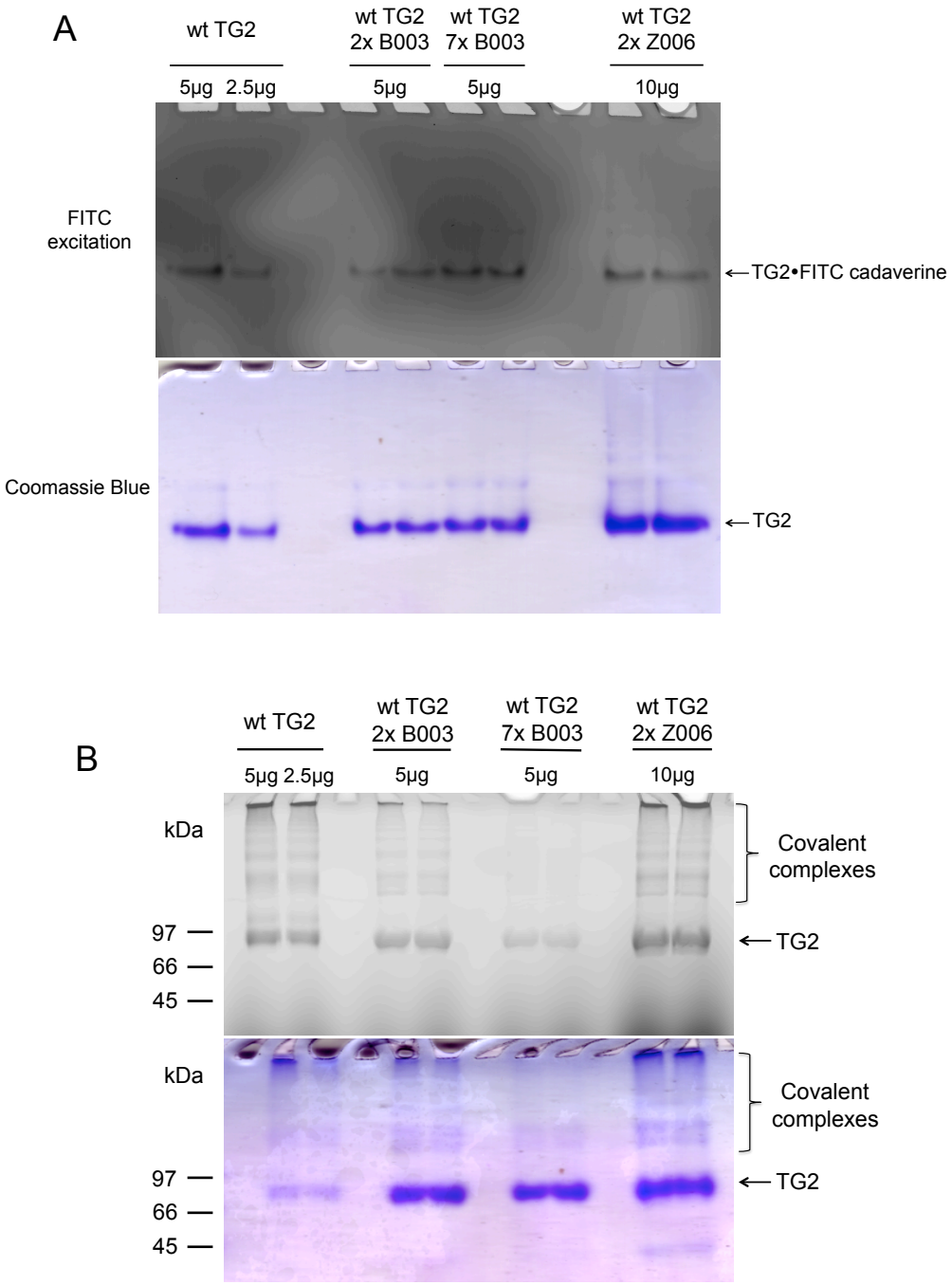

Fig. 4.6 Inhibition of TG2 with B003 or Z006 at 4°C. A: Native PAGE analysis for wt TG2 and inhibited TG2. Top row shows incorporation of FITC-cadaverine by the different variants of TG2 in the 'in gel' assay. Bottom row shows subsequent coomassie blue staining to visualise protein levels. **B:** Samples from A were also run on a SDS-PAGE to assess covalent incorporation of FITC-cadaverine into TG2 following *in vitro* reaction, i.e. to directly assess residual enzyme activity. FITC-excitation is shown on the top row while Coomassie blue staining is shown on the bottom row. FITC-cadaverine binding was visualized using a combination of the 488nm laser line for excitation and a 520nm filter for emission (PMT=500V for A and 400V for B).

Results showed that all variants of the protein demonstrated binding of FITC-cadaverine when in their native conformation (Fig. 4.6A). In fact, 5µg of 7-step B003 inhibited TG2 seemed to bind as much substrate as 5µg of wtTG2. Also, no noticeable changes were observed for 2x and 7x-inhibited protein. However, a clear difference was seen between 2.5µg and 5µg of wtTG2. Therefore, the signal observed appeared to correlate primarily with the amount of protein present rather than the enzymatic activity. When looking at the denaturing electrophoresis, it was evident that the inhibition of wt TG2 with B003 was clearly successful as exemplified by the reduction in formation of high molecular weight complexes and reduction in label incorporation, with 7x inhibitor treatment being more effective than 2x inhibitor treated. In fact, 7x inhibitor treated TG2 displayed very little residual activity (Fig. 4.6B), yet showed similar levels of association with FITC-cadaverine (Fig. 4.6A) suggesting that a high-affinity non-covalent interaction may be involved.

4.2.6 Inhibition of TG2 with Z006 for protein crystallization

The results showing that TG2, extensively treated with active site directed inhibitors, was still able to efficiently bind cadaverine were quite surprising. The fact that the protein-substrate complex did not appear to be related to enzymatic activity and that the binding seemed to be non-covalent, led us to believe that inhibited TG2 may potentially harbour a structural pocket with high affinity for the amine substrate required for the second step during catalysis.

To provide insight on how the amine interacts with the protein at this second pocket, it was decided to crystallize TG2 following modification of the active site cysteine residue with Z006. From previous work in our laboratory, evidence indicated that different amine substrates favour transamidation or deamidation as the outcome of the reaction. Therefore, crystallisation of TG2 with different amine substrates could identify structural determinants important for the deamidation reaction. This in turn would provide insight as

to why deamidation occurs preferentially in the context of the gut in coeliac disease.

The methodology used in the inhibition process of TG2 for use in crystallization experiments can be found in section 2.16 of chapter 2.

Analysis of inhibited TG2 through spectrophotometry showed the classical protein absorbance spectrum, with peak of maximum absorbance at approximately 280nm (Fig. 4.7A). No signs of aggregated protein were observed. Protein was also subjected to an isopeptidase activity assay to assess if inhibition of TG2 was successful. When comparing the wild type control to the Z006 inhibited TG2 (Fig. 4.7B) it was evident that inhibition was overall successful even though Z006 inhibited TG2 still showed some residual enzymatic activity.

Inhibited TG2 was produced at a high enough concentration to allow for protein crystallization.

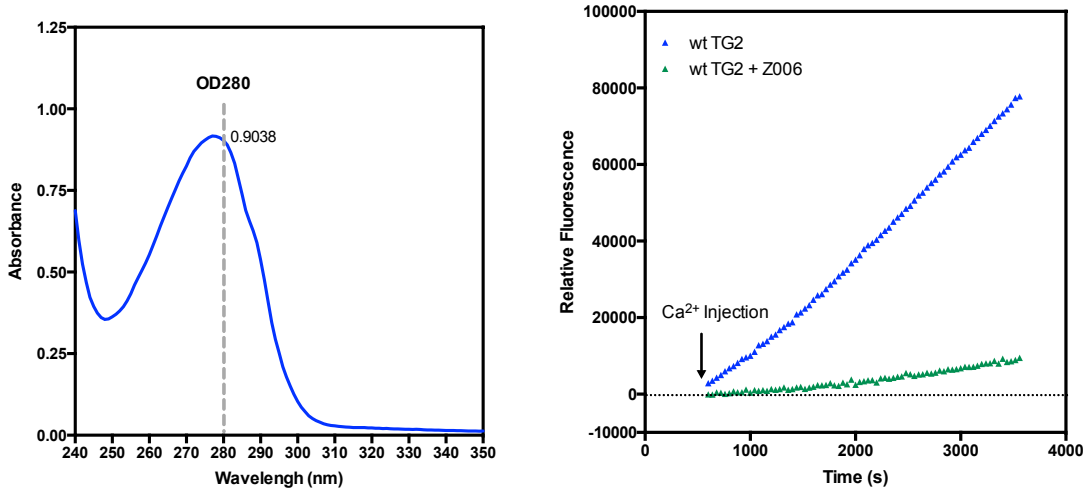

Fig. 4.7 Inhibition of TG2 with Z006. A: Absorbance spectrum of Z006 inhibited TG2. Data was normalized for buffer. Protein was diluted 1:10 to perform the analysis. Concentration of inhibited TG2 was calculated to be 6.8mg/ml. **B:** Enzyme isopeptidase activity for 20µg/ml TG2, normalized for well-specific fluorescence and following subtraction of control curve (no Ca^{2+}) to account for fluorescence bleaching: FLUOstar OPTIMA (gain 1900). Compared to wtTG2 (blue), Z006 inhibited TG2 (green) retained about 12% of its enzymatic activity. Inhibition was overall successful.

4.2.7 Crystallisation of inhibited TG2

TG2 has previously been crystallised in 'open' conformation following modification of the active site with the peptide inhibitor Ac-P(DON)LPF-NH_2 (Pinkas et al., 2007). Hence, the approach used these published conditions as a starting point for attempting crystallisation.

Inhibited TG2 was plated for crystallisation in the presence of either no ligand (Apo) or one of two different amines (ligand A or B). These were selected based on previous work within the group demonstrating that they exclusively promoted deamidation or transamidation, respectively, despite their highly similar structure. Ligands were used at 10-fold molar excess over protein. Crystallisation was performed using vapour diffusion, sitting drop methodology. In this approach, a droplet containing purified protein, buffers and precipitant is in a tightly closed environment with a reservoir containing higher concentrations of similar buffers and precipitants (Fig. 4.8). Initially, the protein and precipitant in the droplet are in an undersaturated state. Due to concentration gradient, water vaporises from the protein droplet and collects in the reservoir thereby increasing concentration of protein to a state of supersaturation. If all parameters including temperature, pH, type of buffer etc. are ideal, protein crystallisation will occur in the drop. The main advantage of this method is that it allows for gradual changes in concentration of protein, which help in the development of larger and well-organized crystals.

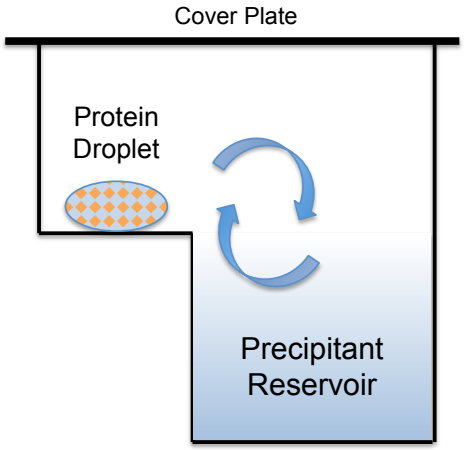

Fig. 4.8 Vapour diffusion, hanging drop method. A protein solution droplet (left) is in a tightly enclosed environment with a reservoir filled with a high concentration precipitant solution (right). Concentration gradient leads water to vaporise from the droplet to the reservoir, gradually increasing protein concentration and ultimately leading to crystallization under ideal conditions.

Detailed methodology of crystallization experiments can be found in section 2.17 of chapter 2.

In order to maximize the chances of obtaining crystals, three different precipitant buffers were used based on the previously published crystallization experiments (Pinkas et al., 2007). The base of all buffers was a 100mM HEPES, pH7.2, solution, to which ammonium sulphate was added to three different concentrations: 1M, 2M and 3M. These buffers were also used in the presence or absence of 15% glycerol, and with or without N-Voy. N-Voy, which has been previously shown to facilitate crystallisation of proteins (Singh et al., 2013), was used at 20-fold molar excess over protein. Even though purified protein was at a concentration of 6.8mg/ml it was possible to seed the protein to ultimately yield different concentrations by changing the protein-precipitant ratio (Table 4.2).

Table 4.2 TG2 crystallization seeding concentrations.

Protein		Precipitant		Final concentration
0.4μl	+	0.2μl	⇔	13.56mg/ml
0.3μl	+	0.2μl	⇔	10.17mg/ml
0.2μl	+	0.2μl	⇔	6.78mg/ml
0.13μl	+	0.2μl	⇔	4.407mg/ml

Ratio between protein and precipitant was changed to yield different final concentrations of TG2 following establishment of the equilibrium in the crystallisation chambers.

Protein was seeded and plates were scanned at day 0, 1, 5, 7, 15 and after 1 month. No TG2 crystals developed during this period.

An attempt the to produce protein crystals under modified conditions was undertaken. The same batch of inhibited TG2 was used. For the new experiment the precipitant buffer used was 100mM HEPES, 2M ammonium sulphate. Since pH does have an effect on the crystallisation process a range of different pHs were set from 6.8 to 7.6. The experiment was carried out with and without 15% glycerol. Final protein concentration in the crystallisation chambers was set to 9mg/ml or 12mg/ml.

The pH of the precipitant was checked when added to the protein solution to make sure that there was no alteration of the pH after the two volumes were mixed (Table 4.3). The highest volume of protein added to the precipitant during crystallisation plating was 0.2μl. After this experiment we decided to use the range of precipitants with initial pH 6.8; 7.2; 7.4; 7.5; 7.7 and 8.0.

Protein solution was centrifuged before use to remove any potential precipitates/aggregates and analysed through spectrophotometry. The final concentration of protein was determined as being 6.1mg/ml and seeding concentrations were set to 9mg/ml and 12mg/ml. Ligands and amount used were kept at the same ratio (10x fold molar excess over protein).

Plates were scanned at day 0 and 1, 5, 7, 13 days and also after 1 month. After this period TG2 crystals were not evident.

Unfortunately, a lot of protein precipitation was seen in the crystallisation droplets, presumably due to protein aggregation. Despite attempting a range of conditions around the parameters successfully used for TG2 crystallisation by others, it was not possible to overcome this problem.

A new batch of inhibited TG2 was produced to allow more crystallisation experiments. Although experiments were successful at obtaining inhibited TG2, the amount of protein that precipitated during the process was such that the final concentration of TG2 was not high enough to use in crystallisation assays.

Table 4.3 pH ranges used in crystallisation study of TG2

Ratio 0.2μl protein + 0.2μl precipitant at RT (≈25°C)	
Initial pH	Final pH
6.8	6.68
7.0	6.86
7.2	6.87
7.4	7.12
7.5	7.25
7.6	7.35
7.7	7.42
7.8	7.52
8.0	7.69

4.3 Discussion

In the previous chapter, experiments revealed that addition of GTP to TG2 prior to the labelling process had a positive effect on the retention of functionality of the protein. Furthermore, the absence of the nucleotide during the labelling process led to an enzymatically inactive protein. This was true when labelling TG2 with two different labels, Atto-565 and Atto-647N. This suggested that absence of GTP lead to labelling at specific sites of TG2 that ultimately influenced the conformation of the enzyme and therefore its inability to adopt a structural state required for catalysis.

Using native PAGE, it was shown here that, when GTP saturation was maintained during electrophoresis, there was a shift in mobility of bands of TG2 labelled in the presence of GTP that was not observed when labelling was performed in the absence of GTP. When GTP saturation was not maintained, labelled TG2 ran at the same level as controls, wt TG2 and open TG2. It is known that when GTP is present, the wild type enzyme will bind to it, and will acquire a closed conformation with a higher apparent negative charge. This will have an effect on how the protein runs in the gel: a more compact and negative protein will have a higher electrophoretic mobility (Pinkas et al., 2007). In contrast, the open conformation TG2 was inhibited by covalent binding of an inhibitor to the catalytic cysteine, making the subsequent conformational changes of the catalytic cycle impossible, including binding of GTP, and consequently it had a lower electrophoretic mobility. This suggested that the ability of TG2 to bind nucleotides was lost in the process of labeling, unless GTP was present at saturating concentrations. Since the band shift was only observed for the preparations of the enzyme that showed isopeptidase activity, it suggested that GTP-binding capacity of TG2 was required for catalytic activity or at least, a conformational transition linked to catalysis.

To further investigate enzyme activity in relation to the shift in bands observed in the native gel electrophoresis, an ‘in-gel’ activity assay was performed. Knowing that cadaverine is an amine donor substrate for TG2 and that TG2 is able to crosslink with the substrate and itself, the use of

cadaverine would be a good method to detect the active fraction of the different TG2 preparations. If TG2 was enzymatically active, it would incorporate FITC-cadaverine auto-catalytically. As previously mentioned, it was suspected that the lower positioned band observed in the gel, i.e. enzyme capable of binding GTP, was the active fraction of the labelled TG2 preparations. This hypothesis was confirmed as FITC-cadaverine was only detectable in the faster migrating bands of both Atto-565 and Atto-647N labelled TG2. There was a clear correlation between the relative abundance of the faster migrating species and the enzymatic activity of the protein preparation, whereby complete transition was seen with the unlabelled wtTG2. This confirmed that the capacity for GTP binding correlated with the enzymatic activity.

The most surprising result obtained during our native PAGE experiments, was the fact that the irreversibly inhibited open TG2 also retained the substrate. This led to the consideration that the inhibited enzyme, trapped in the open conformation, and reflecting the intermediate state during catalysis, had a high-affinity binding site for the amine donor substrate. This binding site could enable tight binding of FITC-cadaverine in a non-covalent way. This serendipitous observation was clearly significant and hence further investigated. If the fluorescent amine donor substrate was not covalently bound to the inhibited enzyme, it should separate from the protein during denaturing gel electrophoresis. However, SDS-PAGE analysis revealed, unexpectedly, that the substrate was at least in part covalently bound to open TG2. This meant that open TG2 retained residual enzymatic activity and hence made the results uncertain. Moreover, the fact that there was not any cadaverine incorporation in the enzymatically inactive forms TG2 E329G and TG2 C277S, confirmed specificity of the results. Even though this suggested that binding of cadaverine to open TG2 may be related to enzyme residual activity it did not exclude the possibility of additional non-covalent substrate binding.

It was decided therefore to tackle the residual activity problem by inhibiting enzyme with the commercially available peptidic inhibitor, B003, with the aim of driving inhibition to completion. Initially, high levels of

protein aggregation were observed and optimization of the inhibition process was required. Addition of N-Voy, an amphiphilic polymer, although effective in preventing protein aggregation, interfered with the assays and was considered not suitable for the experiments being conducted. Decreasing the temperature during TG2 inhibition, from 37°C to 4°C, seemed to be the most effective way of reducing levels of protein aggregation, as shown in subsequent native gel electrophoresis. The isopeptidase assay revealed in house inhibition of TG2 to be successful, as protein showed little or no signs of activity. As transamidation activity assays are more sensitive than the isopeptidase assay, the new inhibited TG2 was pre-incubated with FITC-cadaverine and analysed on a denaturing gel to assess for substrate incorporation. wt TG2 readily incorporated FITC-cadaverine but only when incubated in the presence of calcium. This was expected, as calcium is necessary for enzyme activity. Also, there was a substantial decrease in amide incorporation at 4°C when compared to 37°C, which was also expected as lower temperatures slow down reaction rates. Unexpectedly, both commercially bought and 'in-house' generated 'open' TG2 showed some levels of cadaverine incorporation in the presence of calcium at 37°C.

Despite different approaches to targeting the active site of TG2 it was not possible to completely eliminate catalytic activity. Nevertheless, inhibition over seven consecutive steps proved highly efficient, resulting in only negligible activity in even the most sensitive assays. Surprisingly, when analysing such a preparation side-by-side with wt TG2 in the 'in gel' assay there was no difference in amounts of amine substrate associated with the TG2 band, suggesting that catalytic activity could not explain this result. Furthermore, TG2 E329G, which does undergo the calcium-induced conformational switch, showed no association with the amine substrate in the 'in-gel' assay. These results, along side the absence of enzymatic activity in the isopeptidase assays suggested that the interaction of FITC-cadaverine with the 'open' TG2 is specific, but not due to catalytic activity. This led to the view that there might be a structural pocket with high affinity for an amine substrate that becomes available upon reaction of the enzyme with the first substrate, an event mimicked by reaction with the inhibitor in these

experiments. This is an exciting observation as it opens the door for structural studies investigating the determinants guiding the reactions leading to transamidation and deamidation, respectively.

In conclusion the experiments in this chapter abled the characterization of Inhibited TG2 and have shown for the first time the possibility for the existence of a second structural pocket in the TG2-substrate intermediate structure, with high affinity for an amine substrate.

Chapter 5 Identification of anti-TG2 and anti-TG6 antibody-producing cells in biopsies

5.1 Introduction

Gluten sensitivity classically presents with inflammation of the bowel, triggered by eating gluten, a protein found in wheat and other cereals (Sollid 2002). Gluten loads are particularly high in the upper small intestine, explaining why this is the primary site of GRD manifestation. Current diagnostic assays of this disease are specific for patients with classical gastrointestinal symptoms, as these were developed for coeliac patients, but studies have shown that gluten sensitivity can manifest with symptoms other than those related to inflammation of the bowel, such as neurological symptoms including ataxia and neuropathy (Hadjivassiliou et al. 2003, 2006).

It is crucial to identify these patients, which often do not have overt gastrointestinal symptoms, as they will suffer from irreversible damage to the neural tissue because of the inability of this tissue to regenerate.

TG6 as been shown to be predominantly expressed by a subset of neurons in the central nervous system, including Purkinje cells (D. Aeschlimann & Hadjivassiliou, 2008). Studies have shown that an antibody response, anti-TG6 IgG and IgA, was prevalent in gluten ataxia, independent of intestinal involvement. Furthermore, it was shown that the production of these antibodies in patients is gluten dependent (Hadjivassiliou et al., 2013). Therefore, TG6 has been identified as a possible biomarker to diagnose those patients that may be at risk of developing neurological disease in association with gluten sensitivity (Hadjivassiliou et al. 2008). However, it was unclear whether this immune response developed at the level of the gut or in the CNS. The fact that IgA class antibodies are present suggests that the gut may be involved.

It has been proposed that the production of anti-TG2 IgA in coeliac disease is associated with deamidation of gluten peptides by TG2, i.e. formation of thiolester complexes, and is likely dependent on T-cell help, provided by gluten-specific T-cells to activate TG2-specific autoreactive B-

cells (Sollid et al. 1997). Furthermore, anti-TG2 IgA deposits have been demonstrated in the small intestine of patients with gluten ataxia but not in control patients with other forms of ataxia, suggesting that sub-clinical inflammatory responses at the gut level are a feature in these patients (Hadjivassiliou et al. 2006). However, evidence for a T-cell response in gluten ataxia patients has been found in post mortem studies, where perivascular lymphocytic infiltration of cerebellar tissue by both $CD4^+$ and $CD8^+$ T-cells was observed (Hadjivassiliou et al. 1998). This suggests that inflammation at the blood-brain barrier could also be involved in the expansion of the immune response to additional targets, including TG6.

Since TG6 has been shown to deamidate gluten peptides and generate T-cell epitopes (Stamnaes et al. 2010), it is possible that the immune response in gluten ataxia initiates in the gut, where gluten loads are high.

In this chapter the aim was to shed some light on the mechanistic aspects of autoantibody development in patients with extraintestinal gluten-related disease manifestations. For this purpose, a series of experiments were performed using gut biopsies from GRD and non-GRD patients to investigate the presence of TG2 and TG6-specific B-cells. Detection of such cells *in situ* could help confirm that autoantibody development to TG6 occurs in conjunction with that to TG2, at the level of the gut or, alternatively, has its origin in independent events.

The aims of the chapter:

1. Optimization of an immunofluorescence staining protocol for identification of TG2 and TG6-reactive cells in sections from gut biopsies of a cohort of gluten-related disorders patients and controls.
2. Identify TG6-specific B cells in the human gut and whether these are common among patients with gluten-related disorders or specific to patients with distinct manifestations, e.g., neurology.

5.2 Results

5.2.1 Generation of an Atto-565-labelled control protein conjugate

As described in Chapter 3, experiments successfully led to chemically labelling of TG2 and TG6 for detection of TG2/TG6 specific B cells through immunofluorescent assays. In order to confirm specificity of immunofluorescence, it was necessary to generate an Atto-565-labelled protein conjugate that could be used as a control in cell labelling of tissue sections.

For this purpose labelling of hemocyanin was undertaken. This protein is commonly found in molluscs and no homologues exist in mammalian cells. For this reason, hemocyanin is frequently used as a control, as it is not expected to interact with anything in mammalian tissue, including the human small intestine. Also, its high molecular weight, solubility and abundance of lysine residues make the protein ideal for labelling and to assure staining specificity.

The labelling process was performed as described for TG2 in chapter 3. Briefly, hemocyanin was buffer exchanged into sodium phosphate buffer using gel filtration chromatography. Collected fractions were analysed by spectrophotometry and the fractions with highest absorbance at 280nm were used for labelling reaction (Fig 5.1A). Fluorescent labelling was performed in solution, using 140-fold molar excess of dye over protein to assure protein saturation with label. Gel filtration was again used to separate free label from labelled hemocyanin and fractions containing eluted labeled protein were pooled. Spectroscopic analysis confirmed the success of the labeling process, as a 280nm protein peak was observed along side the expected 565nm absorbance peak for the fluorophore (Fig 5.1B). Final protein concentration and label density were estimated from a standard curve generated from serial dilutions of Atto-565 dye. Labelled hemocyanin was calculated to have a final concentration of ≈458μg/ml and a label density of approximately 100 fluorophores per hemocyanin molecule.

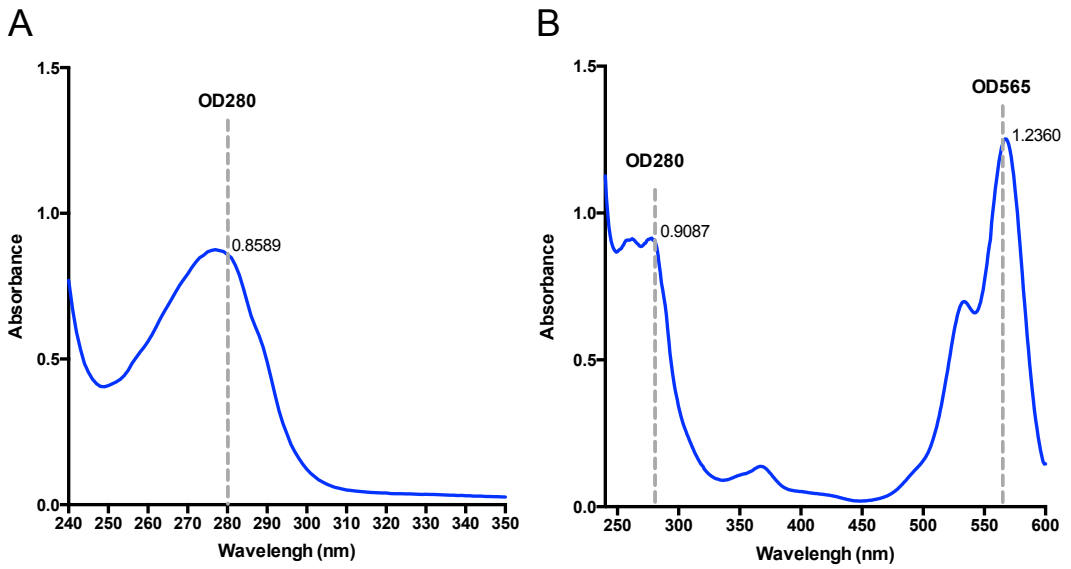

Fig. 5.1 Chemical labelling of hemocyanin with Atto-565 NHS ester dye. A: Hemocyanin (500μg) was applied to PD10 column for buffer exchange. Spectroscopic analysis shows the typical spectrum for protein with maximum absorbance near 280nm. **B:** Absorbance spectrum for Atto-565 NHS ester labelled hemocyanin. Labelled protein was purified using a PD10 column. Graph shows pooled protein. Data shown was corrected for buffer absorbance.

5.2.2 Detection of TG2-specific antibodies with Atto-labelled TG2

As mentioned in chapter 3, coeliac disease and gluten ataxia related autoantigens, TG2 and TG6, were labeled for use in immunofluorescent detection of TG-specific B cells. Although the aim of this research was to ultimately understand the mechanism behind the production of autoantibodies to TG6 in gluten ataxia, labeled TG2 was used as a 'proof of principle'/reference point. Firstly, it is known that TG2-specific plasma cells are present in the intestine in CD patients (Di Niro et al., 2012). Secondly, anti-TG2 IgA deposits have been detected in the small intestine of patients with gluten ataxia, suggesting that anti-TG2 plasma cells may be present also in these patients even if they are serologically negative for anti-TG2 IgA (Hadjivassiliou et al. 2006).

Optimization of labelled TG2 (lTG2) use in tissue labelling studies was required. Frozen sections of a duodenal biopsy of a coeliac disease patient

were available within the group and optimization of ITG2 incubation time was initially performed with these sections.

Unfixed frozen sections were dried overnight and washed with Tris-buffered saline before blocking with 1%BSA/TBS for 30min. Sections were then incubated with 10μg/ml of ITG2 for 2min, 10min or 1h. A 10μg/ml labelled hemocyanin solution was used along side ITG2, as negative control to assess labelling specificity. Detailed methodology can be found in section 2.19 of chapter 2.

Staining for TG2 was detected in the extracellular matrix including basement membrane of the small intestine, especially along the intestinal crypts and also around mucosal vessels (Fig 5.2). This pattern of staining was expected, as TG2 is known to strongly bind to specific ECM components (Aeschliman & Paulsson, 1991; Boscolo et al., 2010; Iversen et al., 2013). This may reflect a combination of binding directly to TG2 in the ECM as well as to autoantibody deposits in the tissue (Korponay-Szabó et al., 2004). From the incubation times used, 2 min gave a comparatively weak signal, while 1h, generated staining with excessive background fluorescence. Overall, the 10min incubation time produced the most appropriate staining, strong enough to be detected without high background fluorescence. Signal specificity can be determined by absence of staining when labelled hemocyanin control was used.

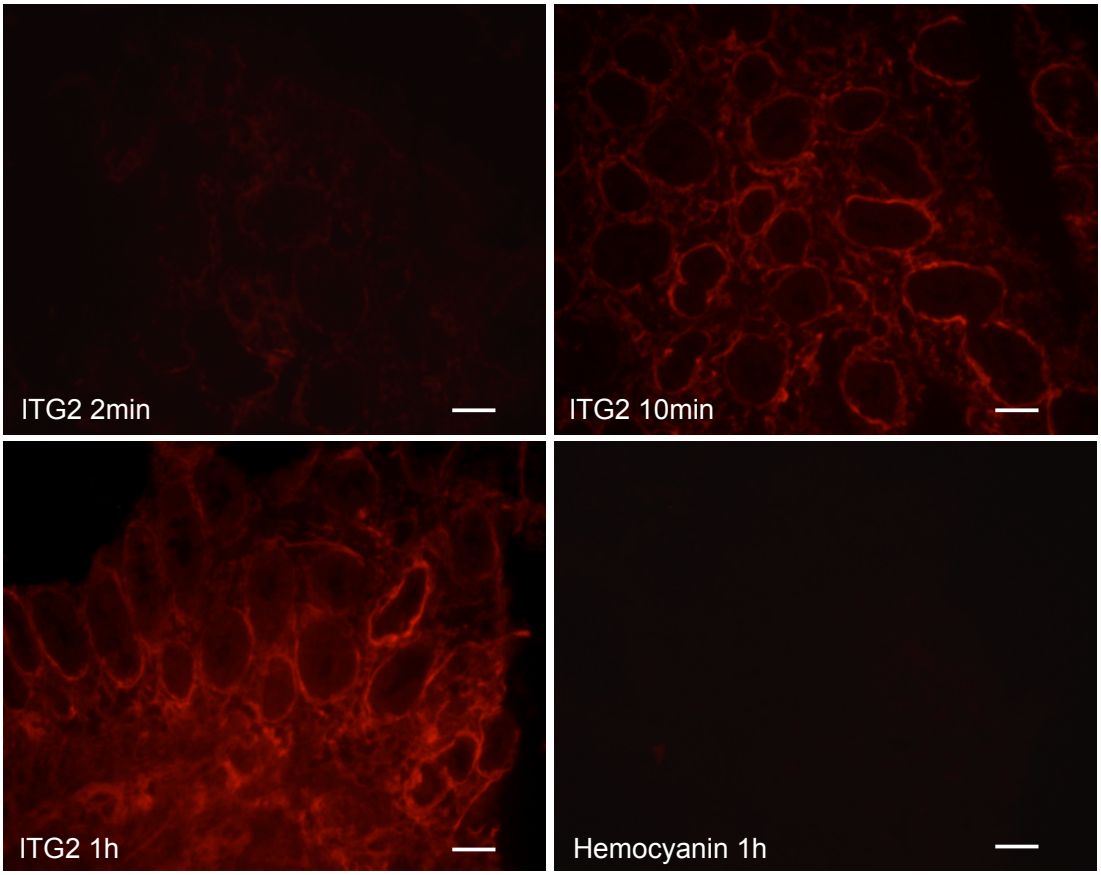

Fig. 5.2 Optimization of labelled-TG2 incubation times with tissue sections. Unfixed frozen sections from a coeliac patient were incubated with Atto-565 labelled TG2 (ITG2) for a period of 2min, 10min or 1h. Atto-565 labelled hemocyanin was used as a negative control to assess staining specificity. Size bar = 50μm

5.2.3 Tissue interaction with labelled TG2 is not mediated via catalytic activity

In chapter 3 it was found that the choice of methodology used for labelling TG2 could affect the enzyme catalytic activity. Since it was possible to produce labelled TG2 in its inactive and active state it was decided to assess binding of the two forms of the enzyme in a coeliac patient gut biopsy. The importance of this experiment comes from the fact that autoantibodies against TG2 have previously been shown to be conformation dependent (Iversen et al. 2013; Seissler et al. 2001). Unfixed frozen sections were prepared as previously described and incubated with 10μg/ml of either

the enzymatically active (labeled in the presence of GTP) or inactive (labeled in the absence of GTP) form of labeled TG2. Sections stained with inactive labeled TG2 (Fig 5.3A top panel) appeared to show a lower level of fluorescent signal when compared to sections incubated with active labeled TG2 (Fig 5.3A bottom panel). This could be related to catalytic activity of labeled TG2, i.e. autocatalytic action of the enzyme could contribute to tissue immobilization. It could also be that inactive labeled TG2 may not be able to interact with the extracellular matrix and may not be recognized by antibodies at the surface of cells, due to its inability to adopt a relevant conformation. As the observed staining is present mainly in the extracellular matrix it was important to rule out that this staining was not a result of labeled TG2 crosslinking to the ECM.

Unfixed frozen sections from the same coeliac disease patient used in the previous experiments were incubated with 10μg/ml labelled catalytically active TG2 for 10min, in the absence or presence of 1mM EDTA. Since calcium is an allosteric regulator of TG2, involved in TG activation, EDTA was used as a chelating agent to prevent TG2 catalytic activity by binding the calcium ion necessary for the reaction.

Results showed no significant difference in the staining pattern obtained for staining in the presence or absence of EDTA (Fig 5.3B). Positive staining was observed in the extracellular matrix. Specificity of labelling was again demonstrated by using an unrelated protein (hemocyanin) carrying the same label. The results allow us to conclude that the TG2 binding to the tissue is specific and not mediated by its catalytic activity.

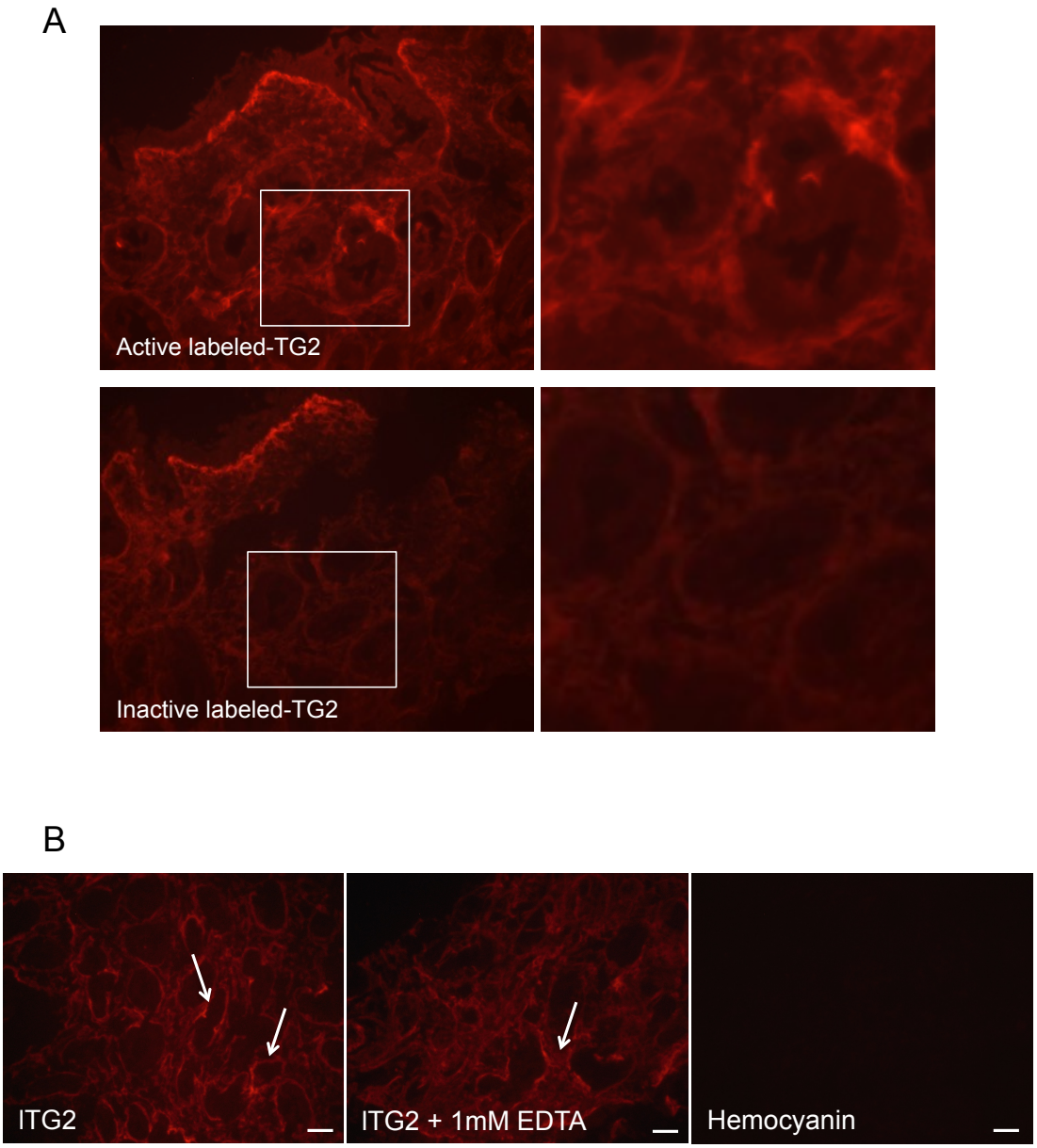

Fig. 5.3 Enzyme conformation state but not transamidation activity impact on labelled TG2 binding to small intestine sections of a coeliac disease patient. A: Comparison of inactive labelled TG2 with active labelled TG2 (10μg/ml) binding to small intestinal tissue after 1h incubation. Size bar 50μm. Pictures on the right are amplification of the selected area (white square) Size bar 25μm. **B:** Comparison of tissue labelling with active ITG2 (10μg/ml) in the presence/absence of 1mM EDTA after 10min incubation. Labelled hemocyanin (10μg/ml) was used as a control. Positive staining is visible in the extracellular matrix (arrows). Size bar = 50μm

5.2.4 Tissue processing and detection of anti-TG IgA deposits in the gut

It is known that fixation and processing methods can substantially influence protein localization studies on tissue sections. The majority of routine diagnosis is based on analysis of formaldehyde fixed and paraffin embedded (FFPE) tissue sections. In the literature however, unfixed frozen tissue sections are the preferred processing method in immunohistochemistry, due to the preservation of antigen structure (Di Niro et al. 2012; Hadjivassiliou et al. 2006). However, this comes at the cost of losing soluble protein and lack of preservation of cellular architecture. It was therefore important to determine which processing method was the most appropriate in detecting TG-specific B cells in human gut sections. This was of clear relevance to subsequent use in diagnostic testing.

In the present study a comparison of 3 different processing methods was undertaken. In the first one, samples were snap frozen in liquid nitrogen immediately after collection. In the second approach, tissue was fixed in paraformaldehyde and then processed using a routine approach. The method was one employed by a certified pathology laboratory, and involved dehydration and paraffin embedding. A third approach was introduced, where gut biopsies were fixed in paraformaldehyde and then gradually soaked in high concentrations of sucrose to prevent ice crystal formation during freezing, before being frozen in liquid nitrogen. Biopsies from each patient were in parallel processed using these 3 approaches.

Snap frozen sections gave us poor cell structure and tissue morphology. The routine formaldehyde-fixed and paraffin embedded (FFPE) sections showed good cell structure but gave high background staining in labelling experiments and lead to poor antigenicity, probably due to modification of surface proteins that made detection impossible or unreliable. The third processing protocol, where samples were sucrose treated and then frozen was the one that yielded the best cell structure without compromising the immunofluorescent assay results. Based on the initial results the FFPE protocol was not employed further in this study, as labelling with either antibodies or labelled enzyme proved unsuccessful. The interest here is in

the features relevant to GRD diagnosis, including detection of TG-specific plasma cells, autoantibodies deposits and the relevant TGs.

In the following sections, I will give one example of the findings regarding tissue processing for illustration purposes. During experimentation with different processing protocols an interesting result was encountered regarding the pattern of IgA distribution between sections processed by snap freezing without fixation and sections snap frozen after fixation. When comparing the human-IgA detection with antibodies, between the two processing protocols, the pattern observed was significantly different (Fig 5.4). On the snap frozen biopsy sections, the IgA deposits, which have been reported to be a specific early feature of CD (Hadjivassiliou et al., 2013), seemed to be associated with specific structures of the extracellular matrix. However, on the fixed frozen section, the IgA presented as a more localized signal, associated with individual cells surrounding the intestinal crypts. It is possible that either TG2 or IgA directed to TG2 in non-fixed biopsies may diffuse from inside the cells to the extracellular matrix during sectioning of the tissue, causing the change in pattern observed in all patients analysed.

Referring back to the literature, colocalization of IgA and TG2 in a characteristic pattern in snap frozen sections of coeliac patients has been reported as evidence for *in situ* formation of IgA deposits in the gut (Korponay-Szabó et al., 2004). Since the pattern observed for IgA deposits in non-fixed frozen sections in the literature (Fig 5.4 left panel) was similar to the one observed in this study, the effect is likely to be an artefact due to the methodology employed. Tissue processing/sectioning seems to critically impact on protein distribution and the colocalization observed in conventional frozen sections may not be representative of protein localization in the gut *in vivo*. The fact that the ‘deposits’ were apparently disease-specific can be explained by the fact that 1: TG2-specific autoantibodies are only present in patients and 2: TG2 is highly upregulated in disease due to the inflammation. Hence, although these ‘deposits’ are most likely an artefact, this artefact is in fact, disease-specific.

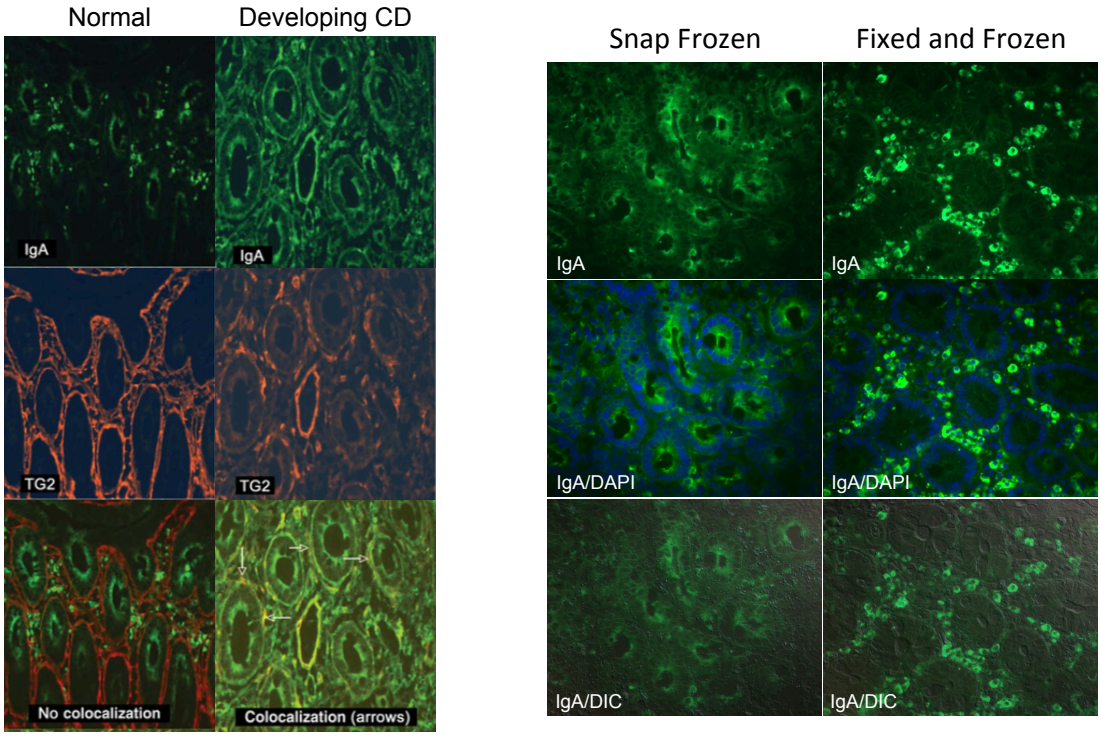

Fig. 5.4 Comparison of TG2-specific IgA deposits between frozen sections processed with and without fixation. The left panel provided example of a negative (normal column) and positive (developing CD column) staining for IgA deposits against TG2 on snap frozen D2 biopsies from 2 patients. The presence of such deposits is a reliable marker of gluten-related disorders (image retrieved from Hadjivassiliou et al. 2013). The right panel shows this study comparison of IgA labelling between snap frozen and fixed frozen D2 biopsy serial sections of one single patient. The pattern observed is significantly different.

5.2.5 Optimization of antibodies for detection of B-cells and plasma-cells

While performing immunofluorecent staining in D2 biopsies a large number of IgA^+ cells were observed in the lamina propria of all patients analysed. This is expected, as the human intestine is the primary place for production of IgA. However, when trying to detect B cells or plasma cells using antibodies against CD20 or CD138 respectively, in the same biopsies, only very few or in some cases no cells were found. This was an unexpected observation as plasma cells are producers of IgA.

To make sure that the results obtained were not related to issues with the antibodies used - some antibodies can be incompatible with some tissue processing methods – and to exclude that this was the reason why an unusual low number of B cells/plasma cells were being detected, it was decided to test these antibodies in a positive control tissue. A human palatine tonsil was obtained through the University Hospital of Wales. The tissue was processed in the same way as our D2 biopsies. Tonsils are intramucosal collections of lymphocytes or aggregated lymphoid tissue closely associated with the overlying epithelium (*Stedman's Medical DIctionary* entry on Tonsil). The palatine tonsils are located at the back of the throat and constitute part of the mucosa-associated lymphoid tissue (MALT), where B cell maturation takes place.

Tonsil tissue sections were used as positive controls to confirm that the anti-B cells/plasma cells antibodies were compatible with the fixed-frozen processing method used in the immunofluorescent experiments. Antibodies against B-cell marker CD20 and plasma cell marker CD138 were tested (Fig 5.5).

The fluorescent signal for B-cell marker CD20 was clear and was present on the membrane of individual cells, which were highly abundant throughout the germinal centres. Fewer cells labelled positive for the plasma cell marker CD138 and although labelling was present, it was not as extensive as for CD20. Individual $CD138^{+}$ cells were observed in the periphery of the germinal centres.

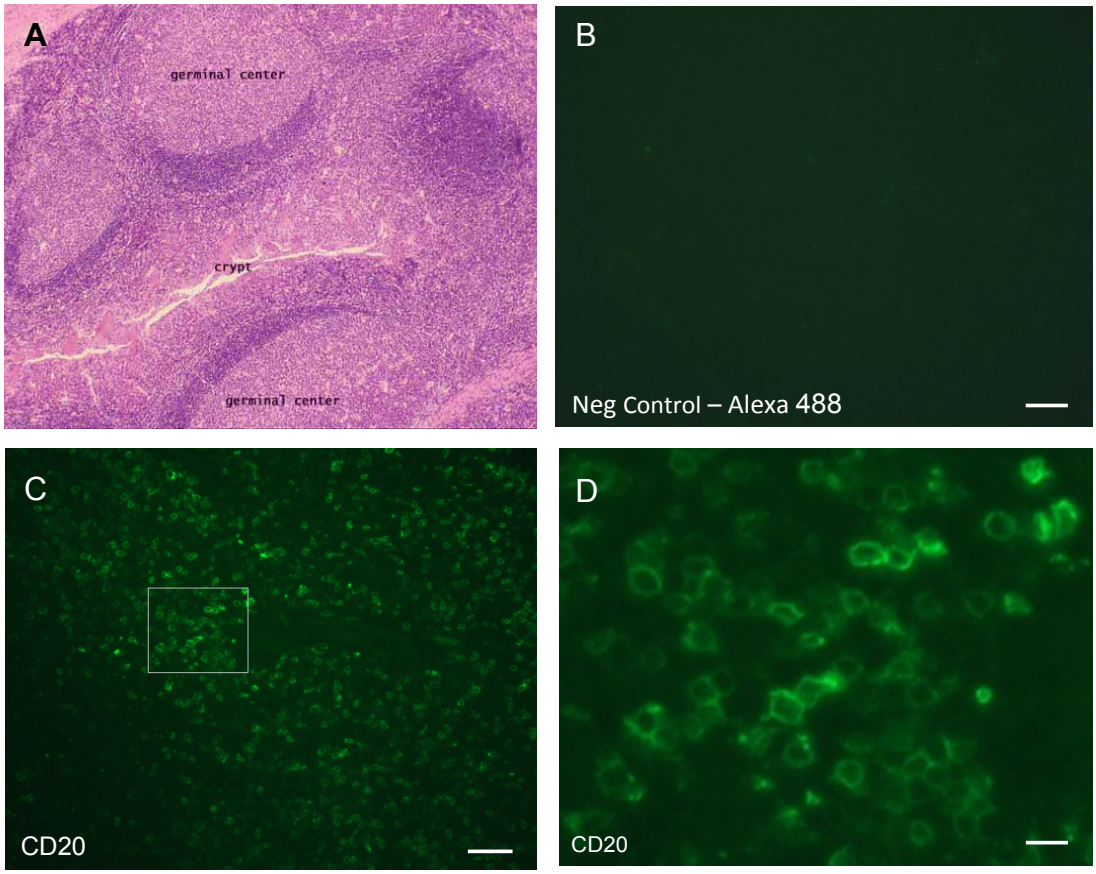

Fig. 5.5 Optimization of antibodies against B-cell and plasma cell markers in tonsil tissue. Tonsil H&E staining (retrieved from Stevens & Lowe, 2004) **(A)**. The tonsillar crypts increase the contact surface between the lymphoid tissue and the environment, while B-cell differentiation occurs in the germinal centres. Tonsillar tissue was positive for B-cell marker CD20 (panel **C** and higher magnification on **D**) and plasma cell marker CD138 (panel **E** and higher magnification **F**). Specificity of staining is demonstrated by negative control **(B)**. Size bars = 50μm in B, C and E. Size bars = 15μm bars in D and F.

5.2.6 Patient selection and biopsy collection for pilot clinical study

Patients were recruited from the ataxia, gluten/neurology, CD, and movement disorders clinics based at the Royal Hallamshire Hospital (Sheffield, UK) with the kind help of Prof. Marios Hadjivassiliou and David Sanders (Table 5.1), and with the approval of the Yorkshire Research Ethics Committee.

The study aimed at comparing classic CD and GRD neurology patients with relevant controls.

Patients were divided into 3 groups: coeliac disease (CD), gluten ataxia (GA) and control group (Table 5.3). Control patients attended the clinic because of non-gluten related disorders (non-GRD). Neurologic controls included a patient with idiopathic sporadic ataxia (ISA) and a patient with cerebellar variant of multiple system atrophy (MSA-C).

All patients attended the gastrointestinal clinic in Sheffield, to receive an endoscopy. Biopsies were collected endoscopically, from the second part of the duodenum (D2), by a specialist gastroenterologist. I personally processed all the biopsies immediately after collection, on site, and according to the methodology mentioned in section 5.2.4, and subsequently transported all tissue to our laboratories in Cardiff. Orientation of biopsies was performed so that a transverse section of intestinal crypts and villi could be observed, although this was not always possible due to the small size of the biopsies. Sectioning of tissue was performed, using a cryostat, in order to obtain 5μm serial sections, but this was also not always possible due to loss of tissue during sectioning process.

Table 5.1 Clinical characteristics of patient cohort.

ID	Age, y	Sex	Clinical Presentation	Serology	Anti-gliadin Ab
2	57	M	CD	Anti-TG2^{+} (low)	IgG
3	24	F	CD	Anti-TG2^{+}	IgA
4	22	F	CD	Anti TG2^{+}	IgG/IgA
5	61	F	GA (not on GFD)	Anti-TG2^{+} (low)	ND
6	52	F	CD	Anti TG2^{+}	ND
7	43	F	CD (not on GFD) WMA	Anti-TG2^{+} Anti TG6^{-} Anti-cardiolipin^{+}	ND
8	37	M	CD	Anti-TG2^{+}	IgA/IgG
9	20	F	CD	Anti-TG2^{+}	ND
10	75	M	GA (not on GFD)	Anti-TG2^{-} Anti-TG6^{+}	ND
11	60	F	GA (not on GFD)	Anti-TG2^{-} Anti-TG6^{+}	ND
12	39	M	ISA Stiff person syndrome	Anti-GAD^{+} Anti-TG2^{-} Anti-TG6^{-}	ND
13	56	F	MSA-C	Anti-TG2^{-}	ND
14	67	M	ISA	Anti-TG2^{-} Anti-TG6^{+}	ND
15	68	F	ISA	Anti-TG2^{-} Anti-GAD^{+} Anti-TG6^{+} (borderline)	ND
16	60	F	GA/myoclonus	Anti-TG2^{-} Anti-TG6^{-}	IgA/IgG
17	61	M	GA	Anti-TG2^{-} Anti-TG6^{+}	ND
18	73	F	CD (on GFD) Ataxia/myopathy	Anti-TG2^{-}	ND
19	44	F	control	Anti-TG2^{+} (low)	IgA/IgG
20	27	F	CD	Anti-TG2^{+}	ND
21	68	M	CD (on GFD) myopathy	Anti-TG2^{-}	ND
22	72	M	control	ND	ND
23	73	F	CD	ND	ND
24	63	F	control	ND	ND
25	28	F	control	ND	ND

Insufficient material of patient 1 was obtained to carry out immunofluorescence analysis.
Abbreviations: CD = coeliac disease; GA = gluten ataxia; GFD = gluten-free diet; WMA = white matter abnormalities; MSA-C = cerebellar variant of multiple system atrophy; ISA = idiopathic sporadic ataxia; ND = not determined

Table 5.2 Patient cohort: histological findings upon biopsy examination

ID	Age, y	Sex	Clinical Presentation	Notes
2	57	M	CD	Residual inflammation related to CD
3	24	F	CD	Some inflammation was observed
4	22	F	CD	Typical CD biopsy
5	61	F	GA (not on GFD)	Normal
6	52	F	CD	Some inflammation was observed
7	43	F	CD (not on GFD) WMA	Normal
8	37	M	CD	Typical CD biopsy
9	20	F	CD	Family history of CD
10	75	M	GA (not on GFD)	Increased IELs
11	60	F	GA (not on GFD)	Normal
12	39	M	ISA Stiff person syndrome	Normal
13	56	F	MSA-C	Normal
14	67	M	ISA	Normal
15	68	F	ISA	Normal
16	60	F	GA/myoclonus	Normal
17	61	M	GA	Normal
18	73	F	CD (on GFD) Ataxia/myopathy	Abnormal
19	44	F	control	Increased IELs
20	27	F	CD	Typical CD biopsy
21	68	M	CD (on GFD) myopathy	Typical CD biopsy
22	72	M	control	Normal
23	73	F	CD	Typical CD biopsy
24	63	F	control	Normal
25	28	F	control	Normal

Insufficient material of patient 1 was obtained to carry out immunofluorescence analysis. Histological analysis was carried out by a specialist pathologist, at the Royal Hallamshire Hospital, Sheffield. Abbreviations: CD = coeliac disease; GA = gluten ataxia; GFD = gluten-free diet; WMA = white matter abnormalities; MSA-C = cerebellar variant of multiple system atrophy; ISA = idiopathic sporadic ataxia; IEL = intra-epithelial leukocytes ND = not determined

Table 5.3 Final grouping of patients for analysis

Coeliac disease	Patients: 2, 3, 4, 6, 7, 8, 9, 18, 2, 21, 23	n = 11
Gluten ataxia	Patients: 5, 10, 11, 16, 17,	n = 5
Controls	Patients: 12, 13, 14, 15, 19, 22, 24, 25	n = 8

5.2.7 Detection of IgA in D2 biopsies

Due to the results obtained when comparing different tissue processing methods, the (immuno)histochemistry assays were undertaken using the fixed-frozen biopsies.

IgA staining was performed on sections from patients 2 to 8 and 10 to 12 (Fig 5.6). The remaining patients were not studied due to lack of time in the project. IgA staining was performed for two reasons: firstly because deposits colocalised with TG2 are considered to be a specific feature in coeliac patients and secondly as the approach identifies cells producing IgA, i.e. plasma cells.

From the patients analysed, all showed IgA staining localized to the lamina propria of the small intestine, around the intestinal crypts and villi. Numerous IgA^+ individual cells were detected. This was not surprising, as immune protection of the intestinal mucosa depends on the secretion of IgA by plasma cells.

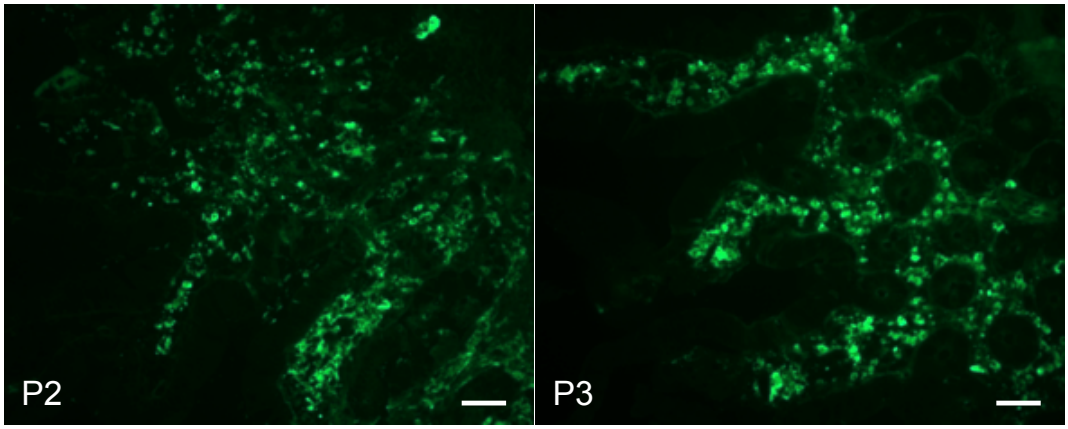

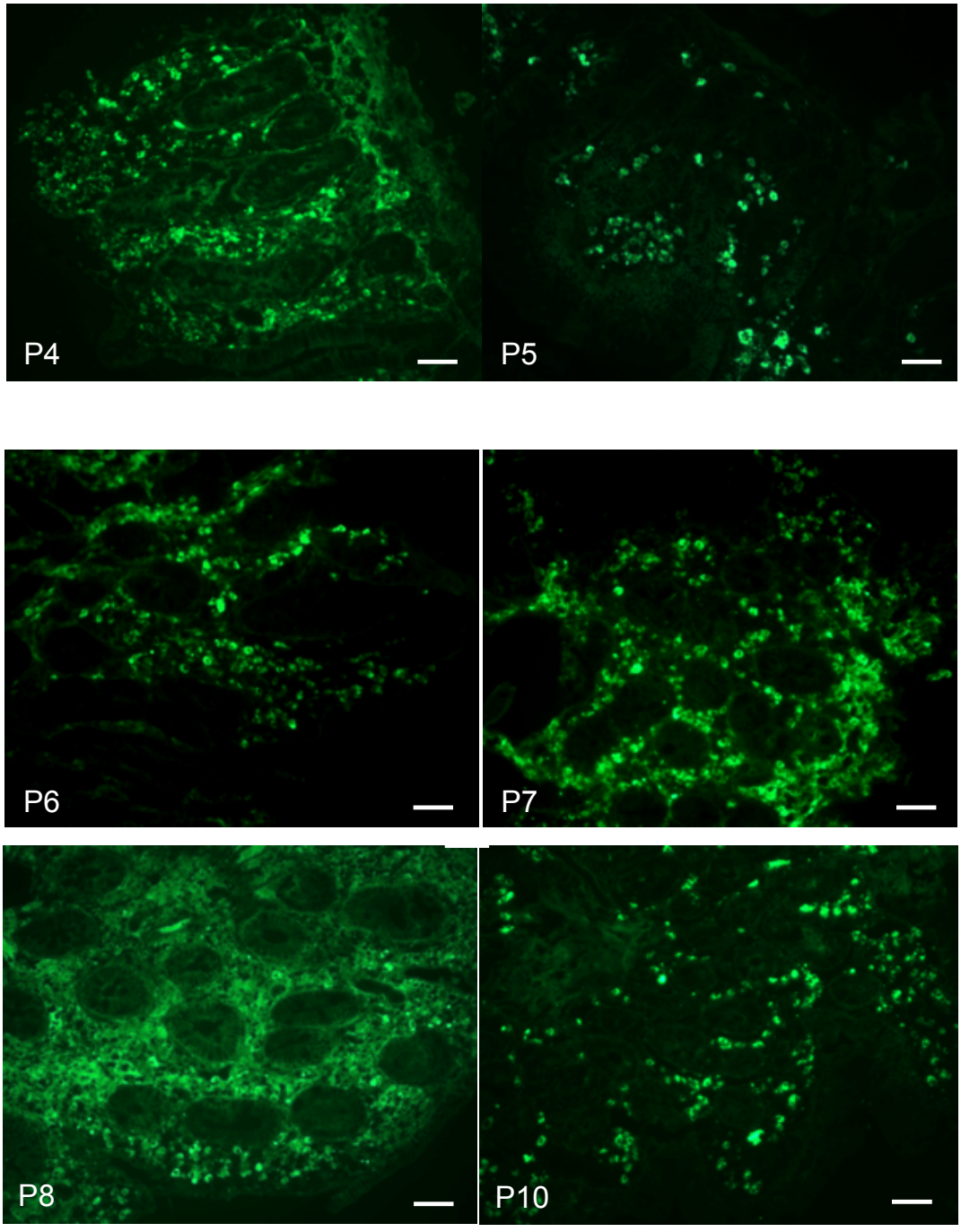
P4
P5
P6
P7
P8
P10

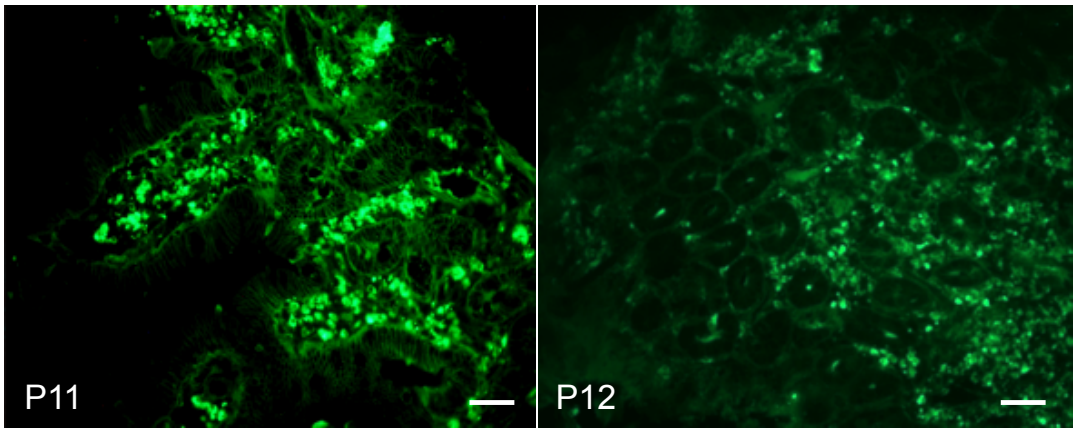

Fig. 5.6 Immunofluorescent staining with anti-IgA FITC-conjugated antibody. All patient sections analysed were positive for IgA. IgA+ individual cells were detected across the lamina propria of the biopsies around the intestinal crypts and also villi when these were present in the section. Size bars = 100μm

5.2.8 Detection of TG2/TG6-specific plasma cells

Detection of TG2-specific plasma cells in patient biopsy D2 sections

Not all patients were tested for labelled TG2 staining, as the priority was to test for anti-TG6 specific antibodies *in situ*. Labelled TG2 (10μg/ml) was incubated on fixed-frozen sections for detection of anti-TG2 antibodies in D2 biopsies. Staining was detected in the lamina propria around the intestinal crypts and villi of all patients tested (Fig 5.7). This may at least in part relate to binding of labelled TG2 to specific ECM components as already discussed in section 5.2.3.

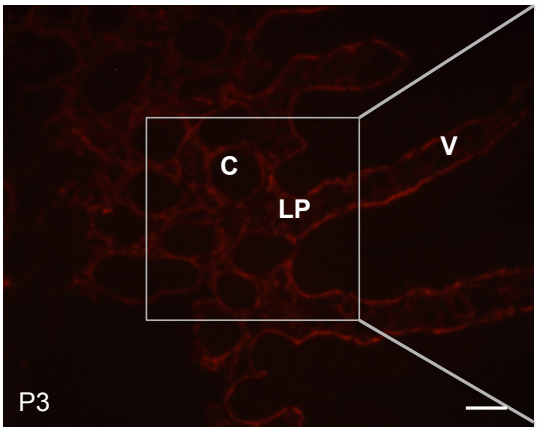
C
V
LP
P3

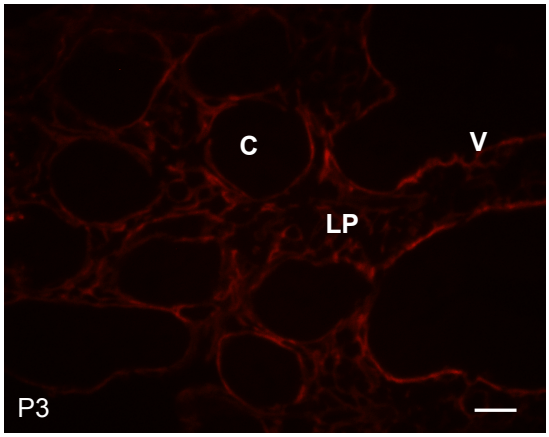
C
V
LP
P3

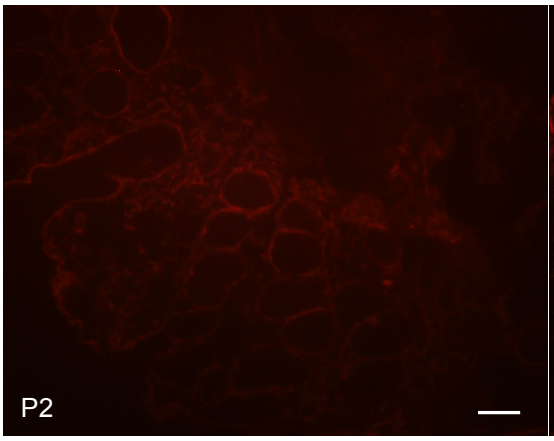
P2

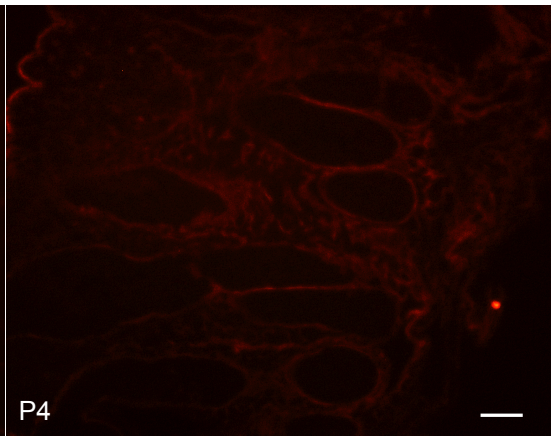
P4

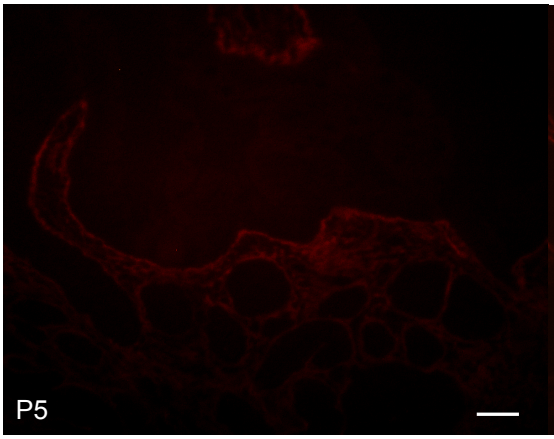
P5

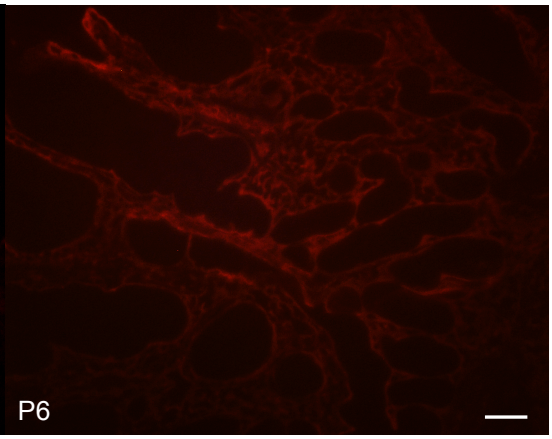
P6

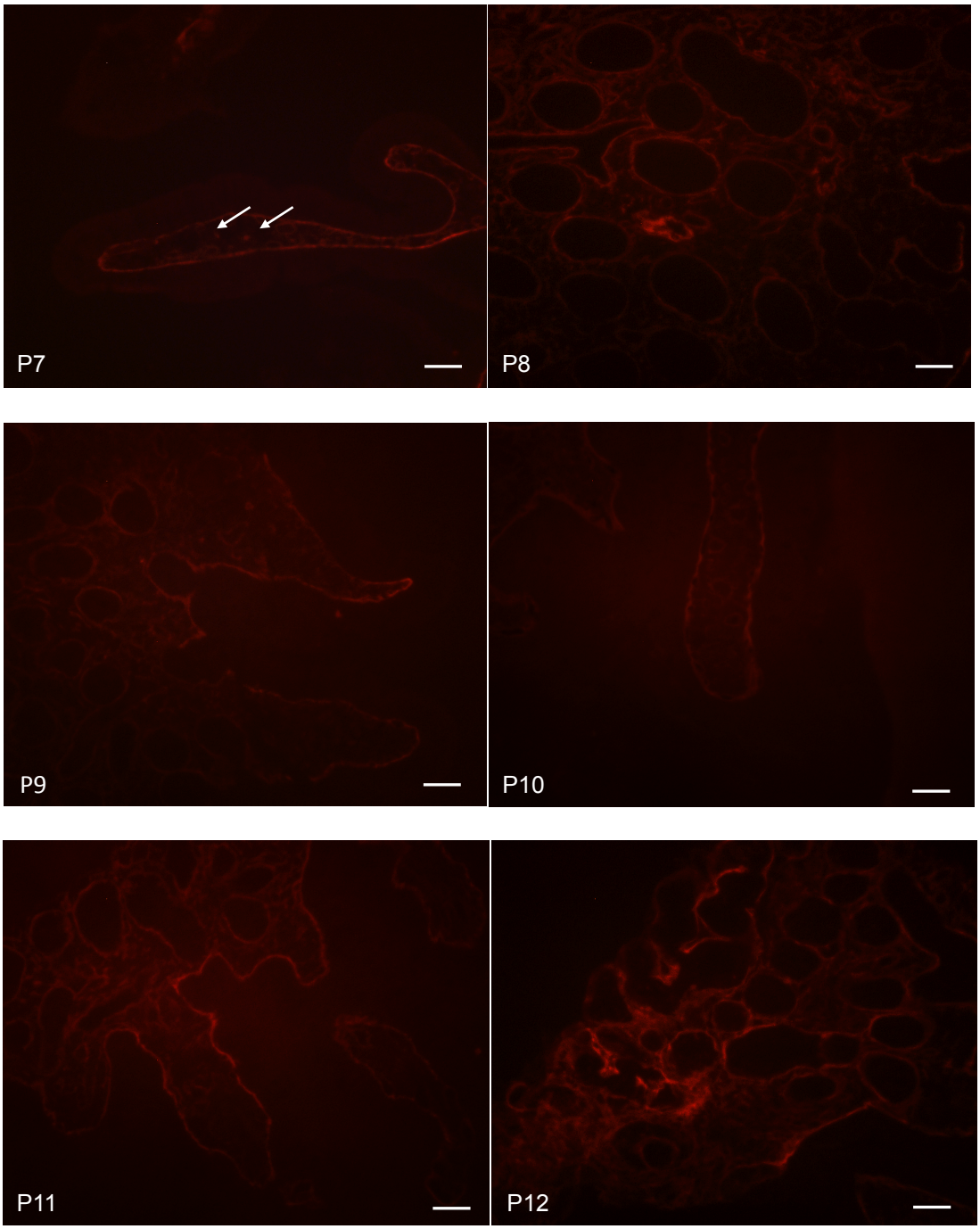

Fig. 5.7 Overview of labelled TG2 staining pattern in different patients. Staining occurred in the lamina propria (LP) of the small intestine, with higher intensity around the intestinal villi (V) and crypts (C). Size bars 100μm A higher magnification of P3, is observed on the top right of the panel for better imaging of intestinal morphology following immunostaining. Size bars = 50μm

A low number of individual cells positive for lTG2 binding were observed in the lamina propria of the small intestine biospies of patients P2, P7 and P9 (Fig 5.8). It is conceivable that other patients also had individual cells expressing anti-TG2 antibodies on the membrane surface, but the abundant matrix-associated staining made it difficult to evaluate this. Patients were considered as having lTG2^{+} cells when individual cells were clearly visible, with nuclei present and staining covering the majority of the cell surface. To further address this, double immunostaining was carried out to assess if cells binding lTG2 were indeed plasma cells expressing TG2-specific antibodies. Results showed that individual cells could be detected, that bind TG2 and express plasma cell marker CD138 (Fig 5.8). However in contrast to what has been reported, such cells were rare in these patient biopsies. Note, none of these 3 patients analysed had classic March 3 biopsy findings (tyipical coeliac disease biospsy) and this could explain this difference.

A

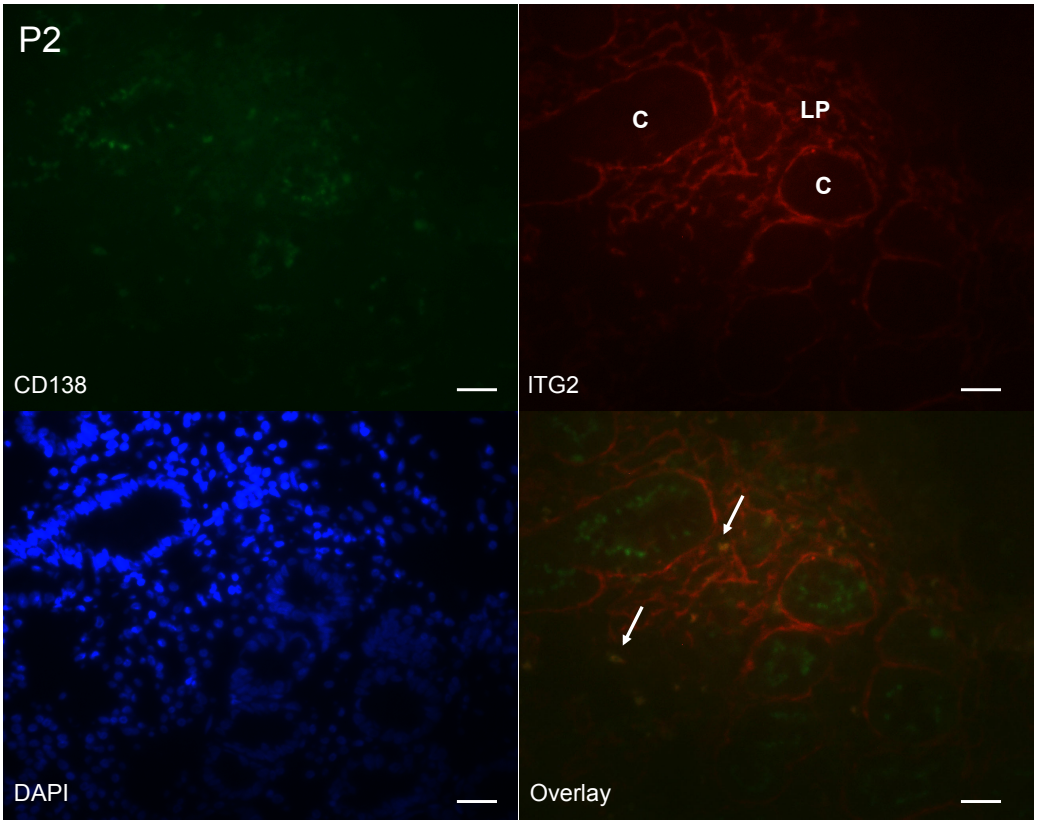
P2
C
LP
C
CD138
ITG2
DAPI
Overlay

B

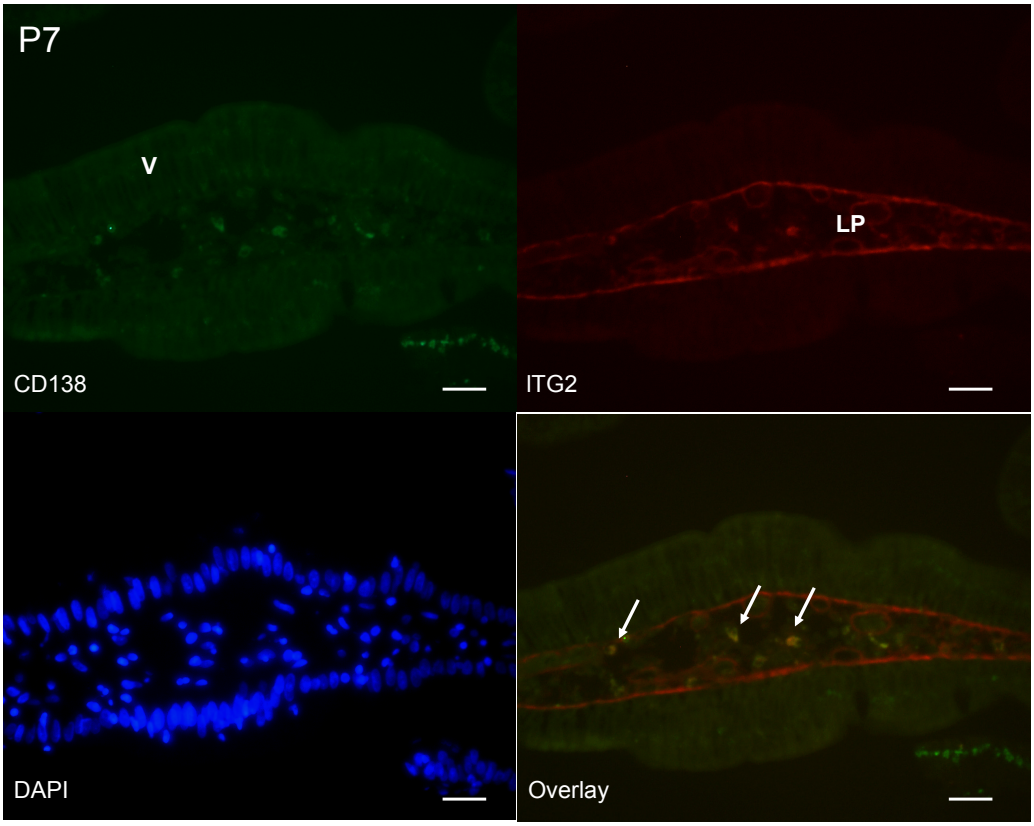
P7
V
LP
CD138
ITG2
DAPI
Overlay

C

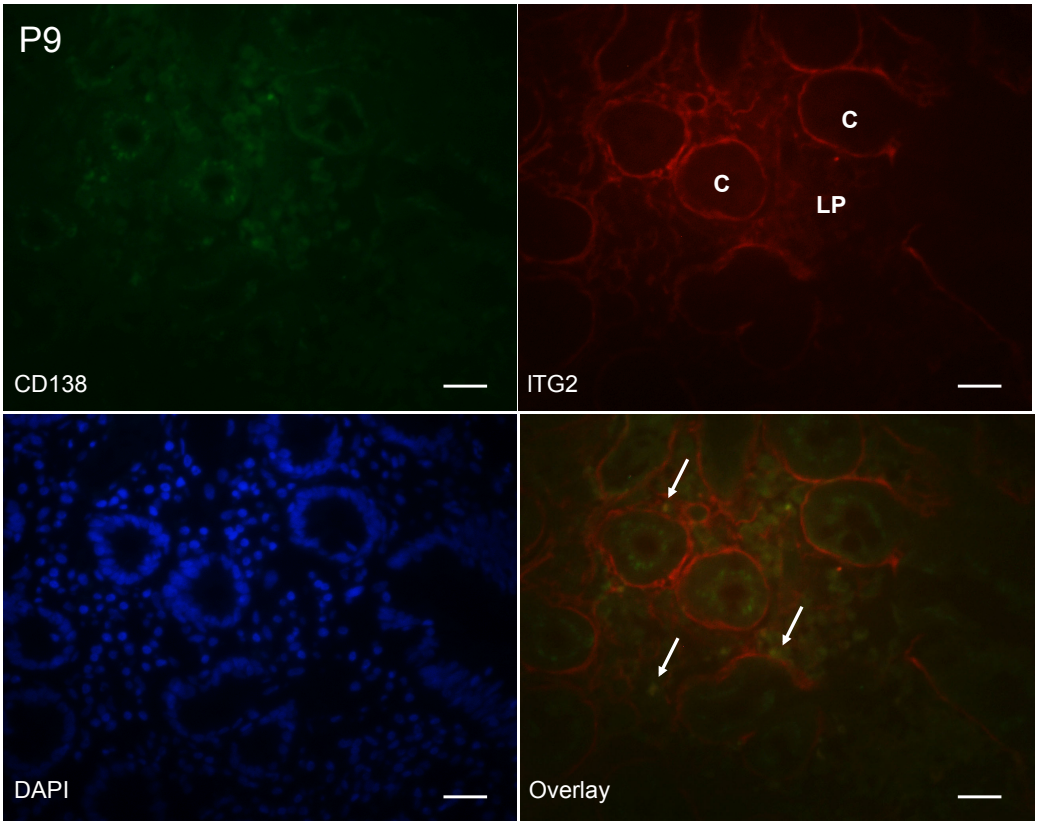

Fig. 5.8 Detection of TG2-specific plasma cells in D2 biopsies for 3 patients. Double immunostaining with labelled TG2 and antibody against plasma cell marker CD138 was performed. Overlay shows colocalization of plasma cell with labelled TG2 binding (arrows). TG2-specific plasma cells were observed in the lamina propria around the intestinal crypts (**C**) in patients P2 and P9 and in the lamina propria (**LP**) of the intestinal villi (**V**) in patient P7. Size bars = 50μm

Detection of TG6-specific B-cells in D2 biopsy section

Atto-565 labelled TG6 (20μg/ml) was incubated with sections for 1h at room temperature to facilitate detection of TG6-specific cells. Patients were considered to have TG6-specific cells when individual cells were observed, where nuclei were fully or at least partially present and ITG6 staining occurred in the majority of the cell surface with a more intense signal than the background. Sometimes, the typical morphology of plasma cells (considerable nucleus-to-cytoplasm ratio, eccentric nucleus) was evident,

e.g. Fig. 5.9 P12, but the section plane was frequently outside the central plane and therefore assessment was more difficult. Nevertheless, efforts were made to count the total number of ITG6$^+$ cells in the section, according to the parameters described. This was done on at least 3 separate occasions for each patient but unfortunately, due to experimental problems, such as tissue loss during staining, data was not available for all attempts for each patient (Table 5.4). Therefore it was decided to mark the patients as positive (Pos) or negative (Neg) for the presence of TG6-reactive cells. Patients were considered negative when the average number of TG6-reactive cells observed in different sections was less than 1.

Cells with positive staining for labelled TG6 were observed in a total of 15 patients: 9/11 (81%) CD group, 4/5 (80%) GA group, 2/8 (25%) control group (Table 5.5). Within the CD group, one of the negative patients was undertaking a gluten-free diet (P18). Within the control group, the 2 positive patients presented with markers related to neurological pathologies: P12 displayed antibodies against multiple autoimmunity marker glutamic acid decarboxylase (anti-GAD) and P13 presented with a cerebellar variant of multiple system atrophy (MSA-C). A link between anti-GAD, ataxia and GRD has been described (Hadjivassiliou et al., 2011). The number of TG6-reactive cells varied from patient to patient and within the same patient, from section to section and ranged from 0 to 27. A significant different was observed for number of patients testing positive for labelled TG6 reactive cells between gluten disorder patients and controls ($p=0.027$).

A panel with an overview of staining observed for the different patients tested is shown in Fig. 5.9. Overall, ITG6$^+$ patients displayed anti-TG6 antibody expressing cells in the lamina propria of the intestinal tissue, particularly around the intestinal crypts and within the intestinal villi.

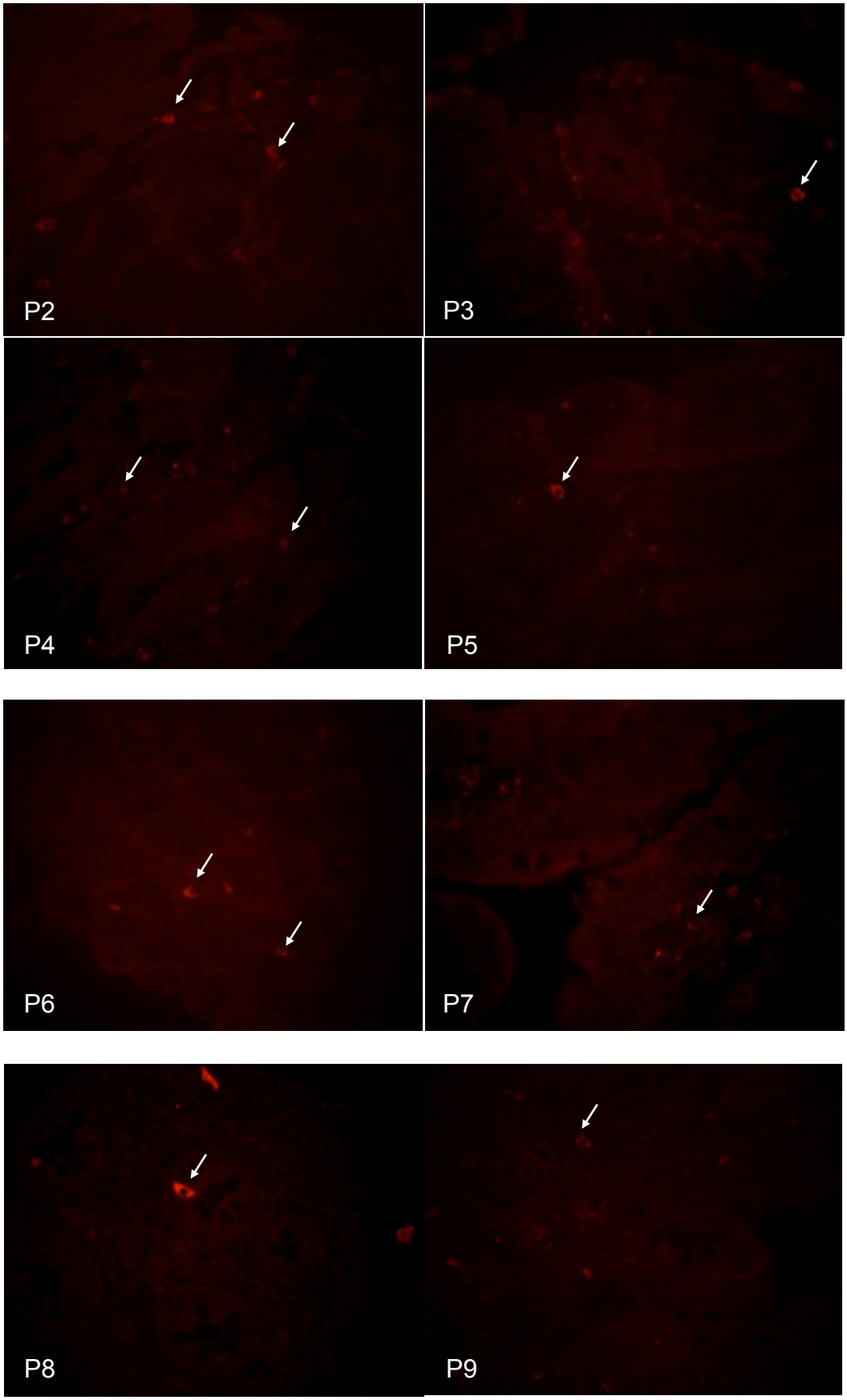
P2
P3
P4
P5
P6
P7
P8
P9

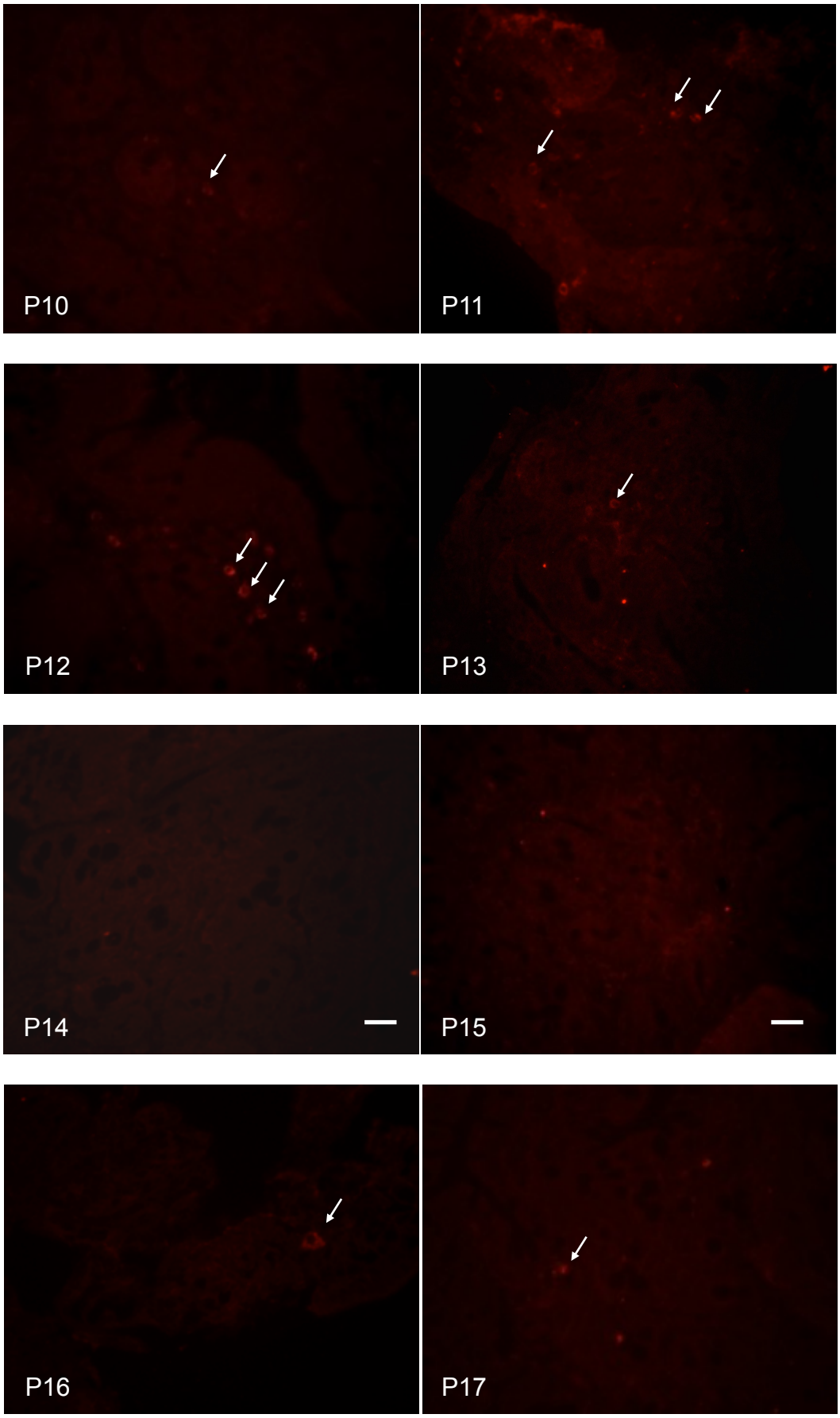
P10
P11
P12
P13
P14
P15
P16
P17

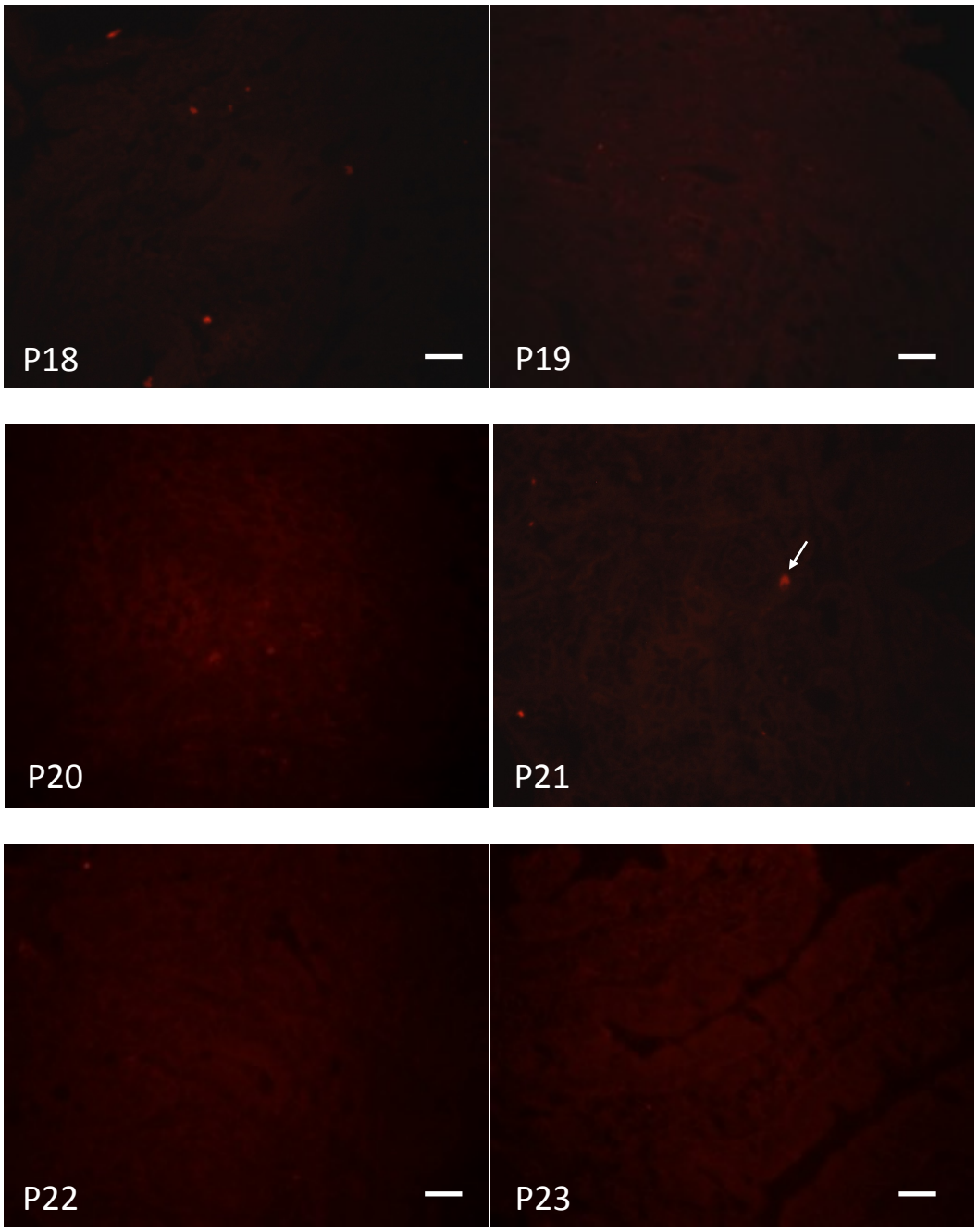
P18
P19
P20
P21
P22
P23

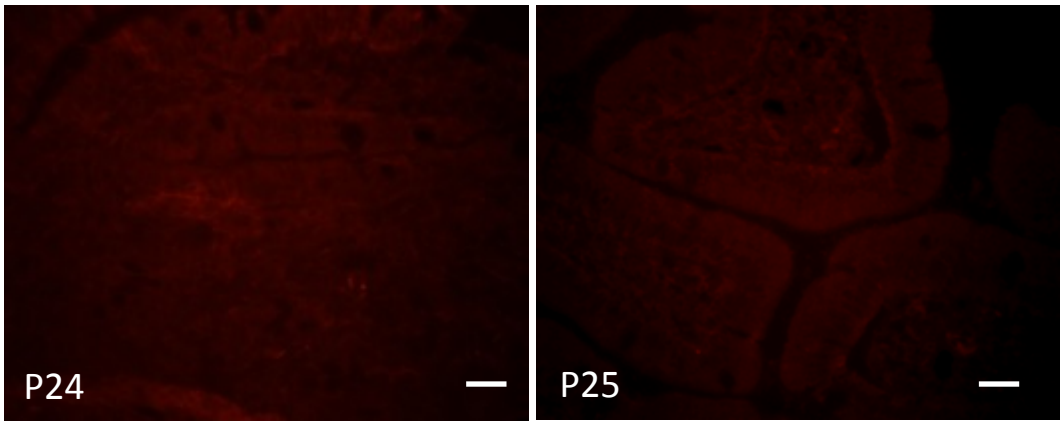

Fig. 5.9 Overview of labelled TG6 staining in patient's D2 biopsies. Fixed-frozen sections were incubated with 20μg/ml of ITG6 for 1h at RT. Size Bar 50μm

Table 5.4 Detection of anti-TG6 antibody expressing cells in different patient groups.

Group	ID	Age, y	Sex	Notes	ITG6	Cell count
Coeliac Disease	2	57	M	Anti-TG2^{+}(low)	Pos	22;3;f
	3	24	F	Anti-TG2^{+}	Pos	f;f;4
	4	22	F	Anti-TG2^{+}	Pos	2;0;4;12;f
	6	52	F	Anti-TG2^{+}	Pos	14;9;11
	7	43	F	Anti-TG2^{+}/ Anti-TG6^{-}	Pos	1;10;f
	8	37	M	Anti-TG2^{+}	Pos	6;f;5
	9	20	F	Anti-TG2^{+}	Pos	0;1;0;14
	18	73	F	Anti-TG2^{-} (on GFD)	Neg	f;0;0;
	20	27	F	Anti-TG2^{+}	Pos	2;0;f
	21	68	M	Anti-TG2^{-} (on GFD)	Pos	3;2;1
	23	73	F		Neg	1;1;0;f
Gluten Ataxia	5	61	F	Anti-TG2^{+}(low) (not on GFD)	Pos	0;5;5;f
	10	75	M	Anti-TG2^{-}/Anti-TG6^{+}/ (not on GFD)	Pos	2;0;4;4;6
	11	60	F	Anti-TG2^{-}/Anti-TG6^{+}/ (not on GFD)	Pos	4;3;4;12
	16	60	F	Anti-TG2^{-}/Anti-TG6^{-}	Neg	1;0;1
	17	61	M	Anti-TG2^{-}/Anti-TG6^{+}	Pos	1;1;2
Control	12	39	M	ISA/ Anti-GAD^{+} Anti-TG2^{-}/Anti-TG6^{-}	Pos	7;6;f;27;f
	13	56	F	MSA-C/ Anti-TG2^{-}	Pos	2;7;f
	14	67	M	ISA/Anti-TG6^{+}/ Anti-TG2^{-}	Neg	0;0;1
	15	68	F	ISA Anti-TG2^{-}/Anti-GAD^{+} Anti-TG6^{+}(borderline)/	Neg	0;0;1
	19	44	F	Anti-TG2^{+}(low)	Neg	0;0;0
	22	72	M		Neg	0;0;0
	24	63	F		Neg	0;0;f
	25	28	F		Neg	0;0;0

Abbreviations: GFD = gluten-free diet; WMA = white matter abnormalities; MSA-C = cerebellar variant of multiple system atrophy; ISA = idiopathic sporadic ataxia. anti-GAD = antibodies against glutamic acid decarboxylase; f = experiment failed

Table 5.5 Summary of results obtained for labelled-TG6 reactive cells in patients gut biopsies.

		Results		
		Negative	Positive	Total
Disease Group	Celiac Disease	2	9	11
	Gluten Ataxia	1	4	5
	Control	6	2	8
Total		9	15	24

A significant different was observed for number of patients testing positive for labelled TG6 reactive cells between gluten disorder patients and controls (p=0.027).

To identify the nature of the cells that were binding labelled TG6, B-cell marker CD20 and plasma cell marker CD138 were also analysed on the same section. Due to poor tissue morphology or loss of tissue during staining process, data was not acquired for all the patients. It was expected that colocalization of ITG6$^+$ with B-cell and plasma cell markers, CD20 and CD138, respectively. Surprisingly, this was not always evident. Since we only performed double labelling in each section, it could be that ITG6$^+$CD20$^-$ cells detected in one section of a patient were in fact ITG6$^+$CD138$^+$ cells and vice-versa. The nature of all ITG6$^+$ cells present in patient sections was therefore impossible to determine based on this approach. Nonetheless, colocalization of ITG6$^+$ cells with either CD20 or CD138 was detected. Below we show a few examples of patients were colocalization between ITG6 staining and CD20 or CD138 was observed (Fig 5.10).

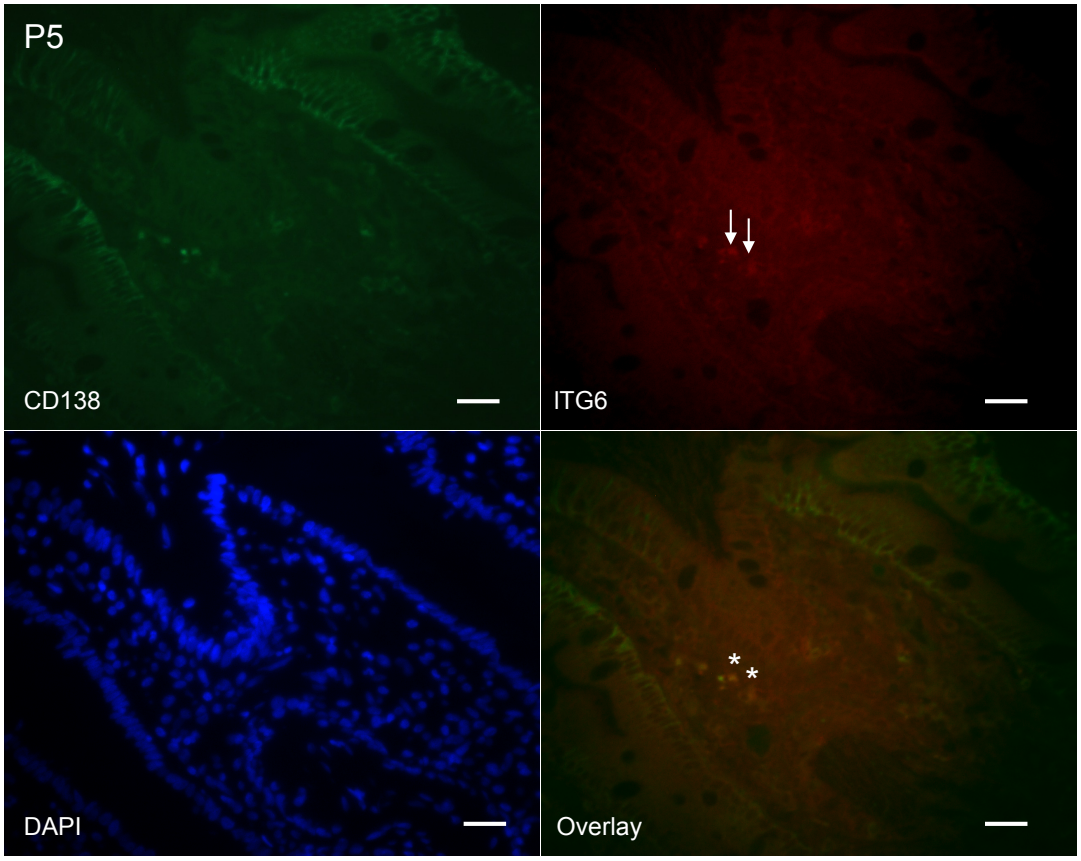
P5
CD138
ITG6
DAPI
Overlay

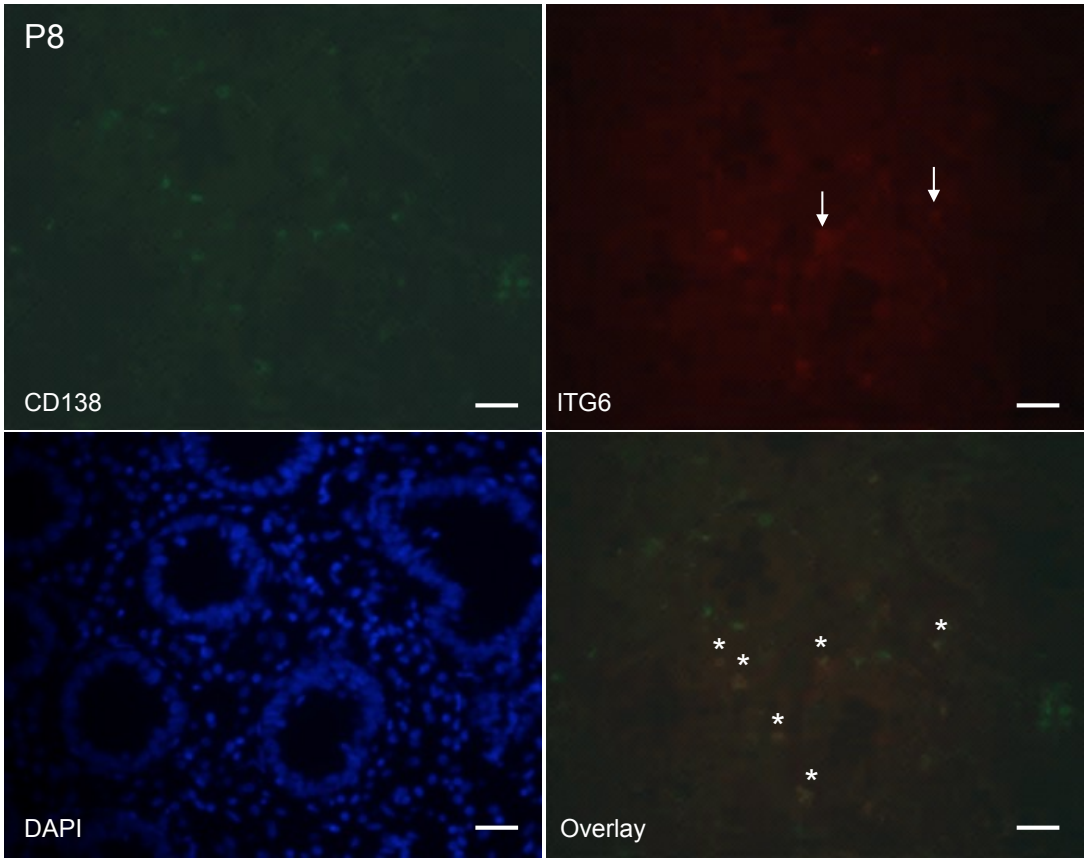
P8
CD138
ITG6
DAPI
Overlay

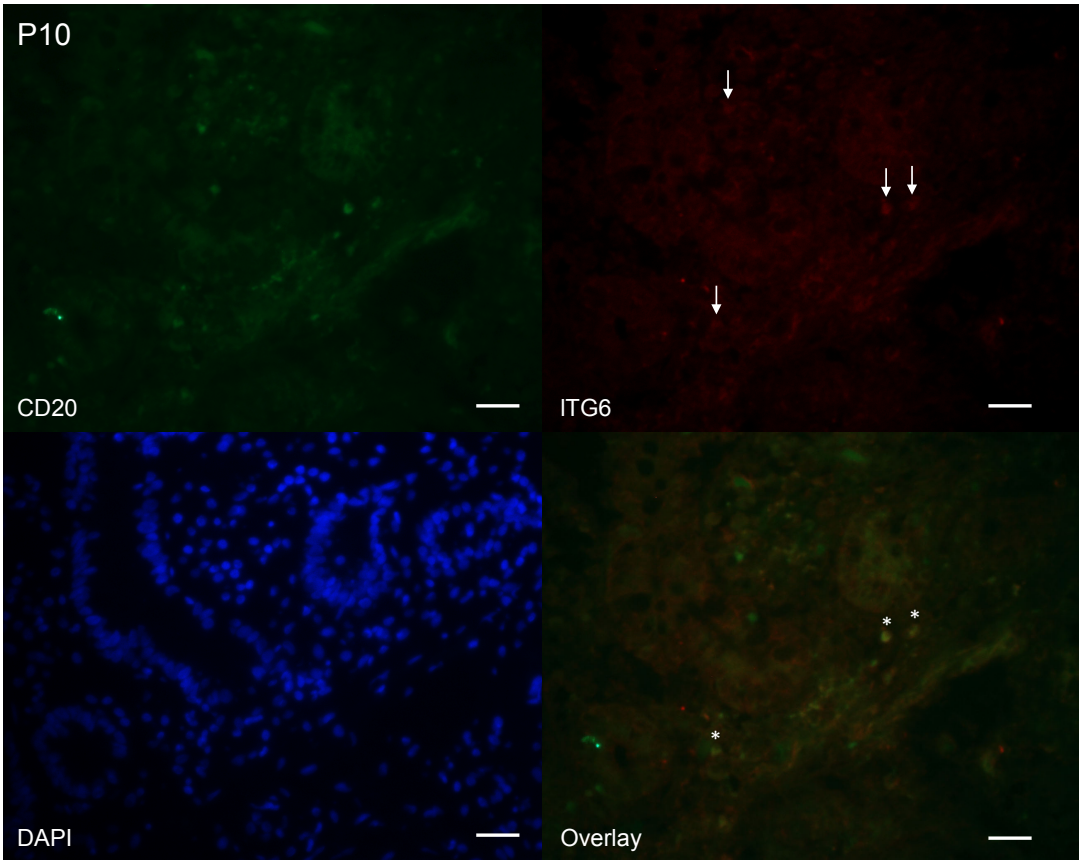
P10
CD20
ITG6
DAPI
Overlay

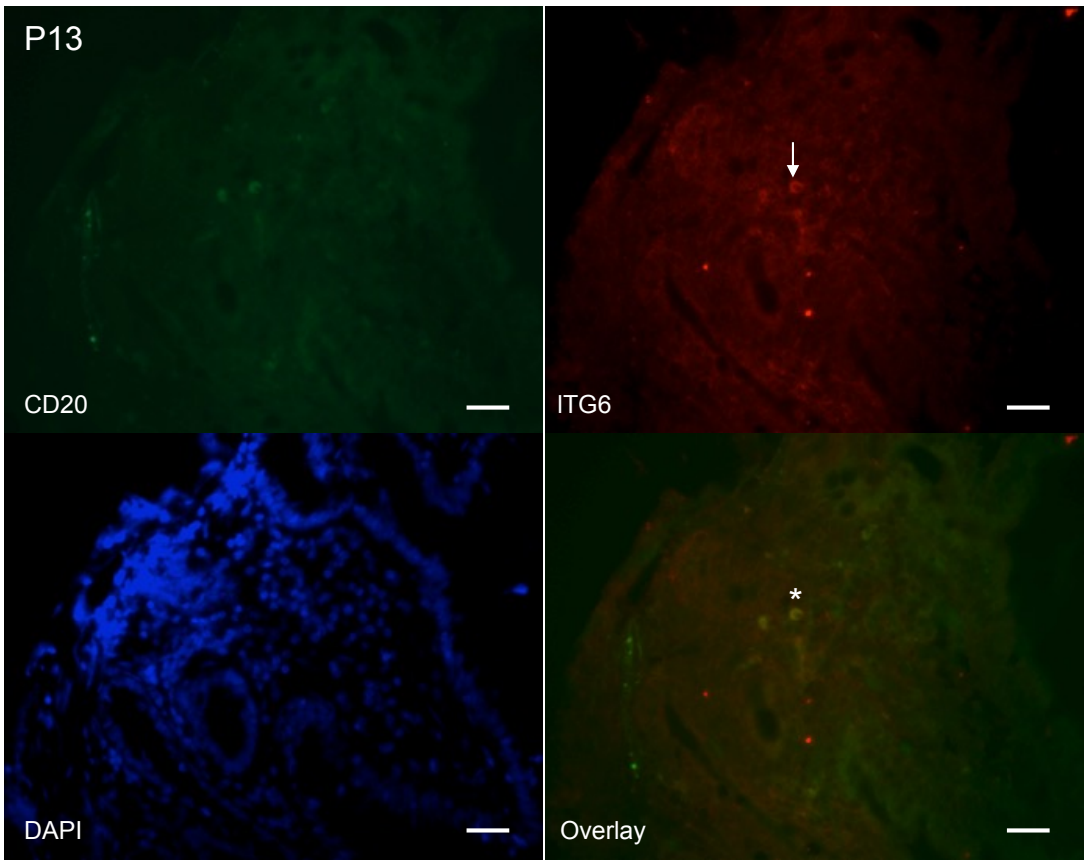
P13
CD20
ITG6
DAPI
Overlay

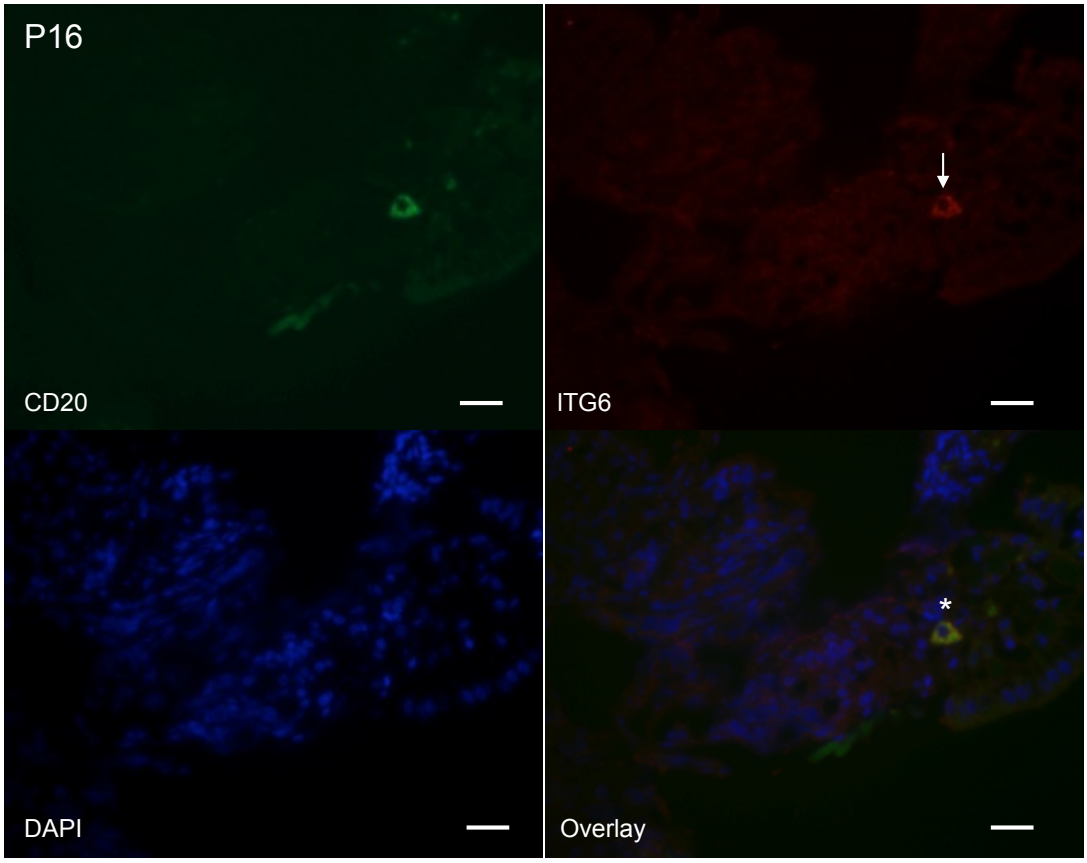

Fig. 5.10 Identity of TG6-reactive cells within the intestinal mucosa. Double immunostaining of fluorescently labelled-TG6 with either antibodies to B-cell marker CD20, or plasma cell marker CD138 in different patients. Colocalization is shown by *. Size bar = 50μm

5.3 Discussion

In this chapter, the presence of TG2 and TG6-specific B-cells in small intestine D2 biopsies of a cohort of patients presenting with GRD or controls was investigated. The main goal of these experiments was to contribute to the mechanistic understanding of autoantibody development in extraintestinal gluten-related disease manifestations, particularly in gluten ataxia.

As previously mentioned, three different, but genetically linked, transglutaminases have been identified as the autoantigens in different gluten related disorders: TG2 in coeliac diease (Dieterich et al., 1997), TG3 in dermatitis herpetiformis (Sárdy et al. 2002) and TG6 in gluten ataxia (Hadjivassiliou et al., 2008). The mechanism for the development of antibodies against these 'self-proteins' is still not fully understood.

A study based on *in situ* detection of autoantibodies with immunofluorescence suggested that anti-TG2 antibodies were produced locally in the small intestine (Korponay-Szabó et al., 2004), although this is still a matter of debate and the exact site of production of anti-TG2 antibodies is still unknown. Plasma cells specific for TG2 have been observed in the small intestinal tissue of coeliac disease patients (Di Niro et al., 2012). In these current experiments, a low number of plasma cells were also detectable when performing double immunofluorescent staining with labelled TG2 and plasma cell marker CD138. Although not all patient sections were studied, plasma cells were present in 2 CD patients and in 1 patient with CD and white-matter abnormalities. This was not surprising, as TG2, although with less specificity than TG6, has also been implicated in gluten ataxia (Hadjivassiliou et al. 2006).

In the context of coeliac disease, Sollid et al (2007) proposed that activation of TG2-reactive B-cells occured through help from gluten-reactive T-cells. This proposed model is based on the possibility that TG2-specific B-cells were able to process and present TG2-gliadin complexes (Sollid et al. 1997). In fact, such an ability was demonstrated by Di Niro and colleagues, therefore favoring this model (Di Niro et al., 2012). More recently, Iversen proposed that B-cell receptors serve as substrates for TG2 and become

cross-linked to gluten-derived peptides. This model links gluten peptide uptake by TG2-specific B-cells directly to peptide deamidation, necessary for the activation of gluten-reactive T-cells (Iversen et al. 2015). It is possible that a similar mechanism is involved in the pathogenesis of the gluten-related neurological pathology, where TG6-specific autoantibodies are produced. In this case, gluten-reactive T-cells would provide help to TG6-reactive B-cells leading to production of antibodies against the neuronal protein TG6 (which are the hallmark of gluten ataxia). In these current experiments it was demonstrated that, although at low numbers, TG6-reactive cells do exist in the lamina propria of the small intestine of GRD patients. These cells were identified mainly in patients diagnosed with coeliac disease and gluten ataxia with a prevalence of 81% and 80%, respectively. The control patients positive for TG6-reactive cells, presented with neurological abnormalities, with 1 of these patients also presenting with elevated anti-glutamic acid descarboxylase antibodies (marker of multiple autoimmunity). Overall, it appears that TG6-reactive B cells were present primarily in patients with a form of gluten-related disorder. Furthermore, some of these cells were identified as being $CD20^+$, the main surface marker for B-cells. This supports the idea that, like TG2-reactive B-cells in Sollid's proposed model, TG6-reactive B-cells are present and could be activated by gluten-reactive T-cells in the gut of susceptible individuals. The knowledge that TG6 is able to deamidate gluten peptides, that constitute T-cell epitopes (Jorunn Stamnaes, Dorum, et al., 2010), in a similar way to TG2, further supports this model. The site where the intestinal biopsy was collected could explain the scarce number of TG6-reactive/$CD20^+$ cells observed. B-cells have been shown to be mainly present in the gut associated lymphoid tissue (GALT) (Spencer & Sollid, 2016). Lamina propria adjacent to GALT may contain B-cells that tend to be large cells resembling plasmablasts or plasma cells, while distant lamina propria contains few, if any, $CD20^+$ B-cells. If patient biopsies were taken from a location that did not contain the GALT, detection of these cells would be difficult.

Additionally, some of the detected TG6-reactive cells that were negative for the B-cell marker CD20, did colocalize with the plasma cell

marker CD138. The overall number of these cells was also low. Recently, a study by Di Niro demonstrated poor correlation between the density of TG2-specific plasma cells in the lesion and IgA anti-TG2 antibody levels in the serum of CD patients (Di Niro et al., 2016). Therefore, it is possible that differentiation of activated B-cells might take place outside the gut. This would explain the low number of TG6-specific plasma cells found in our experiments. These cells could in fact be long-lived plasma cells, as suggested in the study by Mesin (Mesin et al., 2013).

It has to be stated that the number of $CD138^+$ cells detected in patient biopsies was surprisingly low, considering that the intestinal lamina propria is the primary location of plasma cells (review by Fagarasan & Honjo, 2003). Additionally, a high number of IgA positive cells were found in all patients of this study, suggesting that a high number of plasma cells were present in the intestinal sections. The unexpected low number of $CD138^+$ cells detected in this current study could be explained by inefficient detection of CD138 (syndcan-1) by the purchased antibody. In fact, signal for plasma cell marker CD138 in control tonsil tissue was weak, but since plasma cells are not usually abundant in this tissue, the antibody was considered suitable for our experiments. This could perhaps explain the origin of the TG6-reactive cells that stained apparently negative for CD20 and CD138, and some of these may in fact be $CD138^+$, perhaps expressing lower levels of the transmembrane proteoglycan. As serial sections of patient biopsies were not always possible to obtain, and double immunostaining only allowed identification of TG6-reactve cells with either CD20 or CD138 in each case, it could also be that TG6-reactive cells negative for CD20 detected in one section would be staining positively for CD138, and *vice-versa*.

In conclusion optimization of a protocol for immunofluorescence staining of TG2 and TG6-reactive cells in the human gut was achieved. Furthermore, this study shows for the first time that TG6-reactive cells are present in the human gut and they seem to correlate to the presence of a gluten-related disorder. However, there are clear limitations in these experiments and it is premature to conclude whether or not TG6-reactive cells have diagnostic potential in the context of gluten-related disorders.

Nonetheless, the presence alone of such cells supports a model for anti-TG6 antibodies production by plasma cells in the gut and driven by gluten-specific T-cells, similar to the one proposed by Sollid for anti-TG2 antibodies.

Chapter 6 Transglutaminase expression in macrophages

6.1 Introduction

As discussed in the previous chapter, the knowledge of the pathogenic adaptive immune response towards gluten in CD is quite comprehensive. However, an understanding of the role of innate immunity in the disease pathogenesis is still lacking.

Adaptive immunity does not appear to be sufficient for establishment of the CD lesion, and it has been suggested that stress responses in the intestinal epithelium and innate immunity may play a role in the development of CD (J. Stamnaes & Sollid, 2015).

It is established that HLA-DQ molecules are involved in the pathogenesis of CD (Ludvig M Sollid & Jabri, 2011), but is still not understood where and on which cells these molecules exert their function. These molecules are mainly expressed on specialized antigen-presenting cells such as monocytes, macrophages and dendritic cells. Gliadin peptides have been shown to activate monocytes and macrophages *in vitro* with subsequent release of pro-inflammatory factors such as TNF-α (Tucková et al., 2002). A study has also demonstrated a rapid increase of a specific type of dendritic cells, expressing HLA-DQ molecules, in the mucosa of coeliac disease patients after oral gluten challenge (Brottveit et al., 2012). Such findings suggest that a specific subpopulation of cells could present gluten peptides to gluten-reactive T-cells. Likewise, although previous research in this thesis has demonstrated that TG6-specific B-cells and plasma cells are present in the gut, it remains to be shown where TG6 is expressed as, unlike TG2 it appears not to be expressed by the major types of cells making up the tissue. One hypothesis is that TG6 may be expressed by infiltrating immune cells.

In this chapter the focus is the analysis of expression of the gluten-related disorder autoantigens TG2, TG3 and TG6 in different monocytes and macrophages cell populations at baseline and upon stimulation. An insight into the expression of these enzymes might help the understanding of the

role that the innate immune cells play in the pathogenesis of gluten-related disorders, specifically, this might identify the site at which the deamidation reaction linked to these diseases occurs.

The aims of the chapter:

1. To characterize TG2, TG3 and TG6 gene expression in human and murine monocytes before and after differentiation into M1 and M2 macrophages and after bacterial stimulation.

6.2 Results

6.2.1 THP-1 monocyte differentiation into mature macrophages

Initially, a monocyte cell model was chosen to assess expression of transglutaminases during different stages of differentiation and in response to bacterial stimulation.

The human leukemia cell line THP-1 has been reported to express distinct monocytic markers (Tsuchiya et al., 1980) and was, therefore, chosen for this study. More recently, it has been suggested that this cell line is actually a precursor cell linked to dendritic cell differentiation. Additionally, these cells have been reported to express TG2, upon monocyte to macrophage differentiation (Mehta & Eckert, 2005; Mehta & Lopez-Berestein, 1986), making these cells a good starting point to study the involvement of the innate immune response in the context of gluten-related disorders.

Differentiation of THP-1 monocytes was performed in two sequential steps (Fig. 6.1A). Detailed methodology can be found in section 2.21 of chapter 2. Initially, monocytes were stimulated with or without 50ng/ml of 12-O-tetradecanoylphorbol-13-acetate (TPA), for 48h. TPA, or PMA, is a strong tumor-promoting phobol diester, that has been shown to potentiate differentiation of monocytes into macrophages (Shigeru Tsuchiya et al., 1982). Changes in cell morphology were assessed during the differentiation process (Fig. 6.1B). THP-1 monocytes are rounded cells with a smooth surface that grow in suspension. Cells stimulated with TPA, showed the typical morphological changes associated with differentiation. These cells became adherent, increased in size and presented a more granular appearance. This effect was more noticeable after 48h stimulation. No or few morphological changes occurred in THP-1 cells stimulated with medium only or DMSO, which was used as a carrier.

Differentiated THP-1 cells (M0) were then polarized towards classical (M1) or alternatively activated (M2) macrophages by a 3-day stimulation with 20ng/ml GM-CSF or M-CSF, respectively. Morphology of the polarized cells was assessed on the third day (Fig. 6.1C). Both cell populations were

completely adherent and appeared larger, due to extensive cell spreading. M1 and M2 cells presented a very similar morphology, with a granular surface and formation of colonies, as expected after stimulation with colony stimulation factors (CSF).

Both of these cell populations were then incubated with either, 100ng/ml LPS or $1x10^5$ particles of heat killed candida (HKC), for 4 or 24h, to promote activation. M1 cells especially, appeared more elongated. The same effect was also observed when these cells were incubated with HKC, a less powerful stimulator (Fig. 6.1D).

Expression of M1/M2 markers was investigated by quantitative real-time PCR. This allowed confirmation that THP-1 cells were indeed polarized into these respective types of macrophages. M1 macrophages are expected to have a pro-inflammatory profile and tend to express higher levels of IL-12p40 compared to M2 cells (Chanput et al. 2013). M2 cells, on the other hand, are expected to have an anti-inflammatory profile and express higher levels of EBI3 comparing to M1 cells (Zheng et al., 2013).

THP-1 expression of IL-12p40 did not seem to be substantially altered by stimulation of the cells with TPA. However, increase in expression was observed after THP-1 differentiation to M1 or M2 macrophages: M1 cells showed a 3.3-fold increase and M2 cells a 2.4-fold increase in expression of the gene when compared to the control. LPS stimulation further increased the expression of IL-12p40 in M1 and M2 cells. This was expected for the M1 population as LPS is a known activator (Mantovani et al., 2004). However, such an increase of IL-12p40 in the M2 population was not expected as these macrophages usually present an IL-12^{low} profile even upon activation (Mantovani et al., 2004). As this effect was only observed after 4h stimulation it is possible that LPS, as a strong stimuli, has driven the M2 cells towards an M1 profile. This is not surprising as macrophages can be controlled by different changes in environmental signals (Gratchev et al., 2006; Porcheray et al., 2005). Furthermore, a similar LPS-effect has been previously reported in mouse M2 macrophages (Zheng et al., 2013).

Analysis of EBI3 gene expression, further confirmed that THP-1 cells had successfully been polarized to M1 or M2 macrophages. Anti-

inflammatory M2 macrophages showed a higher expression of EBI3 comparing to M1, most clearly evident after 24h of treatment with LPS. Unexpectedly, stimulation of M1 macrophages with LPS, also increased the expression of EBI3. In contrast to LPS, treatment with HKC appeared to have little effect on either expression of IL-12p40 or EBI3.

A

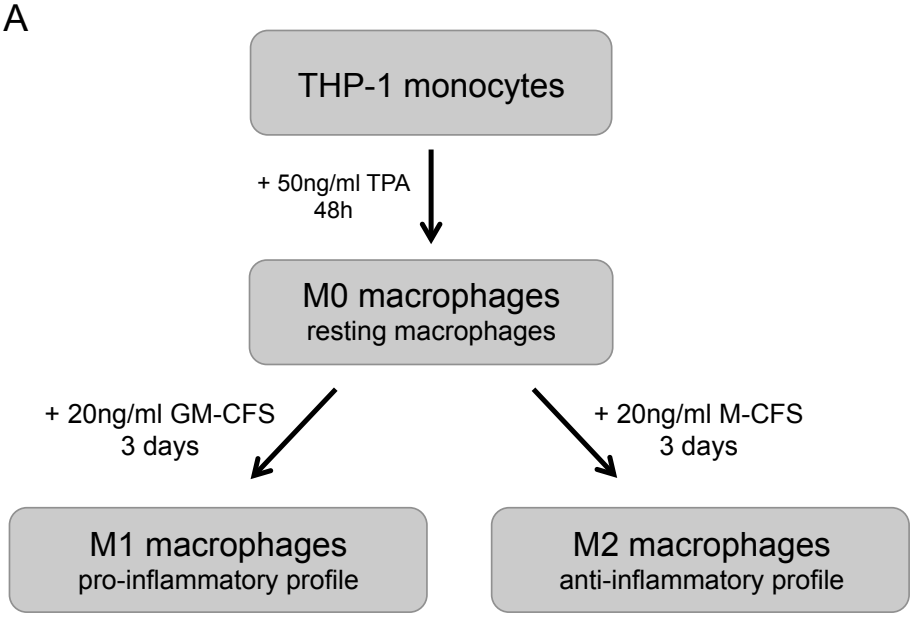

B

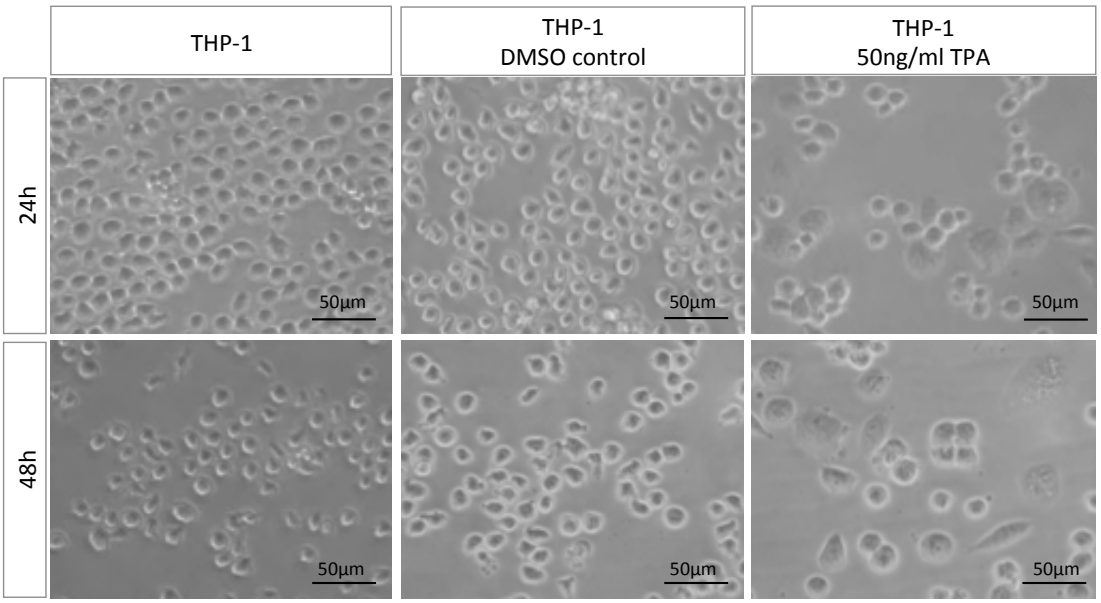

C

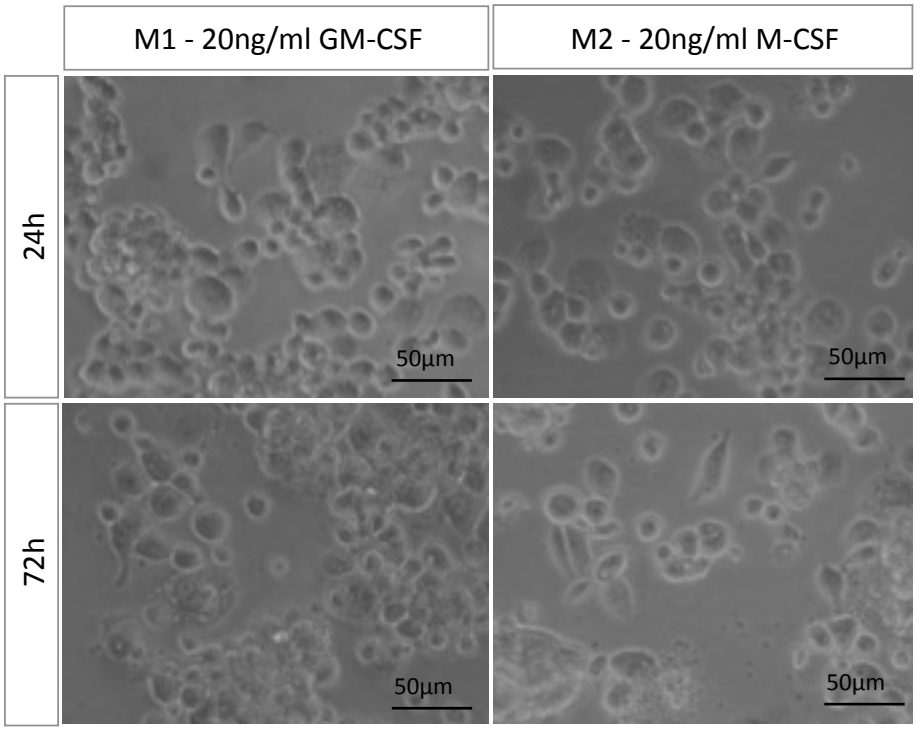
M1 - 20ng/ml GM-CSF
M2 - 20ng/ml M-CSF
24h
72h
50µm
50µm
50µm
50µm

D

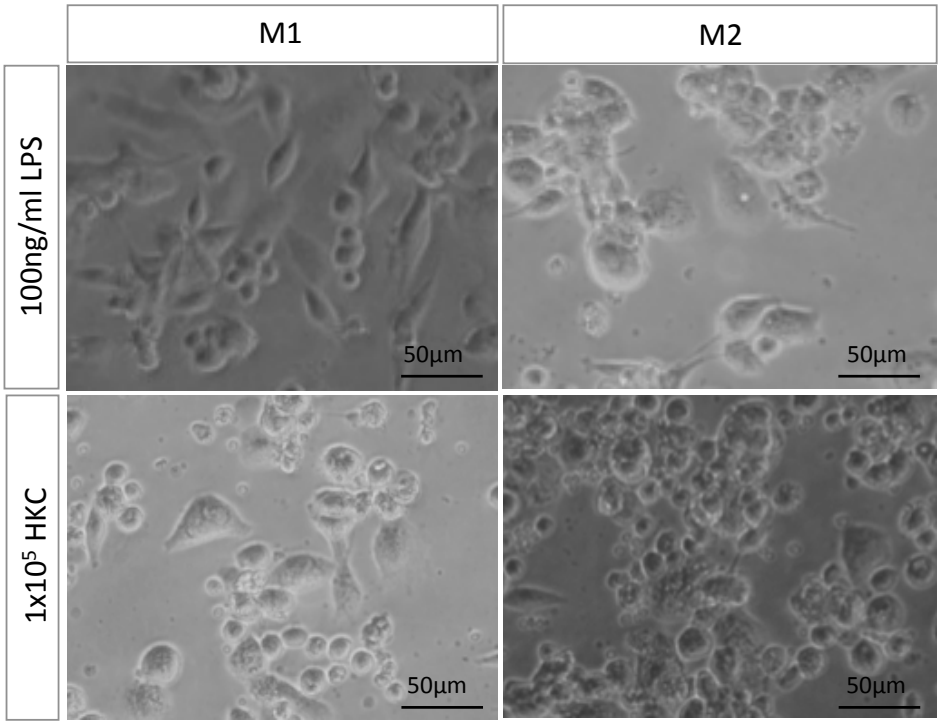
M1
M2
100ng/ml LPS
1x10^5 HKC
50µm
50µm
50µm
50µm

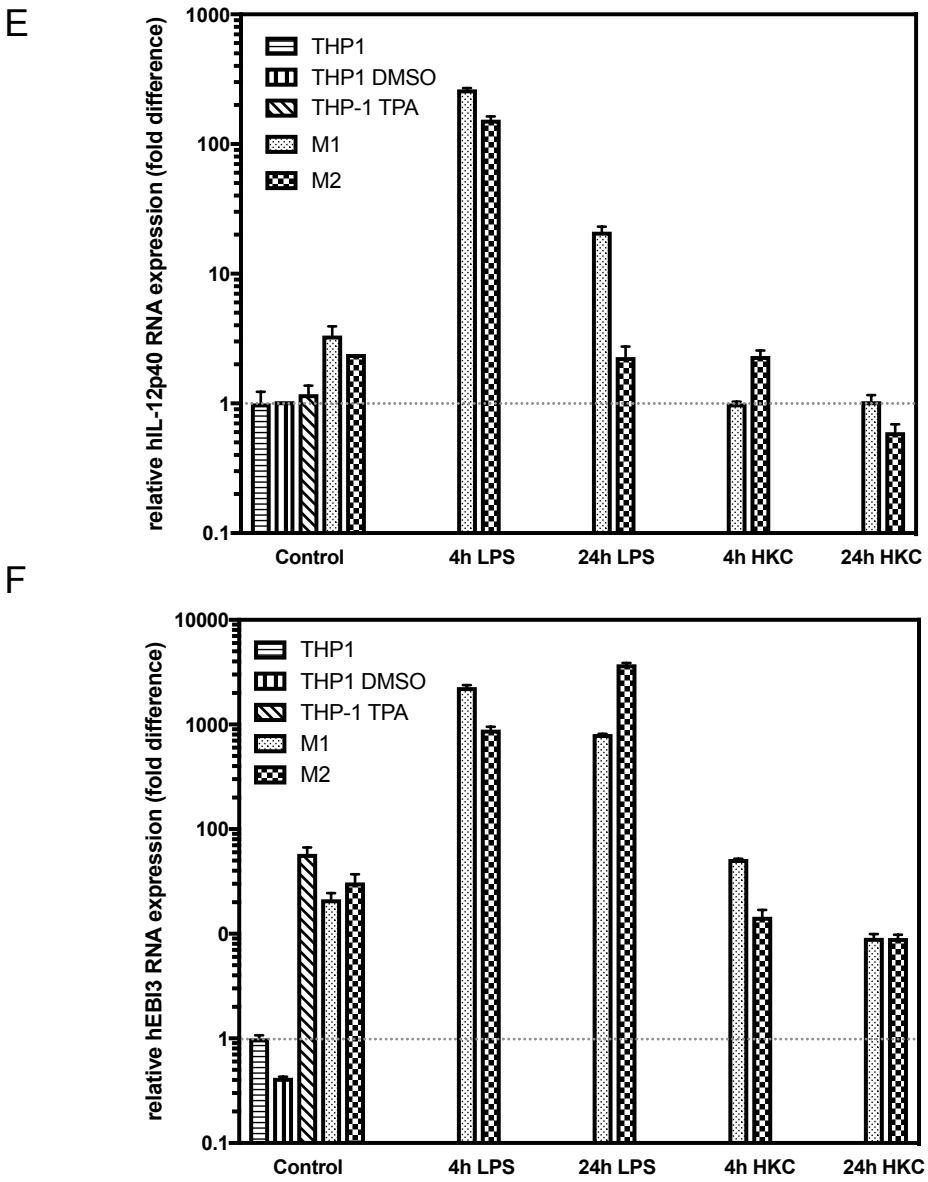

Fig. 6.1 THP-1 monocytes differentiation. A shematic of the process used for diferentiation of THP-1 monocytic cells is shown in panel **A**. THP-1 cells were initially diferentiated into macrophages by stimuation with 50ng/ml TPA over for a 48h period. Morphology of cells after 24 and 48h stimuation was analysed (**B**). Differentiated cells were polarized into M1 or M2-type macrophages by further stimulation with 20ng/ml of rhGM-CSF or rhM-CSF for 3 days. Morphology of cells was analysed after 24h and 72h (**C**). Cells were stimulated with either 100ng/ml of LPS or $1x10^5$ cells of heat killed candida (HKC) (**D**). To confirm success of polarization both stimulated and non-stimulated cells were analysed for expression of M1 macrophage marker, IL-12p40 (**E**) and M2 macrophage marker, EBI3 (**F**). The data is the mean of samples run in triplicate from one experiment. Data reflects sample analysis through the $2^{-\Delta\Delta Ct}$ method, normalized for internal control gene GAPDH, and is given relative to non-stimulated THP-1 population.

6.2.2 Expression of TG2, TG3 and TG6 is linked to inflammatory stimulation

After determining that THP-1 monocytes were successfully differentiated into two different macrophages populations, M1 and M2, a complete screening of TG2 expression was carried by PCR and products were analysed by agarose gel electrophoresis (
Fig. 6.2). Human gene 36B4 (h36B4), encoding for acidic ribosomal phosphoprotein, was used as an internal control. Detailed methodology for these experiments can be found in section 2.26 of chapter 2.

Results for expression of different TG gene products are summarized in Table 6.1. Non-stimulated THP-1 cells did not express gluten-related TGs (TG2, TG3, TG6) (
Fig. 6.2A). Lack of TG2 expression in unstimulated THP-1 cells has been previously reported by Metha & Lopez-Berestein, 1986. Expression of TG4, TG5 and FXIII was also observed in undifferentiated cells.

Upon TPA stimulation, the now M0 macrophage-type cells, showed a decrease in FXIII and, to a lesser extent TG5 expression. Expression of TG4 was no longer detectable. TG2 expression was substantially increased (
Fig. 6.2A). This is in agreement with observations by Metha & Lopez, 1986. Previous work within our group has also demonstrated that TPA and LPS both regulate TG2 expression at protein level in THP-1 cells (Adamczyk, 2013).

Non-activated M1 and M2 cell populations kept the tranglutaminase profile of TPA-stimulated THP-1 cells, with the exception of TG2, that showed a further increase in expression (
Fig. 6.2B and C). Activation of the two types of macrophages with LPS led to an even greater increase of TG2 expression. The same effect was observed with HKC but to a lesser extent. In M2 macrophages, HKC did not elicit an apparent response (
Fig. 6.2C). TG3 and TG6 expression was also induced upon stimulation with LPS but not with HKC, suggesting that a strong stimulus is needed for induction of their expression.

Expression of TG7 could not be determined due to the small product size and the presence of some primer dimers. Internal control gene, h36B4, confirms quality of samples and shows similarity of cDNA levels used for the experiment, across all samples.

In summary, the results showed that FXIII and TG4 were expressed by undifferentiated monocytes but were downregulated upon differentiation, whereas TG2 and to a lesser extent TG3 and TG6 expression was linked to inflammatory stimulation.

Table 6.1 Summary of results for transglutaminase RNA expression levels in THP-1 cells, analysed by gel electrophoresis

Sample	TG1	TG2	TG3	TG4	TG5	TG6	TG7	FXIII
THP-1	-	-	-	++	+++	-	ND	+++
THP-1 (DMSO)	-	-	-	++	+++	-	ND	+++
THP-1 (TPA)	ND	++	-	-	++	-	ND	+
M1	-	++	-	-	++	-	ND	(+)
M1 4h LPS	(+)	+++	(+)	-	++	+	ND	(+)
M1 24h LPS	+	+++	+	-	++	+	ND	(+)
M1 4h HKC	-	+++	-	-	++	-	ND	(+)
M1 24h HKC	-	+++	-	-	++	-	ND	(+)
M2	-	++	-	-	++	-	ND	(+)
M2 4h LPS	(+)	+++	-	-	+++	(+)	ND	(+)
M2 24h LPS	(+)	+++	-	-	++	-	ND	-
M2 4h HKC	-	++	-	-	+++	-	ND	(+)
M2 24h HKC	-	++	-	-	+++	?	ND	(+)

Results represent observations from one experiment.

Marking system: No gene expression (-), low (+), medium (++) and high (+++) expression levels; Borderline gene expression that needs further verification ((+)); Gene expression could not be unequivocally determined (ND).

A

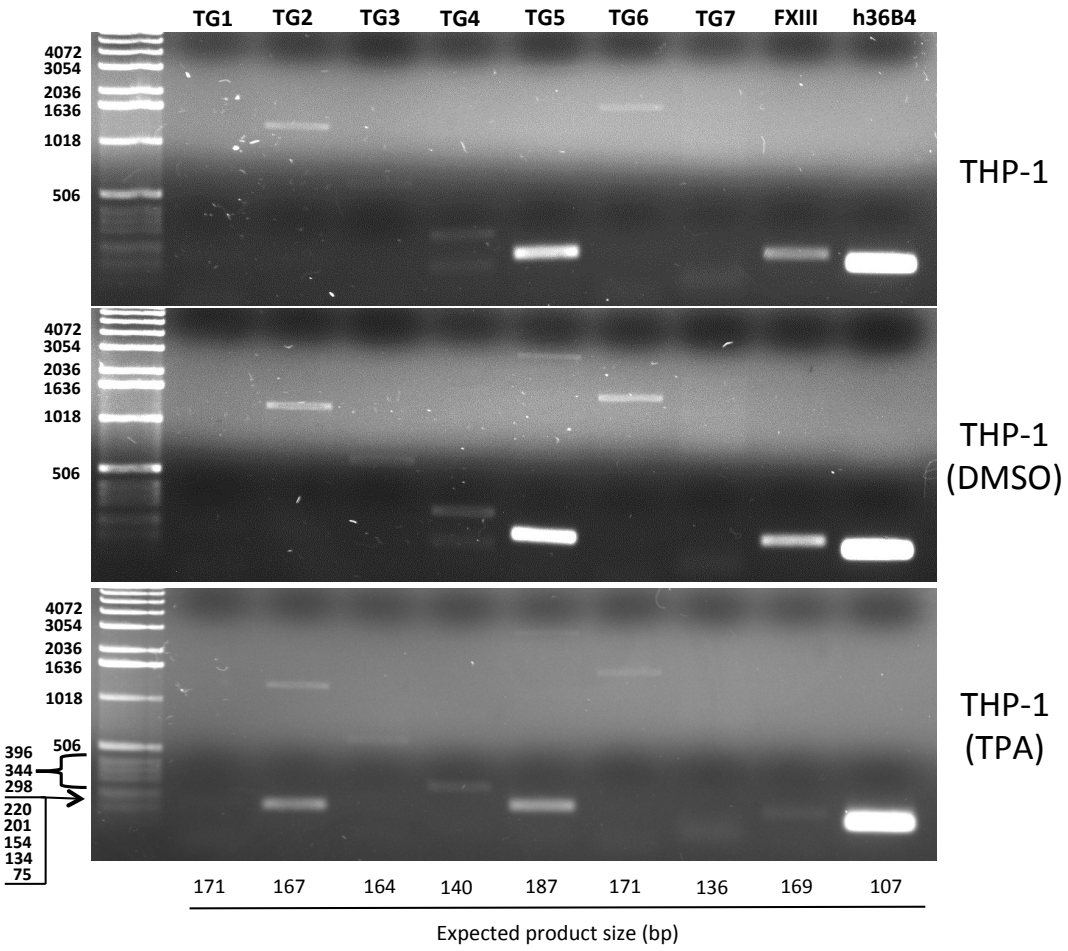
TG1
TG2
TG3
TG4
TG5
TG6
TG7
FXIII
h36B4
4072
3054
2036
1636
1018
506
396
344
298
220
201
154
134
75
THP-1
THP-1 (DMSO)
THP-1 (TPA)
171
167
164
140
187
171
136
169
107
Expected product size (bp)

B

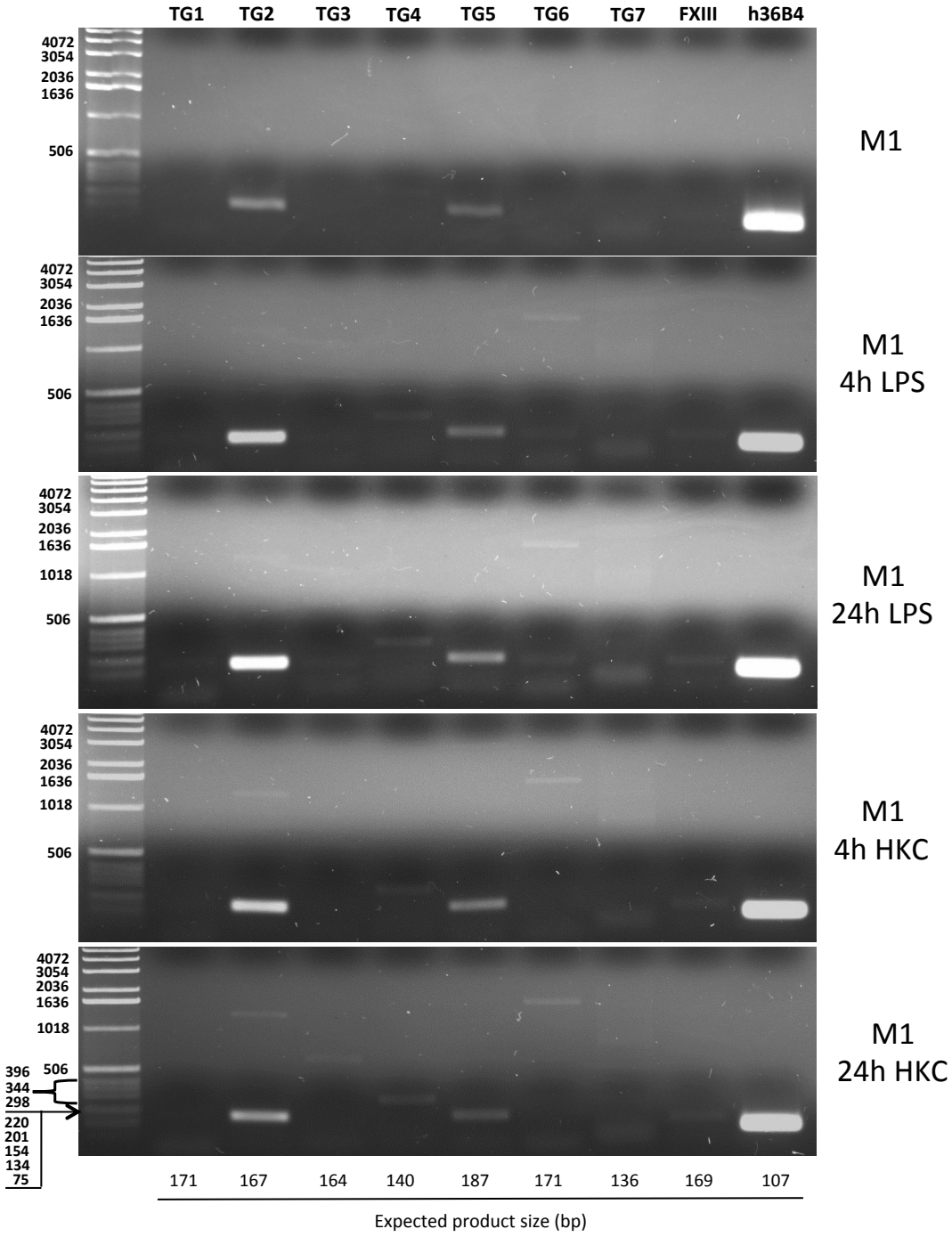
TG1
TG2
TG3
TG4
TG5
TG6
TG7
FXIII
h36B4
4072
3054
2036
1636
1018
506
396
344
298
220
201
154
134
75
M1
M1
4h LPS
M1
24h LPS
M1
4h HKC
M1
24h HKC
171
167
164
140
187
171
136
169
107
Expected product size (bp)

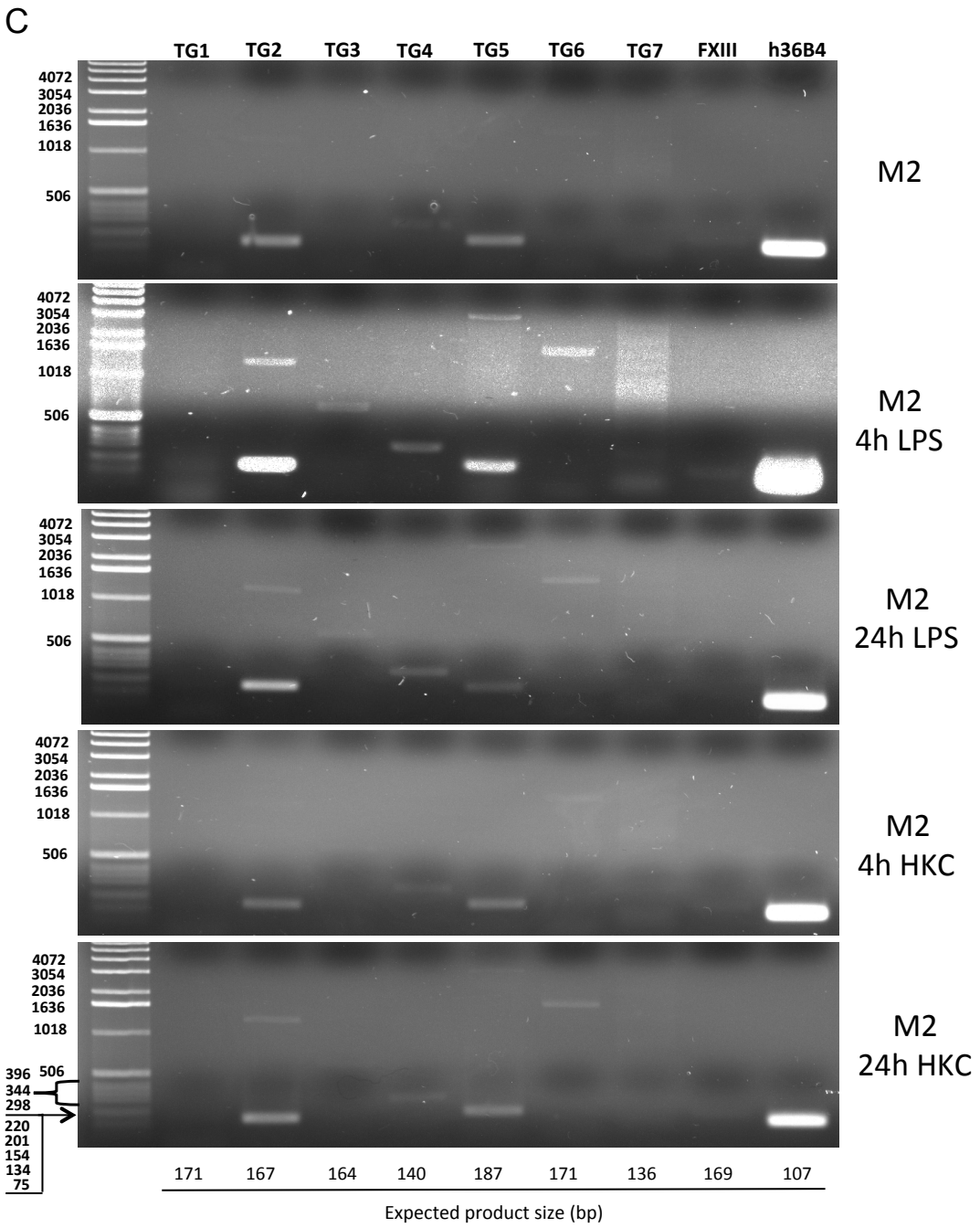

Fig. 6.2 Screening for expression of members of the TG-family in response to differentiation and stimulation of THP-1 cells. Amplified products were obtained by PCR and analysed on 1% agarose gel electrophoresis. EtBr stained products were visualized through UV light using a gel documentation system. Migration of size markers is shown on the left (1Kb ladder). Amplification of housekeeping gene (h36B4) is shown on the right. Factor FXIII and TG4 were expressed by undiferentiated monocytic cells and downregulated upon differentiation, whereas TG2 and, to a lesser extent, TG3 and TG6 expression appear to be linked to strong inflammatory stimuli. TG5 appears to be expressed but not affected by different conditions.

6.2.3 TG2 expression was increased in mouse macrophages after LPS stimulation

After detection of TG2 and TG6 in LPS-activated macrophages, differentiated from THP-1 monocytic cell line, it was decided to assess expression of these genes in primary cells. Initially murine macrophages were used, as it is comparatively easier to access mouse tissue than human tissue.

Detailed methodology for murine macrophages culture can be found in section 2.22 of chapter 2. Briefly, macrophages were isolated from mouse bone marrow and differentiated into M1 and M2 macrophages by stimulation with mouse GM-CSF or M-CSF, for 7 days. After differentiation, cells were trypsinised and reseeded at $2{,}5x10^5$ cells/well and allowed to adhere overnight. Cells were then stimulated with 100ng/ml of LPS and total RNA was extracted at 2, 6 and 24h time points. Total RNA was also extracted from control cells, which were not stimulated with LPS.

Success in terms of cell polarization to M1 and M2 macrophages was determined through analyses of iNOS and Arginase-1 gene expression by real-time quantitative PCR (qPCR). These two genes have been shown to have different expression in the two types of macrophages with M1 cells expressing higher levels of iNOS comparatively to M2. The inverse is seen regarding Arginase-1 expression (Zheng et al., 2013). Analysis of qPCR data showed that expression of these two genes in the mouse M1 and M2 population followed a similar pattern to the one reported by the above study (

Fig. 6.3 A and B). Without stimulation, no apparent difference was observed in the expression of iNOS between the two cell populations. However, an increase in iNOS expression was observed after LPS stimulation, with M1 cells showing higher expression levels (

Fig. 6.3A). This was expected as it has been reported before (Lu et al., 2015). M1 cells continued to show higher expression levels of the gene even after 24h LPS-stimulation.

At baseline, M2 cells showed a ≈300-fold higher expression of Arginase-1 in comparison to M1. These levels of expression were maintained after LPS stimulation of M2 cells, and no increase in expression was observed upon stimulation of M1 cells, at least for the early time points (

Fig. 6.3B). Phenotypic plasticity may contribute to the change seen after 24h.

Overall, the results led to the conclusion that the approach used was able to successfully polarize mouse bone marrow derived macrophages into two different cell populations, M1 and M2.

Analysis of TG2 and TG6 expression was also performed by qPCR, using a TaqMan assay previously optimized within the group.

Expression of TG2 at baseline was higher in the M2 population in comparison to the M1 population, with M2 cells showing 8-fold higher expression (

Fig. 6.3 CI). A substantial increase in expression of TG2 after LPS stimulation was detected, in both cell populations. M1 cells showed a 11-fold increase in expression compared to the corresponding unstimulated cells, whereas M2 showed a 2.6-fold increase (

Fig. 6.3 CII and III).

Therefore, similar to what was observed after stimulation of THP-1 derived macrophages, LPS was able to induce TG2 expression both in M1 and M2 macrophages.

TG6 expression was not detectable in the majority of the samples. TG6 gene expression was detected in M2 cells at baseline and after 6h and 24h of LPS stimulation. M1 cells, stimulated for 6h, also showed some level of TG6 expression. However, when expression was detected, it was at final amplification cycles and hence, near the limit of detection. Apart from 6h-LPS stimulated M2 cells, expression was not detected consistently in all sample replicates, suggesting that the samples contain only a few copies (and hence this is subject to statistical distribution). Therefore no graph of data could be

generated and we should take great caution when making conclusions about the expression level of this gene in mouse macrophages. Although it is likely that TG6 expression is triggered by inflammation, as it was observed for THP-1 derived macrophages, it is clear that this gene is expressed at very low levels. Digital PCR could be used in the future to further clarify this.

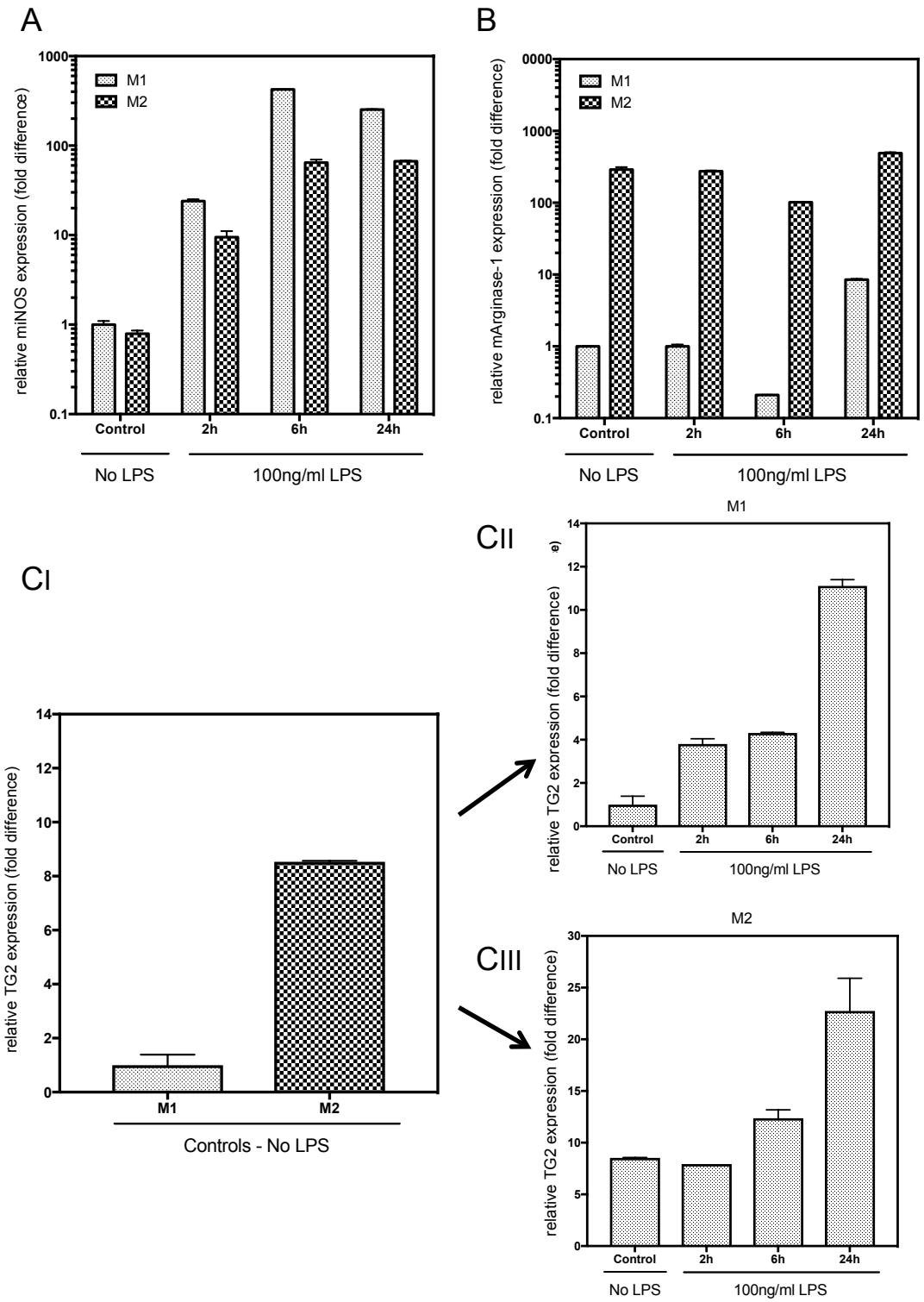

Fig. 6.3 Analysis of gene expression in mouse bone marrow derived macrophages (M1 and M2 populations). Samples in A and B were run in triplicate. Samples in C were run in duplicate. Data reflects sample analysis through the $2^{-\Delta\Delta Ct}$ method, normalized for internal control gene β-Actin (A and B) or h36B4 (C) and is given relative to unstimulated M1 macrophage population.

6.2.4 Is TG2 gene expression increased after stimulation HKC?

Access to different RNA samples of bone marrow derived mouse M1 and M2 macrophages, stimulated with HKC was available. These samples were kindly provided by Dr Xiaoqing Wei. Culture and differentiation and total RNA extraction was performed within Dr Wei's group, following methodology comparable to the one used in our experiments. In this experiment, M1 and M2 cells were stimulated with either medium only, 10^5 cells HKC, 10^6 cells HKC or 10^6 cells HKC+10% MC (melanocyte conditioned medium). Analysis of TG2 and TG6 expression in these samples was performed by qPCR as described for our own samples.

We were able to detect expression of TG2 in control samples in both cell populations, and these showed a similar level of expression (Fig. 6.4A). This was surprising, as previous experiments showed differences in TG2 gene expression between M1 and M2 macrophages (

Fig. 6.3). TG2 gene expression was increased after stimulation with both HKC only or HKC combined with MC in M1 macrophages (Note, data for stimulation with 10^5 cells of HKC was excluded as internal control gene expression wasn't within acceptable limits). Expression of TG6 was not detected by qPCR.

From an independent experiment, new cDNA was obtained from these samples and amplified by PCR. Amplified samples were analysed by agarose gel electrophoresis and EtBr staining. As expected, TG2 gene expression was detected across all samples, although this endpoint PCR did not give any quantitative information (Fig. 6.4B top panel). However, using this simple approach we were able to detect expression of TG6 (Fig. 6.4 bottom panel) and confirm upregulation of its expression upon inflammatory stimulation. M2 macrophages showed expression of TG6 in both baseline and stimulated samples, with an increase in expression after HKC stimulation. With regards to the M1 population, TG6 expression was not detectable in baseline samples but was upregulated in response to HKC stimulation, under all conditions. Although an internal control was not shown

in this gel, a separate experiment using the same cDNA confirmed that a similar amount of amplified product was obtained across all samples (Fig. 6.4).

A

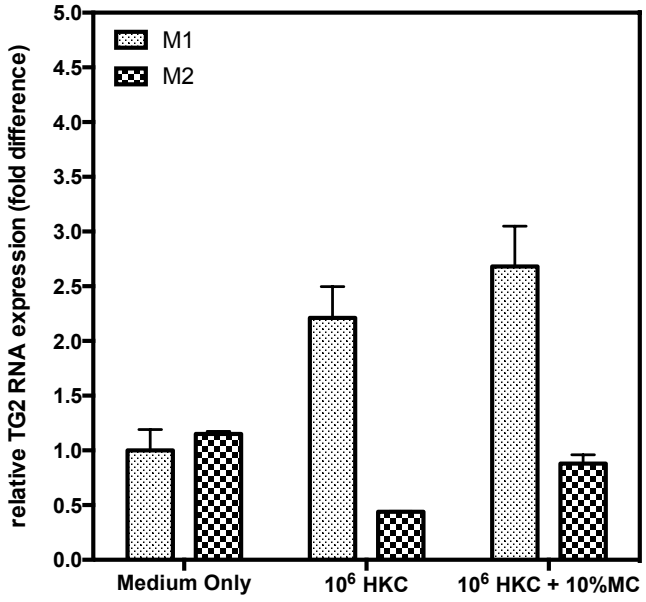

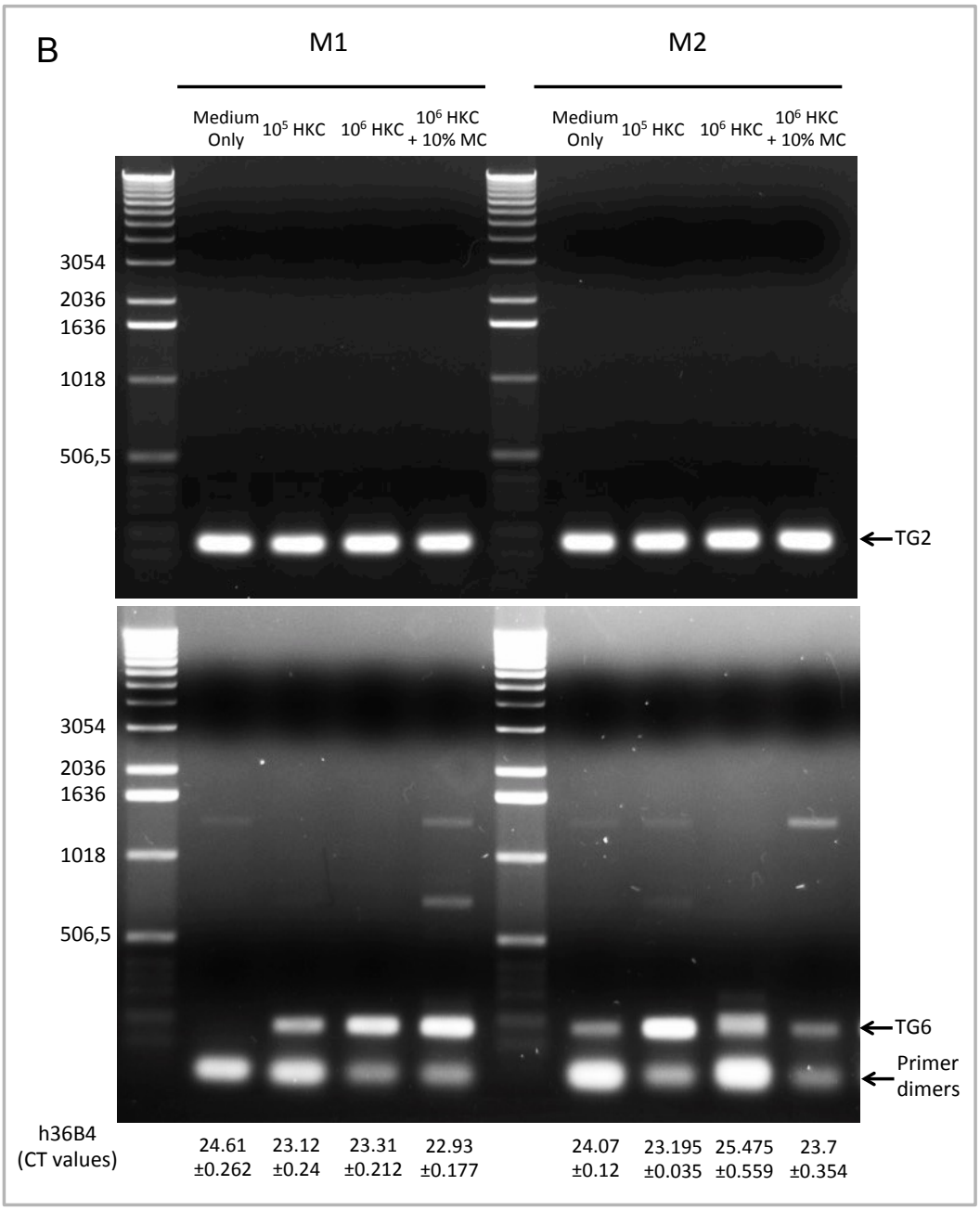

Fig. 6.4 Expression of TG2 and TG6 in mouse macrophages after stimulation with heat killed candida. A: Expression of TG2 was analysed by qPCR. Samples were run in duplicate. Data reflects sample analysis through the $2^{-\Delta\Delta Ct}$ method, normalized for internal control gene h36B4 and data is presented relative to unstimulated M1 population. **B:** Expression of TG2 and TG6 was analysed by PCR. PCR products were separated on 1% agarose gels and visualized using EtBr. Size markers are shown on the left (1Kb ladder) Internal control gene for the same cDNA samples was analysed independently by qPCR, and shown here at the bottom as Ct values. HKC = heat-killed candida; MC= melanocyte conditioned medium.

6.2.5 Expression of TG2, TG3 and TG6 in human PBMC derived macrophages

Expression of TG2 and TG6 gene in human peripheral blood mononuclear cell (PBMC) derived macrophages from 3 healthy volunteers was also analysed.

Detailed methodology of isolation culture and differentiation of human PBMC derived macrophages can be found in section 2.23 of chapter 2. Briefly, a total volume varying between 15-20ml of peripheral blood was collected from 3 healthy volunteers and mononuclear cells were separated using a density gradient media (Ficoll-Paque Premium). Polarization of monocytes into M1 and M2 macrophages was achieved by culturing the cells for 7 days in medium supplemented with 20ng/ml of either rhGM-CSF or rhM-CSF, respectively.

After 7 days of differentiation, a substantial change in morphology was observed for both differentiation regimens across all 3 subjects (Fig. 6.5A). Cells presented a more granular elongated surface, and were completely adherent to the flasks. In M2 cells, achieved by stimulation with M-CSF, irregular protrusions from the cell surface were also observed (Fig. 6.5A).

Cells were trypsinized, counted and re-seeded at a density of $0.5x10^5$cell/cm^2 and stimulated with medium only, 100ng/ml LPS or $1x10^5$ particles of HKC, for 4h, and total RNA was extracted. This time point was chosen based on the results obtained in the THP-1 cell experiments. After 4h stimulation a large increase in TG2, TG3 and TG6 gene expression was observed.

Expression of TG2, TG3 and TG6 was assessed by real-time quantitative PCR. Results represent data acquired by two independent experiments with cells isolated separately at two different times of blood donation (Fig. 6.5B-E). Expression changes are shown relative to unstimulated M1 cells from subject S (at time point t1).

Results showed some variability with regards to the expression of TGs between the three patients. Furthermore, it appears that gene expression in a given patient also differed between different time points. This was not

unexpected, as here, an uncontrolled population is analysed in contrast to mice, which had been maintained germ-free. Although these results were inconclusive a few observations can be made. Contrary to what was observed in mouse macrophages, expression of TG2 was higher in M1 cells at baseline compared to M2 cells in both R and D subjects. The opposite finding was true in subject S but only for time point 2 (t2) (Fig. 6.5B and C). Although differences were small, increase of TG2 gene expression after stimulation was not as clear-cut as expected based on results obtained with previous macrophages. When an increase was observed it was usually a difference of less than 2-fold compared to expression at baseline. A higher increase of expression was observed for subject S in LPS-stimulated M1 cells at t2 and M2 cells at t1.

Regarding TG3 expression, the same level of variability was observed. No substantial increase in TG3 expression was observed after stimulation, for either of the macrophage populations (Fig. 6.5 D and E).

Expression of TG6 was again close to the limit of detection and therefore the data was inconclusive.

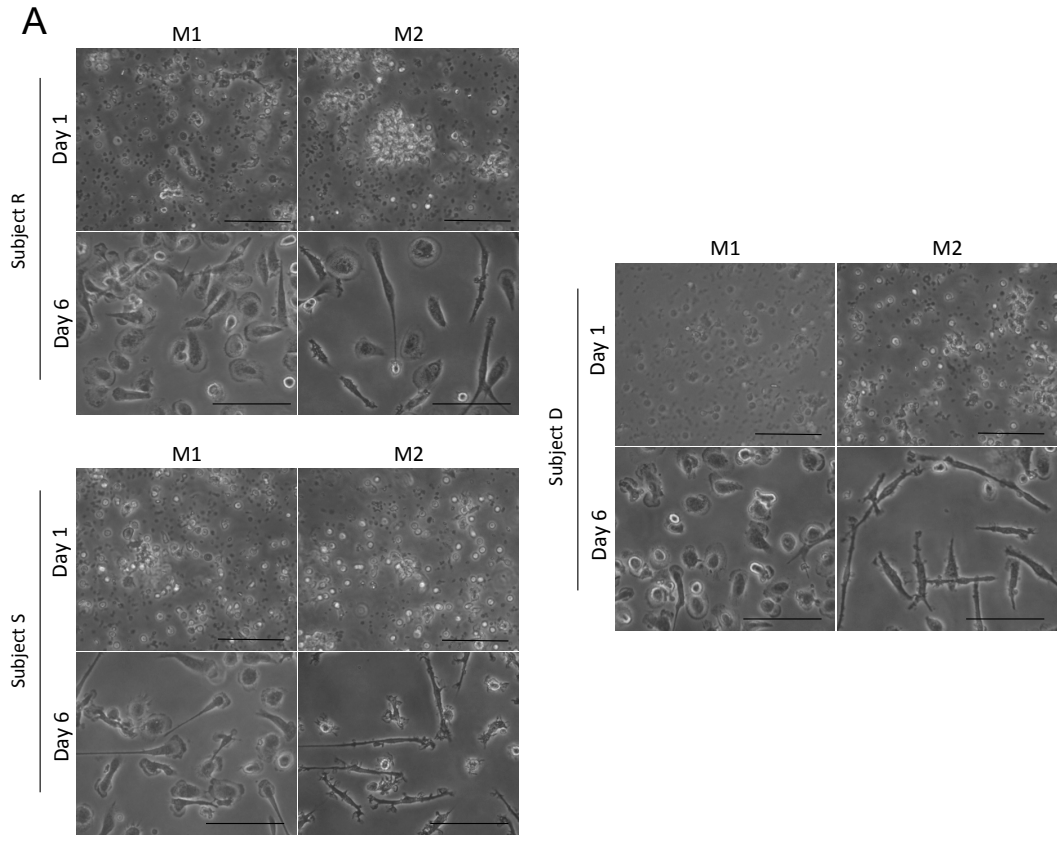

B

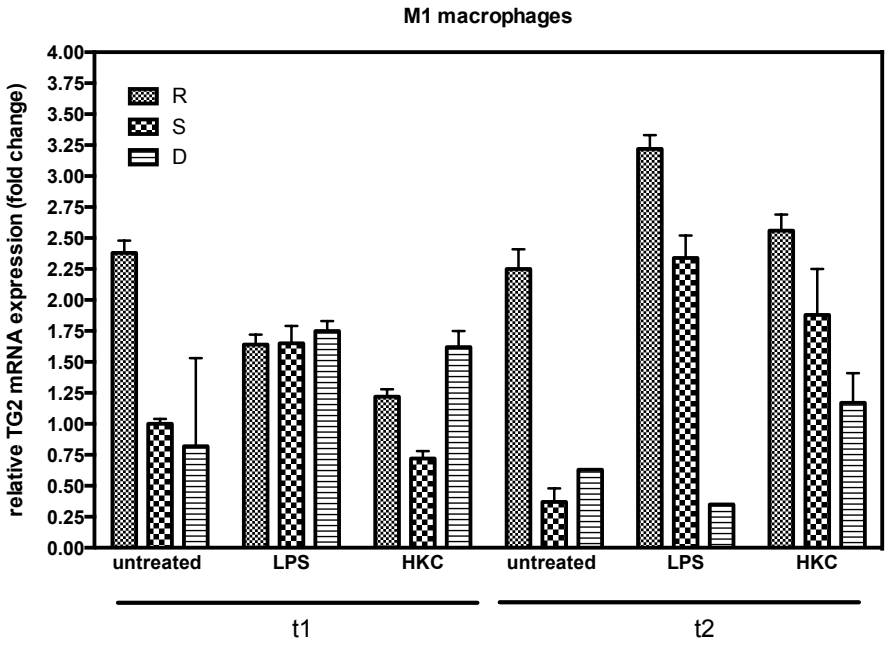
M1 macrophages
relative TG2 mRNA expression (fold change)
4.00
3.75
3.50
3.25
3.00
2.75
2.50
2.25
2.00
1.75
1.50
1.25
1.00
0.75
0.50
0.25
0.00
R
S
D
untreated
LPS
HKC
untreated
LPS
HKC
t1
t2

C

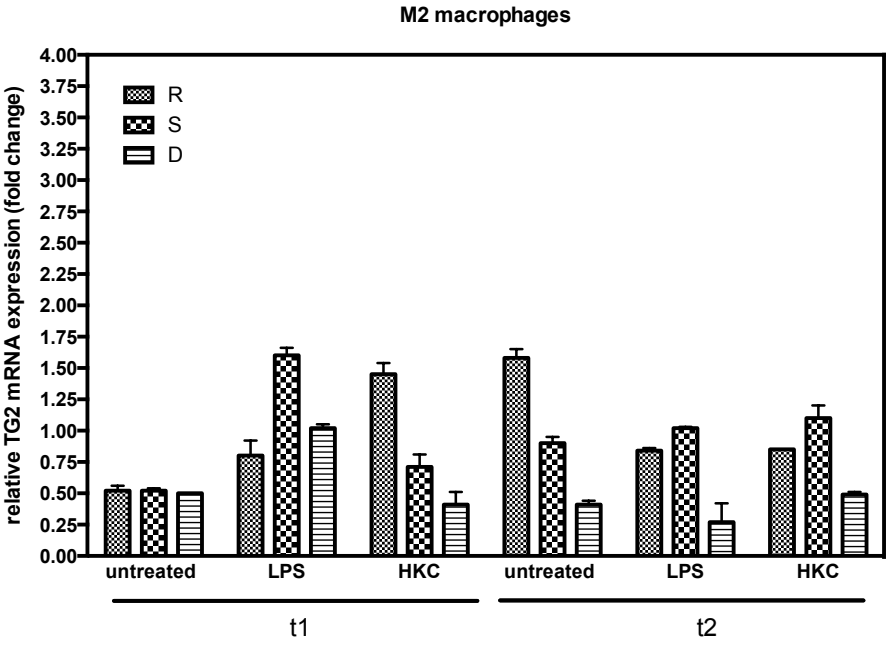
M2 macrophages
relative TG2 mRNA expression (fold change)
4.00
3.75
3.50
3.25
3.00
2.75
2.50
2.25
2.00
1.75
1.50
1.25
1.00
0.75
0.50
0.25
0.00
R
S
D
untreated
LPS
HKC
untreated
LPS
HKC
t1
t2

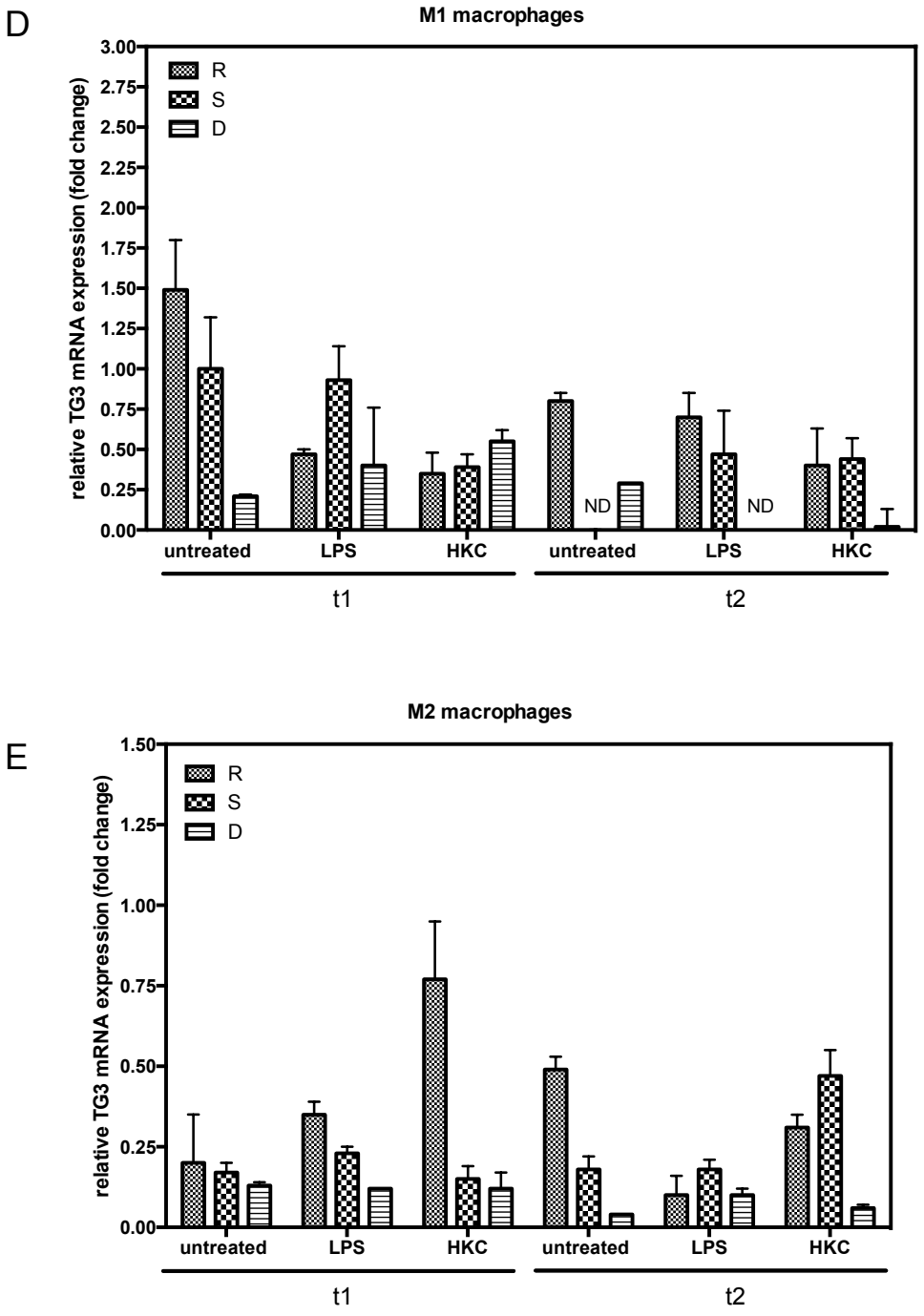

Fig. 6.5 Expression of TG2 and TG3 in human PBMC derived macrophages. A: PBMCs from 3 healthy volunteers were cultured and differentiated with 20ng/ml of either rhGM-CSF or rhM-CSF to obtain, M1 or M2 macrophages populations, respectively. TG2 **(B and C)** and TG3 **(D and E)** expression was analysed by quantitative PCR. All samples were run in duplicate. Data analysis was performed using the $2^{-\Delta\Delta Ct}$ method, after normalizing for internal control h36B4. Results demonstrate data acquired in two independent experiments (t1 and t2) and TG expression is shown relative to non-stimulated M1 cells from subject S (at time point t1).

6.3 Discussion

In this chapter the expression of TG2, TG3 and TG6 genes in monocyte and macrophage cell populations derived from a cell line THP-1, mouse bone marrow or human peripheral blood, was assessed.

Macrophages have been implicated in the pathogenesis of the gluten-related disorder coeliac disease. Studies have shown that gliadin fragments are able to induce activation of macrophages *in vitro*, with a subsequent increase in production of pro-inflammatory cytokines such as TNF-α (Jelínková et al., 2004; Tucková et al., 2002). However, how and where the gliadin peptides interact with macrophages *in vivo* remains elusive. Permeability of the intestinal mucosa might explain this interaction. In fact, studies have found gliadin to be a potent inducer of intestinal permeability (Lammers et al., 2008; Thomas et al., 2006). These studies support a role for the innate immune response to gliadin in the initiation of CD pathogenesis.

Monocytes have been shown to express TG2 at the protein level upon differentiation (Metha & Lopez-Berestein, 1986; Adamczyk, 2013). Furthermore, expression is increased upon LPS stimulation (Adamczyk, 2013). In these current experiments, it was possible to detect TG2 expression at the transcription level in differentiated monocytes derived from the monocytic cell-line THP-1 upon TPA stimulation. Also, expression was further increased after LPS stimulation. These results were consistent with the previous findings by Metha & Lopez-Berestein, 1986 and Adamczyk, 2013, who investigated protein expression. The data confirm dramamtic upregulation in response to Toll-like receptor activation. Additionally, it was also shown that, to some extent, LPS stimulation of these cells was able to increase expression of TG3 and TG6, although a more thorough analysis needs to be carried out. This suggests that all 3 genes relevant to GRD are upregulated in the context of a pro-inflammatory stimulus, but not other members of this gene family.

Upon analysis of primary mouse macrophages, similar results were observed regarding TG2 expression. However, in these cells, a higher expression of this enzyme at baseline was observed in anti-inflammatory M2

macrophages compared to M1 macrophages. However, pro-inflammatory M1 macrophages showed the highest increase in TG2 expression after LPS stimulation.

Differentiated mouse macrophages stimulated with heat-killed candida (HKC) were also analysed. In these cells, expression of TG2 was present across all samples, as expected. However, further analysis of the samples revealed an upregulation of TG6 expression in response to stimulation with HKC. This correlated with the findings described for THP-1 derived macrophages, and further substantiates the link between inflammatory activation and TG6 expression.

Human primary macrophages collected from 3 healthy volunteers and stimulated with LPS or HKC were also analysed for TG expression. Although TG2 and TG3 were both detectable at baseline and in stimulated samples, the great variation in gene expression between and within different subjects did not allow for any clear conclusions to be drawn.

Overall, it was shown that differentiated macrophages are able to express the three transglutaminase enzymes recognized as autoantigens in gluten-related disorders. Furthermore, other studies have shown enzyme activity of TG2 in the membrane of human peripheral blood monocyte derived macrophages and dendritic cells (Hodrea et al., 2010).

Taken together, these results suggest that deamidation of gluten peptides might be linked to an increase in expression of TG2 and also TG3 and TG6, by intestinal macrophages or dendritic cells.

As the highest ratio of TG2 expression upregulation between stimulated and unstimulated macrophages was seen in the pro-inflammatory M1 macrophages, expression of the enzyme could be a response to and take place along side the release of pro-inflammatory cytokines. This is consistent with TG2 being transcriptionally regulated by IL-1, IL-6, TNF-α, IFN-γ and IL-15 (Bayardo et al., 2012). As external TG2 has been shown to undergo reversible inactivation under oxidative conditions (Stamnaes et al., 2010), in the context of the above model, it is possible that the increase in mucosal permeability by gliadin and subsequent activation of macrophages with a release of pro-inflammatory cytokines, could create the optimal conditions for

TG2 externalization and activation and consequent deamidation of gluten peptides. A mechanism for co-secretion of TG2 and thioredoxin-1 has recently been identified (Adamczyk et al., 2015) and could drive generation of active extracellular TG2 in this context.

TG3 and TG6 gene expression following macrophage stimulation was also demonstrated. These enzyme have both been linked to gluten related disorders with extra-intestinal manifestations: TG3 is linked to skin disorder, dermatitis herpetiformis (Sárdy et al., 2002) and TG6 is linked to neurologic disorder gluten ataxia (Hadjivassiliou et al., 2008). If expression of these enzymes could be identified at protein level in skin macrophages or brain microglia, and if these enzymes were shown to be present at the cell surface, this could be the link between gluten challenge at gut level and the extra-intestinal symptoms. However, autoantibodies are likely derived from the circulation as shown in the model for DH (Zone et al., 2011).

Expression of TG2 or TG6 at the surface of microglia cells would allow for this interaction between the self-proteins and circulating autoantibodies. This ultimately could lead to permeability or a breach in the blood–brain barrier and prolonged exposure of the CNS to the gluten-related antibodies. As gluten ataxia may be associated with antibody cross-reactivity between antigenic epitopes on Purkinje cells and gluten protein (Hadjivassiliou et al., 2002), exposure of the CNS to gluten-reactive antibodies could lead to the loss of these cells as detected in GA patients. Alternatively, TG-specific antibodies may be involved directly in causing neuronal damage. In fact, Boscolo and colleagues have demonstrated that antibodies from GRD patients are capable of causing ataxia when transferred into the central nervous system of mice (Boscolo et al., 2007, 2010). Additionally, it was reported that recombinant TG-specific scFv ‘antibodies’ that lack the Fc region lead to a loss of motor function in mice, suggesting an scFv-antigen interaction, independent of complement activation or Fc receptor engagement, as the trigger for the immune response in the disease process (Boscolo et al., 2010).

In conclusion these experiments have shown that TG2, TG3 and TG6 gene expression is indeed upregulated in differentiates macrophages and

upon stimulation. This led to the belief that macrophages could potentially be the source for TG6 and TG3 in the gut of gluten-disorder patients and this way provide the missing link for the hypothesis that autoantibody development against TG6 and TG3 could originate in the gut.

Chapter 7 General Discussion

The aim of this discussion is to summarise the different hypothesis regarding autoantibody production in gluten-related disorders and contrast them to the observations from this study. I am proposing a new model for the pathological mechanism of gluten-related disorders and, more specifically, gluten ataxia: Autoantibodies that drive extraintestinal manifestations of gluten-related disorders are developed in the gut of susceptive individuals. The results presented in this thesis show, for the first time, the presence of TG6 specific B-cells in the small intestine of patients presenting with gluten-related disorders.

With gluten-related disorders affecting 1-2% of the general population, it is crucial to identify the pathological mechanism behind the disease progression. This would allow for the identification of new biological markers and development of new therapeutic targets. In gluten ataxia specifically, an early identification of these patients is essential, as they will suffer from irreversible damage to the neural tissue.

Sollid has proposed a mechanism for production of anti-TG2 antibodies in the context of coeliac disease, where TG2-(deamidated)gluten complexes act as a hapten carrier in the activation of TG2-reactive B cells by gluten-reactive T-cells (Sollid et al., 1997). It is possible that production of autoantibodies against TG6, which have been linked to gluten ataxia, follows a similar model. The presence of TG6-reactive B-cells in the intestinal mucosa of GRD patients reported by this study along side the observation that TG6 is able to deamidate gluten peptides reported elsewhere (Stamnaes et al. 2010), further supports this hypothesis.

Another two important questions linked to this model that require further investigation are: 1) the presence of TG6 at the gut level to allow the formation of TG6-(deamidated) gluten peptide complexes that would act as hapten carrier in the activation of TG6-specific B-cells by gluten-specific T-cells and 2) the catalysis of the deamidation reaction of gluten peptides by TGs in an environment that would favour transamidation.

Although expression of TG6 has been associated with the development of the CNS (H. Thomas et al., 2013), evidence is still lacking when it comes to its expression at the intestinal level.

Regarding the catalysis of deamidation reaction by TGs, studies have shown the selective deamidation of a glutamine residue in the small heat shock protein Hsp20 by TG2, under conditions where other glutamine residues were transamidated (Boros et al. 2006). Another study has also demonstrated that direct deamidation reactions in the presence of an amine-donor are conditioned by peptide sequences as well as enzyme concentration (Stamnaes et al. 2008). These results suggest that deamidation could be influenced by both substrates and reaction conditions. More recently, work performed by Adamczyk, suggested that the nature of the amine also has an impact in the preference for transamidation or deamidation reactions by TG2 (Adamczyk, 2013).

7.1 Expression of TGs by activated macrophages

Previous studies have shown TG2 to be expressed in macrophages differentiated from a monocytic-derived cell line (Mehta & Lopez-Berestein, 1986). Furthermore, TG2 expression was shown to be increased upon LPS stimulation (Adamczyk, 2013). In the present study, expression of this enzyme was also observed in non-stimulated and stimulated pro-inflammatory and anti-inflammatory macrophage populations, derived from the monocytic cell-line and additionally, in macrophages derived from mouse bone marrow or human peripheral blood monocytes.

Moreover, this research reported that expression of TG3 and TG6 genes was also unregulated in response to inflammatory stimuli in both cell-line and primary macrophages. This new finding may have an impact on the understanding of the pathogenesis of the gluten-related disorders dermatitis herpetiformis and gluten ataxia, where TG3 (Sárdy et al., 2002) and TG6 (Hadjivassiliou et al., 2008) are the respective recognized autoantigens.

Macrophages have been implicated in the pathogenesis of the gluten-related disorder coeliac disease. In fact, studies have shown the ability of

gliadin fragments to induce activation of macrophages *in vitro*, with a subsequent increase in production of pro-inflammatory cytokines such as TNF-α (Jelínková et al., 2004; Tucková et al., 2002). Therefore, it is possible that activation of intestinal macrophages by gliadin, could lead to an increase in expression of TG2, TG3 and TG6, in a similar way to what was observed in these current studies after stimulation of macrophages *in vitro* with LPS or HKC. However, how and where the gliadin peptides interact with macrophages *in vivo* remains elusive. Increased permeability of the intestinal mucosa might explain this interaction, as studies have found gliadin to be a potent inducer of intestinal permeability (Lammers et al., 2008; Thomas et al., 2006). Gliadin could then interact with any of these members of the TG family, either within the macrophages or extracelullarly, resulting in the production of deamidated gluten peptides and gluten-TG complexes. In fact, the ability to deamidate gluten peptides with the formation of gluten-TG complexes has been shown for not only TG2 but also TG3 and TG6 (Stamnaes et al., 2010). As in the proposed model by Sollid for TG2 and coeliac disease, gluten-TG3 and gluten-TG6 thiolester complexes would be able to act as hapten carriers and facilitate activation of TG3 or TG6-reactive B cells by gluten-reactive T cells leading to the production of the anti-TG3 or TG6 antibodies, characteristic of dermatitis hermetiformis or gluten ataxia, respectively.

7.2 Production of autoantibodies in gluten ataxia

TG6 has been identified has the autoantigen in gluten ataxia (Hadjivassiliou et al., 2008). However, the mechanism for the development of antibodies against this self-protein is still not fully understood.

In this thesis, the presence of TG2 and TG6-specific B-cells in small intestine D2 biopsies of a cohort of patients presenting with GRD or controls was investigated. The presence of these cells at the intestinal level starts to provide a mechanistic understanding of autoantibody development in extraintestinal gluten-related disease manifestations, particularly in gluten ataxia.

Here, the presence of TG6-reactive cells in the small intestinal mucosa of GRD patients was demonstrated. Furthermore, the studies suggested a prevalence of these cells in approximately 80% of both coeliac disease and gluten ataxia patients. This suggests that there is a link between the occurrence of TG6-reactive cells in the gut and these gluten-related disorders, but not necessarily the type of manifestation present. The studies were also able to identify some of these cells as being B-cells or plasma cells.

Based on this evidence, I propose that the development of anti-TG6 antibodies, the hallmark of gluten ataxia, has its origin in the intestinal mucosa of susceptible subjects.

7.3 Proposed model: Autoantibodies that drive extraintestinal manifestations of GRD are developed in the gut.

Based on the model previously suggested by Sollid for autoantibody development in coeliac disease (L M Sollid et al., 1997), I propose the following revised model for the development of autoantibodies that drive extraintestinal manifestations of gluten-related disorders, in particular gluten ataxia.

Gluten peptide gliadin reaches the intestinal lumen due to its high proline content and subsequent resistance to gastric enzymes (Stepniak & Koning, 2006). Gliadin induces intestinal permeability and is able to enter the intestinal mucosa (Lammers et al., 2008; Thomas et al., 2006). Here, it interacts with and activates intestinal macrophages (Jelínková et al., 2004; Tucková et al., 2002) leading to expression of TG6. TG6 catalyses the deamidation of gliadin (Stamnaes et al., 2010), either within macrophages or extracellularly, with production of TG6-peptide complexes. These complexes act as a hapten carrier and allow activation of TG6-reactive B cells at the GALT, by gluten-reactive T cells, with subsequent development of anti-TG6 antibodies.

7.4 Involvement of microglia in the pathogenesis of gluten ataxia

It is unclear if the CNS pathology associated with gluten sensitivity is the result of access of circulating antibodies that react with brain antigens upon compromise of the blood-brain barrier.

Hadjivassiliou et al, have reported the colocalization of TG6 deposits with perivascular IgA deposits, upon post mortem examination of a gluten ataxia patient (Hadjivassiliou et al. 2008). Additionally, location of these deposits, mainly around brain vessels, suggests that vasculature-centered inflammation may compromise the blood-brain barrier. It is also known that patients with GA have increased serological levels of antibodies primarily directed against TG6 (Hadjivassiliou et al., 2008).

In chapter 6 of this thesis the *in vitro* expression of TG6 by macrophages in response to an inflammatory stimuli was reported.

Microglia are the most abundant and best studied macrophage population of the CNS. These cells play an important role in CNS homeostasis during development, adulthood and ageing. Additionally, they are known to respond not only to changes in the brain's structural integrity but also to very subtle alterations in their microenviroment, such as imbalances in ion homeostasis (Kreutzberg, 1996; Perry & Teeling, 2013).

If microglia were shown to express and externalize TG6 upon activation, it is possible that circulating anti-TG6 autoantibodies would be able to interact with the protein. This interaction could ultimately lead to permeability of the blood–brain barrier and prolonged exposure of the CNS to the gluten-related antibodies. This hypothesis is supported by studies demonstrating that serologic antibodies from GRD patients are capable of causing ataxia, when transferred into the central nervous system of mice (Boscolo et al., 2007, 2010). Additionally, it has been reported that recombinant TG-specific scFv 'antibodies' that lack the Fc region lead to a loss of motor function in mice, suggesting an scFv-antigen interaction, independent of complement activation or Fc receptor engagement, as the trigger for neuronal degeneration in the disease process (Boscolo et al., 2010). Expression of TG6 at the surface of microglia cells would allow for this

interaction between the self-proteins and circulating autoantibodies. A disruption in the blood-brain barrier potentially linked to this interaction would then allow the exposure of the CNS to gluten-related pathogenic antibodies, including anti-TG6 antibodies and anti-gliadin antibodies. As gluten ataxia may be associated with antibody cross-reactivity between antigenic epitopes on Purkinje cells and gluten-derived proteins (Hadjivassiliou et al., 2002), exposure of the CNS to gluten-reactive antibodies could lead to the loss of these cells as detected in GA patients.

7.5 GTP-binding capacity of TG2 is required for catalytic activity

For identification of TG2 and TG6-reactive cells in intestinal biopsies, TG2 and TG6 were successfully produced and chemically labelled using specific fluorophores. These fluorophores were attached using NHS ester chemistry to the primary amine on the side chain of any lysine residue. Effects of amine-labelling on TG2 functionality were analysed. Changes were observed regarding enzyme functionality, dependent on conditions. Surprisingly, when labelling was performed in the absence of GTP, TG2 isopeptidase activity was lost, while addition of the nucleotide during labelling led to an enzymatically active protein. This was observed for NHS ester labelling with two chemically different fluorophores, suggesting that the loss of isopeptidase activity after labelling does not depend on the nature of the fluorophore, but rather structural hindrance caused by label binding to specific lysine residues.

Since TG2 activity is tightly regulated by Ca^{2+}/GTP allosteric conformational changes (Begg et al., 2006; Casadio et al., 1999), it is understandable that interruption of these binding sites, or the adoption of associated conformational states, will lead to the differences in enzyme function.

GTP binding causes a large conformational change, shifting the protein to a closed conformation, limiting active site access to substrates and therefore negatively regulating enzyme activity. The loss of isopeptidase activity observed in labelled TG2 when labelling was performed in the

absence of GTP, suggested incorporation of the fluorophore at a lysine in a position detrimental to either the catalytic region or substrate-binding site. The TG2-GTP binding site has been shown to be located in a pocket between the first β-barrel domain and the loop that connects it to the next β-strand (Jang et al., 2014). Furthermore, two residues from the catalytic core, Lys 173 and Phe 174, have been shown to contribute to the GTP interaction (Begg et al., 2006; Jang et al., 2014; Liu et al. 2002).

Jeon at al., suggested that conformational changes caused by GTP binding may help maintain physiological enzyme stability, to display transamidation activity at high calcium concentrations (Jeon et al., 2002). Furthermore, it has been shown that mutations at S171, involved in GTP-binding, can cause reduction or loss of transamidation activity (Antonyak et al., 2001; Jeon et al., 2002).

As previously mentioned, NHS ester labelling occurs by reaction of the ester group with primary amine found in lysines. During labelling in the presence of GTP, Lys173 would be already bound to the nucleotide and therefore, not available for labelling. Conversely, labelling in the absence of the nucleotide would allow for modification of this catalytic core residue. This could provide an explanation for the loss of isopeptidase activity observed when TG2 was labelled in the absence of GTP and suggests that GTP-binding capacity of TG2 is required for catalytic activity or, at least, a conformational transition linked to catalysis.

In a similar way to S171, it is possible that Lys173 might be implicated in this conformational transition or stabilization of TG2 and may be required for the enzyme to display isopeptidase activity. Therefore, further studies involving mutations at Lys173 should be carried out.

7.6 TG2 displays a second structural pocket with high affinity for an amine substrate

In this study it has been postulated that TG2 may contain a second structural pocket with high affinity for an amine substrate. This hypothesis

comes from evidence collected by analysis of open-conformation TG2 using an ‘in gel’ activity assay.

Initially, native electrophoresis of different forms of TG2 was performed to correlate loss of isopeptidase activity with any structural changes generated by modification of the protein with NHS ester labels.

Labelled proteins were analysed along side native TG2 and a form of TG2 trapped in the ‘open’ conformation, as comparison for any shifts in mobility of bands of TG2 labelled in the presence or absence of GTP. The initial ‘open’- form TG2 used in this assay was commercially purchased TG2, conjugated with an inhibitor at the active site Cys residue in order to stabilize the open conformation. This protein was not expected to display any catalytic activity.

Upon an ‘in gel’ activity assay where, native gels were incubated with a solution containing FITC-cadaverine and calcium, it was observed that inhibited ‘open’ TG2 was somehow able to retain the amine substrate. This led to the speculation that inhibited enzyme, which reflects an intermediate state during catalysis, had a high-affinity binding site for the amine donor substrate. After several experiments performed in order to confirm specificity of the binding, including the in-house inhibition of TG2 with different catalytic site directed inhibitors, it was concluded that interaction of FITC-cadaverine with the ‘open’ TG2 was specific and not due to residual catalytic activity, and untimely the existence of the second structural pocket with high affinity for an amine substrate was proposed. Furthermore, it appears that this pocket becomes available upon reaction of the enzyme with a first substrate, an event mimicked by reaction with the catalytic site-inhibitor in our experiment. This is an important observation that will hopefully clarify, in the future, how the enzyme interacts with the amine substrate, and how exactly this leads to subsequent transamidation or deamidation of the glutaminyl substrate.

7.7 Final conclusions

In summary, the results presented in this thesis have advanced our mechanistic understanding of autoantibody development and extraintestinal manifestations in the context of gluten-related disorders.

It has been successfully shown that both B and plasma-cells reactive to TG6 are present in the gut of patients presenting with a form of gluten-related disorder. Therefore, providing for the first time, evidence that autoantibodies that drive extraintestinal manifestations, such as the ones observed in gluten ataxia, may be developed in the gut.

Furthermore it has been have shown that inflammatory stimulation of macrophages *in vitro*, induces expression of TG6. These cells could therefore be the major source of TG6 at the intestinal level, which would allow for the formation of TG6-gluten complexes necessary for activation of TG6-reactive B-cells by gluten-reactive T-cells.

Additionally, it has been reported that TG2 trapped in an intermediate stage of catalysis is able to bind a second amine-donor substrate. This novel observation opens the door for structural studies investigating the elements directing the reactions leading to transamination and deamidation.

7.8 Future work

While this thesis has provided new knowledge in the field of gluten-related disorders and more specifically in gluten ataxia, there are several lines of research arising from this work that I believe should be pursued further to gain an in-depth understanding of disease process. This section presents some of these directions.

1. Further characterize TG2 and TG6-specific B cells/plasma cells present in the small intestine of GRD patients. Can such B cells be isolated from the circulation?

2. Analyse TG6 expression in the human intestine in helath and in the context of GRD. Are TG6 deposits present in the intestine? Which cells express TG6 (resident cells or infiltrating cells)? Is the expression altered in the presence of a gluten-related disorder?

3. Analyse TG2, TG3 and TG6 expression, at gene and protein level, in human macrophages/dendritic cells after gliadin stimulation of GRD patients as well as appropriate controls.

4. Identify whether autoantibody-binding to microglia cells affects permeability across endothelial-microglia cell barrier.
    a. Confirm TG2 and TG6 expression in human microglial cells at rest and upon inflammatory stimulation
    b. Establish a human brain/blood barrier model to investigate the cellular response to stimulation with TG2/TG6-specific antibodies and whether this could explain the autoantigen antibody reaction in the brain.

References

Achyuthan, K. E., & Greenberg, C. S. (1987). Identification of a guanosine triphosphate-binding site on guinea pig liver transglutaminase. Role of GTP and calcium ions in modulating activity. *Journal of Biological Chemistry*, *262*(4), 1901–1906.

Adamczyk, M. (2013). *Biomarkers for arthritis: Regulation of extracellular transglutaminase activity by non-conventional export*. Cardiff University.

Adamczyk, M., Griffiths, R., Dewitt, S., Knäuper, V., & Aeschlimann, D. (2015). P2X7 receptor activation regulates rapid unconventional export of transglutaminase-2. *Journal of Cell Science*, *7*(November), 1–14.

Adamczyk, M., Heil, A., & Aeschlimann, D. (2013). Real-time fluorescence assay for monitoring of transglutaminase activity by determining isopeptidase activity. Retrieved from http://orca.cf.ac.uk/47001/.

Aeschliman, D., & Paulsson, M. (1991). Cross-linking of Laminin-Nidogen Complexes by Tissue Transglutaminase. *Journal of Biological Chemistry*, *266*(23), 15308–15317.

Aeschlimann, D., & Hadjivassiliou, M. (2008). Transglutaminase 6 as a diagnostic indicator of autoimmune disease.

Aeschlimann, D., Kaupp, O., & Paulsson, M. (1995). Transglutaminase-catalyzed matrix cross-linking in differentiating cartilage: Identification of osteonectin as a major glutaminyl substrate. *Journal of Cell Biology*, *129*(3), 881–892.

Aeschlimann, D., & Knauper, V. (2016). P2X7 receptor-mediated TG2 externalization: a link to inflammatory arthritis? *Amino Acids*, 1–8.

Aeschlimann, D., & Thomazy, V. (2000). Protein crosslinking in assembly and remodelling of extracellular matrices: the role of transglutaminases. *Connective Tissue Research*, *41*(1), 1–27.

Ahvazi, B., Boeshans, K. M., Idler, W., Baxa, U., Steinert, P. M., & Rastinejad, F. (2004). Structural Basis for the Coordinated Regulation of Transglutaminase 3 by Guanine Nucleotides and Calcium/Magnesium. *Journal of Biological Chemistry*, *279*(8), 7180–7192.

Ahvazi, B., Kim, H. C., Kee, S.-H., Nemes, Z., & Steinert, P. M. (2002). Three-dimensional structure of the human transglutaminase 3 enzyme: binding of calcium ions changes structure for activation. *The EMBO Journal*, *21*(9), 2055–67.

Antonyak, M. A., Singh, U. S., Lee, D. A., Boehm, J. E., Combs, C., Zgola, M. M., Page, R. L., & Cerione, R. A. (2001). Effects of Tissue Transglutaminase on Retinoic Acid-induced Cellular Differentiation and Protection against Apoptosis. *Journal of Biological Chemistry*, *276*(36), 33582–33587.

Arentz-Hansen, H., Körner, R., Molberg, O., Quarsten, H., Vader, W., Kooy, Y. M. C., Lundin, K. E. A., Sollid, L.M., & McAdam, S. N. (2000). The Intestinal T Cell Response to -Gliadin in Adult Celiac Disease Is Focused on a Single Deamidated Glutamine Targeted by Tissue Transglutaminase. *Journal of Experimental Medicine*, *191*(4), 603–612.

Bagoly, Z., Koncz, Z., Hársfalvi, J., & Muszbek, L. (2012). Factor XIII, clot structure, thrombosis. *Thrombosis Research*, *129*(3), 382–387.

Bailey, C. H. (1941). A translation of Beccari's lecture "Concerning Grain" (1728). *Cereal Chemistry*, *18*, 555–561.

Bayardo, M., Punzi, F., Bondar, C., Chopita, N., & Chirdo, F. (2012). Transglutaminase 2 expression is enhanced synergistically by interferon-y and tumour necrosis factor-a in human small intestine. *Clinical and Experimental Immunology*, *168*(1), 95–104.

Begg, G. E., Carrington, L., Stokes, P. H., Matthews, J. M., Wouters, M. A, Husain, A., Lorand, L., Iismaa, S. E., & Graham, R. M. (2006). Mechanism of allosteric regulation of transglutaminase 2 by GTP. *Proceedings of the National Academy of Sciences of the United States of America*, *103*(52), 19683–19688.

Beninati, S., & Piacentini, M. (2004). The transglutaminase family: an overview: minireview article. *Amino Acids*, *26*(4), 367–72.

Boehm, J. E., Singh, U., Combs, C., Antonyak, M. A., & Cerione, R. A. (2002). Tissue transglutaminase protects against apoptosis by modifying the tumor suppressor protein p110 Rb. *Journal of Biological Chemistry*, *277*(23), 20127–20130.

Bolotin, D., & Petronic-Rosic, V. (2011a). Dermatitis herpetiformis: Part I. Epidemiology, pathogenesis, and clinical presentation. *Journal of the American Academy of Dermatology*, *64*(6), 1017–1024.

Bolotin, D., & Petronic-Rosic, V. (2011b). Dermatitis herpetiformis: Part II. Diagnosis, management, and prognosis. *Journal of the American Academy of Dermatology*, *64*(6), 1027–1033.

Bonciani, D., Verdelli, A., Bonciolini, V., D'Errico, A., Antiga, E., Fabbri, P., & Caproni, M. (2012). Dermatitis herpetiformis: from the genetics to the development of skin lesions. *Clinical & Developmental Immunology*, *2012*.

Boros, S., Ahrman, E., Wunderink, L., Kamps, B., de Jong, W. W., Boelens, W. C., & Emanuelsson, C. S. (2006). Site-specific transamidation and deamidation of the small heat-shock protein Hsp20 by tissue transglutaminase. *Proteins*, *62*(4), 1044–52.

Boscolo, S., Lorenzon, A., Sblattero, D., Florian, F., Stebel, M., Marzari, R., Not, T., Aeschlimann, D., Ventura, A. Hadjivassiliou, M., & Tongiorgi, E. (2010). Anti transglutaminase antibodies cause ataxia in mice. *PloS One*, *5*(3), e9698.

Boscolo, S., Sarich, A., Lorenzon, A., Passoni, M., Rui, V., Stebel, M., Sblattero, D., Marzari, R., Hadjivassiliou, M., & Tongiorgi, E. (2007). Gluten ataxia: passive transfer in a mouse model. *Annals of the New York Academy of Sciences*, *1107*, 319–28.

Bradford, M. M. (1976). A rapid and sensitive method for the quantitation of microgram quantities of protein utilizing the principle of protein-dye binding. *Analytical Biochemistry*, *72*(1–2), 248–254.

Brottveit, M., Erik, K., Lundin, A., Beitnes, A. R., Ra, M., Jahnsen, L., & Sollid, L. M. (2012). Rapid Accumulation of CD14 + CD11c + Dendritic Cells in Gut Mucosa of Celiac Disease after in vivo Gluten Challenge, *7*(3), 1–9.

Casadio, R., Polverini, E., Mariani, P., Spinozzi, F., Carsughi, F., Fontana, A., de Laureto, P. P., Mauteucci, G., & Bergamini, C. M. (1999). The structural basis for the regulation of tissue transglutaminase by calcium ions. *European Journal of Biochemistry / FEBS*, *262*(3), 672–9.

Catassi, C., & Fasano, A. (2008). Celiac disease. *Current Opinion in Gastroenterology*, *24*(6), 687–691.

Chanput, W., Mes, J. J., Savelkoul, H. F. J., & Wichers, H. J. (2013). Characterization of polarized THP-1 macrophages and polarizing ability of LPS and food compounds. *Food & Function*, *4*, 266–276.

Cotran, R., Kumar, V., & Collins, T. (1999). *Robbins Pathologic Basis of Disease* (6th Edition). Saunders.

Csosz, E., Bagossi, P., Nagy, Z., Dosztanyi, Z., Simon, I., & Fesus, L. (2008). Substrate preference of transglutaminase 2 revealed by logistic regression analysis and intrinsic disorder examination. *Journal of Molecular Biology*, *383*(2), 390–402.

Di Niro, R., Mesin, L., Zheng, N., Stamnaes, J., Morrissey, M., Lee, J., Huang, M., Iversen, R., du Pré, F., Qiao, S., Lundin, K. E. A., Wilson, P. C., & Sollid, L. M. (2012). High abundance of plasma cells secreting transglutaminase 2-specific IgA autoantibodies with limited somatic hypermutation in celiac disease intestinal lesions. *Nature Medicine*, *18*(3), 441–5.

Di Niro, R., Snir, O., Kaukinen, K., Yaari, G., Lundin, K. E. A., Gupta, N. T., Kleinstein, S. H., Cols, M., Cerutti, A., Mäki, M., Shlomchik, M. J., & Sollid, L. M. (2016). Responsive population dynamics and wide seeding into the duodenal lamina propria of transglutaminase-2-specific plasma cells in celiac disease. *Nature - Mucosal Immunology*, *9*(1), 254–264.

Dieterich, W., Ehnis, T., Bauer Michael, Donner, P., Volta, U., Riecken, E., & Shuppan, D. (1997). Identification of tissue transglutaminase as the autoantigen of celiac disease. *Nature Medicine*, *3*(7), 797–801.

Du Pre, M. F., & Sollid, L. M. (2015). T-cell and B-cell immunity in celiac disease. *Best Practice and Research: Clinical Gastroenterology*, *29*(3), 413–423.

Duhring, L. (1884). Dermatitis Herpetiformis. *JAMA*, *III*(9), 225–229.

Fagarasan, S., & Honjo, T. (2003). Intestinal IgA synthesis: regulation of front-line body defences. *Nature Reviews. Immunology*, *3*(1), 63–72.

Fallingborg, J. (1999). Intraluminal pH of the human gastrointestinal tract. *Danish Medical Bulletin*, *46*(2), 183–96.

Feng, J., Readon, M., Yadav, S. P., & Im, M. (1999). Calreticulin Down-Regulates both GTP Binding and Transglutaminase Activities of Transglutaminase II. *Biochemistry*, *38*, 10743–10749.

Ferretti, G., Bacchetti, T., Masciangelo, S., & Saturni, L. (2012). Celiac disease, inflammation and oxidative damage: a nutrigenetic approach. *Nutrients*, *4*(4), 243–57.

Fesus, L., & Piacentini, M. (2002). Transglutaminase 2 : an enigmatic enzyme with diverse functions. *TRENDS in Biochemical Sciences*, *27*(10), 534–539.

Fleckenstein, B., Molberg, Ø., Qiao, S., Schmid, D. G., Mulbe, Von Der Mülbe, F., Elgstøen, K., Jung, G., & Sollid, L. M. (2002). Gliadin T Cell Epitope Selection by Tissue Transglutaminase in Coeliac Disease. *The Journal of Biological Chemistry*, *277*(37), 34109–34116.

Folk, J. E. (1980). Transglutaminases. *Ann. Rev. Biochem*, *49*, 517–531.

Folk, J. E. (1983). Mechanism and basis for specificity of transglutaminase-catalyzed epsilon-(gamma-glutamyl) lysine bond formation. In *Adv. Enzymol. Relat. Areas Mol. Biol. 54* (pp. 1–56).

Folk, J. E., & Finlayson, J. S. (1977). The epsilon-(gamma-glutamyl)lysine crosslink and the catalytic role of transglutaminases. *Advances in Protein Chemistry*, *31*, 1–133.

Fry, L. (1995). Dermatitis herpetiformis. *Baillière's Clinical Gastroenterology*, *9*(2), 371–393.

Godkin, A., Friede, T., Davenport, M., Stevanovic, S., Willis, A., Jewell, D., Hill, A., & Rammensee, H. G. (1997). Use of eluted peptide sequence data to identify the binding characteristics of peptides to the insulin-dependent diabetes susceptibility allele HLA-DQ8 (DQ 3.2). *International Immunology*, *9*(6), 905–911.

Gratchev, A., Kzhyshkowska, J., Köthe, K., Muller-Molinet, I., Kannookadan, S., Utikal, J., & Goerdt, S. (2006). M1 and M2 can be re-polarized by Th2 or Th1 cytokines, respectively, and respond to exogenous danger signals. *Immunobiology*, *211*, 473–486.

Greco, L., Babron, M. C., Corazza, G. R., Percopo, S., Sica, R., Clot, F., Fulchignoni-Lataud, M. C., Zavattari, P., Momigliano-Richiardi, P., Casari, G., Gasparini, P., Tosia, R., Mantovanib, V., de Virgiliis, S., Iacono, G., D'Alfonso, A., Selinger-Leneman, H., Lemainque, A., Serre, J. L., & Clerget-Darpoux, F. (2001). Existence of a genetic risk factor on chromosome 5q in Italian coeliac disease families. *Annals of Human Genetics*, *65*(Pt 1), 35–41.

Grenard, P., Bates, M. K., & Aeschlimann, D. (2001). Evolution of transglutaminase genes: identification of a transglutaminase gene cluster on human chromosome 15q15. *The Journal of Biological Chemistry*, *276*(35), 33066–78.

Hadjivassiliou, M., Aeschlimann, D., Grünewald, R. A., Sanders, D. S., Sharrack, B., & Woodroofe, N. (2011). GAD antibody-associated neurological illness and its relationship to gluten sensitivity. *Acta Neurologica Scandinavica*, *123*(3), 175–80.

Hadjivassiliou, M., Aeschlimann, P., Sanders, D. S., Mäki, M., Kaukinen, K., Grünewald, R. A., Bandmann, O., Woodroofe, N., Haddock, G., & Aeschlimann, D. (2013). Transglutaminase 6 antibodies in the diagnosis of gluten ataxia. *Neurology*, *80*(19), 1740–5.

Hadjivassiliou, M., Aeschlimann, P., Strigun, A., Sanders, D. S., Woodroofe, N. M., & Aeschlimann, D. (2008). Autoantibodies in gluten ataxia recognize a novel neuronal transglutaminase. *Annals of Neurology*, *64*(3), 332–43.

Hadjivassiliou, M., Boscolo, S., Davies-Jones, G. A. B., Grünewald, R. A., Not, T., Sanders, D. S., Simpson, J. E., Tongiorgi, E., Williamson, C. A., & Woodroofe, N. M. (2002). The humoral response in the pathogenesis of gluten ataxia. *Neurology*, *58*, 1221–26.

Hadjivassiliou, M., Davies-Jones, G. A. B., Sanders, D. S., & Grünewald, R. A. (2003). Dietary treatment of gluten ataxia. *Journal of Neurology, Neurosurgery, and Psychiatry*, *74*(9), 1221–4.

Hadjivassiliou, M., Grünewald, R. A., Chattopadhyay, A. K., Davies-Jones, Gibson, A., Jarratt, J. A., Kandler, R. H., Lobo, A., Powell, T., & Smith, C. M. L. (1998). Clinical, radiological, neurophysiological and neuropahtological characteristics of gluten ataxia. *The Lancet*, *352*, 1582–85.

Hadjivassiliou, M., Grünewald, R. A., Kandler, R. H., Chattopadhyay, A. K., Jarratt, J. A., Sanders, D. S., Sharrack, B., Wharton, S. B., & Davies-Jones, G. A. B. (2006). Neuropathy associated with gluten sensitivity. *Journal of Neurology, Neurosurgery, and Psychiatry*, *77*(11), 1262–6.

Hadjivassiliou, M., Grünewald, R. A., Sharrack, B., Sanders, D. S., Lobo, A., Williamson, C. A., Woodroofe, N., Wood, N., & Davies-Jones, A. (2003). Gluten ataxia in perspective: epidemiology, genetic susceptibility and clinical characteristics. *Brain*, *126*, 685–691.

Hadjivassiliou, M., Mäki, M., Sanders, D. S., Williamson, C. A., Grünewald, R. A., Woodroofe, N. M., & Korponay-Szabó, I. R. (2006). Autoantibody targeting of brain and intestinal transglutaminase in gluten ataxia. *Neurology*, *66*(3), 373–7.

Hadjivassiliou, M., Sanders, D. S., Grünewald, R., Woodroofe, N. M., Boscolo, S., & Aeschlimann, D. (2010). Gluten sensitivity: from gut to brain. *Lancet Neurology*, *9*(3), 318–30.

Halstensen, T. S., Scott, H., Fausa, O., & Brandtzaeg, P. (1993). Gluten stimulation of coeliac mucosa in vitro induces activation (CD25) of lamina propria CD4+ T cells and macrophages but no crypt-cell hyperplasia. *Scandinavian Journal of Immunology*, *38*(6), 581–590.

Hodrea, J., Demény, M. Á., Majai, G., Sarang, Z., Korponay-szabó, I. R., & Fésüs, L. (2010). Transglutaminase 2 is expressed and active on the surface of human monocyte-derived dendritic cells and macrophages. *Immunology Letters*, *130*, 74–81.

Hohenadl, C., Mann, K., Mayer, U., Timpl, R., Paulsson, M., & Aeschlimann, D. (1995). Two Adjacent N-terminal Glutamines of BM-40 (Osteonectin , SPARC) Act as Amine Acceptor Sites in Transglutaminase C - catalyzed Modification*. *The Journal of Biological Chemistry*, *270*(40), 23415–23420.

Husby, S., Koletzko, S., Korponay-Szabó, I. R., Mearin, M. L., Phillips, A., Shamir, R., Troncone, R., Giersiepen, K., Branski, D., Catassi, C., Lelgeman, M., Mäki, M., Ribes-Koninckx, C., Ventura, A., & Zimmer, K. P. (2012). European Society for Pediatric Gastroenterology, Hepatology, and Nutrition guidelines for the diagnosis of coeliac disease. *Journal of Pediatric Gastroenterology and Nutrition*, *54*(1), 136–60.

Iismaa, S. E., Mearns, B. M., Lorand, L., & Graham, R. M. (2009). Transglutaminases and Disease : Lessons From Genetically Engineered Mouse Models and Inherited Disorders. *Physiology Review*, 991–1023.

Iversen, R., du Pre, M. F., Di Niro, R., & Sollid, L. M. (2015). Igs as Substrates for Transglutaminase 2: Implications for Autoantibody Production in Celiac Disease ´ ,. *The Journal of Immunology*, *195*(11), 5159–5168.

Iversen, R., Di Niro, R., Stamnaes, J., Lundin, K. E. A., Wilson, P. C., & Sollid, L. M. (2013). Transglutaminase 2-specific autoantibodies in celiac disease target clustered, N-terminal epitopes not displayed on the surface of cells. *Journal of Immunology (Baltimore, Md. : 1950)*, *190*(12), 5981–91.

Jang, T., Lee, D., Choi, K., Jeong, E. M., Kim, I., Kim, Y. W., Chun, J. N., Jeon, J., & Park, H. H. (2014). Crystal Structure of Transglutaminase 2 with GTP Complex and Amino Acid Sequence Evidence of Evolution of GTP Binding Site. *PloS One*, *9*(9), 1–8.

Jelínková, L., Tucková, L., Cinová, J., Flegelová, Z., & Tlaskalová-Hogenová, H. (2004). Gliadin stimulates human monocytes to production of IL-8 and TNF-alpha through a mechanism involving NF-kappaB. *FEBS Letters*, *571*(1–3), 81–5.

Jeon, J., Cho, S., Kim, C., Shin, D., Kweon, J., Choi, K., Park, S., & Kim, I. (2002). GTP is required to stabilize and display transamidation activity of transglutaminase 2. Biochemical and Biophysical Research Communications, *294*, 818–822.

Johansen, B. H., Vartdal, F., Eriksen, J. A., Thorsby, E., & Sollid, L. M. (1996). Identification of a putative motif for binding of peptides to HLA-DQ2. *International Immunology*, 8(2), 177-182.

John, S., Thiebach, L., Frie, C., Mokkapati, S., Bechtel, M., Nischt, R., Rosser-Davies, S., Paulsson, M., & Smyth, N. (2012). Epidermal transglutaminase (TGase 3) is required for proper hair development, but not the formation of the epidermal barrier. *PloS One*, *7*(4), e34252.

Koning, F., Schuppan, D., Cerf-Bensussan, N., & Sollid, L. M. (2005). Pathomechanisms in celiac disease. *Best Practice & Research. Clinical Gastroenterology*, *19*(3), 373–87.

Korponay-Szabó, I. R., Halttunen, T., Szalai, Z., Laurila, K., Király, R., Kovács, J. B., Fésüs, L., & Mäki, M. (2004). In vivo targeting of intestinal and extraintestinal transglutaminase 2 by coeliac autoantibodies. *Gut*, *53*(5), 641–8.

Kreutzberg, G. W. (1996). Microglia: a sensor for pathological events in the CNS. *Trends in Neurosciences*, *19*(8), 312–8.

Lagerqvist, C., Ivarsson, A., Juto, P., Persson, L. Å., & Hernell, O. (2001). Screening for adult coeliac disease - Which serological marker(s) to use? *Journal of Internal Medicine*, *250*(3), 241–248.

Lammers, K. M., Lu, R., Brownley, J., Lu, B., Gerard, C., Thomas, K., Rallabhandi, P., Shea-Donohue, T., Tamiz, A., Alkan, S., Netzel-Arnett, S., Antalis, T., Vogel, S. N., & Fasano, A. (2008). Gliadin Induces an Increase in Intestinal Permeability and Zonulin Release by Binding to the Chemokine Receptor CXCR3. *Gastroenterology*, *135*, 194–204.

Laurenzi, V. De, & Melino, G. (2001). Gene Disruption of Tissue Transglutaminase Gene Disruption of Tissue Transglutaminase. *Molecular and Cellular Biology*, *21*(1), 148–155.

Lee, S.-E., Lee, S.-Y., Jo, E.-J., Kim, M.-Y., Kim, S.-H., & Chang, Y.-S. (2013). Wheat-induced anaphylaxis in korean adults: a report of 6 cases. *Clinical Nutrition Research*, *2*(1), 76–9.

Lesort, M., Tucholski, J., MI, M., Gvw, J., Miller, M. L., & Johnson, G. V. (2000). Tissue transglutaminase: a possible role in neurodegenerative diseases. *Progress in Neurobiology*, *61*(5), 439–463.

Liu, S., Cerione, R. A., & Clardy, J. (2002). Structural basis for the guanine nucleotide-binding activity of tissue transglutaminase and its regulation of transamidation activity. *Proceedings of the National Academy of Sciences of the United States of America*, *99*(5), 2743–7.

Liu, Y., Tang, B., Lan, Y., Song, N., Huang, Y., Zhang, L., Guan, W., Shi, Y., Shen, L., Jiang, H., Guo, J., Xia, K., Ding, Y., & Wang, J. (2013). Distribution of transglutaminase 6 in the central nervous system of adult mice. *The Anatomical Record*, *296*(10), 1576–1587.

Lorand, L., & Graham, R. M. (2003). Transglutaminases: crosslinking enzymes with pleiotropic functions. *Nature Reviews. Molecular Cell Biology*, *4*(2)

Lu, G., Zhang, R., Geng, S., Peng, L., Jayaraman, P., Chen, C., Xu, F., Yang, J., Li, Q., Zheng, H., Shen, K., Wang, J., Liu, X., Wang, W., Zheng, Z., Qi, C., Si, C., He, J. C., Liu, K., Lira, S. A., Sikora, A. G., Li, L., & Xiong, H. (2015). Myeloid cell-derived inducible nitric oxide synthase suppresses M1 macrophage polarization. *Nature Communications*, *6*, 6676.

Ludvigsson, J. F., Leffler, D. A., Bai, J. C., Biagi, F., Fasano, A., Green, P. H. R., Hadjivassiliou, M., Kaukinen, K., Kelly, C. P., Leonard, J. N., Lundin, K. E. A., Murray, J. A., Sanders, D. S., Walker, M. M., Zingone, F., & Ciacci, C. (2012). The Oslo definitions for coeliac disease and related terms. *Gut*.

Mantovani, A., Sica, A., Sozzani, S., Allavena, P., Vecchi, A., & Locati, M. (2004). The chemokine system in diverse forms of macrophage activation and polarization, *25*(12).

Mehta, K., & Eckert, R. (2005). Transglutaminases - Family of enzymes with diverse functions. *Progress in Experimental Tumor Research*, *38*.

Mehta, K., & Lopez-Berestein, G. (1986). Expression of tissue transglutaminase in cultured monocytic leukemia (THP-1) cells during differentiation. *Cancer Res.*, *46*(3), 1388–1394.

Mesin, L., Niro, R. Di, Thompson, K. M., Knut, E., Lundin, A., & Sollid, L. M. (2013). Long-Lived Plasma Cells from Human Small Intestine Biopsies Secrete Immunoglobulins for Many Weeks In Vitro.

Mistry, V., Bockett, N. A., Levine, A. P., Mirza, M. M., Hunt, K. A., Ciclitira, P. J., Hummerich, H., Neuhausen, S. L., Simpson, M. A., Plagnol, V., & Van Heel, D. A. (2015). Exome sequencing of 75 individuals from multiply affected coeliac families and large scale resequencing follow up. *PLoS ONE*, *10*(1), 1–23.

Molberg, Ø., McAdam, S. N., Korner, R., Quarsten, H., Kristiansen, C., Madsen, L., Fugger, L., Scott H., Norén, O., Roepstorff, P., Lundin, K. E. A., Sjöström, H., & Sollid, L. M. (1998). Tissue Transglutaminase selectively modifies gliadin peptides that are recognized by gut-derived T cells in celiac disease. *Nature Medicine*, *4*(6), 713–717.

Perry, V. H., & Teeling, J. (2013). Microglia and macrophages of the central nervous system : the contribution of microglia priming and systemic inflammation to chronic neurodegeneration, 601–612.

Pinkas, D. M., Strop, P., Brunger, A. T., & Khosla, C. (2007). Transglutaminase 2 undergoes a large conformational change upon activation. *PLoS Biology*, *5*(12), 2788–2796.

Porcheray, F., Viaud, S., Rimaniol, A. C., Léone, C., Samah, B., Dereuddre-Bosquet, N., Dormont, D., & Gras, G. (2005). Macrophage activation switching: An asset for the resolution of inflammation. *Clinical and Experimental Immunology*, *142*(3), 481–489.

Porzio, O., Massa, O., Cunsolo, V., Colombo, C., Malaponti, M., Bertuzzi, F., Hansen, T., Johansen, A., Pedersen, O., Meschi, F., Terrinoni, A., Melino, G., Federici, M., Decarlo, N., Menicagli, M., Campani, D., Marchetti, P., Ferdaoussi, M., Froguel, P., Federici, G., Vaxillaire, M., & Barbetti, F. (2007). Missense Mutations in the TGM2 Gene Encoding Transglutaminase 2 Are Found in Patients With Early-Onset Type 2 Diabetes. *Mutation in Brief*, *982*.

Qiao, S.-W., Sollid, L. M., & Blumberg, R. S. (2009). Antigen presentation in celiac disease. *Current Opinion in Immunology*, *21*(1), 111–7.

Rose, C., Armbruster, F. P., Ruppert, J., Igl, B.-W., Zillikens, D., & Shimanovich, I. (2009). Autoantibodies against epidermal transglutaminase are a sensitive diagnostic marker in patients with dermatitis herpetiformis on a normal or gluten-free diet. *Journal of the American Academy of Dermatology*, *61*(1), 39–43.

Rubin, R., Levanony, H., & Galili, G. (1992). Evidence for the presence of two different types of protein bodies in wheat endosperm. *Plant Physiology*, *99*(2), 718–24.

Sander, I., Rozynek, P., Rihs, H.-P., van Kampen, V., Chew, F. T., Lee, W. S., Kotschy-Lang, N., Merget, R., Brüning, T., &Raulf-Heimsoth, M. (2011). Multiple wheat flour allergens and cross-reactive carbohydrate determinants bind IgE in baker's asthma. *Allergy*, *66*(9), 1208–15.

Sapone, A., Bai, J. C., Ciacci, C., Dolinsek, J., Green, P. H. R., Hadjivassiliou, M., Kaukinen, K., Rostami, K., Sanders, D. S., Shumann, M., Ullrich, R., Villalta, D., VOlta, U., Catassi, C., & Fasano, A. (2012). Spectrum of gluten-related disorders: consensus on new nomenclature and classification. *BMC Medicine*, *10*(1), 13.

Sapone, A., Lammers, K. M., Casolaro, V., Cammarota, M., Giuliano, M. T., De Rosa, M., Stefanile, R., Mazzarella, G., Tolone, C., Russo, M. I., Esposito, P., Ferraraccio, F, Cartenì, M., Riegler, G., de Magistris, L., & Fasano, A. (2011). Divergence of gut permeability and mucosal immune gene expression in two gluten-associated conditions: celiac disease and gluten sensitivity. *BMC Medicine*, *9*(1), 23.

Sárdy, M., Kárpáti, S., Merkl, B., Paulsson, M., & Smyth, N. (2002). Epidermal transglutaminase (TGase 3) is the autoantigen of dermatitis herpetiformis. *The Journal of Experimental Medicine*, *195*(6), 747–757.

Sarkar, N. K., Clarke, D. D., & Waelsch, H. (1957). An enzymically catalyzed incorporation of amines into proteins. *Biochim. Biophys. Acta*, *25*(2), 451–2.

Seissler, J., Wohlrab, U., Wuensche, C., Scherbaum, W. A., & Boehm, B. O. (2001). Autoantibodies from patients with coeliac disease recognize distinct functional domains of the autoantigen tissue transglutaminase. *Clinical and Experimental Immunology*, *125*(2), 216–221.

Semrad, C. (2008). Refractory Celiac Disease: What is it? What to do? *Impact*, *8*(3), 8–11.

Shewry, P. R. (2009). Wheat. *Journal of Experimental Botany*, *60*(6), 1537–1553.

Shewry, P. R., Halford, N. G., Belton, P. S., & Tatham, A. S. (2002). The structure and properties of gluten: an elastic protein from wheat grain. *Philosophical Transactions of the Royal Society of London. Series B, Biological Sciences*, *357*(1418), 133–42.

Singh, O., Shillings, A., Craggs, P., Wall, I., Rowland, P., Skarzynski, T., Hobbs, C. I., Hardwick, P., Tanner, R., Blunt, M., Witty, D. R., Smith, K. J. (2013). Crystal structures of ASK1-inhibtor complexes provide a platform for structure-based drug design. *Protein Science*, *22*(8), 1071–1077.

Sjöström, H., Lundin, K. E. A., Molberg, Ø., Körner, R., Mcadam, S. N., Anthonsen, D., Quarsten, H., Norén, O., Roepstorff, P. Thorsby, E., & Sollid, L. M. (1998). Identification of a gliadin T-cell epitope in coeliac disease: General importance of gliadin deamidation for intestinal T-cell recognition. *Scandinavian Journal of Immunology*, *48*(2), 111–115.

Sollid, L. M. (2002). Coeliac disease: dissecting a complex inflammatory disorder. *Nature Reviews. Immunology*, *2*(9), 647–55.

Sollid, L. M., & Jabri, B. (2011). Celiac disease and transglutaminase 2: a model for posttranslational modification of antigens and HLA association in the pathogenesis of autoimmune disorders. *Current Opinion in Immunology*, *23*(6), 732–8.

Sollid, L. M., Molberg, Ø., McAdam, S., & Lundin, K. E. A. (1997). Autoantibodies in coeliac disease : tissue transglutaminase — guilt by association ? *Gut*, *41*, 851–852.

Spencer, J., & Sollid, L. M. (2016). The human intestinal B-cell response. *Nature Publishing Group*, *9*(5), 1113–1124.

Spurkland, A., Ingvarsson, G., Falk, E. S., Knutsen, I., Sollid, L. M., & Thorsby, E. (1997). Dermatitis herpetiformis and celiac disease are both primarily associated with the HLA-DQ (a1*0501, B1*02) or the HLA-DQ (a1*03, B1*0302) heterodimers. *Tissue Antigens*, *49*, 29–34.

Stamnaes, J., Dorum, S., Fleckenstein, B., Aeschlimann, D., & Sollid, L. M. (2010). Gluten T cell epitope targeting by TG3 and TG6; implications for dermatitis herpetiformis and gluten ataxia. *Amino Acids*, *39*(5), 1183–91.

Stamnaes, J., Fleckenstein, B., & Sollid, L. M. (2008). The propensity for deamidation and transamidation of peptides by transglutaminase 2 is dependent on substrate affinity and reaction conditions. *Biochimica et Biophysica Acta (BBA)*, *1784*(11), 1804–1811.

Stamnaes, J., Iversen, R., Pré, M. F., Chen, X., & Sollid, L. M. (2015). Enhanced B-Cell Receptor Recognition of the Autoantigen Transglutaminase 2 by Efficient Catalytic Self-Multimerization, (2012085), 1–19.

Stamnaes, J., Pinkas, D. M., Fleckenstein, B., Khosla, C., & Sollid, L. M. (2010). Redox regulation of transglutaminase 2 activity. *The Journal of Biological Chemistry*, *285*(33), 25402–9.

Stamnaes, J., & Sollid, L. M. (2015). Celiac disease: Autoimmunity in response to food antigen. *Seminars in Immunology*, *27*(5), 343–352.

Stedman's Medical DIctionary. (2006) (28th ed.).

Stephens, P., Grenard, P., Aeschlimann, P., Langley, M., Blain, E., Errington, R., Kipling, D., Thomas, D., & Aeschlimann, D. (2004). Crosslinking and G-protein functions of transglutaminase 2 contribute differentially to fibroblast wound healing responses. *Journal of Cell Science*, *117*(Pt 15), 3389–403.

Stepniak, D., & Koning, F. (2006). Celiac disease - sandwiched between innate and adaptive immunity. *Human Immunology*, *67*(6), 460–8.

Stevens, A., & Lowe, J. (2004). *Human Histology* (3rd ed.). Mosby.

Thomas, H., Beck, K., Adamczyk, M., Aeschlimann, P., Langley, M., Oita, R. C., Thiebach, L., Hils, M., & Aeschlimann, D. (2013). Transglutaminase 6: a protein associated with central nervous system development and motor function. *Amino Acids*.

Thomas, K. E., Sapone, A., Fasano, A., & Vogel, S. N. (2006). Gliadin Stimulation of Murine Macrophage Inflammatory MyD88-Dependent : Role of the Innate Immune Response in celiac disease. *The Journal of Immunology*, *176*, 2512–2521.

Tjon, J. M.-L., van Bergen, J., & Koning, F. (2010). Celiac disease: how complicated can it get? *Immunogenetics*, *62*(10), 641–51.

Tsuchiya, S., Kobayashi, Y., Goto, Y., Okumura, H., Nakae, S., Konno, T., & Tada, K. (1982). Induction of Maturation in Cultured Human Monocytic Leukemia Cells by a Phorbol Diester1. *Cancer Research*, *42*(April), 1530–1536.

Tsuchiya, S., Yamabe, M., Yamaguchi, Y., Kobayashi, Y., Konno, T., & Tada, K. (1980). Establishment and characterization of a human acute monocytic leukemia cell line (THP-1). *International Journal of Cancer*, *26*(2), 171–6.

Tucholski, J., Lesort, M., & Johnson, G. V. (2001). Tissue transglutaminase is essential for neurite outgrowth in human neuroblastoma SH-SY5Y cells. *Neuroscience*, *102*(2), 481–491.

Tučková, L., Novotná, J., Novák, P., Flegelová, Z., Květoň, T., Jelínková, L., Zdeněk, Z., Man, P., & Tlaskalova-Hogenova, H. (2002). Activation of macrophages by gliadin fragments : Isolation and characterization of active peptide. *Journal of Leukocyte Biology*, *71*, 625–631.

Vader, L. W., de Ru, A., van der Wal, Y., Kooy, Y. M. C., Benckhuijsen, W., Mearin, M. L., Drijfhout, J. W., van Veelen, P., & Koning, F. (2002). Specificity of tissue transglutaminase explains cereal toxicity in celiac disease. *The Journal of Experimental Medicine*, *195*(5), 643–9.

van Heel, D. A., Franke, L., Hunt, K. A., Gwilliam, R., Zhernakova, A., Inouye, M., Wapenaar, M. C., Barnardo, M. CNM, Bethel, G. Holmes, G. KT., Feighery, C., Jewell, D., Kelleher, D., Kumar, P., Travis, S., Walters, J. RF., Sanders, D. S., Howdle, P., Swift, J., Playford, R. J., McLaren, W., Mearin, M. L., Mulder, C. J., McManus, R., McGinnis, R., Cardono, L. R., Deloukas, P., & Wijmenga, C. (2007). A genome-wide association study for celiac disease identifies risk variants in the region harboring IL2 and IL21. *Nature Genetics*, *39*(7), 827–829.

Venere, A. Di, Rossi, A., De Matteis, F., Rosato, N., Agrò, A. F., & Mei, G. (2000). Opposite effects of Ca(2+) and GTP binding on tissue transglutaminase tertiary structure. *The Journal of Biological Chemistry*, *275*(6), 3915–21.

Wang, J. L., Yang, X., Xia, K., Hu, Z. M., Weng, L., Jin, X., Jiang, H., Zhang, P., Shen, L., Guo, J. F., Li, N., Li, Y. R., Lei, L. F., Zhou, J., Du, J., Zhou, Y. F., Pan, Q., Wang, J., Wang, J., Qiang, R., & Tang, B. S. (2010). TGM6 identified as a novel causative gene of spinocerebellar ataxias using exome sequencing. *Brain*, *133*(12), 3510–3518.

Yee, V. C., Pedersen, L. C., Le Trong, I., Bishop, P. D., Stenkamp, R. E., & Teller, D. C. (1994). Three-dimensional structure of a transglutaminase: human blood coagulation factor XIII. *Proceedings of the National Academy of Sciences of the United States of America*, *91*(15), 7296–7300.

Zheng, X., Hong, Y., Feng, G., Zhang, G., Rogers, H., Lewis, M. A. O., Williams, D. W., Xia, Z., Song, B., & Wei, X. (2013). Lipopolysaccharide-Induced M2 to M1 Macrophage Transformation for IL-12p70 Production Is Blocked by Candida albicans Mediated Up-Regulation of EBI3 Expression, *8*(5), 4–13.

Zone, J. J., Schmidt, L. A., Taylor, T. B., Hull, C. M., Sotiriou, M. C., Jaskowski, T. D., Hill, H. R., & Meyer, L. J. (2011). Dermatitis Herpetiformis Sera or Goat Anti-Transglutaminase-3 Transferred to Human Skin-Grafted Mice Mimics Dermatitis Herpetiformis Immunopathology. *The Journal of Immunology*, *186*(7), 4474–4480.